



UNIVERSITÀ
DEGLI STUDI
FIRENZE

DOTTORATO DI RICERCA IN SCIENZE CHIMICHE

CICLO XXXII

COORDINATORE Prof. Piero Baglioni

PHYSICAL-CHEMICAL CHARACTERIZATION AND DEVELOPMENT OF
CONSERVATION METHODOLOGIES OF HISTORICAL SILK BANNERS AND
EMBLEMS FROM THE 16-20th CENTURY OF THE NORTH ANDEAN REGION

Settore Scientifico Disciplinare CHIM/12

Dottorando

Dott. Diego Armando
Badillo Sanchez

Tutore

Prof. Alessandra Cincinelli

Coordinatore

Prof. Piero Baglioni

Anni 2016/2019



UNIVERSITÀ
DEGLI STUDI
FIRENZE

DOTTORATO DI RICERCA IN
SCIENZE CHIMICHE

CICLO XXXII

COORDINATORE Prof. PIERO BAGLIONI

PHYSICAL-CHEMICAL CHARACTERIZATION AND
DEVELOPMENT OF CONSERVATION METHODOLOGIES
OF HISTORICAL SILK BANNERS AND EMBLEMS FROM
THE 16-20th CENTURY OF THE NORTH ANDEAN
REGION

Dottorando

Dott. Diego Armando
Badillo Sanchez

Tutore

Prof. Alessandra Cincinelli

TABLE OF CONTENTS

PREFACE	E
Thesis objective	E
Thesis outline	E
PART I INTRODUCTION.....	- 1 -
Chapter 1. Silk	- 3 -
1.1. Silk production	- 4 -
1.1.1. Silk de-gumming.....	- 6 -
1.2. Silk composition	- 7 -
1.2.1 Silk fibroin	- 8 -
1.3. Silk properties	- 10 -
1.4. Degradation factors on silk.....	- 11 -
References.....	- 13 -
Chapter 2. Silk decorations: color and metals	- 15 -
2.1. Color.....	- 15 -
2.2. Metals	- 19 -
References.....	- 21 -
Chapter 3. Silk artificial aging.....	- 23 -
References.....	- 25 -
Chapter 4. Analytical methods on the study of silk	- 27 -
4.1. Microscopy	- 28 -
4.2. Spectroscopic studies	- 28 -
4.3. Thermogravimetric studies.....	- 30 -
4.4. Mechanical studies	- 30 -
4.5. Chromatographic studies.....	- 31 -
4.6. Elemental studies	- 31 -
References.....	- 32 -
Chapter 5. Silk restoration and conservation	- 37 -
References.....	- 40 -
Chapter 6. Historical flags and emblems of the National Museum of Colombia -	
41 -	
6.1. 16 th century.....	- 43 -
6.2. 18 th century.....	- 44 -
6.3. 19 th century.....	- 45 -
6.3.1 European iconography.....	- 45 -
6.3.2. American iconography	- 46 -
6.4. 20 th century.....	- 47 -

TABLE OF CONTENTS

6.5. 21 st century	- 47 -
PART II. STUDY OF METALS AND DYES AS DECORATION OF SILK TEXTILES..	- 49 -
Chapter 7. Microanalytical study of the evolution of metals used as decorations on Spanish and Latin-American flags textiles from 16-20 th -century preserved at the textile collection of the National Museum of Colombia.....	- 51 -
Abstract.....	- 51 -
7.1. Introduction	- 53 -
7.2. Materials and methods.....	- 55 -
7.2.1. Historical samples	- 55 -
7.2.2. Optical microscopy (OM)	- 56 -
7.2.3. Field Emission Scanning Electron Microscopy with Energy Dispersive X-Ray Spectroscopy (FE-SEM-EDS).....	- 56 -
7.2.4. Inductively coupled plasma optical emission spectrometry (ICP-OES)	- 57 -
7.2.5. Multi Collector Inductively coupled plasma with mass spectrometry (MC-ICP-MS).....	- 60 -
7.3. Results and discussion	- 61 -
7.4. Conclusions	- 84 -
References	- 86 -
Supplementary Information Chapter 7.....	- 89 -
Chapter 8. Spectroscopic study of dyes of the flags of the textile collection of the National Museum of Colombia	- 107 -
Abstract.....	- 107 -
8.1. Introduction	- 108 -
8.2. Materials and methods.....	- 109 -
8.2.1. Historical samples	- 109 -
8.2.2 Fiber Optics Reflectance Spectroscopy (FORS).....	- 109 -
8.3. Results and discussion	- 110 -
8.4. Conclusions	- 114 -
References	- 115 -
Supplementary Information Chapter 8.....	- 117 -
PART III. MOLECULAR STUDY OF SILK	- 125 -
Chapter 9. Characterization of the secondary structure of degummed Bombyx mori Silk in modern and historical samples.....	- 127 -
Abstract.....	- 127 -
9.1. Introduction	- 129 -
9.2. Materials and methods.....	- 131 -
9.2.1. Modern and historical silk samples	- 131 -

TABLE OF CONTENTS

9.2.2. Fourier transform infrared (FTIR) 2D Imaging-Chemical mapping	- 132 -
9.2.3. Thermogravimetric analysis (TGA).....	- 134 -
9.2.4. Differential Scanning Calorimetry (DSC).....	- 134 -
9.2.5. Optical microscopy (OM)	- 134 -
9.2.6. Field emission scanning electron microscopy (FE-SEM).....	- 134 -
9.2.7. Accelerated UV-Vis aging of commercial silk samples	- 135 -
9.2.8. Solid-liquid extraction process over silk fibers	- 135 -
9.3. Results and discussion	- 135 -
9.4. Conclusions	- 154 -
References	- 156 -
Supplementary Information Chapter 9.....	- 158 -
Chapter 10. Understanding the structural degradation of Mesoamerican historical silk: A Focal Plane Array (FPA) FTIR and multivariate analysis .-	- 163 -
Abstract.....	- 163 -
10.1. Introduction	- 165 -
10.2. Methods.....	- 168 -
10.2.1. Silk samples	- 168 -
10.2.2. Treatment of modern silk	- 169 -
10.2.3. Fourier Transform Infrared (FTIR) 2D Imaging-Chemical mapping ..-	- 169 -
10.2.4. Statistical data analysis	- 171 -
10.2.5. Fiber Optics Reflectance Spectroscopy (FORS).....	- 172 -
10.3. Results and Discussion.....	- 172 -
10.4. Conclusions	- 184 -
References	- 186 -
Supplementary Information Chapter 10.....	- 190 -
PART IV. SILK CONSOLIDATION	- 205 -
Chapter 11. Self-regenerated silk fibroin with controlled crystallinity for the reinforcement of silk	- 207 -
Abstract.....	- 207 -
11.1. Introduction	- 208 -
11.2. Materials and methods.....	- 212 -
11.2.1. Chemicals used	- 212 -
11.2.2. Pristine and aged silk samples	- 212 -
11.2.3. Self-regenerated silk fibroin (SRSF) solutions.....	- 213 -
11.2.4. SRSF coatings	- 214 -
11.2.5. Fourier Transform Infrared (FTIR) 2D Imaging-Chemical mapping ..-	- 214 -

TABLE OF CONTENTS

11.2.6. Field Emission Scanning Electron Microscopy (FE-SEM)	- 216 -
11.2.7. Differential Scanning Calorimetry (DSC)	- 216 -
11.2.8. Tensile tests	- 217 -
11.3. Results and discussion	- 217 -
11.4. Conclusions	- 230 -
References	- 231 -
Supplementary Information Chapter 11	- 235 -
APPENDIX I	
Appendix 1. List of flags and samples	II
Appendix 2. Sampling protocol	XIV
2.1. Proposal for sampling protocol in art objects and/or cultural heritage goods for scientific research	XV
2.1.1. Sampling process responsible	XVI
2.1.2. Preliminary studies before the sampling process	XVII
2.1.3. Sampling process methods	XVIII
2.1.4. Final consideration	XXIII
References	XXIII
2.2. Sampling protocol agreed with the national museum of Colombia	XXIV
Appendix 3. FPA μ -FTIR 2D chemical mapping on historical samples	XLVII
Appendix 4. Annexed information for different processes on the thesis research	LIII
4.1. Description of the preparation of solutions for silk reconsolidation	LIV
4.2. Tensile tests	LVII
4.3. Lead purification columns for lead isotope analysis on MC-ICP-MS	LIX
4.4. Example of some metal decorations chemically cleaned before SEM-EDS analysis	LX
4.5. Example of the thermal decomposition of silk textile sample on a TGA chamber	LXI
Appendix 5. Raman spectra on the region 200-1800 cm^{-1} of the SRSF films prepared from waste silk	LXII
ACKNOWLEDGEMENTS	LXV

PREFACE

This thesis is submitted to the University of Florence as part of the requirements to obtain the PhD degree in “Science Chemistry Curriculum in Science for the Conservation of the Cultural Heritage”. The presented work was carried out in the years 2016-2019 at the Department of Chemistry "Ugo Schiff", University of Florence.

Thesis objective

The principal aim of this research was to promote/develop culture through an analytical study. For this purpose, it was used a set of historical flags from the National Museum of Colombia which are part of the Latin-American history as base of research. Silk flags/emblems textiles from the transitional period from the Colonial to Republic in the areas of the north of the Andes (Colombia, Peru, Venezuela, Ecuador) were studied to characterize them and understand the natural degradation process on silk textiles to finally propose a preservation method which help to enlarge the life of those valuable textile objects.

Thesis outline

The rational of this research is divided in three conceptual topics: First, a material characterization of the historical objects studied is proposed to evaluate the historical aspects of the different components of the textiles, i.e. fiber analysis, metal decoration detail and the possible dyes present on the textiles; all from a scientific point of view, in aims to give new information to

help on present and future discussions to relate the materials with possible transitions between Europe and America in both, manufacture and exchange of resources on the frame time related with the historical textiles (16th-21st centuries). Second, using modern analytical tools and statistical analysis of data, scientific analysis of the natural degradation path of silk is studied, while it is related with the use of dyes and time. Third, with the previous knowledge a conservation strategy to consolidate degraded silk is proposed. The reader will find this rationale on the thesis following the division of the text as it is organized by parts as follows:

Part I: This section divided in six chapters will give the basic concepts of the main material of study (silk), at the same time that presents the historical objects used on the research, this in aims to give a general introduction where the reader at the end will be familiarized with the state of the art on cultural heritage silk studies.

Part II: This section divided on two chapters explores from a scientific point of view the study of the metal decorations and dyes present on the historical textiles studied in aims to offer to other disciplines scientific data to discuss the evolution of those materials.

Part III: This section which is composed by two chapters, is focused on the scientific study of the degradation of silk from a molecular point of view, at the same time that it is related the possible effect on the silk degradation by the use of the dyes and its age.

Part IV: This final section composed by a single chapter, present a new consolidation process to improve the physical-mechanical properties of degraded silk using waste silk in aims to preserve those valuable textile objects.

PREFACE

Finally, an Appendix section it is available for the reader, which is composed by the photography images and description of the historical objects used on this research, as well the sampling protocol developed to extract the micro samples from the historical objects is presented, and extra information which will complement the information on the main body of the thesis is offered.

PART I.
INTRODUCTION

Chapter 1. Silk

Since prehistoric times humans have used Earth's natural resources to meet their own needs. Nature has been used as a source for food, shelter, and basis to produce tools, clothes, and all kind of accessories around the world, being transformed the natural resources in different cultures in different ways according to the technology available. This transformation of nature it is a consequence of a careful observation of the environment, which starts from the basic but no obvious step to appreciate, contemplate and understand what is around, letting as result the knowledge for inorganic and organic matter.

One of those materials resultant from nature's observation is silk, which according to Confucius, its discovery goes back to 2640 BC. The legend says that Xi Lin Shi, a Chinese princess, saw how a moth fall on her tea cup, and meanwhile she was trying to pull back the insect from the hot cup, she realizes that a fiber was produced [1]. This story tells the discovery of the natural fiber considered until today as a "luxury material" [1], this due to its unique feel, luster, dyeability, tensile strength and elasticity, good thermal stability, hygroscopic nature, and microbial resistance [2]. Nevertheless, recent archaeological findings joint with archaeometric studies have shown that the story is just that, due to evidence can confront the legend, indicating that the ancient knowledge of this material could go back until 8500 years ago [3].

Silk has been used to produce textiles for clothing, fashion accessories, flags, and banners, or as fabrics for furniture, walls tapestry, decoration, and support for different artistic objects, as much as in the past as in the present [4]. Several of those objects nowadays are considered as part of the human cultural

heritage, because of who manufactured it or use it, as well for their artistic value, or for the non-verbal information that relays on them by their iconography, the technique or the technological information present on each shred of textile.

Silk has been used for millennia, and for its value will be used for a longer time, however its full understanding is not complete, being needed to continue researching on it, not only to preserve the ancient objects, but to produce new durable materials.

1.1. Silk production

Silk is a natural proteinaceous fiber material produced by different invertebrates, in particular spiders and insects, which secrete it for various purposes. Trichoptera, Lepidoptera, and some other Holometabola larvae secrete it through their mouth, from labial glands (which acts as silk glands) to produce their cocoons on the chrysalides of the caterpillars [5]. The silk produced by other insects, mainly spiders, is excreted for the making up of their webs [5] (a subject not covered in this research).

The production of silk is denoted as sericulture, which includes plant cultivation to feed the silkworms which spin silk cocoons, till reeling the cocoons to unwind the silk filament for posterior weaving [1].

In the context of this research, the term silk and sericulture will only be referred to the production of silk from the silkworm, in particular from the *Bombyx mori* moth, due to its extended commercial and industrial use, across time and around the world [6]. *Bombyx mori* silk is classified as a mulberry silk, because larvae are only fed with Mulberry leaves. This species is fully

domesticated, in fact, the suppression of flying ability on the insect [1], leads to a controlled process, in which its sericulture is intimately related with the farming of mulberries plants [6]. The successful production of mulberry leaves depends on the variety of the plant, climatic conditions (temperatures from 24 ° C to 28 ° C, humidity in the range of 65–80%, sunshine range of 9–13 h a day, and an annual rainfall ranging from 600 to 2500 mm) and cultivation practices, being cultivated from sea level up to an altitude of 1000 m [6].



Figure 1 Left: Bombyx mori larvae next to B. Mori cocoons over a mulberry leaf. Right: Bombyx mori moth.

The silk production is based on the life cycle of the insect, which has a short life of only about two months, going through four phases: egg; worm or larvae; pupa and moth [6]. The production of fibers is based on the interruption of the cycle before the moth hatches from the cocoon at the third stage. After the cocoon is harvested, a series of processes are followed during the rearing activities, such as cocoon sorting, riddling, stifling, cooking, reeling, re-reeling and twisting; followed by the fiber preparation, spinning weaving and knitting, to finally produce the fabric finishing, including wet processing techniques such as de-gumming, dyeing and printing before the garment manufacture [6].

Silk production was kept in secret in China until 300 AC., later it, was leaked to India with the Buddhist road, where their knowledge spreads, continuing to expand its use by the Mongol expansion, to finally arrive in Europe

and North Africa across the Mediterranean that completes what is actually known as the “silk road” [7]. In the middle ages, its European production began, mainly in Italy, Spain and later in France [8]. This silk expansion finally arrived in America with the first colonizers during the late 15th century but it was only in the late 18th century that in some places in Mexico the sericulture production was allowed to begin [9]. During this period, silk woven started by hand (continuing to the present day), changing in more recent times with the introduction of a variety of looms and tools (not discussed here).

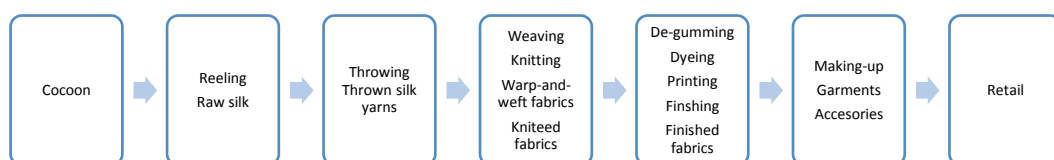


Figure 2 Silk manufacturing process adapted from [1]

1.1.1. Silk de-gumming

It is important to underline from the silk process one operation used very often: the so-called de-gumming process. This process aimed to remove one external component of the natural fiber, the Sericin protein, which if it was not removed, it would confer two disadvantages to the final fabric: it gives the fabric a rigid stiff, cardboard-like feel and prevents dyestuff from penetrating the heart of the fiber [1]. This operation, which has been used for centuries, being the one that mostly modifies the composition of silk, consists in soaking the silk on water with soap (at an alkaline pH) for six hours, and after rinsing it in freshwater, removing in this way only the sericin protein, with a consequent weight loss of around 25-30%, and a slight change in color (turning more yellowish or cream) on the material, which is why, in modern industry this step is followed by an immersion of the fabric/yarn on hydrogen 35% peroxide to bleach the silk and obtain whiter colors [1].

Although this process is suggested to improve the quality of the silk, and has not used for all purposes, this process is mandatory for textile production and it is extremely rare to find a finished textile made of raw silk (Silk that has not had any degumming) [10].

1.2. Silk composition

As mentioned above, silk is a natural fiber, such as cotton, wool, linen, cashmere, and mohair. Silk is a protein fiber with an amino acid composition similar to that found on human skin, which is spun from matured silkworm larvae on two parallel monofilaments (brin) composed of 65–75% fibroin, 20–30% sericin, and 5% wax, pigments, sugars, and other components [2]. The sericin, which has different functions on the larvae, is a protein with molecular weight ranging from 10 to 310 kDa, composed mainly of serine, threonine, aspartic acid, and glutamic acid, due to this protein is removed from the fiber on textile production as a finishing operation and as described above, will not be discussed in this research.

Silk fibers appear as opaque solid rods under a microscope, each raw silk thread has a lengthwise striation, with a width of 10–14 μm and appears in a cross-section like a swollen triangle. Silk fibers contain crystalline and amorphous regions, which break down into fibrils composed of fibrillar regions in a highly organized state, being a not completely homogeneous solid, held together by other regions of the less organized protein, forming a continuous filament which can yield up to 1600 meters each [11].

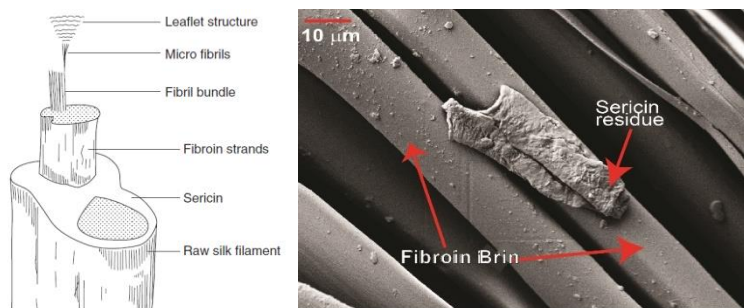


Figure 3 Left: Structure of silk filament taken from [11]. Right: Microphotograph of silk fiber, in detail fibroin fibril and sericin residue after the incomplete de-gumming process.

1.2.1 Silk fibroin

Fibroin is a protein composed of 5507 amino acid repetitions consisting of repeated sequences of six residues of (Gly–Ala–Gly–Ala– Gly–Ser) $_n$ repetitions with molecular weight ranging from 300 to 450 kDa [12]. The chemical analyses of *Bombyx mori* fibroin indicate that it is composed of, 44% glycine, 29% alanine, 12% serine, 5% tyrosine, 2% valine and various other amino acids in even smaller proportions (See Table 1.), with an iso-electric point around pH 5 [11]. The crystalline regions of silk account for 50–60% of the fiber, These contain several repetitions of the basic sequence –(Gly–Ala–Gly–X)– where X is serine or tyrosine, which form in the spun fibers [13].

The SF which is secreted in the lumen of the posterior silk gland of the insect consists of three protein components: heavy chain (H-chain 395 kDa), light chain (L-chain 25 kDa), and glycoprotein, P25 in a 6:6:1 ratio [14]. The L-chain contains 244 amino acid residues, meanwhile H-chain which contains 5263 amino acid residues, with a primary structure rich in glycine, alanine, and serine at a molar ratio of 3:2:1, forming repeating motifs of –(GAGAGS) $_n$ – and –(GAGAGY) $_n$ –, counting for a 64.8% of the total of the H-chain [2]. Two crystalline dimorphs of silk fibroin have been identified, Silk II and Silk I. Silk II mainly consist

of the two repeating motifs present in the H-chain forming a prominent antiparallel β sheet structure, being responsible for the mechanical properties of the fiber, being the resultant structure found after spinning. Silk I is mainly composed of Phe, Tyr, and Try amino acids, groups with residues with larger side groups being part of the L-chain and H-chain hydrophilic regions, as well being related with the hygroscopicity and resistance of the fiber to UV radiation, being this conformation the one found in the solid-state before spinning [2].

Table 1 Amino acid composition of mulberry Silk took from [11]

Amino acid	Percentage
Glycine	43.74
Alanine	28.78
Valine	2.16
Leucine	0.52
Isoleucine	0.65
Serine	11.88
Threonine	0.89
Aspartic acid	1.28
Glutamic acid	1.00
Phenylalanine	0.62
Tyrosine	5.07
Lysine	0.63
Histidine	0.53
Arginine	1.83
Proline	0.35
Tryptophan	0.33

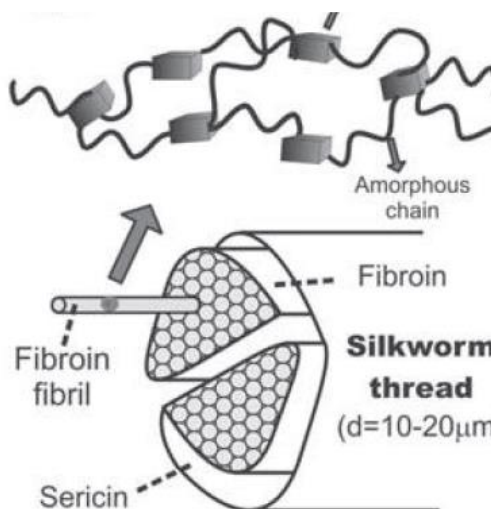


Figure 4 Hierarchical structure of silkworm silk fiber, taken from [15]

The primary structural motifs described above have a preferred secondary structure on the fiber, being those conformations: the random coil, the α -helix, and the β -sheet. The quantity, order, and distribution of those structural conformations will affect the mechanical properties of silk fibers. Due to the special distribution of amorphous and crystalline regions on silk, this material is considered as a semicrystalline polymer with a hierarchical structure in which highly oriented β -sheets crystallites are connected with an amorphous matrix are organized in nanofibrils or fibrillar entities, however, it has been proposed that there exists a third phase, or interphase consisting of weakly oriented β -sheets regions or oriented amorphous domains. The β -sheet crystallite on fibroin is uniformly distributed in the whole fiber matrix, being indexed as a monoclinic space group with a rectangular unit cell parameter of $a=0.938$ nm, $b=0.949$ nm and $c=0.698$ nm, and a size between 20 to 170 nm in the axial direction and 1 to 20 nm in the lateral direction. The non-crystalline regions can be described as amorphous, poorly orientated, or randomly coiled sections, is not well understood yet their distribution on the peptide, existing as well β -turn or β -spiral and helical conformations suggested for amorphous domains [15].

1.3. Silk properties

The different microstructures which compose the silk fibroin fiber confer to them their unique physicochemical characteristics. Silk fibers are smooth, strong, with a tenacity of approximately 4.8 grams per denier, extensible, with an elongation value between 19% and 24% and mechanically compressible and can absorb up to 30 % of its weight in moisture. Compared with other fibers it has better luster and feel, have a higher tensile strength than glass or synthetic

organic fibers. Silk is a non-thermoplastic fiber, normally stable up to 140 ° C and the thermal decomposition temperature is greater than 1500 ° C. The densities of silk fibers are in the range of 1320–1400 kg/m³ with sericin and 1300–1380 kg/m³ without. Silk has a relatively high electrical resistance. At low air humidity, it becomes electrostatically charged when subjected to friction. Silk can absorb considerable amounts of salts. Fibroin is soluble in certain concentrated aqueous chaotropic salt solutions. Silk's natural beauty and properties of comfort in warm weather and warmth during colder months have also made it ideal for high-fashion clothing [2,6,11,16,17].

1.4. Degradation factors on silk

Silk as a natural fiber is susceptible to transformation on its structure by the reaction with natural agents as light, humidity, and biotic attack. Silk has poor resistance to ultraviolet light, producing yellowing/tendering by photochemical degradation, by the decomposition of tryptophan accelerated by the presence of tyrosine. Silk is susceptible to hydrolysis reacting with cations of various inorganic salts, the degree of hydrolysis is much greater with acid than alkali. The least degradation occurs between pH 4 and 8. The rate of hydrolysis is increased by increasing temperature, on the contrary, it is very resistant to hydrolysis by proteolytic enzymes. Oxidative degradation can as well occur and are considered to take place at the side chains of tyrosine; the amino-terminal residues of the main chains; and at the peptide bonds. Silk fiber as well is susceptible to concentrated solutions of certain organic acids such as 98% formic acid, which can cause dissolution and degradation of the protein, or boiling water and steam at 100 °C or more. Hot concentrated acids and alkalis readily decompose silk. The degradative effect of nitric acid is accompanied by

a yellow coloration involving the nitration of phenyl residues in the Xantho proteic reaction. silk is sensitive to acid because of the virtual absence of acid-stable disulfide bridges. However, the absence of alkali-sensitive disulfide bridges gives silk a higher resistance to alkali [2,6,11,16–22].

References

- [1] R.R. Franck, ed., 1 - Silk, in: *Silk, Mohair, Cashmere and Other Luxury Fibres*, Woodhead Publishing, 2001: pp. 1–67. doi:10.1533/9781855737594.1.
- [2] F. Wang, Y.-Q. Zhang, Chapter Eight - Bioconjugation of Silk Fibroin Nanoparticles with Enzyme and Peptide and Their Characterization, in: R. Donev (Ed.), *Advances in Protein Chemistry and Structural Biology*, Academic Press, 2015: pp. 263–291. doi:10.1016/bs.apcsb.2014.11.005.
- [3] Y. Gong, L. Li, D. Gong, H. Yin, J. Zhang, Biomolecular Evidence of Silk from 8,500 Years Ago, *PLOS ONE*. 11 (2016) e0168042. doi:10.1371/journal.pone.0168042.
- [4] N. Luxford, D. Thickett, P. Wyeth, Preserving silk: Reassessing deterioration factors for historic silk artefacts, in: *Natural Fibres in Australasia: Proceedings of the Combined (NZ and AUS) Conference of The Textile Institute, Wilson, C. A. and Laing, R. M, Dunedin, New Zealand, 2009*: pp. 151–156.
- [5] R.S. Weber, C.L. Craig (auth.), T. Asakura, T. Miller (eds.), *Biotechnology of Silk*, 1st ed., Springer Netherlands, 2014. <http://gen.lib.rus.ec/book/index.php?md5=f44d613bf7bb1ca80774ed6fcd3a90f>.
- [6] M. Schoeser, *Silk*, Yale University Press, 2007.
- [7] *The Journey of Maps and Images on the Silk Road*, Brill, 2008. <https://brill.com/view/title/15363> (accessed August 5, 2019).
- [8] G.N. Espinach, El arte de la seda en el Mediterráneo medieval, *En la España medieval*. (2004) 5–51.
- [9] G. Corzo, R. Vanesa, Entramados de la seda en México durante el siglo XIX y principios del XX, (2012). <http://digibuo.uniovi.es/dspace/handle/10651/13416> (accessed August 5, 2019).
- [10] D.A. Badillo-Sanchez, C.B. Dias, A. Manhita, N. Schiavon, The National Museum of Colombia's "Francisco Pizarro's Banner of Arms": A multianalytical approach to help uncovering its history, *Eur. Phys. J. Plus*. 134 (2019) 224. doi:10.1140/epjp/i2019-12747-2.
- [11] K.M. Babu (Auth.), *Silk. Processing, Properties and Applications*, 1st ed., Woodhead Publishing, 2013. <http://gen.lib.rus.ec/book/index.php?md5=96dd28e1fb4d66704ad151972e5d8276>.
- [12] N.S. Koseva, J. Ryzd, E.V. Stoyanova, V.A. Mitova, Chapter Three - Hybrid Protein–Synthetic Polymer Nanoparticles for Drug Delivery, in: R. Donev (Ed.), *Advances in Protein Chemistry and Structural Biology*, Academic Press, 2015: pp. 93–119. doi:10.1016/bs.apcsb.2014.12.003.
- [13] M. Tsukada, G. Freddi, M. Nagura, H. Ishikawa, N. Kasai, Structural changes of silk fibers induced by heat treatment, *Journal of Applied Polymer Science*. 46 (1992) 1945–1953. doi:10.1002/app.1992.070461107.
- [14] S. Inoue, K. Tanaka, F. Arisaka, S. Kimura, K. Ohtomo, S. Mizuno, Silk Fibroin of Bombyx mori Is Secreted, Assembling a High Molecular Mass Elementary Unit Consisting of H-chain, L-chain, and P25, with a 6:6:1 Molar Ratio, *J. Biol. Chem.* 275 (2000) 40517–40528. doi:10.1074/jbc.M006897200.
- [15] X. Liu, K.-Q. Zhang, *Silk Fiber — Molecular Formation Mechanism, Structure- Property Relationship and Advanced Applications*, (2014). doi:10.5772/57611.
- [16] T. Scheibel, H. Zahn, A. Krasowski, *Silk*, in: *Ullmann's Encyclopedia of Industrial Chemistry*, Wiley-VCH Verlag GmbH & Co. KGaA, 2000. doi:10.1002/14356007.a24_095.pub2.
- [17] S. Takeda, Chapter 31 - Bombyx mori, in: V.H. Resh, R.T. Cardé (Eds.), *Encyclopedia of Insects (Second Edition)*, Academic Press, San Diego, 2009: pp. 117–119. <http://www.sciencedirect.com/science/article/pii/B9780123741448000400> (accessed January 26, 2017).
- [18] M. Hacke, Weighted silk: history, analysis and conservation, *Studies in Conservation*. 53 (2008) 3–15. doi:10.1179/sic.2008.53.Supplement-2.3.
- [19] V. DANIELS, M. LEESE, The Degradation of Silk by Verdigris, *Restaurator*. 16 (2009) 45–63. doi:10.1515/rest.1995.16.1.45.
- [20] N. Luxford, Silk durability and degradation, in: P.A. Annis (Ed.), *Understanding and Improving the Durability of Textiles*, Woodhead Publishing Limited, Cambridge, 2012: pp. 205–232. <http://discovery.ucl.ac.uk/1366005/> (accessed December 1, 2016).
- [21] K. Hirabayashi, Y. Yanagi, S. Kawakami, K. Okuyama, W. Hu, Degradation of silk fibroin, *The Journal of Sericultural Science of Japan*. 56 (1987) 18–22. doi:10.11416/kontyushigen1930.56.18.

- [22] Q. Lu, B. Zhang, M. Li, B. Zuo, D.L. Kaplan, Y. Huang, H. Zhu, Degradation Mechanism and Control of Silk Fibroin, *Biomacromolecules*. 12 (2011) 1080–1086. doi:10.1021/bm101422j.

Chapter 2.

Silk decorations: color and metals

The silk textile industry since the early origins has been accompanied to the use of decorative elements to improve or stand out the artifact.

In the manufacturing process of textile objects, different aspects are considered to produce unique objects that transfer not only a piece of fabric to the public, but the charm of fashion, an idea of exclusivity, an expression of art. For this reason, various weavings have been created such as Jacquard, chiffon, among others (this topic will not be discussed on this research but the reader is gently invited to consult it as for example in the book of Hann and Thomas [1]). Nevertheless, not only by playing with the disposition of weft and warp of the fibers it is possible to attract the attention of an audience for centuries, as in the case of silk. For this reason, two main elements are used to transform the silk objects without taking away their valuable properties, namely dyes and metals, which are obtained by changing the color of the object and confer a final added value to the object.

2.1. Color

Silk is a naturally neutral color fiber i.e. it has a white color when it is fresh and a white-cream color after its de-gumming [2–4]. This aspect confers to the fiber an optimal basis for the transformation of its color, a mandatory aspect to be satisfied for a textile in the industry and in the market, where the choice of color depends mainly on the grades of shade, brightness and fastness.

Silk as a proteinaceous material, can be transformed in its appearance through the use of dyes, which will change the color of the full fiber-body, or by the application of pigments such as paints, since the fiber is used only as a support [5]. The technique used to dye the fiber is through an immersion in an aqueous bath where the dyes have been dispersed, in that process the fiber swelled the solution in different degrees depending on the chemical composition of the fiber, which is why the dyeing process could not be homogeneous on all the fiber, due to its different crystalline and amorphous domains.

In the same way that textile industry has evolved over time, even dyes have changed, passing from obtaining basic colors extracted from plants [6–8], to a multicolored world thanks to new and modern synthetic compounds [9,10]. The silk dyeing process has been considered as an art, due to the amazing chromatic results, as well as to the care, attention and skills needed to avoid damages to the fiber [11–13].

The mechanism of silk dyeing depends on free amino and carboxyl groups and also on phenolic with accessible –OH groups on the protein, where the dye–fiber interaction occurs through ionic or covalent bonding, thanks to the –COOH and –NH₂ groups, which ionize at an appropriate pH, letting a wide range of dyes to be used as acid, basic, direct, metal-complex/mordant, natural and reactive dyes [5]. Among these, acid and metal-complex dyes are the most widely used. Acid and metal-complex dyes possess a better affinity for fibers, are easily absorbed, but have poor to moderate washing fastness. The reactive dyes offer good wash fastness and a full range of dischargeable colors with high perspiration fastness. Basic dyed silk has very poor light fastness [5,9,14].

By dyeing with acid dyes it is possible to achieve brilliant shades and good fastness properties, belonging to this type of dyes, compounds with nitro, nitroso, monoazo, bisazo, triphenyl methane, and anthraquinone groups. This process is followed in acidic condition (pH 4–5), creating a zwitter ion on the fibroin protein where the acid dye anions will be adsorbed at the protonated amino groups forming the electrostatic bond or salt linkage. Acid dyes can be classified according to the pH used on the treatment as: leveling acid dyes around pH 2–4 (maintained using sulfuric acid); milling acid dyes around pH 4–6 (maintained using a buffer of acetic acid and sodium acetate); or super milling dyes being applied at pH 6–7 (maintained by the addition of ammonium acetate) [15]. Azo chromophores containing hydroxyl groups can be applied to the dye silk through a mordant/chrome acid process, where chromium atoms are used forming a complex chelation through coordinate bonds, needing from the protein a lone pair of electrons to be donated to chromium atom. This process produces some damages to the material as rigidity, masking its screw, being selected only for some shades, such as some blues and black [15]. Cationic dyes use a dye cation derived from a free or substituted amine group, being applied maintaining an acidic pH around 5 by using acetic acid. To this kind of dyes azo, diphenyl methane, triphenylmethane, oxazine, and thiazine groups are the main dyes found [15]. Dyes with sulphonic acid groups containing sodium salt are used as direct dyes which are fixed by salt linkage with the fibroin, being this process carried out protonating the end amino groups in silk on an acidic medium using 2–5% acetic acid or formic acid, in a hot bath starting at 40 °C, and slowly heat up to 90 °C [15]. A final type of dyes are those denoted as reactive dyes, consisting of chlorotriazine or vinyl sulphone groups, which

react with the amino group of silk at pH around 8 to 10 in the presence of sodium silicate, sodium carbonate, or sodium hydroxide [15].

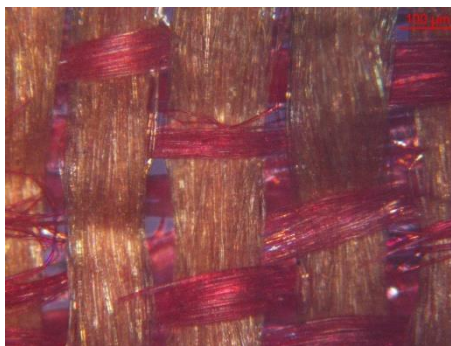


Figure 1 Microphotograph example of a plain historical dyed silk textile with yellow weft fibers and red warp fibers.

Primary colors as blue, yellow, or red, or a full variety of secondary colors and shades including whites and blacks, are achieved during the dyeing process on silk by the use of different types of dyes as noted above, nevertheless, depending on the nature of the dye, as well as the physicochemical interaction with the fiber, the color and tone will be maintained or not on the textile through time, making it sometimes impossible for ancient fabrics to know their original aspect [16–19].

The study of the color on silk textiles can provide information on different aspects as well on the material as about the past cultures. Technological information, change in techniques, economic exchange or merchandizing, source of raw materials, degradation paths due to the use of a specific component, among other data can be extracted from the research of these components, in the same way knowing or revealing the original color of an object, allows to postulate anthropological and communicative details from the people who made, used or stored it.

2.2. Metals

Over time, the beauty of silk textiles has been embellished with different ornaments, making the use of metals as part of the final decoration for the object [20]. Metals have been used in different shapes, proportions, and types, such as textile decorations, being the most common elements gold and silver, being used mainly as metal threads, i.e. a plain metal twisted around a fiber core of finest dimensions (less than 1 mm of width) [21].



Figure 2 Detail of metal decorations used on a 19th century Colombian flag from the National Museum of Colombia textile collection.

These metal decorations, offer different information about the provenance of the object, on their technique, on the kind of decoration, and quantity and quality of the metal used, which can elucidate the age of manufacture, as well as indicate the social relevance of the original owner or its original use [20,21].

After 15th century, international exchange of silver, gold and copper start to have a new competitor to the traditional ores till that date, being the American mines began to contribute the most to the international market after the arrival of the Europeans to American lands [22,23].

Metal decorations can be manufactured in different shapes, as wires, plain strips, paillettes, or in any special shape that the owner of the textile requires. Metal decorations dimensions are usually of thin length and width for threads and long dimensions for larger decorations as leaves, animals or other shapes. Metal decoration can be manufactured combining one or more layers, as in the case of gilded or silvered decorations where an internal metal core is covered by a thinner film of gold or silver.

References

- [1] M.A. Hann, B.G. Thomas, *Patterns of Culture: Decorative Weaving Techniques*, University of Leeds International Textiles Archive, Leeds, 2005.
- [2] S.K. Vyas, S.R. Shukla, Comparative study of degumming of silk varieties by different techniques, *The Journal of The Textile Institute*. 107 (2016) 191–199. doi:10.1080/00405000.2015.1020670.
- [3] R.H. Walters, O.A. Hougen, Silk Degumming I. Degradation of Silk Sericin by Alkalies, *Textile Research Journal*. 5 (1934) 92–104. doi:10.1177/004051753400500213.
- [4] R. Mossotti, R. Innocenti, M. Zoccola, A. Anghileri, G. Freddi, The degumming of silk fabrics: a preliminary near infrared spectroscopy study, *J. Near Infrared Spectrosc.*, *J Near Infrared Spectrosc.* 14 (2006) 201–208. doi:10.1255/jnirs.615.
- [5] T. Scheibel, H. Zahn, A. Krasowski, Silk, in: *Ullmann’s Encyclopedia of Industrial Chemistry*, Wiley-VCH Verlag GmbH & Co. KGaA, 2000. doi:10.1002/14356007.a24_095.pub2.
- [6] M. Yusuf, M. Shabbir, F. Mohamad, Natural Colorants: Historical, Processing and Sustainable Prospects, *Nat Prod Bioprospect.* 7 (2017) 123–145. doi:10.1007/s13659-017-0119-9.
- [7] E.S.B. Ferreira, A.N. Hulme, H. McNab, A. Quye, The natural constituents of historical textile dyes, *Chem. Soc. Rev.* 33 (2004) 329–336. doi:10.1039/B305697J.
- [8] R.A.M. Mussak, T. Bechtold, Natural Colorants in Textile Dyeing, in: T. Bechtold, R. Mussak (Eds.), *Handbook of Natural Colorants*, John Wiley & Sons, Ltd, 2009: pp. 315–337. <http://onlinelibrary.wiley.com/doi/10.1002/9780470744970.ch18/summary> (accessed March 31, 2016).
- [9] H.S. Freeman, J. Sokolowska, Developments in dyestuff chemistry, *Review of Progress in Coloration and Related Topics*. 29 (1999) 8–22. doi:10.1111/j.1478-4408.1999.tb00123.x.
- [10] H. Mustroph, Dyes, General Survey, in: *Ullmann’s Encyclopedia of Industrial Chemistry*, Wiley-VCH Verlag GmbH & Co. KGaA, 2000. http://onlinelibrary.wiley.com/doi/10.1002/14356007.a09_073.pub2/abstract (accessed March 31, 2016).
- [11] G.N. Espinach, El arte de la seda en el Mediterráneo medieval, *En la España medieval*. (2004) 5–51.
- [12] M. Martelli, The Alchemical Art of Dyeing: The Fourfold Division of Alchemy and the Enochian Tradition, in: S. Dupré (Ed.), *Laboratories of Art*, Springer International Publishing, 2014: pp. 1–22. http://link.springer.com.ezproxy.uniandes.edu.co:8080/chapter/10.1007/978-3-319-05065-2_1 (accessed November 19, 2014).
- [13] R.G. Kuehni, H. Henning Bunge, Dyeing, in: *Encyclopedia of Polymer Science and Technology*, John Wiley & Sons, Inc., 2002. <http://onlinelibrary.wiley.com/doi/10.1002/0471440264.pst101/abstract> (accessed March 31, 2016).
- [14] M.R. Fox, Fixation Processes in Dyeing, *Review of Progress in Coloration and Related Topics*. 4 (1973) 18–37. doi:10.1111/j.1478-4408.1973.tb00200.x.
- [15] M.D. Teli, 4 - Advances in the dyeing and printing of silk A2 - Basu, Arindam, in: *Advances in Silk Science and Technology*, Woodhead Publishing, 2015: pp. 55–79. <http://www.sciencedirect.com/science/article/pii/B9781782423119000045> (accessed March 7, 2016).
- [16] S.W. Lewis, 11 - Analysis of dyes using chromatography A2 - Houck, Max M., in: *Identification of Textile Fibers*, Woodhead Publishing, 2009: pp. 203–223. <http://www.sciencedirect.com/science/article/pii/B9781845692667500118> (accessed March 7, 2016).
- [17] V. Rubeziene, S. Varnaite, J. Baltusnikaite, I. Padleckiene, 6 - Effects of light exposure on textile durability A2 - Annis, Patricia A., in: *Understanding and Improving the Durability of Textiles*, Woodhead Publishing, 2012: pp. 104–125. <http://www.sciencedirect.com/science/article/pii/B9780857090874500068> (accessed November 28, 2016).
- [18] N. Shibayama, M. Wypyski, E. Gagliardi-Mangilli, Analysis of natural dyes and metal threads used in 16th -18th century Persian/Safavid and Indian/Mughal velvets by HPLC-PDA and SEM-EDS to

- investigate the system to differentiate velvets of these two cultures, *Heritage Science*. 3 (2015). doi:10.1186/s40494-015-0037-2.
- [19] I. Degano, E. Ribechini, F. Modugno, M.P. Colombini, *Analytical Methods for the Characterization of Organic Dyes in Artworks and in Historical Textiles*, *Applied Spectroscopy Reviews*. 44 (2009) 363–410. doi:10.1080/05704920902937876.
- [20] M. Járó, *Metal Threads in Historical Textiles*, in: *Molecular and Structural Archaeology: Cosmetic and Therapeutic Chemicals*, Springer, Dordrecht, 2003: pp. 163–178. doi:10.1007/978-94-010-0193-9_15.
- [21] V. Costa, D. de Reyer, M. Betbeder, *A note on the analysis of metal threads*, *Studies in Conservation*. 57 (2012) 112–115. doi:10.1179/2047058412Y.0000000001.
- [22] C.H. Haring, *American Gold and Silver Production in the First Half of the Sixteenth Century*, *The Quarterly Journal of Economics*. 29 (1915) 433–479. doi:10.2307/1885462.
- [23] G.E. Dieter, *Mechanical metallurgy*, New York, McGraw-Hill, 1961. <http://archive.org/details/mechanicalmetall00diet> (accessed July 26, 2019).

Chapter 3.

Silk artificial aging

For several years silk has been a subject of investigation in different fields, initially only as part of the textile industry, later as part of the cultural heritage and more recently as source of new biomaterials. By the special properties of the silk, its behavior has been studied using different objects as a reference. Nevertheless, it is not always possible to obtain direct results from pristine or historical objects, it is necessary to use materials which have been altered in their composition, or properties by different stimuli.

Silk aging is a procedure based essentially on the natural degradation that the material undergoes. In this way, the aging procedures use pristine materials to expose them later to different media. Immersion, bathing, or exposure to different chemical reagents are used to produce oxidation, hydrolysis or chemical transformation on the protein. Changes in temperature, the content of water (controlling the relative humidity), or its exposition to a photo-oxidizing source (by radiation with UV, or UV-Vis light), are as well typical procedures to alter the silk. Although different types of treatments have been reported to modify the molecular structure of the silk protein or its mechanical properties, a standardized operation on which a final degradation stage can be achieved on the material by a controlled medium has not yet been reported. Aging treatments have the objective of mimicking the possible stages of silk alteration, however, none of the procedures reported have been used to completely mimic the natural degradation process that the material undergoes.

The aging processes have been carried out on aging chambers (open reactor) or in closed vials, changing the set-ups and the interval of time in which the pristine silk has been stressed, varying these values according to the investigation goals of each researcher. In the same way, some authors have preferred to start from pristine commercial silk, others follow their own sericulture, and others preferred to extract the silk fiber from the insect glands after performing the aging treatments. It is important to underline that all the changes which the silk in the different alteration operations are not reversible.

Examples of aging are present in the literature. Authors as Nilsson et al. used thermo-oxidation (temperature and oxygen), relative humidity (RH), accelerated ultraviolet (UV) exposure, and immersion in solutions of varied pH for aging silk, to find markers which could be related with for chemical and physical properties on silk from the seventeenth-century [1]. Garside et al. have used aging to understand the behavior of tin-weighted silks [2]. Pawcenis et al. used artificial ageing varying time in 1, 3, 5, 7, 14, 21, 28 and 35 days, to monitor the impact of different exogenous factors on silk textiles [3]. Others as Vilaplana et al. have used aging treatments to compare historical silk and artificially aged silk in different environments [4]. In the same way, some authors have used aging to predict damages on the silk after consolidation treatments as Halvorson and Kerr after the use of Parylene-C [5], or to predict the possible degradation on conservation/exhibition processes as the work of Luxford and Thickett, who searched the effect of light, temperature and relative humidity in historic houses [6].

References

- [1] J. Nilsson, F. Vilaplana, S. Karlsson, J. Bjurman, T. Iversen, The Validation of Artificial Ageing Methods for Silk Textiles Using Markers for Chemical and Physical Properties of Seventeenth-Century Silk, *Studies in Conservation*. 55 (2010) 55–65. doi:10.1179/sic.2010.55.1.55.
- [2] P. Garside, P. Wyeth, X. Zhang, Understanding the ageing behaviour of nineteenth and twentieth century tin-weighted silks, *Journal of the Institute of Conservation*. 33 (2010) 179–193. doi:10.1080/19455224.2010.501293.
- [3] D. Pawcenis, M. Smoleń, M.A. Aksamit-Koperska, T. Łojewski, J. Łojewska, Evaluating the impact of different exogenous factors on silk textiles deterioration with use of size exclusion chromatography, *Appl. Phys. A*. 122 (2016) 576. doi:10.1007/s00339-016-0052-5.
- [4] F. Vilaplana, J. Nilsson, D.V.P. Sommer, S. Karlsson, Analytical markers for silk degradation: comparing historic silk and silk artificially aged in different environments, *Anal Bioanal Chem*. 407 (2014) 1433–1449. doi:10.1007/s00216-014-8361-z.
- [5] B.G. Halvorson, N. Kerr, Effect of light on the properties of silk fabrics coated with parylene-C, *Studies in Conservation*. 39 (1994) 45–56. doi:10.1179/sic.1994.39.1.45.
- [6] N. Luxford, D. Thickett, Designing accelerated ageing experiments to study silk deterioration in historic houses, *Journal of the Institute of Conservation*. 34 (2011) 115–127. doi:10.1080/19455224.2011.581118.

Chapter 4.

Analytical methods on the study of silk

Silk has been the subject of different researches, using different analytical instrumentation in their study. The different analytical tools employed in a research on silk vary depending on the aim of the investigation, being microscopic (optical and electronic), spectroscopic (UV, IR, and Raman), thermogravimetric (DSC, TGA and DTG), and physical-mechanical instrumentation (tensile test) the most employed, due to their useful and fast response after different treatments on the fiber or in different stages of the fibroin. As well, chromatographic, spectrometric, NMR, and other more sophisticated tools as genetic (PCR) instrumentation, are used for more detailed information. The details of each technique will not be discussed on this document, nevertheless, it is suggested to the reader to consult specialized literature to detail the characteristics, uses, and principles of the different analytical techniques.

As any cultural heritage object, the analytical study of silk textiles must be as possible non-invasive, non-destructive, and trying to optimize any measure on the material to extract the biggest amount of information possible from it [1–4]. Nevertheless, it is not possible in all type of researches to execute an in-situ measurement, as due to the own nature of the object, or experimental requirements, or by infrastructure difficulties; being mandatory on those cases to proceed through a strategy which just requires a micro-sample which no will

risk the entire object, on the contrary, the possible results achieved will help to understand the object, and preserve it.

4.1. Microscopy

One of the most relevant information on the analysis of silk is its morphology, and its degradation stage. Through optical microscopy it is possible to characterize the fiber to elucidate if it is natural silk and no other type of fiber. Using an instrument which allows to achieve higher spatial resolution as the scanning electron microscopy, fiber details can be measured on the surface of the fiber, elucidate the species of the insect from which the studied silk comes, as well, show if the fiber has been under a de-gumming process, or if its natural tubular morphology has been transformed, damaged by some kind of degradation, or present irregularities or foreign contaminants over its surface. These techniques are extensively found in silk literature by its functionality, and reduced amount of sample needed, being used almost as a starting point for silk studies [5–11].

4.2. Spectroscopic studies

Due to the proteinaceous nature of silk, it allows to use it as an optimal material to be studied through different spectroscopic techniques, thanks to their interaction with light and its response in different wavelengths.

UV-Vis spectroscopy has been used to study the color, the degradation, as well to identify possible dyes and characterize the dyeing process itself [12–16].

Infrared and Raman spectroscopy are the most widely used spectroscopic techniques on silk, this due to the characteristic spectrum of the

protein and its different conformations (amorphous and crystalline). Since early 1950's, infrared spectroscopy has been employed to investigate silk materials, having an increase in its use over the last 20 years, thanks to new possibilities and advance on detectors, coupling with microscopes, and other technical advances that allow to obtain more reliable results at a more reduced scale. As well, IR instruments with ATR, or polarized accessories are used to explore and explain the different molecular groups of silk materials. In the same way, Raman spectroscopy since the late 1970's has been used to investigate silk, being as well as IR, found with more frequency in the last decade. Silk spectrum describes mainly the chain backbone, the interaction between the N-H group of the grafted amino acids of the same or adjacent chains and the motion of the macromolecule chains, the "lattice" modes. Some of the most characteristic IR and Raman bands are the Amide I mode, which shows a well-defined peak at $\sim 1630\text{-}1670\text{ cm}^{-1}$ (originating from the stretching of the ν C=O bond coupled with the C-N bond); the Amide III mode, which present peaks between 1200 and 1300 cm^{-1} (originating from the ν C-N bond) and the isolated ν N-H stretching vibration mode at $\sim 3285\text{ cm}^{-1}$ which offers a very sensitive tool to probe the short-range environment of the N-H bond, being associated with hydrogen bonds [6]. One interesting topic of IR and Raman spectroscopy is the possibility to study the different possible rearrangement of the secondary structure of the protein by spectral or mathematical deconvolution of the Amide I band [17–22]. Literature exposing the broad possibilities of those techniques on silk are widely found [6,17,23–39].

Another spectroscopic technique used on the silk research is the X-ray diffraction spectroscopy, which has been employed in the investigation mainly

to characterize and quantify the crystalline domains in the silk fibers [5,6,17,18,40].

4.3. Thermogravimetric studies

As silk present different conformations in amorphous and crystalline domains on its structure, and due to the possible rearrangement of it after being subject to, either, physical or chemical stress, thermogravimetric studies have been extensively used to elucidate the possible transformations on the silk as fiber, in solution or as film. As example, authors as Tsukada et al., have studied the thermal behavior of silk to elucidate the structural changes on fibers after a thermal treatment [41], Lee and Ha have used DSC to study the bound water in silk fibroin blend films [42], or Hirabayashi et al. have used DTA to evaluate the degradation of silk fibroin [43].

4.4. Mechanical studies

Mechanical tests have been executed on silk materials in aims to test the mechanical properties of silk and how it changes due to degradation, change of phase, the application of consolidants or by the creation of a new material. Breaking stress, breaking strain, fabric stiffness, among other test are applied on fibers, films or fabrics, relating the numerical results with the silk molecular composition. Authors as Huang et al. have shown how the tensile properties of silk are improved through the combination of it with epoxide-ethylene glycol diglycidyl ether [24]. Pérez-Rigueiro et al. have used the tensile test to proof how change the tensile properties of silkworm after de-gumming processes [44], and others as Colombari et al. have found through tensile test the

variability in mechanical behavior of various silks obtained from silkworm, finding five characteristic groups [45].

4.5. Chromatographic studies

Chromatography studies on silk have been performed to answer to questions on nature of dyes used to color the fibers, and to study the amino acid composition of the material and relate it with a possible stage of degradation. Ion chromatography, HPLC, and exclusion size chromatography are the most used techniques on silk research [10,13,29,46–53]

4.6. Elemental studies

Studies related to silk directly or indirectly (as in the case of the study of decorations) use another type of analytical tools, as the ICP, AAS, or EDS to characterize those inorganic elements present in the material and evaluate its possible effect on the silk object [48,54–59].

References

- [1] A.M. Pollard, *Analytical Chemistry in Archaeology*, Cambridge University Press, Cambridge ; New York, 2007.
- [2] J.M. Madariaga, *Analytical chemistry in the field of cultural heritage*, *Anal. Methods*. 7 (2015) 4848–4876. doi:10.1039/C5AY00072F.
- [3] M.E. King, *Analytical Methods and Prehistoric Textiles*, *American Antiquity*. 43 (1978) 89–96. doi:10.2307/279636.
- [4] D.A. Doménech-Carbó, P.D.M.T. Doménech-Carbó, P.D.V. Costa, *Application of Instrumental Methods in the Analysis of Historic, Artistic and Archaeological Objects*, in: D.A. Doménech-Carbó, P.D.M.T. Doménech-Carbó, P.D.V. Costa (Eds.), *Electrochemical Methods in Archaeometry, Conservation and Restoration*, Springer Berlin Heidelberg, 2009: pp. 1–32. http://link.springer.com.biblioteca.uniandes.edu.co:8080/chapter/10.1007/978-3-540-92868-3_1 (accessed February 17, 2013).
- [5] S.K. Vyas, S.R. Shukla, *Comparative study of degumming of silk varieties by different techniques*, *The Journal of The Textile Institute*. 107 (2016) 191–199. doi:10.1080/00405000.2015.1020670.
- [6] P. Colombari, V. Jauzein, 5 - *Silk: Fibers, films, and composites—types, processing, structure, and mechanics*, in: A.R. Bunsell (Ed.), *Handbook of Properties of Textile and Technical Fibres (Second Edition)*, Woodhead Publishing, 2018: pp. 137–183. doi:10.1016/B978-0-08-101272-7.00005-5.
- [7] F. Vollrath, D. Porter, C. Dicko, 5 - *The structure of silk*, in: *Handbook of Textile Fibre Structure*, Woodhead Publishing, 2009: pp. 146–198. [//www.sciencedirect.com/science/article/pii/B9781845697303500056](http://www.sciencedirect.com/science/article/pii/B9781845697303500056) (accessed January 26, 2017).
- [8] P.H. Greaves, 10 - *Alternative and specialised textile fibre identification tests A2 - Houck, Max M.*, in: *Identification of Textile Fibers*, Woodhead Publishing, 2009: pp. 181–202. <http://www.sciencedirect.com/science/article/pii/B9781845692667500106> (accessed March 7, 2016).
- [9] Z. Wu, D. Huang, Z. Hu, Y. Zhou, F. Zhao, Z. Peng, B. Wang, *A new consolidation system for aged silk fabrics: Interaction between ethylene glycol diglycidyl ether, silk Fibroin and Artificial Aged Silk Fabrics*, *Fibers Polym.* 15 (2014) 1146–1152. doi:10.1007/s12221-014-1146-3.
- [10] J. Liu, D. Guo, Y. Zhou, Z. Wu, W. Li, F. Zhao, X. Zheng, *Identification of ancient textiles from Yingpan, Xinjiang, by multiple analytical techniques*, *Journal of Archaeological Science*. 38 (2011) 1763–1770. doi:10.1016/j.jas.2011.03.017.
- [11] Y. Xia, X. Lu, H. Zhu, *Natural silk fibroin/polyaniline (core/shell) coaxial fiber: Fabrication and application for cell proliferation*, *Composites Science and Technology*. 77 (2013) 37–41. doi:10.1016/j.compscitech.2013.01.008.
- [12] C. Septhum, S. Rattanaphani, J.B. Bremner, V. Rattanaphani, *An adsorption study of alum-morin dyeing onto silk yarn*, *Fibers Polym.* 10 (2009) 481–487. doi:10.1007/s12221-009-0481-2.
- [13] M. Ma, M. Hussain, S. Dong, W. Zhou, *Characterization of the pigment in naturally yellow-colored domestic silk*, *Dyes and Pigments*. 124 (2016) 6–11. doi:10.1016/j.dyepig.2015.08.003.
- [14] L.G. Angelini, S. Tozzi, S. Bracci, F. Quercioli, B. Radicati, M. Picollo, *Characterization of Traditional Dyes of the Mediterranean Area by Non-Invasive Uv-Vis-Nir Reflectance Spectroscopy*, *Studies in Conservation*. 55 (2010) 184–189. doi:10.1179/sic.2010.55.Supplement-2.184.
- [15] M.A. Becker, N. Tuross, *Initial Degradative Changes Found in Bombyx mori Silk Fibroin*, in: *Silk Polymers*, American Chemical Society, 1993: pp. 252–269. doi:10.1021/bk-1994-0544.ch022.
- [16] A.-M. Hacke, C.M. Carr, A. Brown, D. Howell, *Investigation into the nature of metal threads in a Renaissance tapestry and the cleaning of tarnished silver by UV/Ozone (UVO) treatment*, *Journal of Materials Science*. 38 (2003) 3307–3314. doi:10.1023/A:1025146207048.
- [17] X. Hu, D. Kaplan, P. Cebe, *Determining Beta-Sheet Crystallinity in Fibrous Proteins by Thermal Analysis and Infrared Spectroscopy*, *Macromolecules*. 39 (2006) 6161–6170. doi:10.1021/ma0610109.
- [18] F. Cilurzo, C.G.M. Gennari, F. Selmin, L.A. Marotta, P. Minghetti, L. Montanari, *An investigation into silk fibroin conformation in composite materials intended for drug delivery*, *International Journal of Pharmaceutics*. 414 (2011) 218–224. doi:10.1016/j.ijpharm.2011.05.023.

- [19] G. Vedantham, H.G. Sparks, S.U. Sane, S. Tzannis, T.M. Przybycien, A Holistic Approach for Protein Secondary Structure Estimation from Infrared Spectra in H₂O Solutions, *Analytical Biochemistry*. 285 (2000) 33–49. doi:10.1006/abio.2000.4744.
- [20] H. Susi, D.M. Byler, Fourier Deconvolution of the Amide I Raman Band of Proteins as Related to Conformation, *Appl. Spectrosc.*, AS. 42 (1988) 819–826.
- [21] K. Rahmelow, W. Hübner, Fourier Self-Deconvolution: Parameter Determination and Analytical Band Shapes, *Applied Spectroscopy*. 50 (1996) 795–804. doi:10.1366/0003702963905682.
- [22] S. Wi, P. Pancoska, T.A. Keiderling, Predictions of protein secondary structures using factor analysis on Fourier transform infrared spectra: Effect of Fourier self-deconvolution of the amide I and amide II bands, *Biospectroscopy*. 4 (1998) 93–106. doi:10.1002/(SICI)1520-6343(1998)4:2<93::AID-BSPY2>3.0.CO;2-T.
- [23] V. Jauzein, P. Colomban, 6 - Types, structure and mechanical properties of silk, in: A.R. Bunsell (Ed.), *Handbook of Tensile Properties of Textile and Technical Fibres*, Woodhead Publishing, 2009: pp. 144–178. //www.sciencedirect.com/science/article/pii/B9781845693879500060 (accessed January 26, 2017).
- [24] D. Huang, Z. Peng, Z. Hu, S. Zhang, J. He, L. Cao, Y. Zhou, F. Zhao, A new consolidation system for aged silk fabrics: Effect of reactive epoxide-ethylene glycol diglycidyl ether, *Reactive and Functional Polymers*. 73 (2013) 168–174. doi:10.1016/j.reactfunctpolym.2012.08.019.
- [25] H. Teramoto, M. Miyazawa, Analysis of Structural Properties and Formation of Sericin Fiber by Infrared Spectroscopy, *Journal of Insect Biotechnology and Sericology*. 72 (2003) 157–162. doi:10.11416/jibs.72.157.
- [26] M.J. Smith, K. Thompson, E. Hermens, Breaking down banners: analytical approaches to determining the materials of painted banners, *Heritage Science*. 4 (2016) 23. doi:10.1186/s40494-016-0095-0.
- [27] D. Chelazzi, A. Chevalier, G. Pizzorusso, R. Giorgi, M. Menu, P. Baglioni, Characterization and degradation of poly(vinyl acetate)-based adhesives for canvas paintings, *Polymer Degradation and Stability*. 107 (2014) 314–320. doi:10.1016/j.polymdegradstab.2013.12.028.
- [28] A. Kljun, T.A.S. Benians, F. Goubet, F. Meulewaeter, J.P. Knox, R.S. Blackburn, Comparative Analysis of Crystallinity Changes in Cellulose I Polymers Using ATR-FTIR, X-ray Diffraction, and Carbohydrate-Binding Module Probes, *Biomacromolecules*. 12 (2011) 4121–4126. doi:10.1021/bm201176m.
- [29] P. Garside, P. Wyeth, Crystallinity and degradation of silk: correlations between analytical signatures and physical condition on ageing, *Appl. Phys. A*. 89 (2007) 871–876. doi:10.1007/s00339-007-4218-z.
- [30] M.A. Koperska, D. Pawcenis, J. Bagniuk, M.M. Zaitz, M. Missori, T. Łojewski, J. Łojewska, Degradation markers of fibroin in silk through infrared spectroscopy, *Polymer Degradation and Stability*. 105 (2014) 185–196. doi:10.1016/j.polymdegradstab.2014.04.008.
- [31] X. Hu, D. Kaplan, P. Cebe, Dynamic Protein–Water Relationships during β -Sheet Formation, *Macromolecules*. 41 (2008) 3939–3948. doi:10.1021/ma071551d.
- [32] C. Mo, P. Wu, X. Chen, Z. Shao, Near-Infrared Characterization on the Secondary Structure of Regenerated Bombyx Mori Silk Fibroin, *Applied Spectroscopy*. 60 (2006) 1438–1441. doi:10.1366/000370206779321355.
- [33] S. Prati, E. Joseph, G. Sciutto, R. Mazzeo, New Advances in the Application of FTIR Microscopy and Spectroscopy for the Characterization of Artistic Materials, *Acc. Chem. Res.* 43 (2010) 792–801. doi:10.1021/ar900274f.
- [34] J. Magoshi, M. Mizuide, Y. Magoshi, K. Takahashi, M. Kubo, S. Nakamura, Physical properties and structure of silk. VI. Conformational changes in silk fibroin induced by immersion in water at 2 to 130°C, *Journal of Polymer Science: Polymer Physics Edition*. 17 (1979) 515–520. doi:10.1002/pol.1979.180170315.
- [35] Ph. Colomban, G. Gouadec, Raman and IR micro-analysis of high performance polymer fibres tested in traction and compression, *Composites Science and Technology*. 69 (2009) 10–16. doi:10.1016/j.compscitech.2007.10.034.

- [36] J. Ming, B. Zuo, Silk I structure formation through silk fibroin self-assembly, *J. Appl. Polym. Sci.* 125 (2012) 2148–2154. doi:10.1002/app.36354.
- [37] Y. Hu, Q. Zhang, R. You, L. Wang, M. Li, The Relationship between Secondary Structure and Biodegradation Behavior of Silk Fibroin Scaffolds, *Advances in Materials Science and Engineering*. 2012 (2012) e185905. doi:10.1155/2012/185905.
- [38] P. Monti, G. Freddi, C. Arosio, M. Tsukada, T. Arai, P. Taddei, Vibrational spectroscopic study of sulphated silk proteins, *Journal of Molecular Structure*. 834–836 (2007) 202–206. doi:10.1016/j.molstruc.2006.11.009.
- [39] S. Ling, Z. Qi, D.P. Knight, Z. Shao, X. Chen, Synchrotron FTIR Microspectroscopy of Single Natural Silk Fibers, *Biomacromolecules*. 12 (2011) 3344–3349. doi:10.1021/bm2006032.
- [40] M. Ballard, R.J. Koestler, C. Blair, N. Indictor, Historical Silk Flags Studied by Scanning Electron Microscopy-Energy Dispersive X-ray Spectrometry, in: *Archaeological Chemistry IV*, American Chemical Society, 1989: pp. 419–428. <http://dx.doi.org/10.1021/ba-1988-0220.ch024> (accessed November 29, 2016).
- [41] M. Tsukada, G. Freddi, M. Nagura, H. Ishikawa, N. Kasai, Structural changes of silk fibers induced by heat treatment, *Journal of Applied Polymer Science*. 46 (1992) 1945–1953. doi:10.1002/app.1992.070461107.
- [42] K.Y. Lee, W.S. Ha, DSC studies on bound water in silk fibroin/S-carboxymethyl keratine blend films, *Polymer*. 40 (1999) 4131–4134. doi:10.1016/S0032-3861(98)00611-9.
- [43] K. Hirabayashi, Y. Yanagi, S. Kawakami, K. Okuyama, W. Hu, Degradation of silk fibroin, *The Journal of Sericultural Science of Japan*. 56 (1987) 18–22. doi:10.11416/kontyushigen1930.56.18.
- [44] J. Pérez-Rigueiro, M. Elices, J. Llorca, C. Viney, Effect of degumming on the tensile properties of silkworm (*Bombyx mori*) silk fiber, *Journal of Applied Polymer Science*. 84 (n.d.) 1431–1437. doi:10.1002/app.10366.
- [45] P. Colombari, H.M. Dinh, A. Bunsell, B. Mauchamp, Origin of the variability of the mechanical properties of silk fibres: 1 - The relationship between disorder, hydration and stress/strain behaviour, *Journal of Raman Spectroscopy*. 43 (2012) 425–432. doi:10.1002/jrs.3044.
- [46] S. Inoue, K. Tanaka, F. Arisaka, S. Kimura, K. Ohtomo, S. Mizuno, Silk Fibroin of *Bombyx mori* Is Secreted, Assembling a High Molecular Mass Elementary Unit Consisting of H-chain, L-chain, and P25, with a 6:6:1 Molar Ratio, *J. Biol. Chem.* 275 (2000) 40517–40528. doi:10.1074/jbc.M006897200.
- [47] N. Shibayama, M. Wypyski, E. Gagliardi-Mangilli, Analysis of natural dyes and metal threads used in 16th -18th century Persian/Safavid and Indian/Mughal velvets by HPLC-PDA and SEM-EDS to investigate the system to differentiate velvets of these two cultures, *Heritage Science*. 3 (2015). doi:10.1186/s40494-015-0037-2.
- [48] J. Nilsson, F. Vilaplana, S. Karlsson, J. Bjurman, T. Iversen, The Validation of Artificial Ageing Methods for Silk Textiles Using Markers for Chemical and Physical Properties of Seventeenth-Century Silk, *Studies in Conservation*. 55 (2010) 55–65. doi:10.1179/sic.2010.55.1.55.
- [49] D. Pawcenis, M. Smoleń, M.A. Aksamit-Koperska, T. Łojewski, J. Łojewska, Evaluating the impact of different exogenous factors on silk textiles deterioration with use of size exclusion chromatography, *Appl. Phys. A*. 122 (2016) 576. doi:10.1007/s00339-016-0052-5.
- [50] X. Zhang, I. Good, R. Laursen, Characterization of dyestuffs in ancient textiles from Xinjiang, *Journal of Archaeological Science*. 35 (2008) 1095–1103. doi:10.1016/j.jas.2007.08.001.
- [51] I. Petroviciu, F. Albu, A. Medvedovici, LC/MS and LC/MS/MS based protocol for identification of dyes in historic textiles, *Microchemical Journal*. 95 (2010) 247–254. doi:10.1016/j.microc.2009.12.009.
- [52] I. Degano, M. Biesaga, M.P. Colombini, M. Trojanowicz, Historical and archaeological textiles: An insight on degradation products of wool and silk yarns, *Journal of Chromatography A*. 1218 (2011) 5837–5847. doi:10.1016/j.chroma.2011.06.095.
- [53] D. Pawcenis, M.A. Koperska, J.M. Milczarek, T. Łojewski, J. Łojewska, Size exclusion chromatography for analyses of fibroin in silk: optimization of sampling and separation conditions, *Appl. Phys. A*. 114 (2014) 301–308. doi:10.1007/s00339-013-8143-z.

PART I. INTRODUCTION

- [54] P. Garside, P. Wyeth, X. Zhang, Understanding the ageing behaviour of nineteenth and twentieth century tin-weighted silks, *Journal of the Institute of Conservation*. 33 (2010) 179–193. doi:10.1080/19455224.2010.501293.
- [55] A.F. Cakir, G. Simsek, H. Tezcan, Characterisation of gold gilt silver wires from five embroidered silk Qaaba curtains dated between the 16th and 19th centuries, *Appl. Phys. A*. 83 (2006) 503–511. doi:10.1007/s00339-006-3527-y.
- [56] A. Manhita, T. Ferreira, A. Candeias, C.B. Dias, Extracting natural dyes from wool--an evaluation of extraction methods, *Anal Bioanal Chem*. 400 (2011) 1501–1514. doi:10.1007/s00216-011-4858-x.
- [57] M. Wojcieszak, A. Percot, S. Noinville, G. Gouadec, B. Mauchamp, P. Colomban, Origin of the variability of the mechanical properties of silk fibers: 4. Order/crystallinity along silkworm and spider fibers, *Journal of Raman Spectroscopy*. 45 (2014) 895–902. doi:10.1002/jrs.4579.
- [58] D. Kaplan, W.W. Adams, B. Farmer, and C. Viney (Eds.), *Silk Polymers*. Materials Science and Biotechnology, American Chemical Society, 1994. <http://gen.lib.rus.ec/book/index.php?md5=46294b434882f15d3cec192f62b11d22>.
- [59] I. Rezić, L. Čurković, M. Ujević, Simple methods for characterization of metals in historical textile threads, *Talanta*. 82 (2010) 237–244. doi:10.1016/j.talanta.2010.04.028.

Chapter 5.

Silk restoration and conservation

Silk as a valuable object, part of the material cultural heritage and susceptible to degradation by its nature, is studied to prevent its damage, which could lead to its disappearing, trying to find reliable methods which allow to protect the material for future generations. For the preservation of textile silk materials (as it is for all kind of historical/archaeological or artistic objects), two types of interventions must be carried out. One is the so-called preventive conservation, which is based to ensure that the object will be maintain in suitable environments for their long-term survival (climate control, light exposition, etc.). The other type of intervention is the conservation, which aims to remedy or ameliorate the effects of deterioration occurred in the past. Conservation treatments for textiles include: cleaning, deacidification; reshaping, support, stitching; immediate pest control, and mounting (over an appropriate structure or frame) for exhibition or storage [1]. It is well established that any intervention held on a historical object, must be reversible, detectable and of course does not produce further damage, at the same time, it is desirable that these processes do not involve the replacement of missing areas of fabric, renewing faded or fugitive dyes, restoring lost function or otherwise modifying the object beyond what is required to stabilize it and minimize the rate of future deterioration [1,2].

As main basis of the different silk conservation studies, as with any archaeological/artistic object, a material characterization must be performed

[3], where through scientific measurements the textile is inspected, knowing in this way, first of all the type of fiber (which is the nature of the fiber, which kind of insect produced it, which kind of weaving was executed, etc.), then, if treatments on its production were executed (de-gumming, dyeing, bleaching, etc.), and finally, if exogenous components have been introduced (mordants, weighing, etc.). After having characterized the fiber, in order to have a full view of the degradation stage of the material and how to treat it in the best way, deeper studies looking at its molecular degradation stage can be carried out. However, this rational is a modern perspective on how to perform a conservation procedure, this being not the rule in the past.

In the past, procedures for the restoration of silk textiles have been executed mainly in an attempt to preserve the object, not always being studied the object from a scientific point of view. The procedures were pointed mainly in two ways: one, to preserve the style, shape or beauty of the object; or second, to maintain the weaving of the fabric. The first procedure follows a technique where is replaced the old-damaged fibers with new fibers, weaving again the object by textile conservators' experts, using materials with the same color and texture than the old object [4]. This procedure has been extensively used on different textile objects since older times. Nevertheless, this procedure replaces all the old material, letting as result an object which has lost information from the past, being only noticeable the modern procedures from the last decades (by the way how is re-woven), but no those performed in previous centuries.

The second procedure follows the application of different materials to the textile to held together the fabric. Weaving crepe silk textile on the back of the fabric where gaps or cuts have appeared is a usual external material added, but any repair is done, neither is prevented a future damage, or stopped the

natural degradation on the material [5], this procedure also known as “mounting”, supports the fragile textile to a more perdurable support, as could be a polymeric one or a silk, nylon or polyester net [6,7] by stitching. Another procedure extensively used is the coating with polymers, where a thick layer of polymer is placed over-around the fabric, as the case of parylene-C [8,9], being this process almost irreversible and producing problems from the own polymer degradation. Use of adhesives has been also employed, using copolymers which could be used in cold-lining, or as well as thermoplastic adhesives, being added to the textile through heating it on a hot table [10–12].

Knowing the difficulty on preserving silk textile materials, in the recent years different researchers have proposed different new-materials to held this operation. Consolidation using bacterial cellulose [13], ethylene glycol diglycidyl ether [14], or epoxide-ethylene glycol diglycidyl ether [15], are some examples.

References

- [1] P. Garside, 10 - Durability of historic textiles A2 - Annis, Patricia A., in: *Understanding and Improving the Durability of Textiles*, Woodhead Publishing, 2012: pp. 184–204. <http://www.sciencedirect.com/science/article/pii/B978085709087450010X> (accessed March 7, 2016).
- [2] N. Luxford, 11 - Silk durability and degradation A2 - Annis, Patricia A., in: *Understanding and Improving the Durability of Textiles*, Woodhead Publishing, 2012: pp. 205–232. <http://www.sciencedirect.com/science/article/pii/B9780857090874500111> (accessed November 28, 2016).
- [3] A.M. Pollard, C.M. Batt, B. Stern, S.M.M. Young, *Analytical Chemistry in Archaeology* by A. M. Pollard, Cambridge Core. (2007). doi:10.1017/CBO9780511607431.
- [4] I. Vanden Berghe, Towards an early warning system for oxidative degradation of protein fibres in historical tapestries by means of calibrated amino acid analysis, *J. Archaeol. Sci.* 39 (2012) 1349–1359. doi:10.1016/j.jas.2011.12.033.
- [5] P. Orlofsky, M. Kaldany, Henri Matisse’s Silkscreen on Linen Editions Océanie, Le Ciel and La Mer, 1946–1949: Development of a Conservation Protocol, *Journal of the American Institute for Conservation.* 53 (2014) 252–274. doi:10.1179/1945233014Y.0000000028.
- [6] J.B. Perjés, K.E. Nagy, M. Tóth, *Conserving Textiles Studies in honour of Ágnes Timár-Balázszy*, ICCROM Conservation Studies 7, ICCROM, Italy, 2009.
- [7] P. Garside, 16 - The role of fibre identification in textile conservation A2 - Houck, Max M., in: *Identification of Textile Fibers*, Woodhead Publishing, 2009: pp. 335–365. <http://www.sciencedirect.com/science/article/pii/B9781845692667500167> (accessed March 7, 2016).
- [8] B.G. Halvorson, N. Kerr, Effect of light on the properties of silk fabrics coated with parylene-C, *Studies in Conservation.* 39 (1994) 45–56. doi:10.1179/sic.1994.39.1.45.
- [9] E.F. Hansen, W.S. Ginell, The Conservation of Silk with Parylene-C, in: *Historic Textile and Paper Materials II*, American Chemical Society, 1989: pp. 108–133. doi:10.1021/bk-1989-0410.ch008.
- [10] L. Hillyer, Z. Tinker, P. Singer, Evaluating the use of adhesives in textile conservation: Part I: An overview and surveys of current use, *The Conservator.* 21 (1997) 37–47. doi:10.1080/01410096.1997.9995114.
- [11] B. Pretzel, Evaluating the use of adhesives in textile conservation Part II: Tests and evaluation matrix, *The Conservator.* 21 (1997) 48–58. doi:10.1080/01410096.1997.9995115.
- [12] History, Technology, and Treatment of a Painted Silk Folding Screen Belonging to the Palace-Museum of Golestan in Iran — *Fibres & Textiles in Eastern Europe*, (n.d.). <http://www.fibtex.lodz.pl/article1265.html> (accessed November 22, 2016).
- [13] S.-Q. Wu, M.-Y. Li, B.-S. Fang, H. Tong, Reinforcement of vulnerable historic silk fabrics with bacterial cellulose film and its light aging behavior, *Carbohydrate Polymers.* 88 (2012) 496–501. doi:10.1016/j.carbpol.2011.12.033.
- [14] Z. Wu, D. Huang, Z. Hu, Y. Zhou, F. Zhao, Z. Peng, B. Wang, A new consolidation system for aged silk fabrics: Interaction between ethylene glycol diglycidyl ether, silk Fibroin and Artificial Aged Silk Fabrics, *Fibers Polym.* 15 (2014) 1146–1152. doi:10.1007/s12221-014-1146-3.
- [15] D. Huang, Z. Peng, Z. Hu, S. Zhang, J. He, L. Cao, Y. Zhou, F. Zhao, A new consolidation system for aged silk fabrics: Effect of reactive epoxide-ethylene glycol diglycidyl ether, *Reactive and Functional Polymers.* 73 (2013) 168–174. doi:10.1016/j.reactfunctpolym.2012.08.019.

Chapter 6.

Historical flags and emblems of the National Museum of Colombia

To execute a research of silk as textile material, where is aimed to understand how it evolves, or how it is their natural degradation process (i.e. how is transformed through time, in the long term, the material by the impact of light, humidity, changes of temperature, bio-attack, use, etc.), it is necessary to guaranty a set of samples which have suffered a natural transformation without an intentional stress, (no artificially aged). The best option is to use historical/archaeological samples, because of their long age, and their naturally altered. Nevertheless, to find a set of objects which guaranties a comparison among them, is not simple, mainly by two reasons: first, textile historical/archaeological samples are difficult to find, being the cultural heritage objects in less proportion of all collections, having an increased value (not only economically, but also culturally), which makes difficult to scientist, and others researchers to access to them; and second, because each object has a unique history, related to its manufacture, use, and preservation stage.

objects are made of silk of different colors, mainly in three colors, red, blue and yellow, and some present the use of metals as decorations.

To study the different objects offered by the Museum, a sampling protocol was developed, which was agreed with the National Museum of Colombia. The protocol and the final agreement are annexed in Appendix 2. Following the sampling protocol, the team of the conservation department of the museum in Bogotá (Colombia) extracted a set of micro-samples from each object, varying the final number of samples depending on the different components present in each textile, arriving to a total of 378 micro samples, which varies in weight around 10 mg the textile samples, and around 20 mg for samples with metals. Each micro-sample was labeled and individually packed to finally been delivered to the Università degli Studi di Firenze, by international mail. At the samples' arrival, each sample was documented to facilitate future inspections on the sample, avoiding their over-handling which could put on risk the micro samples.

The set of objects studied comprise textiles with heraldic symbols from Spain (military and civil), as well as from the new nations which born in the north Andean region of South America in the 19th century. In the next lines, the textile objects will be described for a better understanding of the reader about these historical objects.

6.1. 16th century

From the 16th century survives at the textile collection of the National Museum of Colombia two objects, which were used by the Spaniards during the colony of America. The older is a rectangular tapestry (register number 3305) with a natural design in different colors, which was used by Fray Domingo de las

Casas as decoration for the first catholic mass ceremony on 1538, during the foundation of the new colonial city in America: Santafé; on what is now known as Bogotá (Colombia). The second object is an embroidered coat of arms of large dimensions (register number 97), finely decorated with metallic threads, which presents the full heraldic symbols of King Felipe II of Spain, this object which was emplaced in the Royal Audience of Santafé building, possibly over another textile (disappeared at the present), served as a symbol for the institution where was imparted justice, and as a chancellery later at name of the Spanish kingdom in America, for the region of what is nowadays known as Colombia, Venezuela, and Guyana. Those two objects if well were located in America, it is well known that their manufacture was European according to the history of textile industry, in special the silk one, as well by the kind of technology employed which is different from those used by the native Americans before the arrival of the Europeans.

6.2. 18th century

From the 18th century, three objects were investigated. The first is a large red textile flag (register number 99), embroidered with the Carlos III of Spain coat of arms, surrounded by cannons, the pillars of Hercules and the “Non plus ultra” inscription, doing reference to the new world (America) and possibly being part of a Royal military group, this flag was captured in the 19th century in the revolution process for America’s independence. The second object is a red “V” shape flag, embroidered with the simplified Royal coat of arms of Spain (register number 116), composed by the symbols of Castilla and Leon, the Borbon and Granada, surrounded by decorative flags and cannonballs. The third is a red rectangular flag with the coat of arms of Carlos IV of Spain, surrounded

with the pillars of Hercules, flags, cannons, and a text which claims for the King. This last textile, contrary to the first one of this frame of time, does not present any embroidery, being all the decorations painted on top of the textile.

6.3. 19th century

Thanks to the National Museum of Colombia, which have kept and protect different objects that have marked the Latin-American and especially the Colombian history through time, we have a large set of objects to study in this important century. 19th century in the Latin American context is full of changes, the society passes from a colony to become independent republics, the industrialization starts, and different conflicts/wars are held on the new nations. This period of time offers to us the biggest number of objects studied in this research, 26 in total, which can be divided into two, one as the Europeans and a second as the American.

6.3.1 European iconography

From this period of time, eight objects were used for this research. Three textiles which can be related to political or civilian Spanish use, two from 1808 and one from 1815. Five textiles related with the military units sent to America to fight the revolution against the Spanish Crown, two from 1813, two from 1815 and one from 1824. The three political flags correspond to one red and two white “V” shape flags, the red one (register number 117) has lost its coat of arms, meanwhile, extra decorations painted remains. The older white flag (register number 118) preserved its embroidered coat of arms with the simplified Royal coat of arms of Spain, similar to those used in the past, nevertheless, its elegance is markedly decreased compared with those of previous time, at the same time, the younger white flag presents a painted

decoration with the symbols of the coat of arms of Spain as used by Fernando VI, till Fernando VII (1746-1808). The military flags correspond to five white flags captured during the revolution process (register numbers 100, 101, 102, 103, 104), each one of the textiles presents decorations which represents the type of the army and their provenance. All of the five textiles have embroidery and metal decorations as part of their decoration.

6.3.2. American iconography

A total of 18 textile flags and coat of arms framed in the years 1823 till 1899 are studied in this period (register numbers 105, 106, 107, 108, 110, 111, 112, 113, 114, 122, 124, 129, 131, 1948, 3044, 3245, 3615, 6079). Ten of them were made for a military purpose, and 8 to a political or civil purpose. Almost all flags have in common the use of the colors yellow, blue and red in a horizontal way, changing on some of them the color order or the width of each color band, meanwhile the coat of arms follow the iconography of the Colombian one, with exception with one object which is the Arequipa coat of arms.

These textile objects are historical proof of how the independent populations after the revolution in America started to establish new countries, with different political systems, trying to find ideas which link them as a nation. These flags show the evolution of the different military/political groups and the resultant nations, as for example, the flag created in 1819 for the republic of “La Gran Colombia” which uses three horizontal bands, each one with the same width, one yellow, one blue and one red, representing the union of the nations of what is nowadays known as Colombia, Panama, Venezuela, Ecuador and part of the north of Peru. In the same way, the flag of the resultant country after the division of the “La Gran Colombia” in 1831, the “Republic of the New Grenade”,

which used the same tricolor flag but in an inverted distribution of the colors. As well flags which represent the population who preferred a federal political system are present, as those of the regional groups which fight on civil wars for their territory, or the flag of the resultant federal country known as “The United States of Colombia” in 1861, formed by actual Colombia, Panama and some parts of North Peru and West Brazil.

6.4. 20th century

Four textile objects were selected from the 20th century for this research, two flags corresponding to the Republic of Colombia (register number 7354 and 126) from 1900 and 1929, one coat of arms with the symbols of Colombia (register number 125) from 1932, and one final flag which corresponds to the Venezuelan flag (register number 120) from 1901. The flags from Colombia and Venezuela use the same colors and in the same distribution, yellow, blue and red in a pattern of twice the width of the first band by one by the second and the third.

6.5. 21st century

In aims to have a starting point on the possible changes that could suffer the silk and have a reference material to execute clear comparisons with historical silk materials, pristine non-dyed *Bombyx mori* silk textiles waved with different densities were acquired on the textile commercial market in Florence and used as a reference for this research. Physicochemical characteristics for the pristine silk was used as the starting stage for the material, in other words, as time zero for possible changes or degradation.

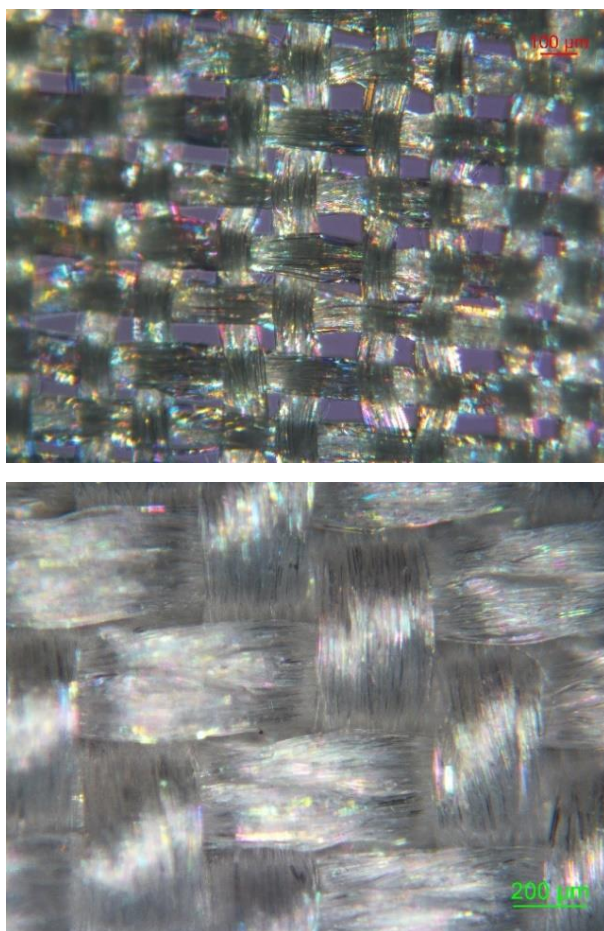


Figure 2 Microphotography of pristine silk at 20X. Top panel: Low-density silk (Georgette). Bottom panel: High-density silk (Taffeta)

PART II.
STUDY OF METALS AND DYES AS
DECORATION OF SILK TEXTILES

Chapter 7.

Microanalytical study of the evolution of metals used as decorations on Spanish and Latin-American flags textiles from 16-20th-century preserved at the textile collection of the National Museum of Colombia

Abstract

Metals have been used in textile manufacture as part of the textile decorations for centuries on diverse cultures. Textile emblems and flags are common objects where metal decorations are regularly found. After 15th century with the arrival of the Europeans in America the use of flags and emblems was introduced. Some of those textile objects considered part of the Latin American cultural heritage is kept as historical record at the textile collection of the National Museum of Colombia. Following a microanalytical study over a large set of micro samples coming from twenty flags of the textile collection of the National Museum of Colombia, which covers a frame time since 16th century till 20th century, metal decorations were investigated to

Chapter 7. Microanalytical study of the evolution of metals used as decorations on Spanish and Latin-American flags textiles from 16-20th-century preserved at the textile collection of the National Museum of Colombia

characterize them both in their material composition, as in their manufacture style. Optical microscopy, Scanning Electron Microscopy with Energy Dispersive Spectroscopy, Inductively Coupled Plasma coupled to Optical Emission Spectroscopy and Multicollector Inductively Coupled Plasma coupled to Mass Spectrometry were used. Results allowed to evidence patterns between flags, understand the provenance of the silver used, and the evolution of this decorative element on this kind of artifacts on the evolution of time.

7.1. Introduction

The international exchange of resources and its development after the arrival of Christopher Columbus to America in 1492 is today an open field for discussion and research in different disciplines, being a topic of special interest the trade of minerals and metals after the meet of the two civilizations. The impact in the daily life of both, Americans and Europeans inhabitants [1–5], created a phenomenon of exchange not only of the resources but also of ideas, technologies, and techniques, which will change both worlds [2,5,6].

Metals can be found in several kinds of artifacts, used as pure metal [7], in composite materials (as layers of different metals for example) [8] or in alloys [9], each with a specific manufacturing technique and technology, which can be associated with a time frame and the community on which was created [10–12]. Metals, such as gold, copper and silver are special elements, have been classified throughout history as objects of great value based on their use, opportunity for exchange, availability or representativeness of the social status, in relation to their use or accumulation with wealth, deities, and power, as well being used as basis for economic trades, or payment reference (coins/money) [13,14].

One interesting case of study is to investigate their use as metal decoration on textiles, because it is possible to obtain a deeper knowledge of the society related, depending on the culture and age in which it was employed, as for example, from Europe to Asia since the first millennium BC, where their use was mainly as metallic embroidery threads i.e. as metal threads, stripes, paillettes or wires of millimetric dimensions; used not only to embellish several kind of artifacts, as ecclesiastical as well as on secular vestments, on different

Chapter 7. Microanalytical study of the evolution of metals used as decorations on Spanish and Latin-American flags textiles from 16-20th-century preserved at the textile collection of the National Museum of Colombia

accessories like gloves, shoes, headdresses, or even on other objects like hangings, carpets, etc. [15], but also to create full vests as in the case of medieval armors [16]. In contrast, in the pre-Hispanic Americas, archaeological finds describe the use of metallic decorations not only as a material used to finish a textile, but also as a full garment itself, i.e. large dimensions body accessories, masks, crowns, etc. [17,18].

Studies of metals as decorative items on textiles have been of particular interest due to the possibility to relate those with a possible location and/or period of textile manufacture, according to the technique and raw materials found on its making [19,20]. Analytical studies have been focused on the characterization of the metal decoration and its respective stylistic classification. Optical Microscopy (OM) has been used as a first approach to analyze this kind of material, giving the possibility to classify the object as wire, metal thread, stripe, etc. and to give the first clue about its manufacture technique [21,22]. Scanning Electron Microscopy coupled to Energy Dispersive Spectroscopy (SEM-EDS) analysis has been used to characterize the morphology, degradation, presence of pollutants, combination/distribution of materials in the manufacture of the metal decorations, as well to clarify the presence/type or not of internal fibers [23–26]. X-Ray Fluorescence (XRF) analysis has been employed to characterize the elemental composition of the metals, similar to EDS [25]. Ion Coupled Plasma (ICP) analysis has been employed to get deeper knowledge in the composition of the metals including major and trace elements [23,27]. The combination of these two techniques can give a complete characterization of the metal decoration, being extensively used in European collections, letting open the possibility to performing similar

studies on American objects, letting the possibility to compare them to elucidate patterns or similar compositions to understand the influence of the Europeans after their arrival in American lands.

The study of the metal decorations present in flags and emblems of the textile collection of the National Museum of Colombia (Bogota-Colombia) by an analytical approach will allow to understand the transitional period between the colonial ages (16-19th centuries) and Republican ones (19-20th centuries) in America. It will be possible to describe the use of metals in non-common artifacts as the metal decorations are, to elucidate the change of techniques and possible trades of technology and raw materials on these transitional periods of time. In this study, a selection of a large number of flags (20) with a subset of micro samples (80>) from different locations, (Spain, Colombia, Peru, Venezuela) were studied through Optical microscopy (OM), scanning electron microscopy with energy dispersive spectroscopy (SEM-EDS), Ion coupled plasma (ICP) with optical spectroscopy and, by the first time multi-collector coupled to Ion coupled plasma mass spectrometry (MC-ICP-MS) was used to evaluate the lead isotopes in order to elucidate the possible provenance of the silvered metals compared with reported isotope lead values [28,29].

7.2. Materials and methods

7.2.1. Historical samples

Twenty textiles, covering the republic, independence and Spanish colonial periods (16-20th centuries), on the north of South-America (i.e. the present countries Colombia, Peru, Venezuela, Ecuador and Panama) (On SI Table 1. are listed the studied flags), which were property of the textile collection of the National Museum of Colombia, were subject of a

microextraction campaign by the conservators of the institution. As result, a set of 81 metals' micro-samples (See Supplementary information Table 2.) were collected from the metal decorations present in the flags with dimensions inferior to 1 cm in length and inferior to 2 mg in weight. Any of the flags studied has been under a restoration treatment in the past, stored in the museum, kept in the same environmental conditions (relative humidity, temperature, light, exposition).

7.2.2. Optical microscopy (OM)

The full set of micro samples were visualized under a microscope (Reichert, Austria) coupled to a digital camera (Nikon Digital sights DS-F12) with objective lenses Epi 5,5 (20X) and Epi 11 (40X), and polarized filter light.

7.2.3. Field Emission Scanning Electron Microscopy with Energy Dispersive X-Ray Spectroscopy (FE-SEM-EDS)

The topography of a subset of 20 samples (See Supplementary Information Table 2.) was analyzed using an FE-SEM SIGMA instrument (Carl Zeiss Microscopy GmbH, Germany). Samples were no coated, and images were acquired using the secondary electron detector as well in-lens secondary electron detector with an acceleration potential of 20 kV. EDS mapping was held over the surface of the samples to investigate the elemental distribution over the surfaces of the metals. To clarify the elemental composition found due to the presence of original elements or by corrosion sub-products on the samples, each sample was measured twice, one as obtained and a second time after a cleaning process. The cleaning process was executed as follows: a tiny part of each micro-sample was cut and introduced in an Eppendorf with 0.5 mL of

HNO₃ 0.1% (Nitric acid ACS reagent, Merck), then the closed vessel was introduced in an ultrasound bath for 1 minute; after that the acid was removed and the metal rinsed 3 times with mQ-water to finally let dry at room conditions.

7.2.4. Inductively coupled plasma optical emission spectrometry (ICP-OES)

A subset of 40 micro-samples (See Supplementary Information Table 2.) were weight and around 1 mg of each were put in a reflux glass vessel for digestion. Two digestion systems were executed simultaneously for each sample: one containing a solution of concentrated nitric acid (HNO₃), and a second containing aqua regia (Chlorhydric acid – Nitric acid HCl:HNO₃ 3:1 Sigma Aldrich Ultrapure). Digestions were conducted on a heat plate, letting the samples boiling for 48 hours, time after, solutions resultant from the acid digestion presented not dissolved gold residues, as well, aqua regia solutions presented white precipitate coming from silver chlorides. After digestion samples were let overnight at room temperature to decant. Next, supernatant was diluted to a final volume of 30 mL with mQ-water (18.2 Ω). Diluted solutions were injected as aerosol through a quartz spray and measured on an Optima 2000 Perkin Elmer ICP-OES dual Vision instrument. Silver (Ag), aluminum (Al), arsenic (As), gold (Au), Cobalt (Co), chromium (Cr), copper (Cu), iron (Fe), mercury (Hg), iridium (Ir), nickel (Ni), osmium (Os), lead (Pb), palladium (Pd), platinum (Pt), antimony (Sb), tin (Sn), titanium (Ti), vanadium (V), zinc (Zn) were measured and compared with standards to evaluate their presence and concentration on the samples as well as in blank solutions. CZ9090 mix010 was used for Al, As, Cr, Cu, Fe, Ni, Pb, Ti, and Zn; CZ9042(1C) was used for Os; CZ9027 was used for In; Au (Au, Pt, Pd); Pt; CZ9001 was used for Ag, Hg.

7.2.4.1. Calculation of the elemental concentration

Because micro samples presented degradation (some in higher proportion than others), it was impossible after weighting to know with precision the amount corresponding to the original metal and how much comes from degradation or contaminants. As micro samples had a reduce dimension and mass (around 1 mg), no cleaning was intended on the samples before the ICP-OES measurements, avoiding in this way the possible loss of mass from the bulk of the sample, as well knowing that part of the patina and oxides are formed by the original metal, it was intended to measure the complete sample as a whole and after execute a mathematical approximation to eliminate the possible interferences, in this way obtaining a value which will related to the original composition of the object after its manufacture, calculating the possible original weight of each sample. This procedure which looks to evaluate the real weight of the samples, allowing to compare the values among samples was followed without taking in consideration sulfur, chlorine, magnesium, calcium, silicon, sodium, oxygen and carbon elements, which were not measured at all, since those elements could be present mainly as a result of degradation processes i.e. the oxides and sulfurs over the metal patina, pollutant residues, foreign contaminants and/or micro attached organic matter not related with the metallurgical process, as well as if they are part of the metallurgical process their original concentration on the micro samples will be too low to be detected, having that values from those elements will be bias for the pollutants. In this way, the mathematical approximation was as follows:

1- ICP-OES result for each micro-sample after their digestion (on Aqua regia or nitric acid), was evaluated: negative values and values under the limit of detection of the instrument were discarded.

2- Silver concentration from the aqua regia measurements were discarded, and gold concentration discarded from the nitric acid ones. The other analyzed elements were compared among digestions, obtaining that elemental values were almost equal on both experiments. Aqua regia and nitric acid blanks do not reflect the introduction of any relevant concentration of foreigner elements to the solutions.

3- Concentration in weight per each element on each sample was taken (silver concentration from nitric acid digestion and gold from aqua regia digestion) and its values added arithmetically.

4- The resultant sum was selected as the real original mass value for each sample.

5- The concentration in weight% for each element on the sample was recalculated taking as 100% of sample the value obtained in point 4.

7.2.4.2 Principal component analysis (PCA)

The elemental composition of the metal decorations as obtained by ICP-OES were subjected to multivariate statistical analysis through Principal Components Analysis (PCA), using the Origin Pro Software Vs. 9.0 (OriginLab Corporation, Northampton, USA). PCA fundamentals of data treatment can be found elsewhere [30,31]. Autoscaling was selected as pre-treatment for PCA: the mean of the column element was subtracted from the individual elements

and divided by the standard deviation of the respective column; each column has then zero mean and unit variance [32].

7.2.5. Multi Collector Inductively coupled plasma with mass spectrometry (MC-ICP-MS)

Digestion and lead purification were executed in the clean laboratory at the radiogenic isotope laboratory of the department of earth sciences of the Università degli studi di Firenze. HNO₃ (Ultra-pure nitric acid Romil) dissolution of 3-10 mg of sample, depending of the available amount of the historical microsample, followed by standard ion-exchange chromatographic techniques using an AG1-X8 ion exchange resin (Bio-Rad) and a standard HBr (Ultrapure Romil) and HCl (Ultrapure Romil) elution procedure was employed for lead purification. Pb isotope ratios on the selected subset of micro samples were determined at the Institute of Geosciences and Earth Resources (CNR) of Pisa using a Neptune Plus MC-ICP-MS (Thermo Fisher Scientific Inc., Bremen, Germany). The dilute nitric acid solutions (2%UPA) were injected into the mass spectrometer as aerosol through a quartz spray chamber. The measurement of Pb isotopes has been performed in static mode, using seven of the nine Faraday cup collectors of the Neptune MS, being each one of the collectors associated with a 10¹¹ Ω amplifier, except for ²⁰⁴Pb and ²⁰²Hg which were associated with 10¹² Ω amplifier due to their low intensity. Mercury (²⁰²Hg) was monitored for the correction of isobaric interference with ²⁰⁴Pb, so the effect of this interference was negligible as a matter of fact, being unnecessary a further correction. Mass bias during lead isotopic analysis was corrected for by using sample-standard bracketing, assuming that the same mass bias characterizes standards and unknown samples. Measured values were compared with the

international standard NBS981: $^{208}\text{Pb}/^{204}\text{Pb}$: 36.7265, $^{207}\text{Pb}/^{204}\text{Pb}$: 15.5000, $^{206}\text{Pb}/^{204}\text{Pb}$: 16.9418 (Baker et al, 2004 [33]). The reproducibility of the results of replicate analyses of the standard over the measuring period was 0.052–0.099% for the $^{206}\text{Pb}/^{204}\text{Pb}$, $^{207}\text{Pb}/^{204}\text{Pb}$, and $^{208}\text{Pb}/^{204}\text{Pb}$ ratios. Evaluation of resulting data were executed offline, first subtracting the blank intensity to each sample and then being corrected for the isotopic fractionation using the two standards which bracket the sample. All the errors were fully propagated using Montecarlo simulation. Control blank samples were processed and measured along with the samples obtaining values under the 52 pg of lead. Isotopic results were compared with literature [34–36].

7.3. Results and discussion

Metal decorations have been studied in the past by several authors in different locations as in Europe by Costa et al., Ferreira et al, or Weiszburg et al. [24,33,34], or in the Latin-American context by Muros et al. [25], nevertheless, there is still a lack of information on these elements and especially, on the transformation of this technique after the arrival in America. In order to fill this gap through analytical methods, a set of textile objects, which were preserved at the National Museum of Colombia were selected to study the metal decorations present on them.

As a pre-analytical step, all documentation present at the National Museum of Colombia was consulted to collect all information on each object. It was possible to get information on the acquisition, material integrity, cleaning operations, previous restoration, exhibition and scientific studies on the objects after their arrival in the museum. By this way, it was possible to know that the flags studied were not subject to any intervention (cleaning neither restoration),

Chapter 7. Microanalytical study of the evolution of metals used as decorations on Spanish and Latin-American flags textiles from 16-20th-century preserved at the textile collection of the National Museum of Colombia

except those planned to avoid plagues infestation, which could lead damages on the textiles, and had not been part of any previous scientific study.

Flags were all manufactured, used, and time later arrived to be part of the museum collection. Each flag has suffered a unique history, being those manufactured before the museum foundation at 1823, the ones which were used for longer time, contrary to the most recent flags which were used for short time and were carried in a short time to become part of the museum collection. In the same way, the documentary system data and the iconography of the objects, allow to discriminate the full set of flags on two main groups: one group composed by 54% of the total of flags, corresponding to the colonial period of America (16-18th centuries) and the Spanish armies arrived in America on the reconquest time (early 19th century), which are known that have a European manufacture (presumably Spanish); and a second group formed by 46% of the total of flags with iconography representing the newborn nations (19-20th century) of the north of South America (what is nowadays Colombia, Venezuela, Ecuador, Panama and Peru;), presumably manufactured in America. It is important to underline, that all the flags are different among them, and represent different moments of the history. According to their iconography, both groups of flags are divided into two main representations, military or political (See Figure 1 and Supplementary information Table1.), resembling their original identity and function [35]; for example, some show the coat of arms of the Spanish king (at the time), indicating the use of the flag as a representative symbol of possession and control of the land in which it was placed; others show military symbols of an army, reflecting the joint of a group of men with a military mission; meanwhile, others reflect the joint of ideas, cultures and people and

their need to be identified as a nation by the use of a combination of colors and/or symbols in a flag, such as in the new republic flags from the republic period.

All flags selected for this research are manufactured with a main silk textile body [36]. The flags are textiles of big format (more than 1 m²) with different shapes (squares, rectangles, “V” shape), some of made of one plane textile, and some composed by the combination of different sewn textiles. All the historical objects present different colors, which are obtained using a dye on the silk textile before to be displayed in a specific pattern. The flags contain metals used as decorations, to create or highlight some figures, to outline some areas of the textile, or just employed as an ornament on purpose to give to the textile a higher aesthetical and/or economic value.

Due to the conservation status of the historical objects here studied, and the lack of both, scientific information of the objects and the possibility of in-situ research [37,38], a microsampling campaign was followed. To maximize the possibility to gain new scientific information after the micro intrusive sampling procedure, the extraction of the micro samples was based in an in-situ inspection on each flag, where was determined the number of samples necessary to fully describe the different metal decorations on the textiles, and the minimal amount required of each sample to held an investigation at different analytical scales, and with different analytical tools [39,40]. As result, a total of 81 micro samples for the 20 flags were extracted, due to the presence (or possible presence) of more than one type of metal decoration on some flags (See Supplementary Information Table 2.).

Chapter 7. Microanalytical study of the evolution of metals used as decorations on Spanish and Latin-American flags textiles from 16-20th-century preserved at the textile collection of the National Museum of Colombia



Figure 1. Example of military or political iconography on the flags studied. Top left: Flag with the Castilla and Leon coat of arms ca. 1700; Top right: Infantry battalion Spanish flag ca. 1813; Bottom left: Military flag of the Gran Colombia's first hussars squad battalion ca.1824; Bottom right: Flag of the United States of Colombia ca.1861. Photographs © National Museum of Colombia.

As a first analytical step, all samples were inspected through optical microscopy. Characteristic information is reported on Supplementary information Table 3. The microscopical inspection of all the metal micro samples allowed to identify and classify the samples according to their shape [15] in plain or twisted samples (See Figure 2.). Plain metal decorations were detailed as

plane metal (a plane metallic layer without a characteristic shape); paillette (circular and flat metals with a concentric gap); strip (a flat linear rectangular sheet); and wire (a tubular linear metal). Twisted metal decorations used as metal threads (a metal twisted around an internal core fiber [15]) were detailed as spring wire (a wire twisted in a spring shape around a fiber); spring strip (a strip twisted as a spring around a fiber); and a strip twisted (a strip twisted around a fiber). Strip twisted samples showed that mainly silk was used as internal fiber on the manufacture of the metal threads with exception of some modern samples which use cotton, almost all strip twisted samples presented a left ("S") metal twist and some few exceptions of right ("Z") twist. The core fibers of the different metal threads did not present any color which could indicate the use of dyed fibers. The metal micro samples presented different colorations on their surfaces as silvered, golden or copper, as well some black, green or earth colors which indicate possible corrosion and/or presence of contaminants.

Organizing the different types of samples according to their age, it is possible to see a trend in the metal decorations over the time (See Figure 2.), it seems that in the 16-18th century it is used one or two types of metal decorations (strip, strip twisted metal threads) in the manufacture of the flags, meanwhile a diversification is evident at the beginning of the 19th century, while the use of only one type of decorations returns in the 20th century. This observation can be explained as result of the change of availability of resources in the population, as well as a change in fashion and market, where, in the older flags, the manufacturing of the metal decorations were performed by specialized techniques, and specialized handcrafters only to satisfy specific

Chapter 7. Microanalytical study of the evolution of metals used as decorations on Spanish and Latin-American flags textiles from 16-20th-century preserved at the textile collection of the National Museum of Colombia

requirements on high value objects [26,41], presenting a variety in color, probably due to different composition or coating to satisfy the needs of that

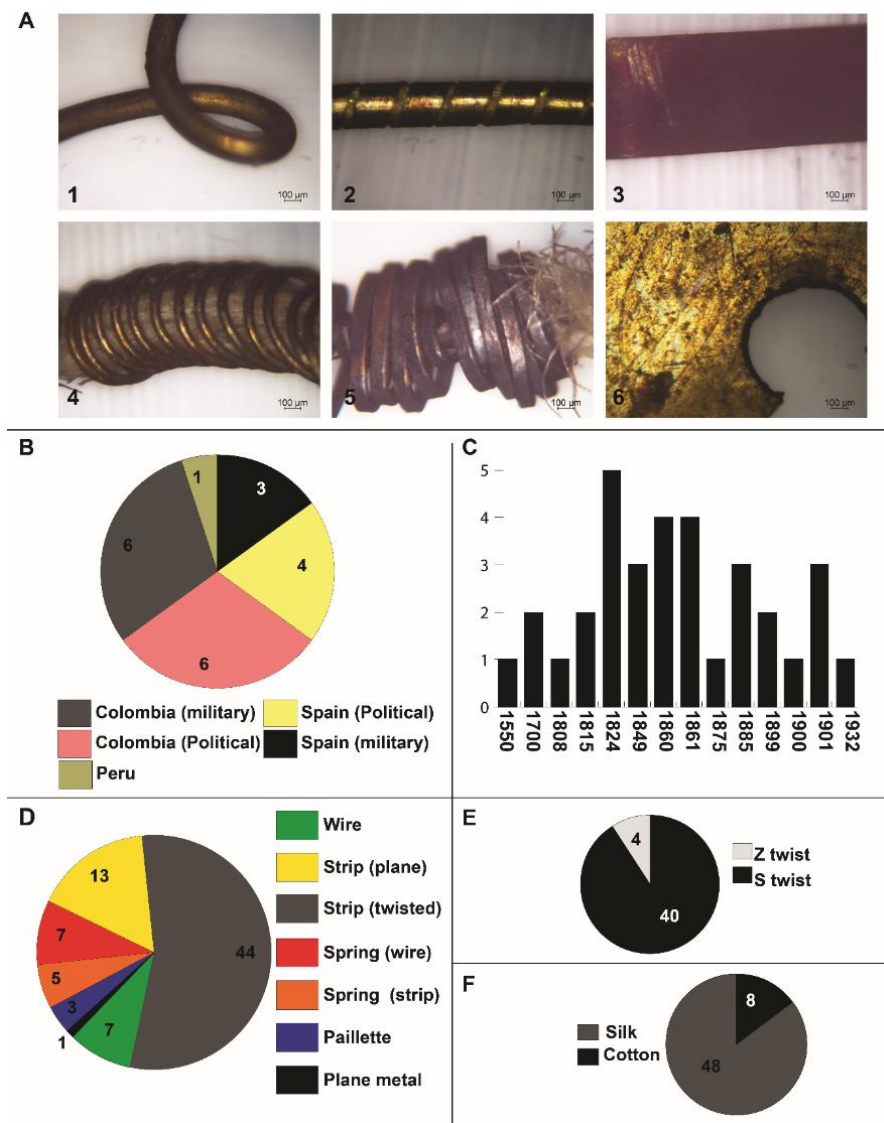


Figure 2. Images and Classification of the metal micro samples according with the visual and Microscopical inspection A) microphotograph of one representative sample as an example of the different types of metal decoration identified by OM 1)Wire, 2)Strip (plane), 3) Strip (twisted), 4) Spring (wire), 5) Spring (strip), 6) Paillette B) Number of flags per its main iconography; C) histogram of the number of types of metal decoration per year; D) Number of samples per type of metal decoration; E) Number of stripe (twisted) samples with "S" or "Z" twisting; F) number of samples with internal core from stripe (twisted), spring (wire and stripe) samples.

time, meanwhile, after the industrialization in the 19th century, the access to materials and new techniques in the production of these elements, opened the market for different social groups, allowing in this way an increase of styles to satisfy the new demand of these product for different customers, obtaining in this way a diversification of the metal decorations, producing wires and paillettes (find in samples after the first quarter of the 19th), being used as a simple wire or as springs twisted around a silk internal cores (technique already used in the past in other regions [23]). Finally, due to the introduction of new decorative techniques (as painting, stamp, extensile, etc.) the use of the metal decorations in flags decrease, conducing to disuse, which is evident in modern flags which prefer the use of other type of decorations than metals [42,43].

Detailing the micro samples over time, type by type, it was found that each type of metal decoration preserved its basic shape over time, indicating a continuation on the know-how of its production, regardless of age, the possible location of production and final use. Notwithstanding, comparing the dimensions on each type of decoration, similar values are found in samples of the same time frame (but subtle changes are found when are compared in a larger frame of time), indicating that the technique has undergone some modifications in the years. To detail the similarities or changes on metal decorations, different plots were created, to represent the relationship between the length of the metal decoration (strip or wire) and the age of the sample (Figure 3.A.); the relationship between the length of the metal decoration and the diameter of the metal thread (Figure 3.B.); the relationship between the number of twists per millimeter on the metal thread versus the arithmetical ratio of the diameter of the thread per length of the strip (Figure 3.C-D).

Chapter 7. Microanalytical study of the evolution of metals used as decorations on Spanish and Latin-American flags textiles from 16-20th-century preserved at the textile collection of the National Museum of Colombia

The relationship between the length of the strip or wire decoration and the age of the sample (See Figure 3A) shows two main groups. One group composed of Spanish military flags of the 18th century which used strips around 0.8 mm, and a second group composed of civilian and military, Spanish and American flags from 19th to 20th century, with metal decorations around 0.1 mm length for the wires and around 0.2-0.3 mm for the strips, being thinner with respect the first group. This change suggests that for reasons that cannot be explained here, the use of the strip and wire metal decoration suffers a reduction in length in recent centuries, compared with those older, maybe due to a restriction in the use of metals for this purpose, or due to the cost of the materials, or by a fashion style, or due to an evolution on the technology which allow to achieve shorter/finest dimensions with a higher reproducibility in the process than in the past.

The relationship between the length of the metal decoration and the diameter of the metal thread Figure 3.B. shows three groups and two isolated samples (S274 and S325). The first group confines the strip (twisted) samples with a diameter thread around 0.4 mm and a length between 0.2 and 0.45 mm, being inside samples with representations from Spain and America for both civilian and military, in a range of time from the 17th to the 20th century. A second group is composed by the 16th-century civilian flags samples, which have a uniform diameter around 0.4 mm, but with a length of the strip variable between 0.3 mm and 0.8 mm. Finally, a third group enclose the springs (wires and strips) samples which have a diameter between 0.5-0.8 mm and a reduced length strip around 0.1 mm, for both 19th century Spanish and American civilian flags, one interesting point of this group is that springs made of wire have a

variety of diameter, meanwhile the springs made of strips even from different years have similar dimensions.

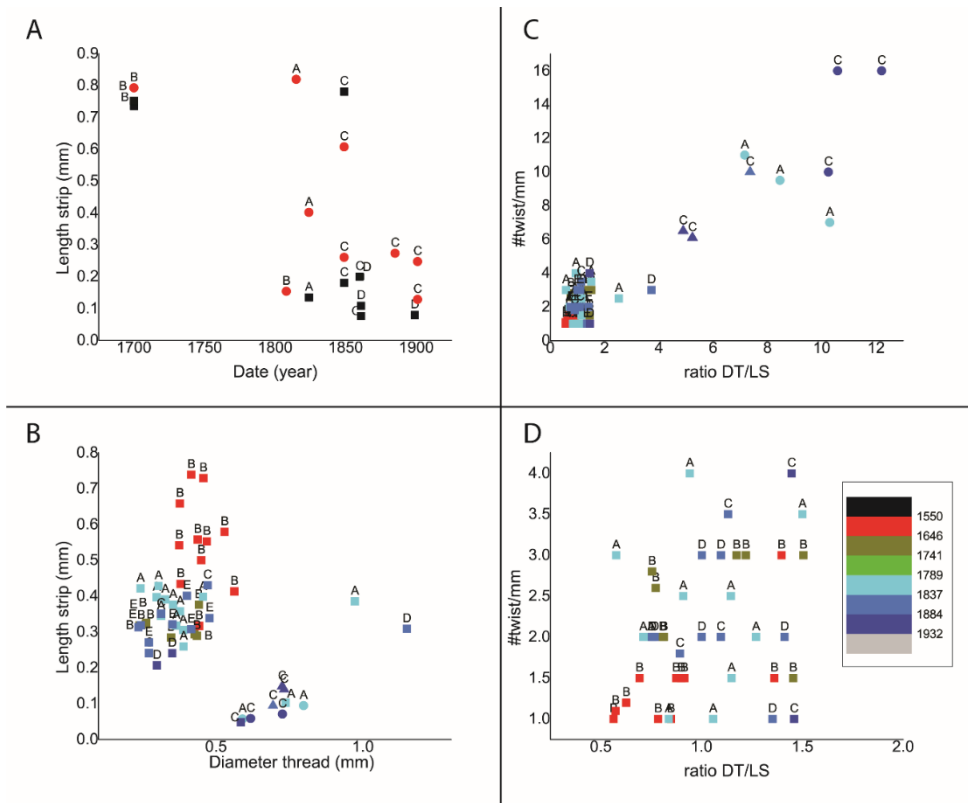


Figure 3. A) Plot of length of the strip versus its date on wires and strips; B) Plot of length of the strip versus the diameter in the thread; C) Plot of the ratio of number of twists per mm versus ratio of the diameter per length in metal threads; D) Zoom of the plot C in the region 0.0 to 2.0. The labels of the plots describe the iconography of the flag as follows: A=Spanish military, B= Spanish kingdom, C=Colombian flag, D= Colombian army, E= Peruvian coat of arms. Shapes in plots B-D describes the type of metal decoration as follows: Square=Strip (twisted), Circle= Spring (wire), Triangle= Spring (Strip). Colors of points in plots B-D describe the age of the sample as explained in the color map.

The relationship between the number of twists per millimeter on the metal thread versus the arithmetical ratio of the diameter of the thread per length of the strip (Figure 3.C-D), reflects how the strip (twisted) samples are grouped, indicating that even in different years, uses (military or civilian) and different (probable) provenance (Spain or America), this kind of objects continue to have a similar pattern in their manufacture (Figure 3C.). In the same way it reflects, how a different type of decoration (the springs), the number of

Chapter 7. Microanalytical study of the evolution of metals used as decorations on Spanish and Latin-American flags textiles from 16-20th-century preserved at the textile collection of the National Museum of Colombia

twists increased, meanwhile the length of the strip decreases for similar diameters. Nevertheless, it is interesting how the American spring (wire) samples are not grouped with the European ones, indicating that possibly were not manufactured following the same parameters. Figure 3.D. shows a peculiarity on the strip samples, where Spanish kingdom flags of the 16th century are mainly grouped with less twist per length on the decoration, meanwhile for the rest of American and Spanish the samples on the subsequent centuries, have no an established pattern, presenting different values. This could be a result of spreading of the technique and manufacture centers in the following years, meanwhile, in the 16th century, the manufacture centers could be centralized in a unique factory. In conclusion, the dimensions of the metal decorations analyzed under the optical microscope indicates a subtle change on the manufacturing process across the time of these objects, although the concept of each type of decoration continues during the six centuries studied, their manufacture technique changes, being possibly a response to different factors (economic, political, change of fashion or manufacture school among others) that experimentally are not possible to discuss.

As a first attempt to characterize the elemental composition and its distribution at a micrometrical scale on the body of the metal decorations and visualize their morphology, a subset of twenty samples of metal decorations were analyzed by SEM-EDS. This technique was used knowing their limitations and was not intended to discriminate the thickness of the possible different layers, neither to obtain a quantitative elemental composition on the samples measured [44–46], but results were correlated with the previous subtle changes detected by optical microscopy analysis.

The SEM observations over the surfaces of the samples showed the presence of aggregation of extra particulates as an alteration of the metals in both faces of the micro samples i.e. the frontal face which is the one that the spectator can see, and the rear one, which is hidden from the spectator view. EDS analysis over the surface allow to detect chlorine, sulfur, aluminum, calcium, magnesium and oxygen as non-metallic elements, being these associated (by their location, shape and color under the optical microscope) with the formation of chlorine salts, sulfur salts, deposition of soil dust and metal oxidation (See Figure 4A-B). This kind of corrosion and/or contamination are characteristic on this kind of objects by their interaction with the environment due to a natural process and are not related with the metal decoration manufacture [47–50].

To put in evidence the original surface of the samples, a soft chemical cleaning of the samples was performed, and each sample was observed again under the SEM instrument, obtaining in this way that the content of contaminants over the surface of the metal was diminished (almost completely removed), and the original composition was evidenced (See Figure 4.C). Strips and wires samples (gild, silvered and not) presented a uniaxial striation parallel to the central axis of the metal, indicating that the material suffered an external mechanical force on their manufacture, possibly as a drawn wire [51]. Gild strips presented a gold layer around the full-body, indicating that before to be flattened, a cylinder was first made and after was pressed and pulled unidirectionally to give its final shape to the metal decoration.

On Table 1, the elements detected by EDS on the different samples are presented, together with the description of the distribution of the elements on the metal decorations, before and after the soft acid treatment. With the clean

Chapter 7. Microanalytical study of the evolution of metals used as decorations on Spanish and Latin-American flags textiles from 16-20th-century preserved at the textile collection of the National Museum of Colombia

surface, three types of metal decorations were found: first type is wires and strips metal decorations made by only one element (silver) or one alloy (bronze); the second type are strips, wires, and plain metals decorations made by two metal layers, one thick core (silver or copper) full surrounded by a thin film of another metal (mainly gold and some samples with silver); finally, a third type is the paillettes, which present three layers, an inner core (copper), followed by a thick silver layer, which is surrounded by a thin gold film. Gold, silver, and copper were found as the elements used in the manufacture of all-metal decorations, being used as a unique element or in layers. The use of these metals during all time and in all kind of decorations and purposes, proof that these objects as decorations have been intentionally used to increase the value of the textile. It is important to underline that was not found any sample with multiple layers on which gold was used as inner core. Paillette samples elemental distribution suggest the use of a thinner copper core surrounded by a thicker layer of silver to form a cylinder which was after gilded, being next flattened, twisted and cut to obtain its final circular shape (See Figure 4.I-J).

One interesting result of the EDS measurements over the gilded sample was the identification of copper together with the gold film, all around the surface of the metal in a homogenous distribution, but, at a low concentration (See Figure 4.D-F). When samples were analyzed in a lateral cut, the two layers were evidenced, the inner core and the thin gold film used as an external layer (See Figure 4.G-H), but no evidence of copper inside the inner metal core as inclusions was detected, as also reported by Costa et al. [24]. This result suggests that a copper substance was used to weld the golden external layer to the inner core metal during the manufacturing process. This result also evidences a

transformation of the metal decoration process over time, and a change in the selection of the metals used for its manufacture. After the 19th century, copper was introduced as inner core of the decoration, replacing the traditional use of silver as the main element in the decorations as in previous time, in the same way, alloys start to be employed in the manufacture of these artifacts, effect that reduce the cost of the production, but can give some colors similar to those of gilded objects.

Chapter 7. Microanalytical study of the evolution of metals used as decorations on Spanish and Latin-American flags textiles from 16-20th-century preserved at the textile collection of the National Museum of Colombia

Table 1. EDS results of the subset of metal micro samples

Sample	Main elements detected by EDS	Impurities detected by EDS	Type	Core	External layer
S10	Ag, Cu	S, Cl, Mg, O	Strip (twisted)	Silver	None
S17	Ag, Au, Cu	Na, Mg, S, Cl, O	Strip (twisted)	Silver	Gold
S26	Ag, Au, Cu	Cl, O, Ca, Si, S, Al, Na,	Strip (twisted)	Silver	Gold
S27	Ag	Cl, S, Si, Mg, O	metal	Silver	None
S281	Ag, Cu	S, Cl, O, Mg, Al, Ca,	Strip (twisted)	Copper	Silver
S55	Ag, Au	Ca, Cl, S, Si, Mg, Al, Na, O	Strip (twisted)	Silver	Gold
S133	Ag, Au, Cu	Ca, Cl, O, S	wire	Silver	Gold
S135	Ag, Au	Cl, S	Strip (twisted)	Silver	Gold
S247	Ag, Au, Cu	O	paillette	Copper Silver	Gold
S268	Ag, Au, Cu	Cl, O, S, Si, Al, Na, Ca	Strip (twisted)	Silver	Gold
S269	Ag, Au, Cu	Cl, S, Si, O	Strip (twisted)	Silver	Gold
S274	Ag	Cl, S, O, Mg, Al, Si, Ca	Strip (twisted)	Silver	None
S217	Cu, Zn	Cl, S, Si, O	Strip (twisted)	Bronze	None
S226	Ag, Au, Cu	Cl, O	wire	Silver	Gold
S228	Ag, Au	S, Si, O	metal	Silver	Gold
S237	Ag, Au, Cu	Cl, O, S	wire	Silver	Gold
S327	Ag, Cu	Cl, S, O	wire	Copper	Silver
S82	Ag, Cu,	Cl, S, Si, O	Strip (twisted)	Copper	Silver
S347	Ag, Au, Cu	Cl, O	wire	Silver	Gold
S252	Cu, Zn, Fe	Cl, S, Si, Al, O	wire	Bronze	None

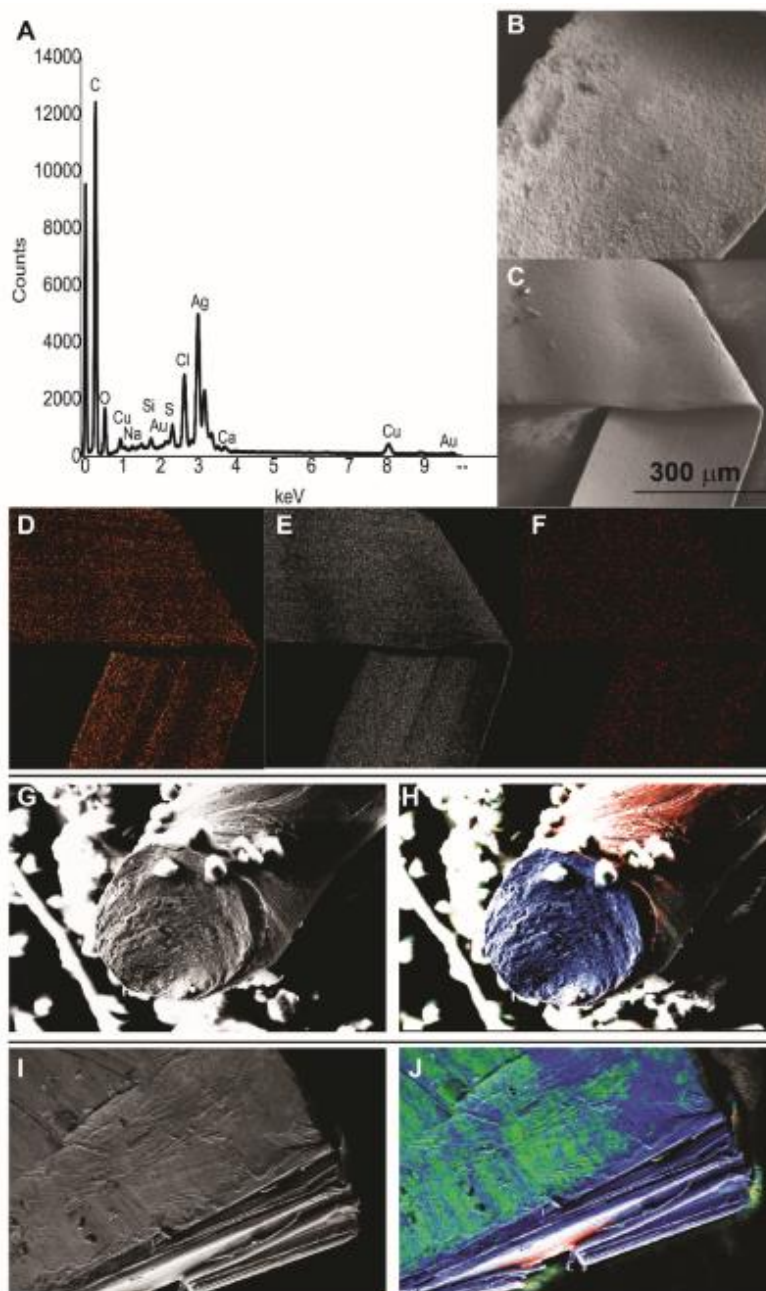


Figure 4. Example of SEM-EDS results over metal decorations A) EDS spectra of the metal surface of S268 without cleaning; B) SEM image of the surface of the metal S268; C) SEM image of the cleaned surface of the metal S268; D) EDS mapping of gold over metal S268; E) EDS mapping of silver over metal S268; F) EDS mapping of copper over metal S268 G) SEM image of the cut of the metal wire S133; H) EDS cameo on wire S133, blue=silver, red= gold; I) SEM image of the paillette S247; J) EDS cameo on paillette S247, blue=silver, red= copper, green=gold.

Chapter 7. Microanalytical study of the evolution of metals used as decorations on Spanish and Latin-American flags textiles from 16-20th-century preserved at the textile collection of the National Museum of Colombia

SEM measurements reflect similarities between samples analyzed and those reported in the literature for the different periods of time [15,25,26,34], confirming the authenticity in time of the objects analyzed. Samples gilded on one side were not found, neither the use of linen or other materials as inner cores, neither organic strips. When strips or wires of different times or locations were compared, among them, structural differences, which could indicate a difference in their manufacture process, were not found, suggesting that all wires and all strips followed similar technique conditions on their manufacture, regardless their age.

To get a complete quantitative elemental characterization on the metal decorations, overpassing the EDS difficulties [24,44], and obtain new and useful information in this kind of objects, ICP-OES analysis was performed over a subset of forty samples (See supplementary Information Table 2.), where patterns or differences among samples were looked for. ICP-OES results (See supplementary information Table 4.) were obtained after the calculation of the weight for each sample discarding the non-metallic elements, corresponding to impurities/corrosion detected by SEM-EDS previously (see Materials and methods 2.4.2). A difference between the initial mass (mass-weighted initially before the digestion) and the calculated one (the final weight calculated from the concentration of the elements selected on the ICP-OES measurement), was obtained after the ICP-OES measurements, letting as result a variance in weight around the 25 % for the silver core samples, and 5-10 % on the copper core samples. This due to the high content of corrosion products on the samples, where, silver samples due to their own nature and due to in general, are older than the copper samples, being exposed to a longer deterioration presented a

higher presence of nonmetallic elements on their body than copper samples. In the same way, ICP-OES results, corroborate the use of copper, silver, and gold as main elements on the manufacture of the metal decorations, as was evidenced by the SEM-EDS results. There was not possible to use the ICP-OES results to find a specific element which could be used as a reference to discriminate the samples according to a possible provenance, neither as a possible indicator of change through time of the manufacturing technique.

To analyze the results of the full set of samples and all the selected elements on the ICP-OES measurements, a PCA model was performed and optimized, obtaining that As, Os, Ir, Pt, Sb, Sn, and Ti were excluded as variables because its low representativity; while Ag, Al, Au, Co, Cr, Fe, Ni, Pb, Pd, and Zn as variables (See Figure 5.). The PCA model which explains the 54.01 % of variability on the forty samples on their first two principal components (PC1=37.4%; PC2=16.62%), presents the samples in two main groups, one grouping those samples with a silver core and a second group composed by those samples with a copper core. Both groups are described by multiple types of metal decorations (strips, wires, etc.), with different chronologies (from 16-20th century), and representing different provenances (American and European).

Chapter 7. Microanalytical study of the evolution of metals used as decorations on Spanish and Latin-American flags textiles from 16-20th-century preserved at the textile collection of the National Museum of Colombia

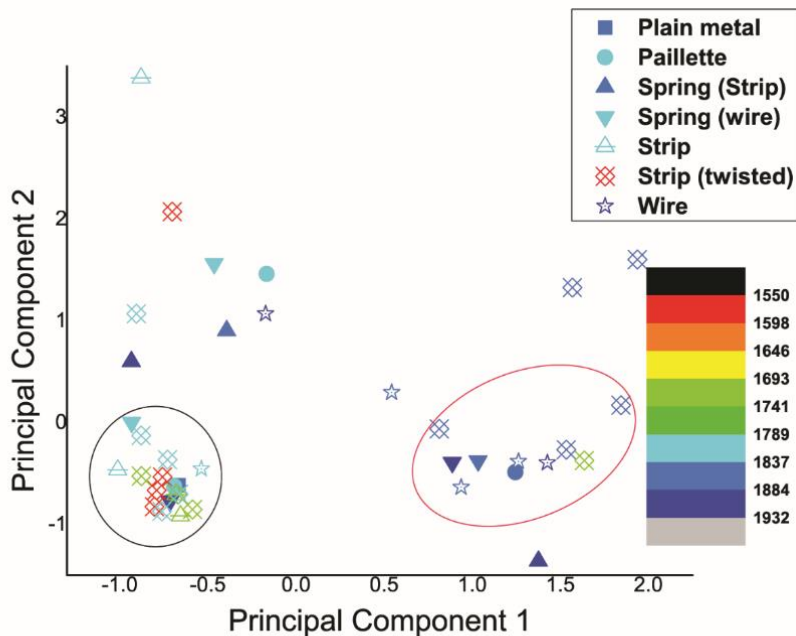


Figure 5. PCA score plot of the elemental analysis by ICP-OES. Black circle silver core samples. Red ellipse, copper core samples. Samples are colored by date as the map color indicates.

Using PCA information, samples were split into two groups, the metal samples composed by a silver core and the samples composed by a copper core, to detail the Cu vs Au, Au vs Ag, and Cu vs Ag ratios detailed (See Supplementary Information Figure 1. and 2.). Detailing the silver core samples, the Cu vs Au relationship shows a group of samples without copper neither gold, being those corresponding to the metal decorations made of pure silver. The gilded silver core samples show that all samples, from all provenances, ages, and types, without matter the gold content, have a similar amount of copper, except by 16th century Spain strip (twisted) and the paillette (copper core) samples. Both groups, one which proves that the silver employed has no as much copper as the gilded ones, could confirm the hypothesis of the use of a copper substance to join the gold film to the silver core in the gilding process, the reason why it is

present in similar amounts regardless the gold concentration found. The Au vs Ag and the Cu vs Ag relationships show that, samples of a same frame of time, no matter the type of metal decoration, neither final use (for a Spanish or American flag), present similar concentration of gold and copper, respectively, indicating that a proportion of raw materials were used in each time, being carefully respected.

Copper core samples, which are composed mainly by American samples from the late 18th century till 20th century, does not presented in the different relationship analyzed specific trends or sub-groups, only showing differences among them in the content of gold or silver, which can be attributed to the thickness of the gilded and silvered samples. The values obtained in the relation of gold-copper, or silver-copper, reflects how the copper concentration it is comparable to the silver concentration in the metal decorations with a silver core, demonstrating how was replaced one metal by the other.

Finally, to elucidate a possible exchange in raw materials from America to Europe, or a possible manufacture in America after the 19th century of this metal decorations, MC-ICP-MS was executed as complementary tool to correlate the provenance of the metal silver in one sample for each flag (See Supplementary information Table 2.). By using lead isotopic analysis, it was aimed to correlate the possible ore or mine of the silver/copper metals with a possible origin of the respective metal decoration used on each flag. MC-ICP-MS results are presented in supplementary information in Table 6. When $^{206}\text{Pb}/^{204}\text{Pb}$, $^{207}\text{Pb}/^{204}\text{Pb}$, $^{208}\text{Pb}/^{204}\text{Pb}$ ratios are compared among samples, a single group is formed for all samples, except by metals S82 and S372 which presented distant values (See Supplementary information Figure 3.), this could be explained as a lower amount in the three lead isotopes (^{206}Pb , ^{207}Pb , ^{208}Pb),

Chapter 7. Microanalytical study of the evolution of metals used as decorations on Spanish and Latin-American flags textiles from 16-20th-century preserved at the textile collection of the National Museum of Colombia

or more reasonable as a higher content in ^{204}Pb , indicating a possible reuse of metals for the manufacturing process of these two samples in a recycling process. When S82 and S372 are excluded of the lead isotopically analysis, and $^{206}\text{Pb}/^{204}\text{Pb}$, $^{207}\text{Pb}/^{204}\text{Pb}$, $^{208}\text{Pb}/^{204}\text{Pb}$ ratios 3D plot, two groups are found (See Figure 6.), and easily analyzed when the ratios $^{207}\text{Pb}/^{204}\text{Pb}$ vs $^{206}\text{Pb}/^{204}\text{Pb}$ and $^{208}\text{Pb}/^{204}\text{Pb}$ vs $^{206}\text{Pb}/^{204}\text{Pb}$ are plot (See Figure 7.). The first group is mainly composed of the samples representing the Spanish iconography of the 16th and 19th century, having similar $^{206}\text{Pb}/^{204}\text{Pb}$, and $^{208}\text{Pb}/^{204}\text{Pb}$ values. The second group is mainly conformed by samples with American iconography, having a similar trend with common values of $^{207}\text{Pb}/^{204}\text{Pb}$, and $^{208}\text{Pb}/^{204}\text{Pb}$.

Due to the history of the flags, and their iconography, the lead isotope values for the metal decoration samples studied here were compared with Mexican, Peruvian, Spanish and Italian ores, and with Spanish objects. The isotopic ratios obtained by MC-ICP-MS were compared with literature values and using the Oxford archaeological lead isotope database (OXALID), to postulate the provenance of the main metal employed for the manufacture of the metal decoration [52–54].

When values of lead isotopes of the metal decorations samples are compared with values for Mexican and Peruvian ores (See Supplementary information Figure 4.), no correlation are obtained between them, indicating that none of the samples were extracted from an American ore, letting open a question for future discussions in other disciplines: if big amounts of metals were extracted from America, why were those not used in the manufacture of this kind of objects?.

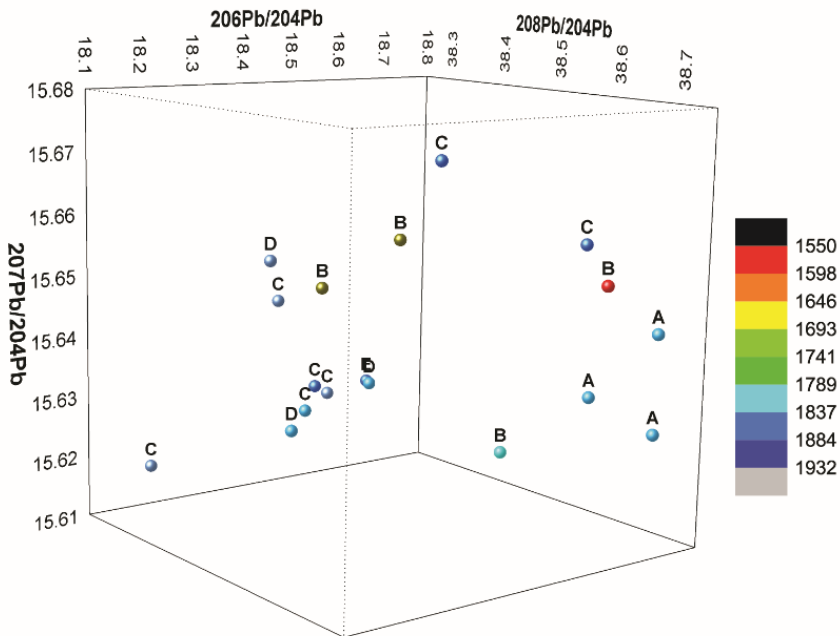


Figure 6. 3D plot of the isotopic ratio of the metal decorations studied by MC-ICP-MS. Labels of the plots describe the iconography of the flag as follows: A=Spanish military, B= Spanish kingdom, C=Colombian flag, D= Colombian army, E= Peruvian coat of arms. Colors of points describe the age of the sample as explained in the color map.

Comparing the isotopic values obtained for the samples with Spanish and Italian ores, some samples presented a close correlation with Italian ores, nevertheless, all samples presented an almost full correspondence of the samples with those from Spain (See supplementary Information Figure 5 and 6.). In detail, samples of the first group (Spanish iconography of the 16th and 19th century) match with samples coming from “Sierra Almagro” lead’s ore at Almeria (Spain) and Cartagena lead’s ore at Murcia (Spain), meanwhile the second group (samples with an American iconography from 19th to 20th century), present similar values to those samples coming from “Los Molares” lead’s ore at Huelva (Spain). This result indicates that all metal samples come from Spain, nevertheless, the possible provenance of the metallurgical factory, differs from the Spanish flags to the American ones.

Chapter 7. Microanalytical study of the evolution of metals used as decorations on Spanish and Latin-American flags textiles from 16-20th-century preserved at the textile collection of the National Museum of Colombia

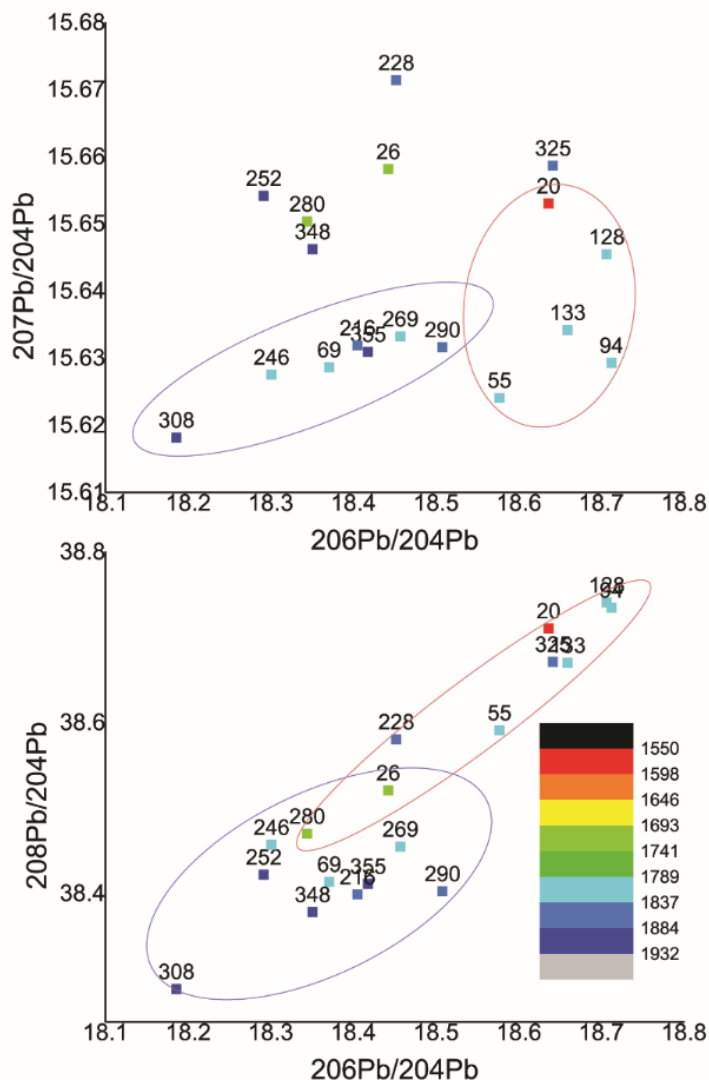


Figure 7. Isotopic composition of metal decorations on flags from the National Museum of Colombia. Top panel, $^{207}\text{Pb}/^{204}\text{Pb}$ vs $^{206}\text{Pb}/^{204}\text{Pb}$. Bottom panel, $^{208}\text{Pb}/^{204}\text{Pb}$ vs $^{206}\text{Pb}/^{204}\text{Pb}$. Samples are colored representing their age according to the age map. Red ellipse= First group (Spanish flags samples); Blue ellipse= Second group (American flag samples)

To confirm the provenance of the metal decorations previously found with the Spanish ores, the lead isotopic results were compared with objects reported in the literature for Spanish kings' objects (See Supplementary information Figure 7.), obtaining an optimal match between the metal

decorations and reported objects. The historical samples here studied shown similar values with objects of a frame time similar to them, as for example, those metal decorations of the 16th century have similar values to the objects related to Phillip III, or samples from metal decorations later than 17th century, shown values similar to samples of Louis XI, or Philip V.

7.4. Conclusions

The multianalytical study of the different microsamples coming from the flags preserved at the National Museum of Colombia, showed how in those textiles from the 16th-20th century the idea and use of metals as decorative elements was a common and extended practice, which underwent different changes over time.

Microscopical analysis of the objects shows that metal decorations underwent a change across the time, where some types are introduced in new factories as the use of spring metal decorations, as well classic techniques as the strip or twisted strip (metal threads) change in their dimensions as a possible result of a change in technique.

Elemental analysis of the studied objects reflects a preferential use of gold, silver, and copper in the manufacture of these decorative elements, nevertheless, its concentration varies in time.

The different samples studied, does not show a noticeable difference in their composition, however, subtle changes are present, but are not easily associated with a drastic change of location, or manufacture idea, being maybe just as the result of economic changes and an opening of new manufacturing places in more recent times without a specialization so accurate as in the past.

The isotopic analysis reflects the use of European raw materials in the production of metal decorations for textiles, for a European and for an American costumer; this suggests that the exchange/merchandising of these objects continued after the creation of the new republics, as in previous periods of time,

but maybe, not being restricted to specialized artisan manufacture centers which created in a meticulous way precious objects (as in the samples of older flags), but producing this materials for an audience not so exclusive or fussy.

It is important to underline that even if these objects were used in American textile manufacture there is no evidence that the raw metal decoration has been done in America, letting for future discussions how, when and why occurs the transferring or not of this knowledge and industry from Europe to America.

References

- [1] C.H. Haring, American Gold and Silver Production in the First Half of the Sixteenth Century, *The Quarterly Journal of Economics*. 29 (1915) 433–479. doi:10.2307/1885462.
- [2] G.D. Hubbard, The Influence of the Precious Metals on American Exploration, Discovery, Conquest and Possession, *Bulletin of the American Geographical Society*. 42 (1910) 594–602. DOI:10.2307/199959.
- [3] J.E. Kicza, R. Horn, R. Horn, Colonial Spanish America and Its Impact on the Sedentary Imperial Societies, *Resilient Cultures*. (2016). DOI:10.4324/9781315509891-11.
- [4] J.B. Legg, D.B. Blanton, C.R. Cobb, S.D. Smith, B.R. Lieb, E.A. Boudreaux, An Appraisal of the Indigenous Acquisition of Contact-Era European Metal Objects in Southeastern North America, *Int J Histor Archaeol*. 23 (2019) 81–102. DOI:10.1007/s10761-018-0458-1.
- [5] G. Montenegro, Conquistadors and Indians “Fail” at Gift Exchange: An Analysis of Nikolaus Federmann’s *Indianische Historia* (Hagenau, 1557), *MLN*. 132 (2017) 272–290. DOI:10.1353/mln.2017.0017.
- [6] J. Parry, M. Bloch, *Money and the Morality of Exchange*, Cambridge University Press, 1989.
- [7] B.V. Hampshire, K. Butcher, K. Ishida, G. Green, D.M. Paul, A.D. Hillier, Using Negative Muons as a Probe for Depth Profiling Silver Roman Coinage, *Heritage*. 2 (2019) 400–407. DOI:10.3390/heritage2010028.
- [8] R. Cesareo, Gold, gildings, and tumbaga from the Moche tomb of the Lady of Cao: An EDXRF test for the internal ratio method, *X-Ray Spectrometry*. 48 (2019) 202–207. DOI:10.1002/xrs.3021.
- [9] A.M. Pollard, R. Liu, J. Rawson, X. Tang, From Alloy Composition to Alloying Practice: Chinese Bronzes, *Archaeometry*. 61 (2019) 70–82. DOI:10.1111/arcm.12415.
- [10] H. Hodges, *Artifacts*, Edición: New edition, Bloomsbury 3PL, 1995.
- [11] C.C. Patterson, Native Copper, Silver, and Gold Accessible to Early Metallurgists, *American Antiquity*. 36 (1971) 286–321. DOI:10.2307/277716.
- [12] D. Killick, T. Fenn, *Archaeometallurgy: The Study of Preindustrial Mining and Metallurgy*, *Annual Review of Anthropology*. 41 (2012) 559–575. DOI:10.1146/annurev-anthro-092611-145719.
- [13] M.E. Solt, P.J. Swanson, On the Efficiency of the Markets for Gold and Silver, *The Journal of Business*. 54 (1981) 453–478.
- [14] A.M. Watson, Back to Gold and Silver, *The Economic History Review*. 20 (1967) 1–34. DOI:10.2307/2592033.
- [15] M. Járó, Metal Threads in Historical Textiles, in: *Molecular and Structural Archaeology: Cosmetic and Therapeutic Chemicals*, Springer, Dordrecht, 2003: pp. 163–178. DOI:10.1007/978-94-010-0193-9_15.
- [16] E. Bérard, C. Verna, V. Toureille, A. Williams, P. Dillmann, FABRICATION AND CIRCULATION OF MEDIEVAL ARMOR: AN ARCHAEOLOGY APPROACH, (2017). <https://hal.archives-ouvertes.fr/hal-01632474> (accessed June 13, 2019).
- [17] J. Mitchell, *The Art of Precolumbian Gold: The Jan Mitchell Collection*, Metropolitan Museum of Art, 1985.
- [18] I. Shimada, J.A. Griffin, Precious Metal Objects of the Middle Sicán, *Scientific American*. 270 (1994) 82–89.
- [19] M. Járó, Gold embroidery and fabrics in Europe: XI – XIV centuries, *Gold Bull*. 23 (1990) 40–57. DOI:10.1007/BF03214711.
- [20] J.L. Perez-Rodriguez, A. Albardonedo, M.D. Robador, A. Duran, Spanish and Portuguese Gilding Threads: Characterization Using Microscopic Techniques, *Microscopy and Microanalysis*. 24 (2018) 574–590. DOI:10.1017/S1431927618015167.
- [21] T. Yurdun, E. Dolen, R. Karadag, C. Mathe, A.K. Tsakalof, K.A. Bairachtari, E.A. Varella, A. Spinella, D. Capitani, S. Bastone, C.D. Stefano, E. Caponetti, E. Pavlidou, M. Kyranoudi, L. Puchinger, F. Sauter, A.

- Gössl, *Applying the Techniques on Materials I*, in: E.A. Varella (Ed.), *Conservation Science for the Cultural Heritage*, Springer Berlin Heidelberg, 2013: pp. 163–246. http://link.springer.com.ezproxy.uniandes.edu.co:8080/chapter/10.1007/978-3-642-30985-4_5 (accessed November 20, 2014).
- [22] A.-M. Hacke, C.M. Carr, A. Brown, D. Howell, Investigation into the nature of metal threads in a Renaissance tapestry and the cleaning of tarnished silver by UV/Ozone (UVO) treatment, *Journal of Materials Science*. 38 (2003) 3307–3314. DOI:10.1023/A:1025146207048.
- [23] A.F. Cakir, G. Simsek, H. Tezcan, Characterisation of gold gilt silver wires from five embroidered silk Qaaba curtains dated between the 16th and 19th centuries, *Appl. Phys. A*. 83 (2006) 503–511. DOI:10.1007/s00339-006-3527-y.
- [24] V. Costa, D. de Reyer, M. Betbeder, A note on the analysis of metal threads, *Studies in Conservation*. 57 (2012) 112–115. DOI:10.1179/2047058412Y.0000000001.
- [25] V. Muros, S.K.T.S. Wärmländer, D.A. Scott, J.M. Theile, Characterization of 17th–19th Century Metal Threads from the Colonial Andes, *Journal of the American Institute for Conservation*. 46 (2007) 229–244.
- [26] D.A. Badillo-Sanchez, C.B. Dias, A. Manhita, N. Schiavon, The National Museum of Colombia’s “Francisco Pizarro’s Banner of Arms”: A multianalytical approach to help uncovering its history, *Eur. Phys. J. Plus*. 134 (2019) 224. DOI:10.1140/epjp/i2019-12747-2.
- [27] I. Rezić, L. Ćurković, M. Ujević, Simple methods for characterization of metals in historical textile threads, *Talanta*. 82 (2010) 237–244. DOI:10.1016/j.talanta.2010.04.028.
- [28] L. Balcaen, L. Moens, F. Vanhaecke, Determination of isotope ratios of metals (and metalloids) by means of inductively coupled plasma-mass spectrometry for provenancing purposes — A review, *Spectrochimica Acta Part B: Atomic Spectroscopy*. 65 (2010) 769–786. DOI:10.1016/j.sab.2010.06.005.
- [29] E. Pernicka, Provenance Determination of Archaeological Metal Objects, in: B.W. Roberts, C.P. Thornton (Eds.), *Archaeometallurgy in Global Perspective: Methods and Syntheses*, Springer New York, New York, NY, 2014: pp. 239–268. DOI:10.1007/978-1-4614-9017-3_11.
- [30] H. Martens, T. Næs, Multivariate calibration. I. Concepts and distinctions, *TrAC Trends in Analytical Chemistry*. 3 (1984) 204–210. DOI:10.1016/0165-9936(84)85008-6.
- [31] T. Næs, H. Martens, Multivariate calibration. II. Chemometric methods, *TrAC Trends in Analytical Chemistry*. 3 (1984) 266–271. DOI:10.1016/0165-9936(84)80044-8.
- [32] N. Ratola, J.M. Amigo, A. Alves, Comprehensive assessment of pine needles as bioindicators of PAHs using multivariate analysis. The importance of temporal trends, *Chemosphere*. 81 (2010) 1517–1525. DOI:10.1016/j.chemosphere.2010.08.031.
- [33] T.G. Weiszburg, K. Gherdán, K. Ratter, N. Zajzon, Z. Bendő, G. Radnóci, Á. Takács, T. Váci, G. Varga, G. Szakmány, Medieval Gilding Technology of Historical Metal Threads Revealed by Electron Optical and Micro-Raman Spectroscopic Study of Focused Ion Beam-Milled Cross Sections, *Anal. Chem*. 89 (2017) 10753–10760. DOI:10.1021/acs.analchem.7b01917.
- [34] T. Ferreira, H. Moreiras, A. Manhita, P. Tomaz, J. Mirão, C.B. Dias, A.T. Caldeira, The liturgical cope of D. Teotónio of Braganza: material characterization of a 16th century pluviale, *Microsc. Microanal.* 21 (2015) 2–14. DOI:10.1017/S1431927614013440.
- [35] Shanafelt Robert, The nature of flag power, *Politics and the Life Sciences*. 27 (2008) 13–27. DOI:10.2990/27_2_13.
- [36] D. Badillo-Sanchez, D. Chelazzi, R. Giorgi, A. Cincinelli, P. Baglioni, Characterization of the secondary structure of degummed *Bombyx mori* silk in modern and historical samples, *Polymer Degradation and Stability*. 157 (2018) 53–62. DOI:10.1016/j.polymdegradstab.2018.09.022.
- [37] C. Miliani, F. Rosi, B.G. Brunetti, A. Sgamellotti, In Situ Noninvasive Study of Artworks: The MOLAB Multitechnique Approach, *Acc. Chem. Res*. 43 (2010) 728–738. DOI:10.1021/ar100010t.
- [38] E. Richardson, G. Martin, P. Wyeth, X. Zhang, State of the art: non-invasive interrogation of textiles in museum collections, *Microchim Acta*. 162 (2008) 303–312. DOI:10.1007/s00604-007-0885-x.
- [39] I. Crina Anca Sandu, M.H. de Sá, M.C. Pereira, Ancient ‘gilded’ art objects from European cultural heritage: a review on different scales of characterization, *Surf. Interface Anal.* 43 (2011) 1134–1151. DOI:10.1002/sia.3740.

Chapter 7. Microanalytical study of the evolution of metals used as decorations on Spanish and Latin-American flags textiles from 16-20th-century preserved at the textile collection of the National Museum of Colombia

- [40] J.M. Madariaga, Analytical chemistry in the field of cultural heritage, *Anal. Methods*. 7 (2015) 4848–4876. DOI:10.1039/C5AY00072F.
- [41] C. King, The King's Flags and Some Others, *The Mariner's Mirror*. 38 (1952) 84–105. DOI:10.1080/00253359.1952.10658112.
- [42] F. Lennard, N. Pollak, C. Lin, W.-P. Chen, Blue flag with yellow tiger? Flags, authenticity and identity, *Journal of the Institute of Conservation*. 36 (2013) 3–17. DOI:10.1080/19455224.2013.744698.
- [43] M. Ballard, R.J. Koestler, C. Blair, N. Indictor, Historical Silk Flags Studied by Scanning Electron Microscopy-Energy Dispersive X-ray Spectrometry, in: *Archaeological Chemistry IV*, American Chemical Society, 1989: pp. 419–428. <http://dx.doi.org/10.1021/ba-1988-0220.ch024> (accessed November 29, 2016).
- [44] K. Tronner, A.G. Nord, J. Sjöstedt, H. Hydman, Extremely Thin Gold Layers on Gilded Silver Threads, *Studies in Conservation*. 47 (2002) 109–116. DOI:10.1179/sic.2002.47.2.109.
- [45] G.M. Ingo, S. Balbi, T. de Caro, I. Fragalà, E. Angelini, G. Bultrini, Combined use of SEM-EDS, OM and XRD for the characterization of corrosion products grown on silver roman coins, *Appl. Phys. A*. 83 (2006) 493–497. DOI:10.1007/s00339-006-3533-0.
- [46] E. Figueiredo, R.J.C. Silva, M.F. Araújo, J.C. Senna-Martinez, Identification of ancient gilding technology and Late Bronze Age metallurgy by EDXRF, Micro-EDXRF, SEM-EDS and metallographic techniques, *Microchim Acta*. 168 (2010) 283–291. DOI:10.1007/s00604-009-0284-6.
- [47] M.C. Bernard, S. Joiret, Understanding corrosion of ancient metals for the conservation of cultural heritage, *Electrochimica Acta*. 54 (2009) 5199–5205. DOI:10.1016/j.electacta.2009.01.036.
- [48] E. Pańczyk, B. Sartowska, L. Waliś, J. Dudek, W. Weker, M. Widawski, The origin and chronology of medieval silver coins based on the analysis of chemical composition, *Nukleonika*. 60 (2015) 657–663. DOI:10.1515/nuka-2015-0108.
- [49] F. Corvo, T. Perez, L.R. Dzib, Y. Martin, A. Castañeda, E. Gonzalez, J. Perez, Outdoor–indoor corrosion of metals in tropical coastal atmospheres, *Corrosion Science*. 50 (2008) 220–230. DOI:10.1016/j.corsci.2007.06.011.
- [50] L. 't Hart, P. Storme, W. Anaf, G. Nuyts, F. Vanmeert, W. Dorriné, K. Janssens, K. de Wael, O. Schalm, Monitoring the impact of the indoor air quality on silver cultural heritage objects using passive and continuous corrosion rate assessments, *Appl. Phys. A*. 122 (2016) 923. DOI:10.1007/s00339-016-0456-2.
- [51] G.E. Dieter, *Mechanical metallurgy*, New York, McGraw-Hill, 1961. <http://archive.org/details/mechanicalmetall00dieter> (accessed July 26, 2019).
- [52] Z.A. Stos-Gale, N.H. Gale, Metal provenancing using isotopes and the Oxford archaeological lead isotope database (OXALID), *Archaeol Anthropol Sci*. 1 (2009) 195–213. DOI:10.1007/s12520-009-0011-6.
- [53] A.-M. Desaulty, P. Telouk, E. Albalat, F. Albarède, Isotopic Ag–Cu–Pb record of silver circulation through 16th–18th century Spain, *PNAS*. 108 (2011) 9002–9007. DOI:10.1073/pnas.1018210108.
- [54] Baker J., Stos S., Waight T., Lead isotope analysis of archaeological metals by multiple-collector inductively coupled plasma mass spectrometry*, *Archaeometry*. 48 (2006) 45–56. DOI:10.1111/j.1475-4754.2006.00242.x.

Supplementary Information

Chapter 7

Supplementary Information Chapter 7

Supplementary Table 1. List of micro samples and its respective analytical method used to study

Sample ID	Iconography	Flag ID	OM	ICP-OES	SEM-EDS	MC-ICP-MS
S1	Spanish Kingdom	97	x			
S2			x			
S8			x	x		
S10			x	x	x	
S12			x			
S15			x			
S16			x			
S17			x		x	
S19			x	x		
S20			x	x		x
S21			x			
S24	Spanish Kingdom	99	x	x		
S25			x			
S26			x	x	x	x
S27			x	x	x	
S28			x			
S30			x			
S32			x	x		
S33			x			
S38	x					
S280	Spanish Kingdom	16	x	x		x
S281			x	x	x	
S55	Spanish Kingdom	17	x	x	x	x
S92	Spanish army	100	x			
S94			x	x		x
S95			x			
S105			x			
S110			x			
S125	Spanish army	101	x	x		
S128			x	x		x
S69	Colombian flag	111	x	x		x
S133	Spanish army	102	x	x	x	x
S134			x			
S135			x	x	x	

PART II. STUDY OF METALS AND DYES AS DECORATION OF SILK TEXTILES

S136			x			
S139			x			
S242	Colombian army	122	x			
S246			x	x		x
S247			x	x	x	
S268	Colombian army	106	x	x	x	
S269			x	x	x	x
S273			x			
S274			x	x	x	
S275			x			
S213	Colombian flag	3044	x			
S215			x			
S216			x	x		x
S217			x	x	x	
S218			x			
S372	Colombian flag	3245	x	x		x
S373			x			
S374			x	x		
S378			x			
S226	Colombian flag	114	x	x	x	
S228			x	x	x	x
S234			x			
S237			x	x	x	
S239			x			
S324	Colombian flag	131	x			
S325			x	x		x
S327			x	x	x	
S290	Family coat of arms (from Peru)	124	x	x		x
S291			x	x		
S293			x			
S294			x	x		
S298			x			
S299			x			
S300			x			
S82			Colombian flag	129	x	x
S90	x					
S340	Colombian flag	3615	x			

Supplementary Information Chapter 7

S347			x	x	x	
S348			x			x
S252	Colombian army	7354	x	x	x	x
S355	Colombian flag	1948	x	x		x
S356			x			
S357			x			
S358			x			
S359			x	x		
S307	Colombian flag	125	x			
S308			x	x		x

OM= Optimal microscopy; ICP-OES= Inductively coupled plasma coupled to Optical emission spectroscopy; SEM-EDS= Scanning Electron Microscopy coupled to Energy dispersive spectroscopy; MC-ICP-MS= Multi collector Inductively coupled plasma coupled to mass spectrometry.

Supplementary information Table 3. Dimensions and description of the meal decoration after optical microscopy analysis.

Sample	Metal Twist	Type	Diameter thread mm	Length strip	Ratio DT/LS	Twist/mm	Internal fiber
S1	S	Strip twisted	0.375	0.542	0.7	1.5	Silk
S2	S	Strip twisted	0.450	0.500	0.9	1.5	Silk
S8	S	Strip twisted	0.443	0.317	1.4	3	Silk
S10	S	Strip twisted	0.416	0.739	0.6	1	Silk
S12	S	Strip twisted	0.563	0.413	1.4	1.5	Silk
S15	S	Strip twisted	0.530	0.579	0.9	1.5	Silk
S16	S	Strip twisted	0.469	0.552	0.8	1	Silk
S17	S	Strip twisted	0.380	0.434	0.9	1.5	Silk
S19	S	Strip twisted	0.438	0.558	0.8	1	Silk
S20	S	Strip twisted	0.457	0.729	0.6	1.2	Silk
S21	S	Strip twisted	0.377	0.658	0.6	1.1	Silk
S24	S	Strip twisted	0.435	0.289	1.5	3	Silk
S25	-	Strip	-	0.736	-	-	-
S26	-	Strip	-	0.753	-	-	-

PART II. STUDY OF METALS AND DYES AS DECORATION OF SILK TEXTILES

S27	-	Strip	-	0.793	-	-	-
S28	S	Strip twisted	0.263	0.326	0.8	2	Silk
S30	S	Strip twisted	0.246	0.318	0.8	2.6	Silk
S32	S	Strip twisted	0.261	0.321	0.8	2	Silk
S33	S	Strip twisted	0.427	0.294	1.5	1.5	Silk
S38	S	Strip twisted	0.240	0.318	0.8	2.8	Silk
S280	S	Strip twisted	0.441	0.376	1.2	3	Silk
S281	S	Strip twisted	0.347	0.285	1.2	3	Silk
S55	-	Strip	-	0.154	-	-	-
S92	S	Strip twisted	0.388	0.306	1.3	2	Silk Double thread
S94	S	Strip twisted	0.327	0.391	0.8	1	Silk
S95	S	Strip twisted	0.378	0.357	1.1	1	Silk
S105	S	Strip twisted	0.365	0.318	1.1	1.5	Silk
S110	S	Strip twisted	0.354	0.376	0.9	4	Silk
S125	S	Strip twisted	0.456	0.398	1.1	2.5	Silk
S128	-	Strip	-	0.819	-	-	-
S69	-	paillette	1.680	-	-	-	-
S133	-	Spring wire	0.798	0.094	8.5	9.5	Silk
S134	-	Spring wire	0.737	0.103	7.2	11	Silk
S135	S	Strip twisted	0.243	0.422	0.6	3	Silk
S136	S	Strip twisted	0.298	0.397	0.8	2	Silk
S139	S	Strip twisted	0.305	0.429	0.7	2	Silk
S242	-	Strip	-	0.306	-	-	-
S246	-	Spring wire	0.590	0.057	10.3	7	Silk
S247	-	paillette	1.939	-	-	-	-
S268	S	Strip twisted	0.313	0.345	0.9	2.5	Silk
S269	-	Wire	-	0.135	-	-	-
S273	-	Strip	-	0.402	-	-	-

Supplementary Information Chapter 7

S274	S	Strip twisted	0.973	0.386	2.5	2.5	Silk
S275	S	Strip twisted	0.390	0.260	1.5	3.5	Silk two twisted threads
S213	-	Wire	-	78.095	-	-	-
S215	-	Strip	-	0.608	-	-	-
S216	-	Wire	-	0.181	-	-	-
S217	-	Spring wire	?	0.166	-	-	-
S218	-	Strip	-	0.261	-	-	-
S372	-	Spring strip	0.694	0.094	7.4	10	Cotton twisted thread
S373	-	Wire	-	0.200	-	-	-
S374	-	Spring strip + Paillette	1.893	-	-	-	Cotton twisted thread
S378	Z	Strip twisted	0.313	0.351	0.9	1.8	Cotton twisted thread
S226	S	Strip twisted	0.471	0.430	1.1	2	Cotton
S228	-	metal	?	?	-	-	-
S234	S	Strip twisted	0.272	0.241	1.1	3.5	Silk
S237	-	Wire	-	0.077	-	-	-
S239	-	-	-	-	-	-	-
S324	-	Strip	-	0.200	-	-	-
S325	Z	Strip twisted	1.149	0.308	3.7	3	Cotton with a laze in Cotton Thick
S327	-	Wire	-	0.109	-	-	-
S290	S	Strip twisted	0.416	0.308	1.4	1	Silk
S291	S	Strip twisted	0.478	0.339	1.4	2	Silk
S293	S	Strip twisted	0.245	0.319	0.8	2	Silk
S294	S	Strip twisted	0.401	0.401	1.0	2	Silk
S298	S	Strip twisted	0.236	0.313	0.8	2	Silk
S299	S	Strip twisted	0.271	0.271	1.0	3	Silk
S300	S	Strip twisted	0.352	0.321	1.1	3	Silk

PART II. STUDY OF METALS AND DYES AS DECORATION OF SILK TEXTILES

S82	-	Spring strip+ Wire	1.215	0.157	7.7	?	Cotton
S90	-	Strip	-	0.274	-	-	-
S340	Z	Strip twisted	0.351	0.241	1.5	1	Cotton
S347	-	Wire	-	0.080	-	-	-
S348	Z	Strip twisted	0.299	0.207	1.4	4	Cotton
S252	-	Spring strip	-	0.154	-	-	-
S355	-	Spring strip	0.725	0.148	4.9	6.5	Silk
S356	-	Strip	-	0.247	-	-	-
S357	-	Spring strip	0.732	0.140	5.2	6.1	-
S358	-	Strip	-	0.128	-	-	-
S359	-	Spring wire	0.726	0.071	10.2	10	Silk
S307	-	Spring wire	0.618	0.058	10.6	16	Silk
S308	-	Spring wire	0.585	0.048	12.2	16	Silk

Supplementary Information Chapter 7

Supplementary Information Table 4. Elements identified by ICP-OES of the subset of metal decorations, results are presented in weight%

Sample	Ag	Al	As	Au	Co	Cr	Cu	Fe	Ir	Ni	Os	Pb	Pd	Pt	Sb	Sn	Ti	Zn	% metal
S8	88.377	0.013	ND	0.712	ND	ND	10.570	ND	ND	0.010	ND	0.144	ND	ND	ND	ND	ND	0.173	77.6
S10	90.036	0.129	ND	0.145	ND	0.095	8.828	0.267	ND	0.096	ND	0.273	ND	ND	ND	ND	ND	0.130	46.0
S19	91.380	0.107	ND	0.052	ND	ND	8.201	ND	ND	ND	ND	0.260	ND	ND	ND	ND	ND	ND	85.5
S20	90.750	0.505	ND	0.149	ND	ND	8.287	0.007	ND	ND	ND	0.267	ND	ND	ND	ND	ND	0.034	70.9
S24	97.591	0.116	ND	1.130	ND	0.004	1.120	ND	ND	ND	ND	0.040	ND	ND	ND	ND	ND	ND	77.0
S26	96.866	0.583	ND	0.798	ND	ND	1.166	0.049	ND	0.017	ND	0.040	ND	ND	ND	ND	ND	0.480	73.7
S27	99.295	0.428	ND	0.061	ND	ND	0.116	ND	ND	ND	ND	0.083	ND	ND	ND	ND	ND	0.017	87.5
S32	99.596	0.224	ND	0.031	ND	ND	0.049	ND	ND	ND	ND	0.029	ND	ND	ND	ND	ND	0.069	86.2
S280	99.554	0.012	ND	0.034	ND	ND	0.277	ND	ND	ND	ND	0.093	ND	ND	ND	ND	ND	0.031	72.7
S281	2.279	0.228	ND	ND	0.009	ND	97.340	0.024	ND	0.104	ND	ND	0.016	ND	ND	ND	ND	ND	106.5
S55	98.072	0.029	ND	1.347	ND	ND	0.102	ND	ND	ND	ND	0.107	ND	ND	ND	0.285	ND	0.057	72.4
S94	99.179	ND	ND	0.077	ND	ND	0.059	ND	ND	ND	ND	0.083	ND	ND	0.124	0.413	ND	0.066	73.7
S125	99.570	0.047	ND	0.004	ND	ND	0.055	ND	ND	0.061	ND	0.263	ND	ND	ND	ND	ND	ND	72.7
S128	97.444	0.030	ND	1.212	ND	0.133	0.393	0.409	ND	0.121	ND	0.136	ND	ND	ND	ND	ND	0.123	78.4
S69	98.251	ND	ND	0.616	ND	ND	1.113	ND	ND	0.001	ND	0.018	0.001	ND	ND	ND	ND	ND	77.9
S133	98.017	0.041	ND	1.551	ND	0.013	0.255	0.058	ND	0.021	ND	0.022	ND	ND	ND	ND	ND	0.021	82.2
S135	97.645	0.078	ND	1.748	0.001	0.012	0.386	0.027	ND	0.017	0.003	ND	ND	ND	ND	ND	ND	0.082	74.8
S246	94.130	0.210	ND	0.401	ND	0.070	1.289	0.253	ND	0.109	ND	0.023	ND	ND	ND	2.918	0.464	0.133	80.9
S247	72.193	0.077	ND	0.640	ND	0.001	26.332	0.712	ND	0.014	ND	0.010	0.007	ND	ND	ND	0.001	0.013	76.4
S268	92.914	0.072	ND	1.511	ND	0.071	5.248	0.055	ND	0.058	ND	0.050	ND	ND	ND	ND	ND	0.022	71.2
S269	93.493	0.407	ND	1.597	ND	ND	4.263	0.044	ND	0.013	0.005	0.049	0.016	0.018	ND	ND	0.003	0.092	76.6

PART II. STUDY OF METALS AND DYES AS DECORATION OF SILK TEXTILES

S274	99.144	0.499	ND	0.094	ND	ND	0.051	0.010	ND	ND	ND	0.170	ND	ND	ND	ND	0.032	87.5	
S216	0.321	0.084	ND	0.275	ND	0.030	98.992	0.027	ND	0.125	ND	0.073	ND	ND	ND	ND	0.073	101.1	
S217	0.220	0.054	ND	0.287	ND	ND	99.264	0.010	ND	0.096	0.001	ND	0.018	ND	ND	ND	0.002	0.047	99.3
S372	96.644	0.186	ND	0.704	ND	0.035	1.518	0.129	ND	0.156	ND	0.009	ND	ND	ND	ND	0.485	0.134	76.8
S374	0.734	0.272	ND	ND	ND	ND	94.732	0.021	3.675	0.107	ND	ND	0.022	ND	ND	ND	0.002	0.435	99.6
S226	0.108	0.150	0.022	0.007	0.002	0.002	98.340	0.132	ND	0.111	ND	0.097	ND	ND	ND	ND	0.016	1.013	99.4
S228	99.123	0.152	ND	0.506	ND	0.005	0.203	0.002	ND	0.009	ND	ND	ND	ND	ND	ND	0.001	ND	74.2
S237	3.269	0.144	ND	0.292	ND	ND	96.167	ND	ND	0.053	ND	ND	0.020	ND	ND	ND	ND	0.055	110.3
S325	1.053	0.289	ND	ND	ND	0.026	93.653	0.210	ND	0.302	ND	0.073	0.020	ND	ND	3.482	ND	0.892	104.0
S327	0.884	0.182	ND	ND	0.004	0.002	98.722	ND	ND	0.115	ND	ND	0.014	ND	ND	ND	0.002	0.076	102.3
S290	0.569	0.109	ND	ND	0.005	ND	98.089	0.059	ND	0.205	ND	0.072	0.026	ND	ND	ND	ND	0.858	102.4
S291	0.670	0.298	ND	0.059	0.008	0.035	97.944	0.455	ND	0.153	ND	ND	0.027	ND	ND	ND	0.003	0.344	86.8
S294	0.728	0.325	ND	ND	0.008	ND	98.733	0.037	ND	0.134	ND	ND	0.012	ND	ND	ND	ND	0.023	105.0
S82	0.339	0.017	0.105	0.010	0.008	0.006	99.303	ND	ND	0.066	0.009	0.042	0.016	ND	ND	ND	0.001	0.076	84.6
S347	97.230	0.197	ND	0.233	ND	0.050	1.322	0.183	ND	0.126	ND	ND	0.007	ND	ND	ND	0.474	0.178	82.3
S252	ND	ND	ND	0.059	ND	ND	94.148	ND	ND	0.014	ND	ND	0.017	ND	ND	ND	0.002	5.760	90.4
S355	97.463	0.108	ND	0.729	ND	0.035	0.631	0.127	ND	0.047	ND	0.239	ND	ND	ND	ND	0.581	0.041	82.6
S359	97.688	0.287	ND	0.728	ND	ND	1.257	ND	ND	ND	ND	ND	ND	ND	ND	ND	ND	0.040	91.7
S308	0.365	0.061	ND	0.373	ND	0.012	97.802	0.050	ND	0.037	ND	0.078	0.019	ND	ND	ND	ND	1.202	99.2

ND= Not detected or under the analytical limit of detection

Supplementary Information Chapter 7

Supplementary Information Table 5. PCA results

	Eigenvalue	Percentage of Variance	Cumulative	Degrees of Freedom
1	4.11384	37.40%	37.40%	65
2	1.82769	16.62%	54.01%	54
3	1.26992	11.54%	65.56%	44
4	1.13176	10.29%	75.85%	35
5	0.83909	7.63%	83.48%	27
6	0.55492	5.04%	88.52%	20
7	0.45143	4.10%	92.62%	14
8	0.40021	3.64%	96.26%	9
9	0.21349	1.94%	98.20%	5
10	0.19752	1.80%	100.00%	2
11	1.22E-04	0.00%	100.00%	0

	Coefficients of PC1	Coefficients of PC2	Coefficients of PC3	Coefficients of PC4	Coefficients of PC5
Ag	-0.47276	0.03019	0.06582	-0.07356	0.06013
Al	0.00921	-0.10419	0.62874	-0.24447	0.67143
Au	-0.27325	0.13408	-0.38611	-0.47473	0.02176
Co	0.32974	0.02309	0.23485	-0.26478	-0.37971
Cr	-0.09191	0.65026	-0.05879	0.1267	0.01652
Cu	0.47218	-0.03571	-0.05615	0.06984	-0.08001

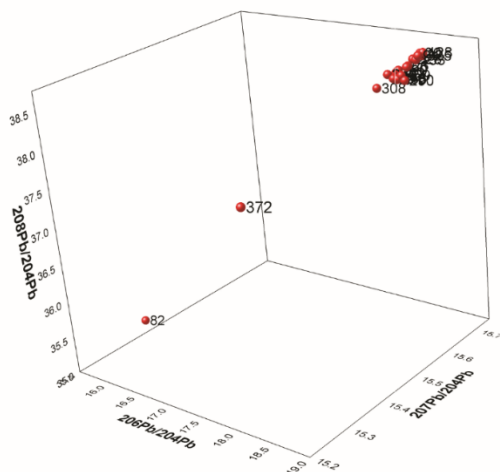
PART II. STUDY OF METALS AND DYES AS DECORATION OF SILK TEXTILES

Fe	0.03666	0.5932	-8.17E-04	-0.06619	0.23435
Ni	0.3171	0.41619	0.14912	0.0437	0.00311
Pb	-0.20293	0.06334	0.36046	0.65464	-0.17432
Pd	0.4322	0.00662	-0.05647	-0.11229	0.11791
Zn	0.17818	-0.12824	-0.48389	0.41348	0.54316

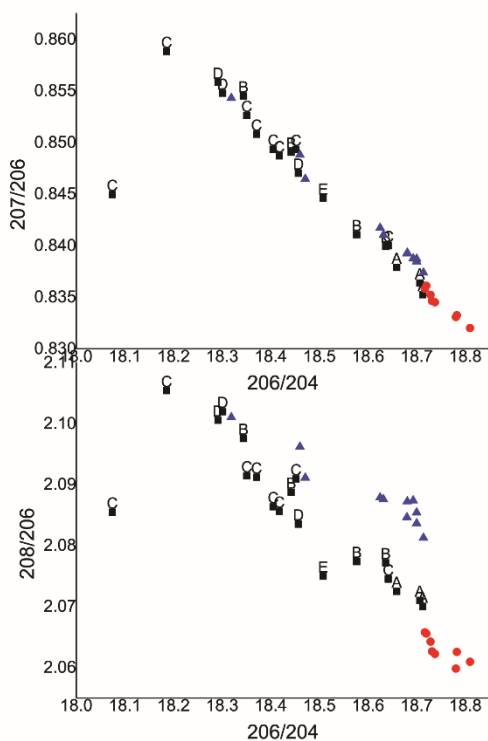
Supplementary Information Chapter 7

Supplementary information Table 6. MC-ICP-MS results of the metal decorations analyzed

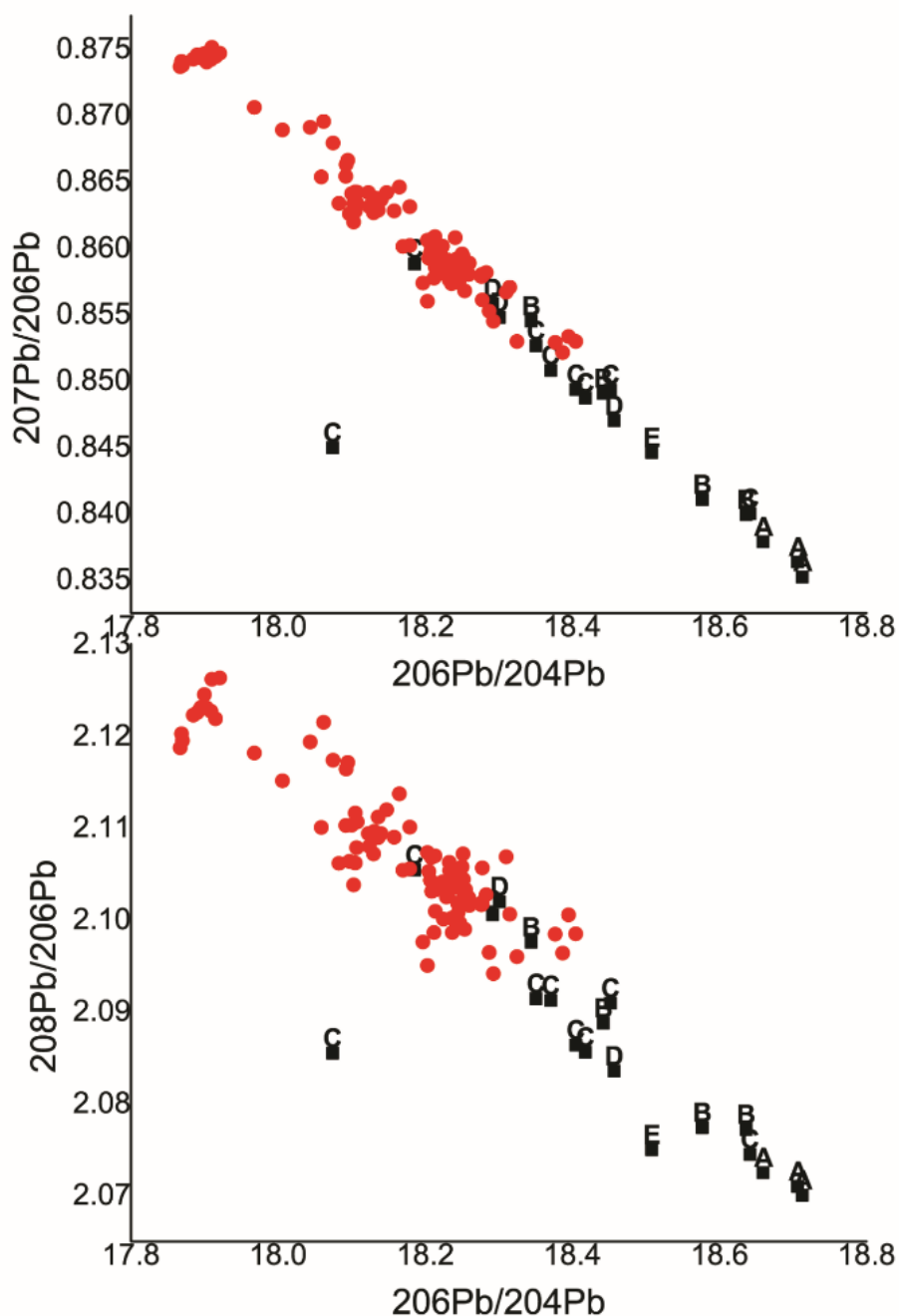
Sample	206Pb/204Pb	± 1σ	207Pb/204Pb	± 1σ	208Pb/204Pb	± 1σ	208Pb/206Pb	± 1σ	207Pb/206Pb	± 1σ
S94	18.712	0.008	15.629	0.006	38.735	0.017	2.0700	0.0008	0.8352	0.0003
S246	18.301	0.032	15.628	0.027	38.457	0.068	2.1020	0.0031	0.8548	0.0013
S252	18.292	0.004	15.654	0.004	38.423	0.010	2.1006	0.0005	0.8558	0.0002
S372	18.074	0.915	15.258	0.773	37.656	1.878	2.0855	0.0905	0.8450	0.0355
S348	18.351	0.003	15.646	0.003	38.379	0.006	2.0914	0.0003	0.8526	0.0001
S26	18.442	0.039	15.658	0.032	38.521	0.078	2.0888	0.0037	0.8490	0.0015
S325	18.641	0.030	15.659	0.026	38.672	0.065	2.0745	0.0030	0.8400	0.0012
S269	18.457	0.016	15.633	0.014	38.455	0.035	2.0835	0.0016	0.8470	0.0007
S55	18.577	0.005	15.624	0.004	38.591	0.011	2.0774	0.0005	0.8411	0.0002
S82	15.842	0.002	15.333	0.002	35.416	0.006	2.2355	0.0003	0.9678	0.0001
S308	18.186	0.023	15.618	0.020	38.289	0.049	2.1054	0.0023	0.8588	0.0010
S355	18.418	0.003	15.631	0.002	38.412	0.006	2.0856	0.0003	0.8487	0.0001
S133	18.659	0.008	15.634	0.007	38.671	0.017	2.0725	0.0008	0.8379	0.0003
S128	18.706	0.003	15.646	0.003	38.741	0.006	2.0710	0.0003	0.8364	0.0001
S20	18.636	0.005	15.653	0.004	38.711	0.010	2.0772	0.0007	0.8399	0.0003
S280	18.344	0.006	15.650	0.006	38.470	0.013	2.0976	0.0010	0.8545	0.0004
S69	18.371	0.169	15.629	0.146	38.414	0.364	2.0912	0.0268	0.8508	0.0105
S216	18.405	0.032	15.632	0.027	38.399	0.064	2.0864	0.0048	0.8493	0.0020
S290	18.508	0.040	15.632	0.035	38.403	0.090	2.0750	0.0063	0.8446	0.0024
S228	18.452	0.090	15.671	0.081	38.581	0.200	2.0909	0.0137	0.8493	0.0054



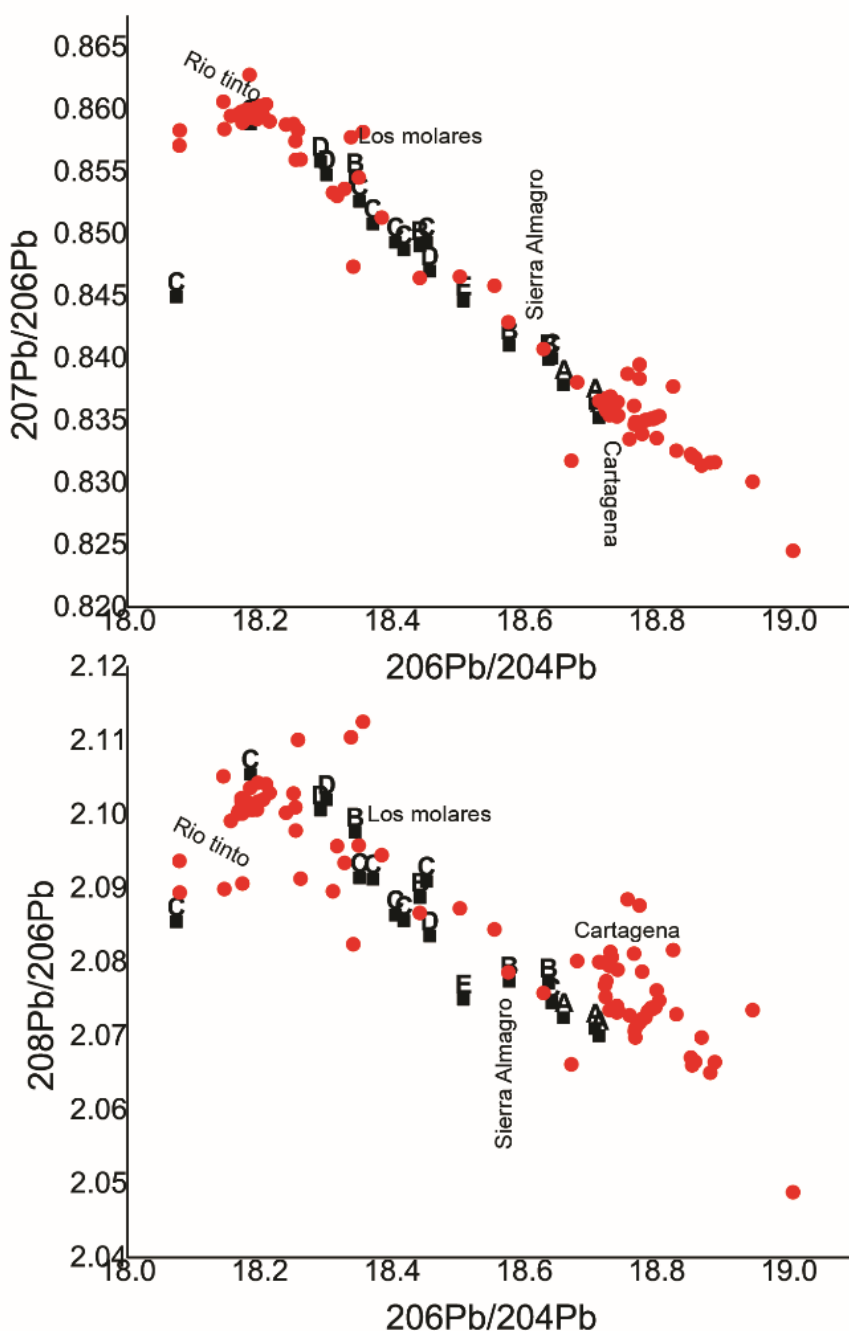
Supplementary Information Figure 3. 3D plot of lead isotope ratios of analyzed samples of metal decorations



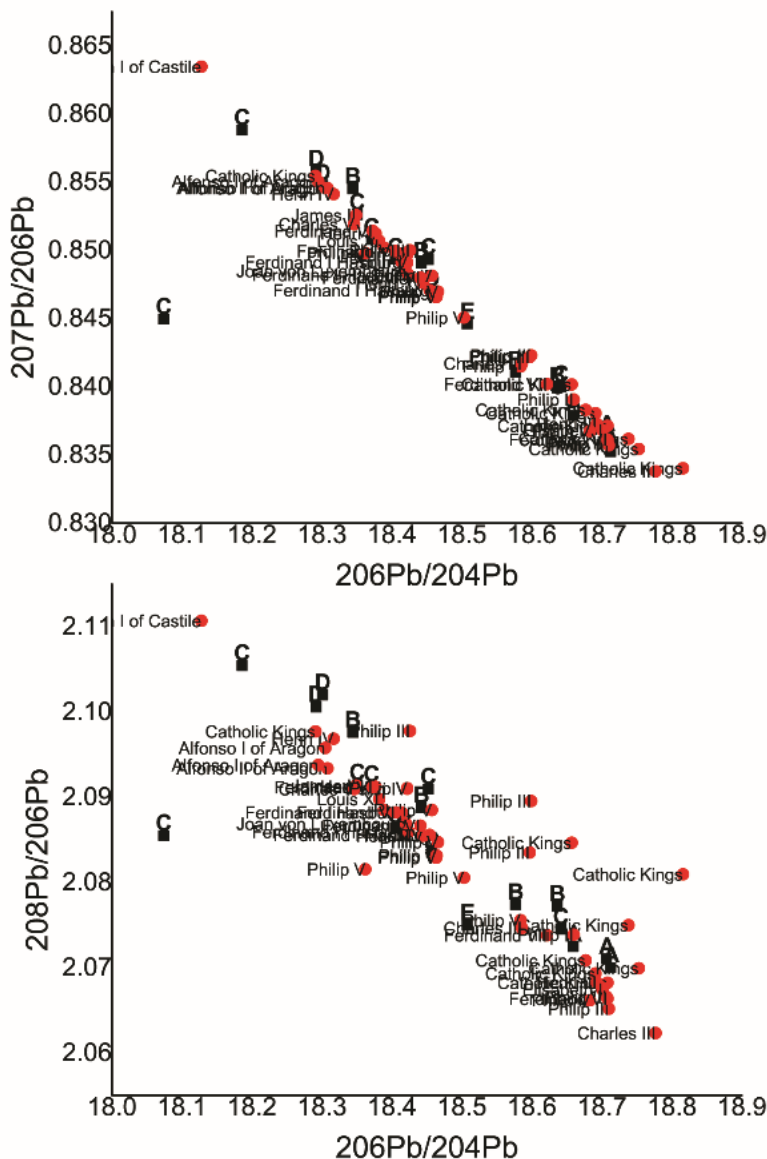
Supplementary Information Figure 4. Isotopic composition of metal decorations on flags from the National Museum of Colombia, and Mexican and Peruvian samples from literature. Top panel, $^{207}\text{Pb}/^{206}\text{Pb}$ vs $^{206}\text{Pb}/^{204}\text{Pb}$. Bottom panel, $^{208}\text{Pb}/^{206}\text{Pb}$ vs $^{206}\text{Pb}/^{204}\text{Pb}$. Labels of the plots describe the iconography of the flag as follows: A=Spanish military, B= Spanish kingdom, C=Colombian flag, D= Colombian army, E= Peruvian coat of arms. Triangle=Peruvian literature samples; Square= metal decorations analyzed; Circle= Mexican literature samples.



Supplementary Information Figure 5. Isotopic composition of metal decorations on flags from the National Museum of Colombia, and Italian samples from literature. Top panel, $^{207}\text{Pb}/^{206}\text{Pb}$ vs $^{206}\text{Pb}/^{204}\text{Pb}$. Bottom panel, $^{208}\text{Pb}/^{206}\text{Pb}$ vs $^{206}\text{Pb}/^{204}\text{Pb}$. Labels of the plots describe the iconography of the flag as follows: A=Spanish military, B= Spanish kingdom, C=Colombian flag, D= Colombian army, E= Peruvian coat of arms. Square= metal decorations analyzed; Circle= Spanish literature samples.



Supplementary Information Figure 6. Isotopic composition of metal decorations on flags from the National Museum of Colombia, and Spanish samples from literature. Top panel, $207\text{Pb}/206\text{Pb}$ vs $206\text{Pb}/204\text{Pb}$. Bottom panel, $208\text{Pb}/206\text{Pb}$ vs $206\text{Pb}/204\text{Pb}$. Labels of the plots describe the iconography of the flag as follows: A=Spanish military, B= Spanish kingdom, C=Colombian flag, D= Colombian army, E= Peruvian coat of arms. Square= metal decorations analyzed; Circle= Spanish literature samples.



Supplementary Information Figure 7. Isotopic composition of metal decorations on flags from the National Museum of Colombia, and Spanish kingdom objects from literature. Top panel, $^{207}\text{Pb}/^{206}\text{Pb}$ vs $^{206}\text{Pb}/^{204}\text{Pb}$. Bottom panel, $^{208}\text{Pb}/^{206}\text{Pb}$ vs $^{206}\text{Pb}/^{204}\text{Pb}$. Labels of the plots describe the iconography of the flag as follows: A=Spanish military, B= Spanish kingdom, C=Colombian flag, D= Colombian army, E= Peruvian coat of arms. Square= metal decorations analyzed; Circle= Spanish literature samples.

Chapter 8.

Spectroscopic study of dyes of the flags of the textile collection of the National Museum of Colombia

Abstract

Dyes have been used to transform the appearance of textiles since prehistoric times. Dyes were used in flags and emblems to produce the specific iconography needed to transmit the information on it. In an American context, the iconography of flags and emblems suffered a transformation from the representation of the Spanish Kingdom until the newborn republics. By using Fiber Optics Reflectance Spectroscopy was studied a large set of flags and emblems of the textile collection of the National Museum of Colombia to investigate the use of dyes in objects related to Europe and America in the frame of time of the 16th to 20th century. Cochineal, brazilwood and madder were identified as red dyes, Prussian blue and indigo were identified as blue dyes, meanwhile yellow dyes were just ascribable to natural dyes.

8.1. Introduction

Textile artifacts have been used since prehistoric times, where some of them have survived through time, carrying with them socio-cultural information, as well technological and technical information about previous societies [1]. Those objects which can reflect some part of the past and transfer to new generations a cultural meaning, are denoted as cultural heritage objects, being relevant their study, preservation, and save through the combination of different disciplines [2–5]. One of those textile objects are the flags/banners used for different societies as a mean for non-verbal communication [6–10].

Textiles are manufactured mainly by fiber threads weaved among them in weft and warps in different combinations, transforming a linear material in a bidimensional object [2,11,12]. This transformation is sometimes accompanied with the introduction of some decorative elements which change the appearance of the material in a deeper way, as the case of the use of dyes, pigments or metals [13–15]. In the case of dyes, the change over the material is mainly perceived as a change in the color of the textile, which can be durable, or being as well transformed after ageing [16–20].

Dyes have been used since prehistoric time, first by the use of molecules extracted from animal or vegetable resources, and in more recent times through the use of synthetic chemical products [15,21–26]. Dyes study can allow to understand the economical exchange, immigrational processes, understand the value of the object for the elements employed on its manufacture, or to gain knowledge about its degradation [8,27–32].

By using a large set of flags from the textile collection of the National Museum of Colombia, it is intended to elucidate how was or was not, the

transition on the use of dyes to elaborate the different flags which represent the different historical periods of the north of south America, transforming silk textiles in different colors, shapes and iconographies to transmit the idea of power, nation and culture on their societies.

8.2. Materials and methods

8.2.1. Historical samples

35 flags corresponding to five centuries of Latin-American history coming from the textile collection of the National museum of Colombia were sampled by the experts of the museum obtaining a total of 244 micro samples, presenting them the different colors on the textiles, mainly yellow, blue and red, with some of them, black, orange, purple and green.

8.2.2 Fiber Optics Reflectance Spectroscopy (FORS).

FORS analysis was performed to identify dyes on the silk fibers, using a portable optical fiber spectrophotometer Prime™ X (B&W Tec Inc., Newark, DE, USA) with a back-thinned CCD array detector (1024 pixel), connected to a Deuterium/Tungsten light source and a bifurcated fiber reflectance probe that combines optical fibers (7 fibers, $\varnothing = 200 \mu\text{m}$ each). Spectra were collected for each sample in the 200-900 nm interval, avoiding areas affected by noticeable defects; a 99 % Teflon diffuse reflectance metrological standard from BW Tech (Newark, DE, USA) was employed for calibration. Each spectrum was collected averaging 50 cycles of 50 ms each to enhance S/N; both incident and acquisition angles are perpendicular to the surface. A dedicated software (BWSpec 3.27 by B&W Tec Inc.) was used for spectra acquisition and colorimetric data collection.

Spectra collected were compared with those reported in the literature for the identification of dyes [33–36].

8.3. Results and discussion

The different microsamples were measured through the FORS instrument obtaining their LABS value and their respective spectra between 200 and 950 cm^{-1} . Labs values are plotted on Figure 1. after a PCA model, showing that the samples are grouped according with their color, suggesting that the perceptible color (the resultant reflected light over the textile and later perceived by the eye) of the sample it corresponds to the actual spectral color of the sample (the resultant shift of the light wavelength by the physical interaction between the light and the chemical composition of the material) [37].

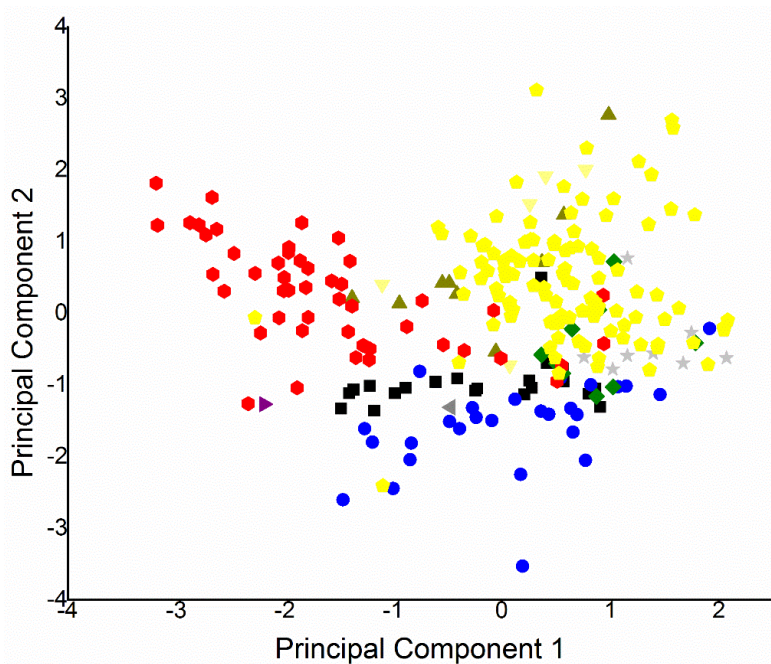


Figure 1 PCA model for LABS results over historical micro samples

FORS measurements allowed to identify the dyes used to color the blue and red samples (See Supplementary information table 1), nevertheless, as it is well known the yellow spectra achieved are not possible to be used to discriminate a possible source for those dyes.

Blue color was mainly present on American flags, as due to was selected as one of the representative colors to describe the new republics i.e. Colombia, Ecuador and Venezuela; meanwhile it was scarcely found on the textiles with European iconography. The FORS spectra allowed to postulate that for blue dyeing Indigo, and Prussian blue was used (See Figure 2.). In the same way, it was noticed that Prussian blue was used only after the 19th century, only on those samples with American iconography, in contrast with the indigo one, which were found in both (American and European) during all the frame time studied here.

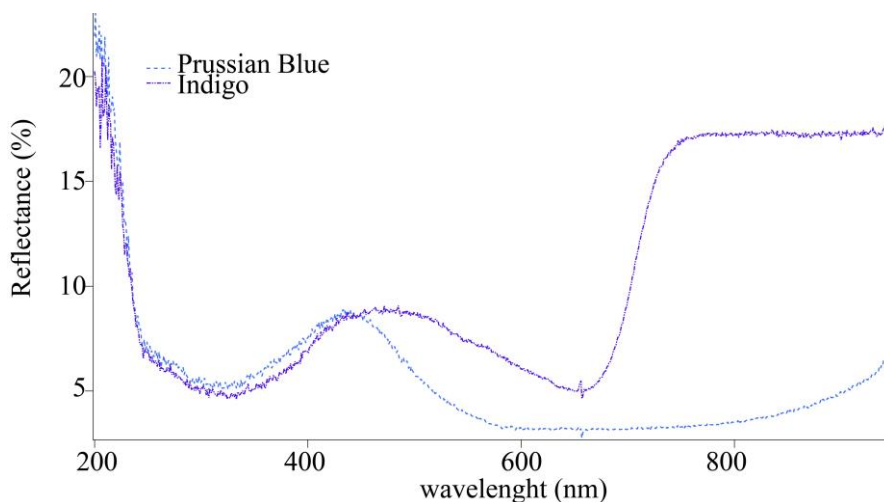


Figure 2 Example of FORS Spectra of blue dyes present on the silk textiles. The spectra match with reference spectra of, respectively, Indigo and Prussian blue, reported in the literature

Red color was present on most of the textiles during all the studied time. FORS spectra could be associated to three different sources Brazil Wood,

Chapter 8. Spectroscopic study of dyes of the flags of the textile collection of the National Museum of Colombia

cochineal and Madder (See Figure 3.). Cochineal and madder are found in samples both European and American from all times, meanwhile, brazilwood were just found in American samples since the first quarter of the 19th century.

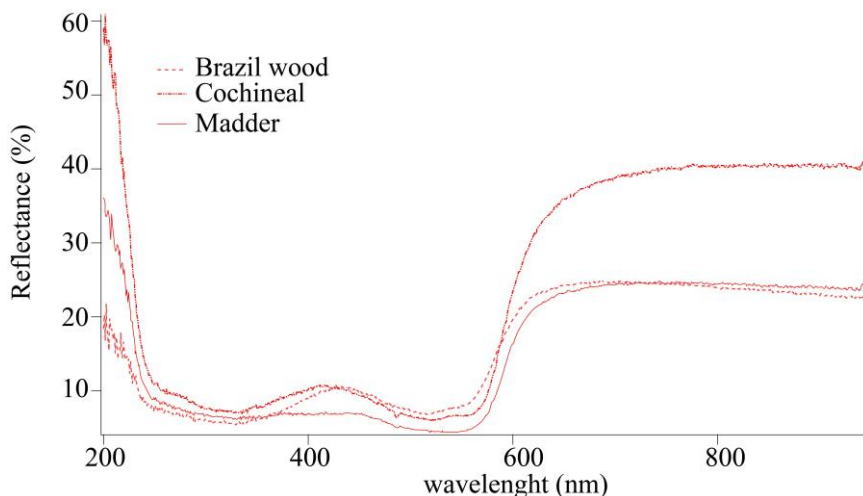


Figure 3 Example of FORS Spectra of red dyes present on the silk textiles. The spectra match with reference spectra of, respectively, Cochineal, Brazil wood, and red madder, reported in the literature

Yellow samples were present on almost all samples, from European as well American iconography. It is important to underline that even if the samples presented a coloration, it is not possible to postulate directly that a dye was applied on the original textile, this due to silk on their natural ageing process, it suffers a yellowing, which transforms its white appearance to more yellowish tones. FORS spectra on yellow samples does not lead on positive identification of a possible dye source (See Figure 4.), this due to the FORS spectra of yellow dyed samples presents similar shapes, as the molecule which produce the color on different dyes could present similar spectra. Nevertheless, the FORS spectra obtained indicated that only natural plant dyes were used, maybe of flavonoid sources.

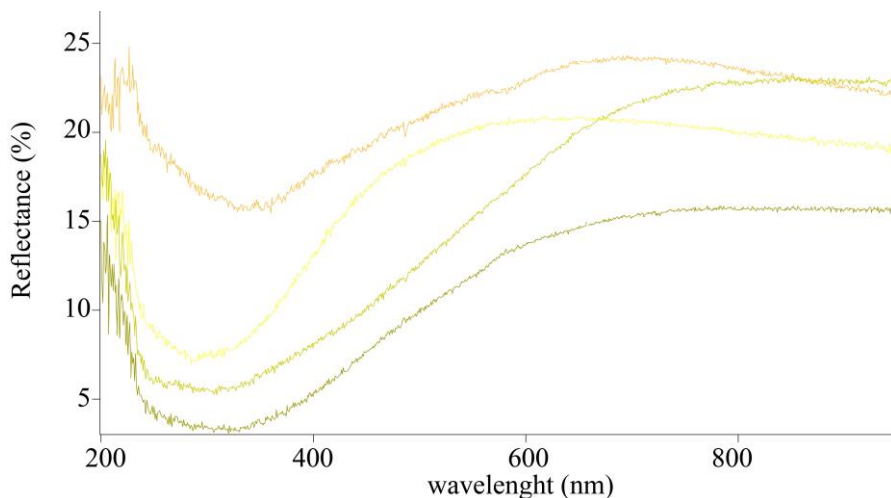


Figure 4 Example of FORS Spectra of yellow dyes present on the silk textiles. Even though it was not possible to unequivocally identify the yellow dyes by FORS, their spectra resemble those of some natural dyes commonly and historically used, such as hydroxy and methoxy derivatives of flavones and isoflavones, dihydropyrans, anthocyananidins and carotenoids

Green and purple samples showed similar spectra with the blue samples dyed with Indigo, indicating the possible use of this blue dye as part of the process to obtain the secondary colors on the textiles (See Figure 5). Black samples did not show a spectral result which could lead on a positive identification.

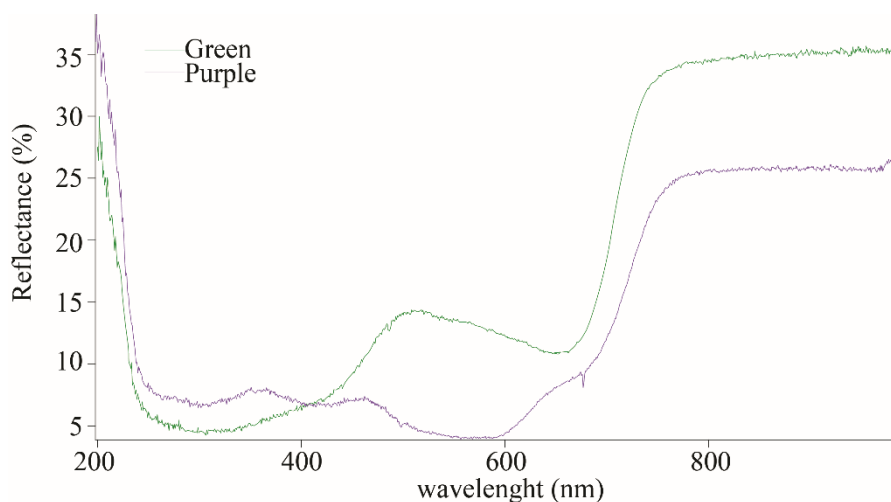


Figure 5 Example of FORS Spectra of green and purple hues on silk textiles. Both present the use of Indigo plus another dye to achieve the final color; purple hue uses a red dye; meanwhile green uses a yellow dye.

8.4. Conclusions

By using FORS was possible to identify the red and blue dyes used on the manufacture of the different objects studied. It was no evidenced the use of native American compounds for dyeing on the manufacture of the flags or emblems, except by those controlled, and produced by Europeans at the time (cochineal, indigo and brazil wood).

A change on the use of red dyes across time was found, showing that older textiles have been mainly dyed with cochineal, meanwhile, most recent ones use for the same purpose brazilwood. Blue colors were obtained using mainly Indigo, but it was proof how in the 19th century Prussian blue was introduced.

Yellow dyes were characterized as natural dyes, being necessary to continue the research on them using other analytical techniques.

Secondary colors were achieved through the double dyeing of two principal colors of the fibers.

References

- [1] D. Cardon, Colours in Civilizations of the World and Natural Colorants: History under Tension, in: T. Bechtold, R. Mussak (Eds.), Handbook of Natural Colorants, John Wiley & Sons, Ltd, 2009: pp. 21–26. <http://onlinelibrary.wiley.com/doi/10.1002/9780470744970.ch2/summary> (accessed March 31, 2016).
- [2] P. Garside, 10 - Durability of historic textiles A2 - Annis, Patricia A., in: Understanding and Improving the Durability of Textiles, Woodhead Publishing, 2012: pp. 184–204. <http://www.sciencedirect.com/science/article/pii/B978085709087450010X> (accessed March 7, 2016).
- [3] A. Choudhary, M. Mausom, Conservation of Cultural Heritage: The Necessities, Trends, and the Analysis of Current Practices, in: Understanding Built Environment, Springer, Singapore, 2017: pp. 15–28. doi:10.1007/978-981-10-2138-1_2.
- [4] E. Varella, Conservation Science for the Cultural Heritage, Springer, 2012.
- [5] P. Frediani, M. Frediani, L. Rosi, eds., Cultural Heritage: Protection, Developments and International Perspectives, Nova Science Pub Inc, New York, 2013.
- [6] K.A. Cerulo, Symbols and the world system: National anthems and flags, Sociol Forum. 8 (1993) 243–271. doi:10.1007/BF01115492.
- [7] B. Karl, Silk and Propaganda — Two Ottoman Silk Flags and the Relief of Vienna, 1683, Textile History. 45 (2014) 192–215. doi:10.1179/0040496914Z.00000000047.
- [8] D. Hobbs, Royal Ships and Their Flags in the Late Fifteenth and Early Sixteenth Centuries, The Mariner's Mirror. 80 (1994) 388–394. doi:dye.
- [9] M. Ballard, R.J. Koestler, C. Blair, N. Indictor, Historical Silk Flags Studied by Scanning Electron Microscopy-Energy Dispersive X-ray Spectrometry, in: Archaeological Chemistry IV, American Chemical Society, 1989: pp. 419–428. <http://dx.doi.org/10.1021/ba-1988-0220.ch024> (accessed November 29, 2016).
- [10] Shanafelt Robert, The nature of flag power, Politics and the Life Sciences. 27 (2008) 13–27. doi:10.2990/27_2_13.
- [11] M.M. Houck, 2 - Ways of identifying textile fibers and materials, in: Identification of Textile Fibers, Woodhead Publishing, 2009: pp. 6–26. <http://www.sciencedirect.com/science/article/pii/B9781845692667500027> (accessed March 7, 2016).
- [12] M.E. King, Analytical Methods and Prehistoric Textiles, American Antiquity. 43 (1978) 89–96. doi:10.2307/279636.
- [13] E. Yi, J.-Y. Cho, Color analysis of natural colorant-dyed fabrics, Color Res. Appl. 33 (2008) 148–157. doi:10.1002/col.20390.
- [14] M. Járó, Metal Threads in Historical Textiles, in: Molecular and Structural Archaeology: Cosmetic and Therapeutic Chemicals, Springer, Dordrecht, 2003: pp. 163–178. doi:10.1007/978-94-010-0193-9_15.
- [15] M. Martelli, The Alchemical Art of Dyeing: The Fourfold Division of Alchemy and the Enochian Tradition, in: S. Dupré (Ed.), Laboratories of Art, Springer International Publishing, 2014: pp. 1–22. http://link.springer.com.ezproxy.uniandes.edu.co:8080/chapter/10.1007/978-3-319-05065-2_1 (accessed November 19, 2014).
- [16] V. Rubeziene, S. Varnaite, J. Baltusnikaite, I. Padleckiene, 6 - Effects of light exposure on textile durability A2 - Annis, Patricia A., in: Understanding and Improving the Durability of Textiles, Woodhead Publishing, 2012: pp. 104–125. <http://www.sciencedirect.com/science/article/pii/B9780857090874500068> (accessed November 28, 2016).
- [17] M.D. Teli, 4 - Advances in the dyeing and printing of silk A2 - Basu, Arindam, in: Advances in Silk Science and Technology, Woodhead Publishing, 2015: pp. 55–79. <http://www.sciencedirect.com/science/article/pii/B9781782423119000045> (accessed March 7, 2016).
- [18] T.H. Morton, Apparent Colour Yield in Dyed Textiles, Journal of the Society of Dyers and Colourists. 92 (1976) 149–157. doi:10.1111/j.1478-4408.1976.tb03282.x.

Chapter 8. Spectroscopic study of dyes of the flags of the textile collection of the National Museum of Colombia

- [19] M.P. Colombini, A. Andreotti, C. Baraldi, I. Degano, J.J. Łucejko, Colour fading in textiles: A model study on the decomposition of natural dyes, *Microchemical Journal*. 85 (2007) 174–182. doi:10.1016/j.microc.2006.04.002.
- [20] M. Bide, Dyeing, in: *Kirk-Othmer Encyclopedia of Chemical Technology*, John Wiley & Sons, Inc., 2000. <http://onlinelibrary.wiley.com/doi/10.1002/0471238961.0425051907121522.a01.pub2/abstract> (accessed March 31, 2016).
- [21] A. Thomson, The Dyeing of Natural Silk, *Journal of the Society of Dyers and Colourists*. 44 (1928) 202–205. doi:10.1111/j.1478-4408.1928.tb01504.x.
- [22] R.S. Blackburn, Natural dyes in madder (*Rubia* spp.) and their extraction and analysis in historical textiles, *Coloration Technol*. 133 (2017) 449–462. doi:10.1111/cote.12308.
- [23] H.T. Linh, Natural Dyes in Eastern Asia (Vietnam and Neighbouring Countries), in: T. Bechtold, R. Mussak (Eds.), *Handbook of Natural Colorants*, John Wiley & Sons, Ltd, 2009: pp. 65–72. <http://onlinelibrary.wiley.com/doi/10.1002/9780470744970.ch6/summary> (accessed March 31, 2016).
- [24] M. Yusuf, M. Shabbir, F. Mohammad, Natural Colorants: Historical, Processing and Sustainable Prospects, *Nat Prod Bioprospect*. 7 (2017) 123–145. doi:10.1007/s13659-017-0119-9.
- [25] R.A.M. Mussak, T. Bechtold, Natural Colorants in Textile Dyeing, in: T. Bechtold, R. Mussak (Eds.), *Handbook of Natural Colorants*, John Wiley & Sons, Ltd, 2009: pp. 315–337. <http://onlinelibrary.wiley.com/doi/10.1002/9780470744970.ch18/summary> (accessed March 31, 2016).
- [26] Z.C. Koren, Modern Chemistry of the Ancient Chemical Processing of Organic Dyes and Pigments, in: *Chemical Technology in Antiquity*, American Chemical Society, 2015: pp. 197–217. <http://dx.doi.org/10.1021/bk-2015-1211.ch007> (accessed November 22, 2016).
- [27] E.A. Strand, K.M. Frei, M. Gleba, U. Mannering, M.-L. Nosch, I. Skals, Old Textiles — New Possibilities, *European Journal of Archaeology*. 13 (2010) 149–173. doi:10.1177/1461957110365513.
- [28] D. Das, D.B. Datta, P. Bhattacharya, Simultaneous Dyeing and Finishing of Silk Fabric With Natural Color and Itaconic Acid, *Clothing and Textiles Research Journal*. 32 (2014) 93–106. doi:10.1177/0887302X14520964.
- [29] D.A. Badillo-Sanchez, C.B. Dias, A. Manhita, N. Schiavon, The National Museum of Colombia's "Francisco Pizarro's Banner of Arms": A multianalytical approach to help uncovering its history, *Eur. Phys. J. Plus*. 134 (2019) 224. doi:10.1140/epjp/i2019-12747-2.
- [30] P. Velmurugan, A. TamilSelvi, P. Lakshmanaperumalsamy, J. Park, B.-T. Oh, The use of cochineal and *Monascus purpureus* as dyes for cotton fabric, *Coloration Technol*. 129 (2013) 246–251. doi:10.1111/cote.12032.
- [31] J. Liu, D. Guo, Y. Zhou, Z. Wu, W. Li, F. Zhao, X. Zheng, Identification of ancient textiles from Yingpan, Xinjiang, by multiple analytical techniques, *Journal of Archaeological Science*. 38 (2011) 1763–1770. doi:10.1016/j.jas.2011.03.017.
- [32] S. Geissler, Economic Aspects of Natural Dyes, in: T. Bechtold, R. Mussak (Eds.), *Handbook of Natural Colorants*, John Wiley & Sons, Ltd, 2009: pp. 367–384. <http://onlinelibrary.wiley.com/doi/10.1002/9780470744970.ch21/summary> (accessed March 31, 2016).
- [33] M.A. Maynez-Rojas, E. Casanova-González, J.L. Ruvalcaba-Sil, Identification of natural red and purple dyes on textiles by Fiber-optics Reflectance Spectroscopy, *Spectrochimica Acta Part A: Molecular and Biomolecular Spectroscopy*. 178 (2017) 239–250. doi:10.1016/j.saa.2017.02.019.
- [34] M. Bacci, Fibre optics applications to works of art, *Sensors and Actuators B: Chemical*. 29 (1995) 190–196. doi:10.1016/0925-4005(95)01682-1.
- [35] L. de Ferri, R. Tripodi, A. Martignon, E.S. Ferrari, A.C. Lagrutta-Diaz, D. Vallotto, G. Pojana, Non-invasive study of natural dyes on historical textiles from the collection of Michelangelo Guggenheim, *Spectrochimica Acta Part A: Molecular and Biomolecular Spectroscopy*. 204 (2018) 548–567. doi:10.1016/j.saa.2018.06.026.
- [36] C. Montagner, M. Bacci, S. Bracci, R. Freeman, M. Picollo, Library of UV–Vis–NIR reflectance spectra of modern organic dyes from historic pattern-card coloured papers, *Spectrochimica Acta Part A: Molecular and Biomolecular Spectroscopy*. 79 (2011) 1669–1680. doi:10.1016/j.saa.2011.05.033.
- [37] Lee, D., 2010. *Nature's Palette: The Science of Plant Color*. University of Chicago Press.

Supplementary Information

Chapter 8

Supplementary Information Chapter 8

Supplementary Table 1. FORS results for micros samples

Date	lc	Flag	Sample	L*	a*	b*	B	Y	R	Bk	G	P	Br	W	
1538	CS	3305	310	60.08	1.251	7.478		YA							
1538		3305	311	46.7	-4.982	-3.663	Ind								
1538		3305	312	51.51	-3.135	-0.492	Ind								
1538		3305	313	23.75	1.74	2.697			Mad						
1538		3305	314	60.45	-1.438	32.527		YE							
1538		3305	316	55.3	4.194	18.198								YC	
1538		3305	317	35.99	30.188	4.488			Coc						
1538		3305	318	39.47	-7.263	6.135						Ind+			
1538		3305	319	71.95	-1.551	6.158		YC							
1538		3305	320	71.44	-4.781	3.015						Ind+			
1538		3305	321	53.56	-0.02	-0.206					A				
1538		3305	322	50.82	9.148	11.89			YF						
1550	CS	97	3	37.96	15.259	8.105			Mad						
1550		97	5					YF							
1550		97	6	44.11	-6.457	-11.464	Ind								
1550		97	7	34.43	0.086	-0.772				A					
1550		97	9	40.76	-3.518	2.648				A					
1550		97	11	25.61	9.467	-5.274			Coc						
1550		97	13					YG							
1550		97	14						Coc						
1550		97	18							A					
1550		97	22										Ind+c oc		
1700	CS	99	23 a	35	17.727	6.185			Coc						
1700		99	23 r	46.47	11.387	12.924									
1700		99	29	49.98	-0.284	23.183		YE							
1700		99	31	19.37	0.204	-0.721				A					
1700		99	34	61.73	-0.908	6.601		YA							
1700		99	35y	49.84	-2.22	12.39		YF							
1700		99	35g	42.82	-7.678	9.589					Ind				
1700		99	36	36.8	27.097	3.377									
1700		99	37	34.26	18.696	-1.101			Coc						
1700		99	39	69.64	-1.879	-2.027		W?							
1700		CS	116	277	58.23	0.673	6.224		YA						
1700	116		278	37.28	16.119	4.995			Coc						

PART II. STUDY OF METALS AND DYES AS DECORATION OF SILK TEXTILES

1700		116	282	51.11	-0.416	5.983		YA						
1700		116	283	59.26	-2.429	4.836		YA						
1700		116	284	33.71	12.917	6.533			Coc					
1700		116	287	28.75	12.659	0.729			Mad					
1790	CS	109	49	33.73	20.332	5.776			Coc					
1790		109	50b	23.28	-0.777	-3.096				Ma d				
1790		109	50g	47.39	3.632	20.834								
1790		109	50r	34.26	19.518	11.726			Mad					
1790		109	51	58.02	-0.846	6.247		YA						
1808	CS	117	52	32	17.842	3.357			Coc					
1808		117	53	34.46	8.188	-0.199				A				
1808		117	54	49.95	4.221	12.278		YB						
1808		117	56	32.82	8.051	0.529			Mad					
1808		117	57	45.21	2.467	12.194		YB						
1808	CS	118	191	37.91	3.21	12.538		YB						
1808		118	192	31.79	21.313	4.063			Coc					
1808		118	193	50.37	0.999	10.178		YB						
1808		118	194	70.89	-3.117	-4.992	Ind							
1808		118	195	65.9	-4.114	2.606		YC						
1808		118	199	50.85	4.914	17.234		YA						
1808		118	200	42.31	4.052	15.526		YA						
1813	MS	103	142	42.13	5.764	15.884		YB						
1813		103	143	45.69	1.413	8.376		YB						
1813		103	144	55.29	1.021	5.734		YB						
1813		103	145	44.44	0.65	8.582		YB						
1813		103	146	55.96	-0.345	-2.828			Mad					
1813		103	147	37.87	17.712	-0.956			Coc					
1813		103	151	59.7	-3.398	6.093		YC						
1813		103	153	54.68	0.318	5.754							YC	
1813		103	154	54.01	-6.117	-1.819					Ind			
1813		103	155	62.24	-2.932	21.761		YC						
1813	MS	104	159g	35.68	-1.618	-3.567								
1813		104	159y	36.99	1.608	10.442		YA						
1813		104	161	18.32	-0.05	-2.58				A				
1813		104	162	51.45	2.787	9.432		YA						
1813		104	163	52.26	1.116	33.992							Y	
1813		104	164	63.93	-1.29	2.746		YB						

Supplementary Information Chapter 8

1813		104	165	46.69	18.535	-0.778			Coc				
1813		104	166	40.62	-0.822	-2.188				A			
1813		104	167	50.42	2.14	13.177						YC	
1813		104	168	33.73	25.086	-0.536			Coc				
1813		104	169	44.29	0.04	7.357		YB					
1813		104	170	53.1	-3.946	15.961					Ind+		
1815	MS	100	91	51.71	-0.642	6.447		YB					
1815		100	93	52.81	-1.468	0.534					Ind+		
1815		100	96	23.1	0.429	-0.209				A			
1815		100	97	50.24	-0.619	-3.923				A			
1815		100	98	42.12	-0.121	-2.419				A			
1815		100	99	55.73	-0.396	-1.682		W?					
1815		100	100	53.91	0.715	4.895		YA					
1815		100	103	45.88	3.586	13.086		YB					
1815		100	104	33.02	26.433	1.219			Coc				
1815		100	106	25.02	6.361	8.85						YC	
1815		100	107	41	2.14	12.978		YD					
1815		100	108	42.12	15.434	-2.292			Coc				
1815		100	109	55.96	-0.668	-1.56					Ind		
1815	MS	101	111	44.47	1.318	12.478		YA					
1815		101	113	43.77	0.151	2.426						YA	
1815		101	116	59.62	-2.02	-4.18				A			
1815		101	118	34.34	13.051	4.337			Coc				
1815		101	120	19.7	0.036	-0.188				A			
1815		101	121	65.06	1.606	31.565		YC					
1815		101	122	60.09	2.451	18.412		YA					
1815		101	123	28.06	-0.581	-0.521				A			
1815		101	126	49.84	1.095	16.177		YA					
1815		101	127	49.23	-1.256	-1.568							
1815		101	129	78.18	-3.549	4.811		YB					
1815	CS	115	201	27.9	-6.468	-2.268	Pr b						
1815		115	202	52.54	3.558	22.718		YA					
1815		115	203	33.32	19.38	7.771			Mad				
1815		115	204	47.4	3.812	13.504		YB					
1815		115	205	43.04	1.303	9.696		YB					
1815		115	207	41.87	0.21	6.342		YB					
1823	MA	107	40	35.15	1.244	10.841						YC	

PART II. STUDY OF METALS AND DYES AS DECORATION OF SILK TEXTILES

1823		107	41	52.78	0.983	15.431		YA						
1823		107	42g	53.17	6.206	22.778								
1823		107	42b	25.58	-1.038	-0.766				A				
1823		107	44	33.46	19.052	4.412			Coc					
1823		107	45	52.77	-0.32	6.146		YA						
1823		107	46	54.1	-7.085	-10.295	Pr b							
1823		107	47	36.89	3.447	11.106							Br	
1823		107	48	43.99	3.813	24.156		YC						
1824	CA	111	59	34.11	15.054	11.863			Mad					
1824		111	60	25.23	-5.116	-7.976	Pr b							
1824		111	61	46.61	1.61	16.945		YB						
1824		111	62	54.89	2.598	14.033		YA						
1824		111	64	77.01	-4.055	4.176		YC						
1824		111	65	55.21	1.041	4.772		YA						
1824		111	66	61.58	2.897	-2.95			Mad					
1824		111	67	62.95	-2.43	-3.348					Ind+			
1824		111	68	57.27	-3.235	1.672		YG						
1824	MS	102	131	57.38	-0.847	8.333		YA						
1824		102	132	32.58	-5.078	-4.475	Ind							
1824		102	138	52.35	-0.536	2.341		YB						
1824		102	140	60.6	-1.465	-0.759		YB						
1824	MA	105	261	28.35	16.746	-1.584			Coc					
1824		105	262	64.59	-2.876	-3.208	Pr b							
1824		105	263	44.54	-8.886	12.66					Ind+			
1824	MA	122	241	30.93	34.314	10.219			BW					
1824		122	243	57.66	-0.578	6.99		YC						
1824		122	244	62.34	3.525	19.939		YC						
1824		122	245	52.32	0.365	8.304		YB						
1824		122	248	54.11	-0.566	6.339		YB						
1824		122	249	53.61	-4.924	-4.947	Ind							
1824		122	b122w	65.28	1.744	12.232								
1824		122	b122b	38.7	-12.84	-20.425	Ind							
1824		122	b122y	55.78	11.578	31.795		YC						
1824	MA	106	266	34.7	-5.21	-3.069	Ind							
1824		106	270	54.27	0.024	3.201		YB						
1824	MA	108	171	55.77	4.327	27.339		YH						
1824		108	172	51.86	-2.891	0.646				A				

Supplementary Information Chapter 8

1824		108	174	46.24	2.178	16.374		YA						
1824		108	176g	56.05	3.856	24.566								
1824		108	177	44.32	1.958	11.912		YA						
1824		108	178	30.38	-4.389	2.427			A					
1824	MA	110	179	51.32	1.109	8.975		YB						
1824		110	180	62.68	-1.915	-6.374			A					
1824		110	181	43.85	10.486	14.55		YI						
1824		110	182	20.49	-1.989	-4.683	Pr b							
1824		110	183	28.11	-1.5	2.196	Pr b							
1824		110	185	38.11	4.865	10.238							YC	
1824		110	186	48.62	8.698	-1.45			Coc					
1849	CA	3044	208	45.76	0.883	7.655		YA						
1849		3044	209	60.91	1.579	10.005		B						
1849		3044	210	57.09	-1.568	8.015			A					
1849		3044	211	57.7	-1.223	7.459		YA						
1849		3044	214	50.99	1.832	13.545		YC						
1849		3044	219	31.97	28.99	6.954			BW					
1849		3044	220	57.02	-3.145	-8.654	Pr b							
1850	MA	112	187	56.27	0.647	15.076		YA						
1850		112	188	78.66	-3.203	3.229		YC						
1850		112	189	64.49	0.195	17.805		YC						
1850		112	190y	49.41	7.872	16.755		YI						
1850		112	190r	45.4	24.804	2.554			Coc					
1850		112	b112y	53.32	0.471	11.05		YA						
1850	MA	113	70	43.37	1.732	13.03		YB						
1850		113	71	19.8	-3.654	-5.636	Pr b							
1850		113	72	45.27	3.061	9.534		YD						
1850		113	73b	23.02	-5.936	-4.989	Pr b							
1850		113	73y	42.53	2.968	14.788		YB						
1850		113	74	40.36	2.214	11.91		YB						
1860	CA	3245	375	70.06	-1.521	4.817		YA						
1860		3245	376	66.95	-0.184	4.79		YB						
1860		3245	377	57.2	-2.601	26.974		YA						
1861	CA	114	225	55.7	2.548	10.787		YE						
1861		114	227	24.76	0.348	-16.238	Pr b							
1861		114	233	45.23	-1.495	18.432		YA						
1861		114	235	53.2	-5.627	-0.408	Ind							

PART II. STUDY OF METALS AND DYES AS DECORATION OF SILK TEXTILES

1861		114	236	30.63	29.229	7.269			BW					
1861	CA	131	323	60.06	4.39	13.134		YE						
1861		131	326	33.96	9.081	-1.814			BW					
1861		131	328	82.12	-2.419	-1.447								?
1861		131	329	42.14	3.74	13.258								
1861		131	330	34.61	6.691	6.89							?	
1861		131	331	54.31	5.436	-2.332			BW					
1861		131	332	38.13	20.836	1.228			BW					
1861		131	333	66.06	1.794	0.215			BW					
1875	CA	124	288	57.17	-1.39	2.443		YA						
1875		124	289	22.55	10.652	-7.835						Ind+C oc		
1875		124	290	49.02	17.413	2.531								
1875		124	296	49.78	-1.437	-2.544				?				
1875		124	297	42.1	2.549	1.531			Mad +					
1875		124	300	43.25	-2.48	14.043				?				
1880	CA	6079	368	66.72	-1.786	8.711		YA						
1880		6079	369	66.94	-0.682	-4.674	Ind							
1880		6079	371	55.92	3.843	18.53		YA						
1885	CA	129	81	40.74	8.644	1.979			BW					
1885		129	83	39.19	-1.933	-3.886	Ind							
1885		129	86	46.35	1.322	7.406		YD						
1885		129	87	55.1	8.256	2.827			BW					
1885		129	88	61.12	-2.777	10.269		YC						
1885		129	89	58.66	-0.821	0.439								
1899	CA	3615	341	67.39	-0.328	-0.556								?
1899		3615	343	72.03	-0.536	0.572								?
1899		3615	344	49.77	-6.267	-2.953	Ind							
1899		3615	345	48.65	6.451	-2.834			BW					
1899		3615	346	73.6	-2.746	3.191								
1899		3615	349	80.41	-1.672	-2.553								?
1899		3615	350	19.17	10.391	-7.228			BW					
1899		3615	351	66.83	5.648	10.085		YMIX						
1899		3615	352lb	68.09	-7.719	6.837	Ind							
1899		3615	352	54.93	2.041	11.752		YB						
1900	MA	7354	250	60.01	-0.646	12.359		YC						
1900		7354	251	49.96	-0.517	18.785		YH						
1900		7354	253	64.89	-0.685	-1.968								?

Supplementary Information Chapter 8

1900		7354	254	66.02	-2.169	2.047		YC						
1900		7354	255	34.34	28.314	6.414			Mad					
1900		7354	256	40.63	-5.297	-1.154	Ind							
1900		7354	257	54.16	-2.04	-1.799				?				
1900		7354	258	43.48	-7.753	-2.354	Ind							
1900		7354	259	28.63	31.441	6.033				BW +				
1901	CA	120	75	40.25	23.461	5.64				Mad				
1901		120	76	1.79	2.625	10.564		YB						
1901		120	77	27.18	-1.982	-13.367	Pr b							
1901		120	78	57.05	-0.635	2.735		YC						
1901		120	80	49.84	3.752	15.541		YC						
1901	CA	1948	353	40.63	33.495	7.565				Coc				
1901		1948	360	73.15	-3.572	2.215		YA						
1901		1948	363	48.85	2.159	13.544		YB						
1901		1948	364	27.42	-3.058	-13.257	Pr b							
1901		1948	365	39.14	19.692	2.09				Coc				
1901		1948	366	66.3	3.628	5.979				Coc +				
1929	CA	126	334	52.32	14.519	1.347				Mad BW				
1929		126	335	44.96	-1.117	-6.715	Ind							
1929		126	336	63.51	-4.897	21.812		YMIX						
1929		126	337	60.78	-1.88	-3.614				A				
1929		126	338	71.02	-0.9	-0.342								?
1929		126	339	75.52	-1.814	-1.758								?
1932	CA	125	302	53.17	-0.942	1.033		YB						
1932		125	309	63.59	2.84	25.349		YC						

PART III.
MOLECULAR STUDY OF SILK

Chapter 9.

Characterization of the secondary structure of degummed *Bombyx mori* Silk in modern and historical samples

Abstract

Understanding the degradation mechanisms of silk is fundamental to improve preventive conservation measures, and to develop consolidation materials to restore the degraded fibers. Here, pristine and historical silk samples were analyzed with an inclusive set of analytical techniques, in order to investigate the changes in the protein secondary structure that occurred upon natural aging or manufacturing processes. FTIR 2D Imaging-Chemical mapping allowed the non-invasive characterization of the structure, and the obtained information was supported by Optical microscopy (OM), Scanning electron microscopy (SEM) and thermal analysis (Thermogravimetry, TGA, and Differential Scanning Calorimetry, DSC). Based on the acquired data, a different degradation mechanism was proposed for each historical sample, highlighting a heterogeneous conservation status.

THIS CHAPTER HAS BEEN PUBLISHED ON: “Polymer Degradation and Stability” [Diego Badillo-Sanchez, David Chelazzi, Rodorico Giorgi, Alessandra Cincinelli, Piero Baglioni, Characterization of the secondary structure of

Chapter 9. Characterization of the secondary structure of degummed *Bombyx mori* Silk in modern and historical samples

degummed *Bombyx mori* silk in modern and historical samples, Polymer Degradation and Stability 157 (2018) 53-62]

9.1. Introduction

Silk has been used for over 5000 years [1,2] to produce numerous types of objects and artifacts. In order to preserve such a vast cultural heritage from natural aging, it is necessary to detail the mechanisms by which the structure and chemical composition are affected by degradation. This will allow the improvement of preventive conservation measures and the development of consolidation materials to restore the degraded artifacts. In this study, we specifically refer to the fibroin fiber (75e83% w/w of the original spun off fiber [3]) obtained by the domesticated moth *Bombyx mori* after the removal of the sericin coating (degumming process [4]). Silk is a poly-amino acid-based fibrous material [5], with a hierarchical structure composed of crystalline and cross-linked amorphous domains to form tubular fibrils, which in turn assemble into fibers with an average diameter of 10-14 μm . The latter form smooth filaments (maximum length between 600 and 1500 m) with a trilobal cross-section [1,3,5]. The structural proteins in silk are H-fibroin (Heavy Chain), L-fibroin (Light Chain), and P25, in a proportion of 6:6:1 [6]. Several non-structural minor polypeptides are also present [7]. H-fibroin is composed of ordered domains with a highly repetitive (Gly-Ala)_n sequence motif (the ratio of glycine to alanine is ca. 3:27), and tyrosine-rich domains. L-fibroin is described as a relatively elastic structure with unordered domains [7]. P25 is thought to play a role in maintaining the integrity of the complex as chaperonin-like protein, mainly linked to H-Fibroin by non-covalent bonds [7]. Both the composition and the hierarchical structure of the fibers determine their tensile strength, wet tenacity, elongation, hygroscopic capacity, thermal and electrical resistance [1,3,5].

The deterioration of silk fibroin has been widely observed [8-10], and several studies have investigated the accelerated aging of the fibers [11]. Degradation is favored by high humidity and temperature, UV radiation, some enzymes, pH lower than 4 and above 8, salts and metal components [1,12,13]. Oxidation, hydrolysis, chain scission and chain rearrangements have been proven to be the main degradation pathways [12], and free radicals have been identified on degraded fibers [14]. However, no agreement exists concerning the change in the internal structure of silk during degradation. Some authors propose a first degradation stage characterized by random scission of the main chains in the amorphous regions, followed by a subsequent stage in which the crystalline structures are involved [15,16]. Others propose a gradual reduction in the degree of polymerization with a loss of alignment of the crystals with the fiber axis, along with the breakdown of the amorphous component of fibroin, leaving the crystals intact [15,16]. Finally, other authors propose a mechanism where degradation occurs mainly in the amorphous regions during the initial stage, followed by combined amorphous-crystalline degradation at the same speed [17]. Regardless the mechanism, changes in the internal morphology, secondary structure, degree of orientation, and thermal stability of the fibers occur with degradation.

The aim of the present contribution is to investigate the degradation mechanisms of silk proteins as a textile material through the non-invasive measurement of the distribution of crystalline and amorphous domains in the fibers. To this purpose, both modern commercial (pristine and UV-Vis aged) and historical silk samples have been analyzed with micro-FTIR (Fourier Transform Infrared Spectroscopy), using a Focal Plane Array (FPA) detector. The use of micro-FTIR in reflectance mode allows the characterization of the secondary

structure of silk, without samples pre-treatment or alteration. The selected FPA detector currently allows the highest spatial resolution available (i.e. few microns) [18], which results in chemical maps with high sensitivity, in particular when the sample exhibits inhomogeneous structure and chemical composition on the micron-scale. Optical microscopy (OM), Scanning electron microscopy (SEM) and thermal analysis (Thermogravimetry, TGA, and Differential Scanning Calorimetry, DSC) were also performed to complement and confirm the results obtained by FTIR.

9.2. Materials and methods

9.2.1. Modern and historical silk samples

Two textiles of industrial production (used as representative modern commercial silk) and three historical silk micro-samples (weight < 2 mg; area <1 cm²) were analyzed. The modern samples consisted of a white silk (named “Mod1”), having a density of 2.57 g/cm³, obtained from the Opificio Delle Pietre Dure (Florence, Italy), and a beige silk (“Mod2”) with a density of 13.95 g/cm³, obtained from a local market in Florence. The historical samples came from the textile collection of the National Museum of Colombia, and comprised a blue silk sample from a Spanish tapestry dated on 1538 (“Hist1”), and two samples (yellow, “Hist2”, and red “Hist3”) from Spanish banners dated on 1815 and 1808, respectively. It must be noticed that these artifacts had not undergone any restoration or consolidation treatment.

9.2.2. Fourier transform infrared (FTIR) 2D Imaging-Chemical mapping

Single fibers (length ≤ 5 mm) were manually separated from the original textile samples and analyzed (without any pre-treatment) with a Cary 670 FTIR spectrophotometer coupled to a Cary 620 FTIR microscope (Agilent Technologies). Measurements were carried out in reflectance mode over a gold plated reflective surface; background spectra were collected directly on the gold plated surface. The FTIR settings were as follows: 512 scans for each acquisition, spectral resolution of 2 cm^{-1} , open windows, and spectral range of $3900\text{--}900\text{ cm}^{-1}$. Data were collected using a 15x objective and a Focal Plane Array (FPA) detector of 128×128 pixels, where each pixel provides an independent spectrum related to an area of $5.5\text{ mm} \times 5.5\text{ mm}$. Each analysis can produce either a “tile” map of $700\text{ mm} \times 700\text{ mm}$ or a “mosaic” map composed of multiple tiles. In the maps, the chromatic scale shows the bands’ intensity following the order red > yellow > green > blue.

9.2.2.1. Analysis of the secondary protein structures

An IR map was collected on a chosen spot for each silk fiber. Then, from each map, five spectra with high Amide A absorbance, and fifteen spectra of the golden platelet were selected. The spectra of the Au surface were averaged to obtain a single spectrum, which was used as a reference to subtract environmental water absorptions from the spectra of the fiber. Then, each of the five fiber spectra underwent the following process: 1) Manual spectral subtraction of the reference Au spectrum; the subtraction factor was adjusted manually until no absorption at 1654 cm^{-1} (OH bending, H₂O) was observable in the fiber spectra; 2) Smoothing with an SG quad-cubic function of 13-15 points,

taking care not to alter any diagnostic feature of the spectra; 3) Spectrum truncation down to the 1720-1480 cm^{-1} range (Amide I-II region); 4) Baseline correction using a linear function connecting the two extremes of the truncated spectra; 5) Each spectrum was normalized to the maximum absorbance value of the Amide I band. Operations 1-5 were carried out using the Agilent Resolution Pro software (Agilent technologies). Each resultant spectrum was deconvoluted and fitted using the multipeak fitting package of the Igor Pro software, version 7 (WaveMetrics, Inc). First, the second derivative of the convoluted spectra was used to locate the position of bands. Then, the spectra were deconvoluted using Gaussian curves and a constant baseline (constrained at zero absorbance), in two steps: 1) The position and width of the bands were hold; the height of all bands constrained to a maximum of 80 and a minimum of 0; the fitting was then iterated until no changes were reported between two successive iterations; 2) The width was let change in the 0-20 limit, and the height was let change with a minimum limit of 0; the fitting was iterated until no changes were reported between two successive iterations. The resultant deconvoluted bands composing amide I were assigned to the different secondary structures of the protein as follows [19,20]: (Tyr) side chains/aggregated strands, 1605-1615 cm^{-1} ; aggregate b-strand/intermolecular β -sheets (weak), 1616-1621 cm^{-1} ; intermolecular β -sheets (strong), 1622-1627 cm^{-1} ; intramolecular β -sheets (strong), 1628-1637 cm^{-1} ; random coils/extended chains, 1638-1646 cm^{-1} ; random coils, 1647-1655 cm^{-1} ; α -helices, 1656-1662 cm^{-1} ; turns, 1663-1670, 1671-1685, and 1686-1696 cm^{-1} ; intermolecular β -sheets (weak), 1697-1703 cm^{-1} ; oxidation bands, 1703-1720 cm^{-1} .

9.2.3. Thermogravimetric analysis (TGA)

1 mg of sample was put in the aluminum pan of an SDT Q600 instrument (TA Instruments, Milan, Italy). The temperature program was set as follows: heating scan rate of 10 °C/min from 30 °C to 400 °C, nitrogen flux of 100 mL/min. The obtained data were elaborated with the Q Series software, version 5.4.0.

9.2.4. Differential Scanning Calorimetry (DSC)

A Q2000 DSC (TA Instruments, New Castle, DE, USA) instrument was used. Aluminum hermetic pans (TZero Aluminum Hermetic, TA Instruments) were used as sample holders and as a reference. The DSC measurements were done with the following temperature program: initial isothermal for 5 min at -50 °C, heat ramp of 5 °C/min from -50 °C to 400°C; nitrogen atmosphere (flow rate 50 mL/min). Reproducible results could be obtained using ca. 1 mg of silk sample for each measurement. The obtained data were elaborated with the Q Series software, version 5.4.0.

9.2.5. Optical microscopy (OM)

A petrographic microscope (Reichert, Austria) was used, equipped with a polarizer, objectives Reichert Epi 5,5 (20x) and Epi 11 (40x), and coupled to a Nikon Digital sights DS-F12 camera.

9.2.6. Field emission scanning electron microscopy (FE-SEM)

FE-SEM investigation of the silk samples was carried out using a SIGMA instrument (Carl Zeiss Microscopy GmbH, Germany). Samples were gold coated, and images acquired using the secondary electron detector as well in-lens secondary electron detector with an acceleration potential of 5 kV.

9.2.7. Accelerated UV-Vis aging of commercial silk samples

Modern silk samples (“Mod2”) were aged using UV-Vis light to compare with naturally aged silk samples. A Neon Light Color 765 Basic daylight Beghelli Lamp was used (160 mW/lm, 380-700 nm), placing the silk samples in a closed chamber for 30 days at room conditions (36 °C, RH 40%), where the samples’ surface was exposed to ca. 11000 Lux of homogeneous illumination. These conditions are meant to accelerate the natural aging that would be experienced by objects on display in museums, where illuminations of 50-100 lux are typically used.

9.2.8. Solid-liquid extraction process over silk fibers

Microsamples from Mod1 (14 mg) and Hist2 (1 mg) samples were immersed in ethanol (EtOH) (Fluka ACS 99.8%), in sealed flasks, at room temperature for 120 min under continuous agitation. Every 30 min, the solvent in the flask was dripped over an aluminum vessel, and replaced with fresh solvent. Both the silk fibers and the extracted solution were let dry at room temperature for 2 h, before being analyzed with micro-FTIR, OM, FE-SEM, DSC, and TGA.

9.3. Results and discussion

All the silk samples show characteristic tubular-like fibers under the optical microscope. The color of the historical fibers (Hist1-3) is reasonable due to the presence of natural dyes (e.g. vegetal compounds), considering the age and provenance of the samples [21]. All the fibers show iridescent colors under

polarized light (See Fig. 1.), indicating the possible presence of microcrystalline structures [22,23].

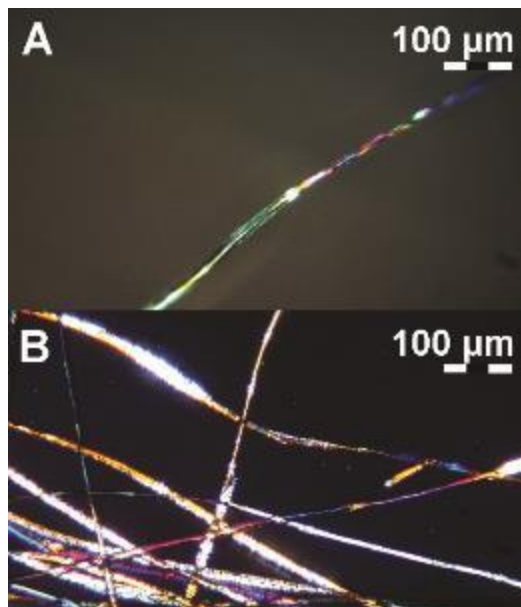


Figure 1 Optical image under polarized Vis-light of silk fibers (transmittance mode): A) modern commercial silk fiber (Mod1); B) historical silk fiber (Hist3).

The silk morphology was further investigated through FE-SEM observation. Mod1-2 samples are made of threads with no evident twisting (see Fig. 2. A, B), each thread being composed of fibers 10-12 mm thick. The fibers show a smooth surface with striae running parallel to the fiber axis (see Fig. 2. C). Small particles on the fibers surface (Fig. 2. C) can be attributed to sericin residues from the degumming process [1,4,24]. Hist1-3 showed bigger aggregates over the surface, possibly due to larger amounts of sericin residues, which might be explained considering that historical degumming processes were less accurate and controlled than modern ones [4,24]. The historical fibers exhibit different morphologies ascribable to natural aging. Hist2 shows tubular fibers (10-12 mm thick) with transversal cracks (see Fig. 2. E). Hist1 and Hist3 show flattened fibers with irregular shape, “vein-like” features, edges running

along the fiber axis, and large unidentified surface aggregates (Fig. 2. D, F). Micro-crystallites were observable inside the Hist3 fibers, within cracks and ruptures (Fig. 2. F).

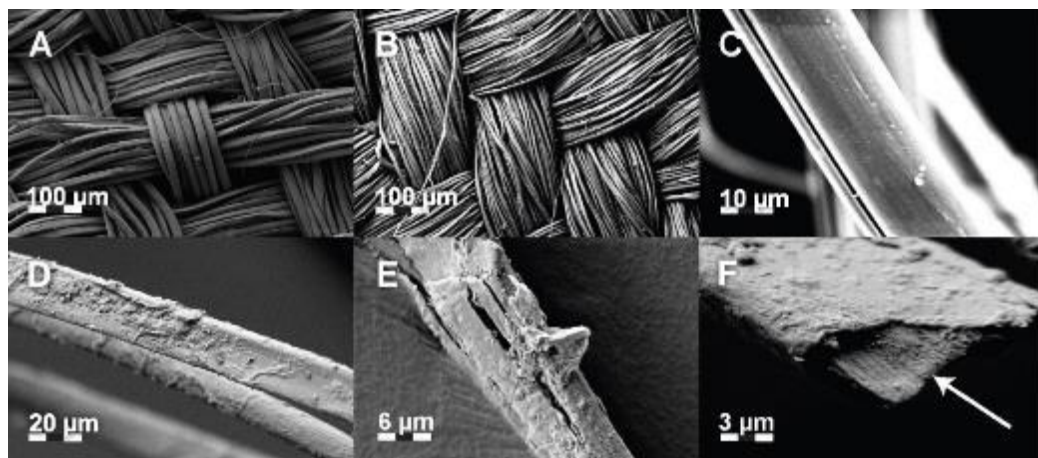


Figure 2 Field emission scanning electron microscopy images of modern commercial and historical silk samples. A) Mod1 textile; B) Mod2 textile; C) Mod2 fiber; D) Hist1 fiber; E) Hist2 fiber; F) Hist3 fiber (the arrow indicates the repetitive “crystalline-like” structures inside the fiber).

FTIR 2D Imaging-Chemical mapping was used to correlate the morphology of the fibers with the secondary structure of the fibroin. The spectra show all the characteristic bands of *Bombyx Mori* silk fibroin, at 3300 (Amide A), 3073 (Amide B), 2975, 2931, 2873 (CH stretching), 1654 (Amide I), 1532 (Amide II), 1443 (vibration modes of residues), 1388 (CH₂ bending), 1260 (Amide III, β -sheet), 1230 (Amide III, random coil and helical conformation), 1160 (N-Ca stretching), and 1069 cm⁻¹ (skeletal stretching) [12,25,26]. No bands ascribable to other types of synthetic or natural fibers were observed. According to the literature, the width of the Amide A band (N-H stretching of H-bonded NH groups) is related to the secondary structure of proteins, where crystalline domains exhibit sharp bands centered around 3300 cm⁻¹, and amorphous regions show broader bands around that wavenumber [27-29]. Therefore, mapping the intensity of the Amide A band in a narrow range

($3300 \pm 30 \text{ cm}^{-1}$) allowed visualizing the distribution of crystalline regions (red pixels in the maps) along the silk fibers. As shown in Fig. 3, for sample Mod2, red regions are continuously found along the fiber, while Mod1 and Hist1-3 samples exhibit a discontinuous distribution of crystalline areas. For historical samples, this indicates that natural aging affected the internal structure of the proteins. In the case of sample Mod1, the discontinuous pattern could be the result of degradation due to some manufacturing process, e.g. bleaching considering that the fibers appear white and shining under visible light.

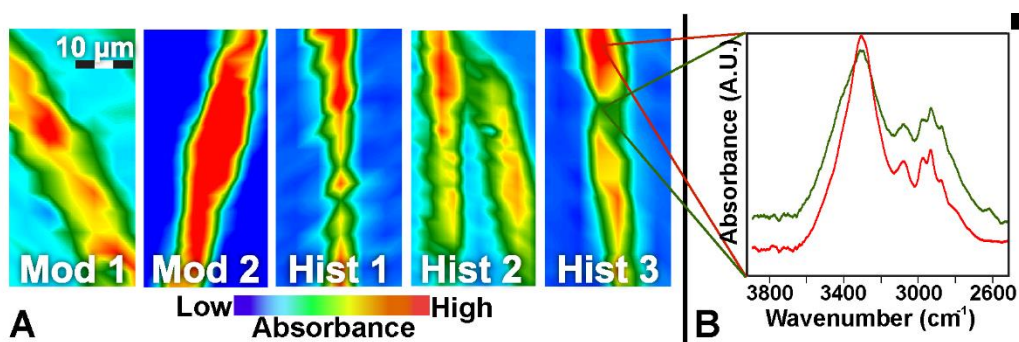


Figure 3 A) FTIR 2D Imaging-Chemical mapping of historical and modern silk samples; the intensity of the Amide A band was mapped in the $3330 \pm 30 \text{ cm}^{-1}$ region. B) Examples of FTIR spectra corresponding to different pixels in the map: Red spectrum: high intensity Amide A band (red pixels in the maps); Green spectrum: low intensity Amide A band (green pixels in the maps).

A deeper insight in the structure of the silk protein was obtained by the deconvolution of the amide I band for the different samples. In this case, analyzing only spectra with high intensity in the $3300 \pm 30 \text{ cm}^{-1}$ range would lead to an overestimation of the crystalline domains over the amorphous regions. Therefore, for each sample, spectra were selected from areas where the intensity of the whole amide A band ($3440\text{-}3160 \text{ cm}^{-1}$) is high. It was also verified that all the main silk absorptions were clearly observable in the selected spectra, allowing the characterization of the secondary structure of portions where degradation is still in process, before the complete loss of spectral information.

Thus, an estimation of the status of the different samples could be made. It must be noticed that a direct mapping of the amide I band would be affected by the presence of environmental water (yielding absorptions in the 1800-1400 cm^{-1} region), while pre-treatment of the samples (e.g. drying, heating, etc.) might affect the actual structure of the fibers.

The wide-range amide A maps typically show higher absorbance intensity in the internal regions of the fibers (red areas), and lower intensity in the lateral edges (green areas) (see Fig. 4.). This is explained considering that the IR beam is transmitted through the fiber, reflects on the golden platelet, and then crosses the fiber again. Therefore, thicker fiber sections give enhanced contrast in the intensity map. In fact, the maps of Mod1-2 show continuous red areas along the fiber axis, while Hist1-3 exhibit a discontinuous intensity of the amide A band. In the low-intensity areas, the spectra show amide A broadening, along with deformation and decreased intensity of the amide I and II bands (up to disappearance), suggesting the loss of the fibroin secondary and primary structure. Overall, this indicates that the degradation processes in the historical samples occurred heterogeneously across and along the fibers, with no evident pattern.

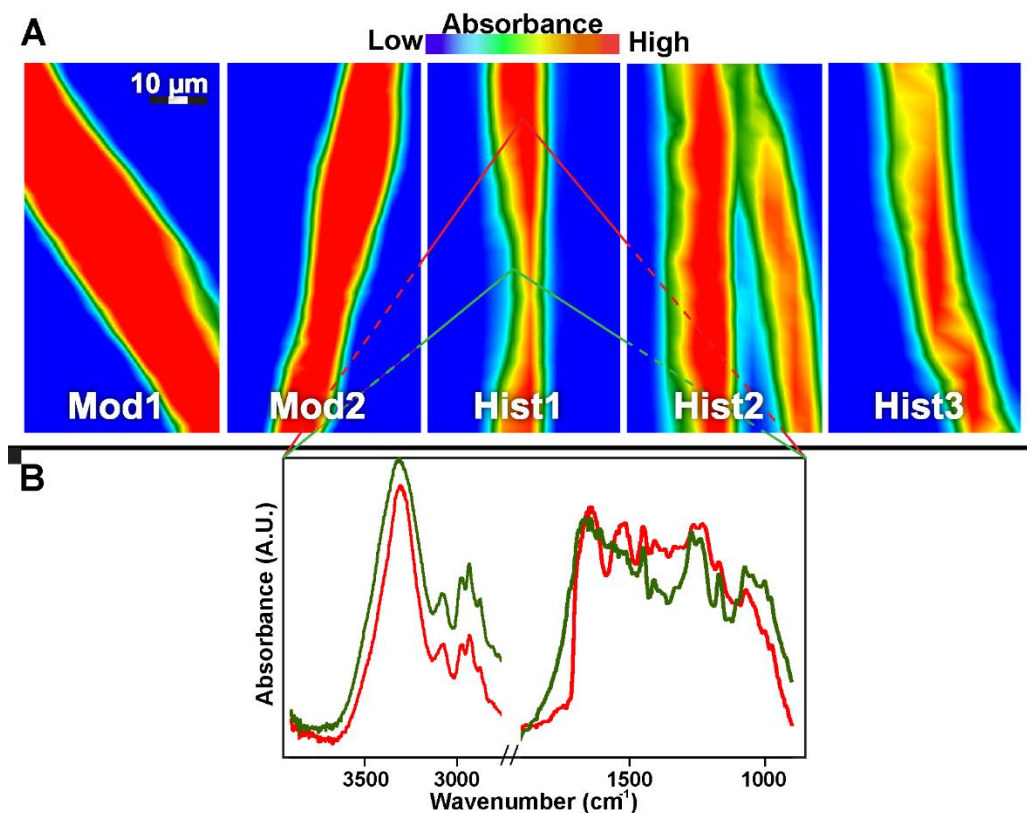


Figure 4 A) FTIR 2D Imaging-Chemical mapping of historical and modern silk samples; the intensity of the whole Amide A band (3440-3160 cm^{-1}) was mapped. B) Examples of FTIR spectra corresponding to different pixels in the map: Red spectrum: high intensity Amide A band (red pixels in the maps); Green spectrum: low intensity Amide A band (green pixels in the maps).

Fig. 5 shows the amide I deconvolution and fitting results averaged on five different map pixels for each sample. It is important to underline that the protein structure varies significantly along the same fiber on a scale of few microns, i.e. two neighboring pixels from a high intensity amide A area can exhibit significant spectral differences due to the naturally heterogeneous distribution of crystalline and amorphous domains (See SI).

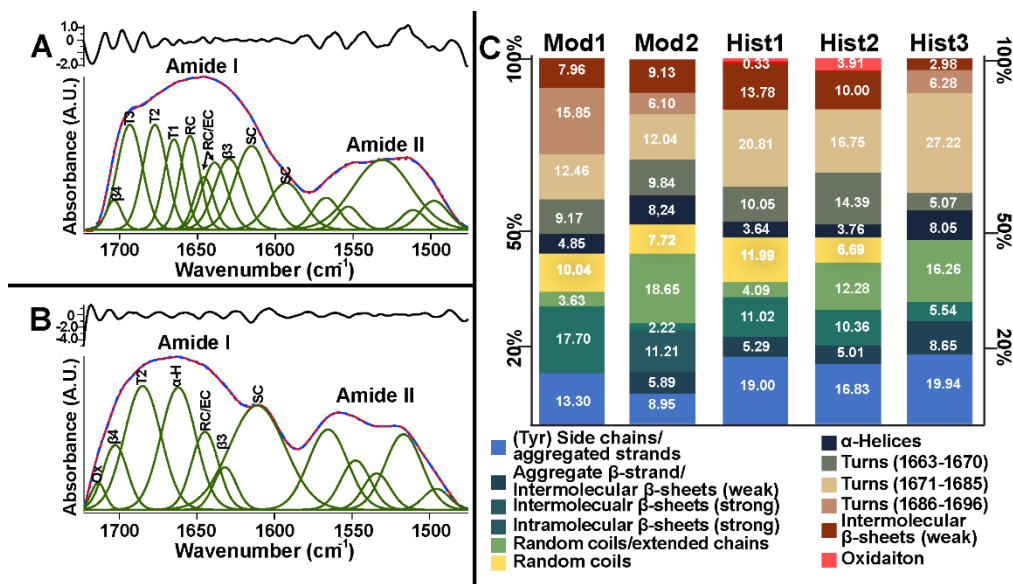


Figure 5 Panels A and B show examples of the deconvolution and fitting of the Amide I band for modern and historical silk samples. Black curve: difference between fitted and experimental spectra. Red curve: experimental spectrum. Blue segmented curve: fitted spectrum. Green curves: deconvoluted bands, which were assigned to secondary protein structures according to the literature [19,20]. SC: (Tyr) side chains/aggregated strands; b3: intramolecular β -sheets (strong); RC/EC: Random coil/Extended Chain; RC: Random coil; α -H: α -Helices; T1: Turn (1663-1670 cm^{-1}); T2: Turn (1671-1685 cm^{-1}); T3: Turn (1686-1696 cm^{-1}); b4: intermolecular β -sheets (weak); Ox: Oxidation. A) Results obtained on one spectrum (i.e. one pixel of the Amide A FTIR 2D Imaging-Chemical mapping) of Mod1. B) Results obtained for Hist1. C) Distribution of protein secondary structures for the Mod1-2 and Hist1-3 samples; for each sample, the distribution is averaged on five pixels from the Amide A FTIR 2D Imaging-Chemical mapping.

Mod2, which is the most recent modern sample, shows a diversified set of secondary structures. β -sheets (inter and intramolecular) and b-turns are predominant ($\sim 56\%$), followed by random coils and, to a lesser extent, α -helices and side chains. No oxidation bands were found. This result is in agreement with evaluations of crystalline domains obtained via X-ray diffraction (XRD) on *Bombyx Mori* silk [4,16]. The diversified motifs are representative of the different sub-proteins that compose fibroin (e.g. H-fibroin, L-fibroin, P25), as expected in modern commercial silk samples right after the manufacturing process. Compared to Mod2, Mod1 shows an increase in intramolecular β -sheet domains and b-turn structures (around 1686 cm^{-1}), and accordingly a decrease of extended chains; a decrease in random coils and α -helices was found as well.

Interestingly, no intermolecular β -sheets were found. According to FTIR and XRD studies reported in the literature, the molecular conformation and the crystalline structure of silk fabrics remain unchanged through degumming, regardless of the agents used in the process (while the tensile strength is affected, possibly due to changes in the orientational order of amorphous fractions) [4,25,30-33]. Degumming of commercial silk typically consists in submerging cocoons in boiling water; salts, alkalis or detergents are commonly used to increase the effectiveness of removal (as in the conventional soap-soda ash method), but the use of enzymes and organic acids has also been reported [4,34,35]. We hypothesized that the structural differences in Mod1 could be ascribed to other manufacturing processes (e.g. bleaching).

Each historical sample showed a unique secondary structure, even though an increase in the side chain component was found in all cases with respect to Mod1-2, indicating a larger number of free peptides or unfolded structures, probably as a result of protein chain scission through natural aging. Considering that the three historical banners have been stored under the same conditions at the National Museum of Colombia since ca. 1815, the different degradation status of Hist1-3 can be ascribed to the natural aging of the samples prior to that date, and to differences in their chemical composition (e.g. presence of dyes, products from the manufacturing process). Hist1 exhibited a complete absence of intermolecular β -sheets and b-turns (around 1686 cm^{-1}), a reduction of α -helices and extended chains, and an increase of random coil structures compared to Mod1-2, which suggests that degradation took place through the transformation of β -sheets into amorphous structures. Hist2 showed a similar structure to Mod1, with a loss of intermolecular aggregate β -strand/ β -sheets structures and β -turns. A larger oxidation component was

found in this case. Hist3 showed an increase of b-turns, and a significant loss of random coils and intermolecular aggregate β -strand/ β -sheets. The number of α -helices is comparable to Mod2. This result can be explained with the presence of small aggregates of β -sheets (linked together by b-turns), rather than extended sheet structures (where the β -sheet/turn ratio would be higher).

Table 1 DSC and TGA measurements on historical and modern commercial silk samples.

Thermal Event	Mod1	Mod2	Mod2 (EtOH extraction)	Hist1	Hist3
DSC main event 1	148.5 °C	145.4 °C	144.6 °C	143.8 °C	73.6 °C
	148.6 - 148.8 °C	145.6 -145.9 °C	144.9 °C		
DSC main event 2	248.7 °C	211.3 °C	204.3 °C	175.5 °C	ND
DSC main event 3	273.8-312.8 °C	303.9 - 315.5 °C	290.0-312.9 °C	269.3-313.9 °C	262.5-380.0 °C
DSC minor event 1	159.5 °C	153.8 °C	ND	ND	144.2 °C
DSC minor event 2	218.0 °C	192.3 °C	ND	ND	ND
TGA minor event	25.0 - 68.9 °C WL 6.3 %	28.7 - 67.1 °C WL 6.6 %	22.5 – 35.0 °C WL 4.9 %	NM	27.1 - 64.6 °C WL 4.9 %
TGA main event	317.4 °C WL 46.2 %	322.9 °C WL 48.9 %	322.0 °C WL 44.3 %	NM	315.2 °C WL 27.3 %

Thermal analysis was used to complement the FTIR data, in order to better understand the effects of natural aging on the secondary structure of the protein samples. Both DSC and TGA have been coupled with spectroscopic measurements in previous reports on silk degradation [36-38] and characterization. Therefore, we carried out measurements on Mod1-2 and Hist3 using both thermal techniques; however, owing to the scarce number of historical samples available for destructive analysis, DSC was carried out only on Hist1, while no measurement could be done on Hist2. The results are shown in Table 1.

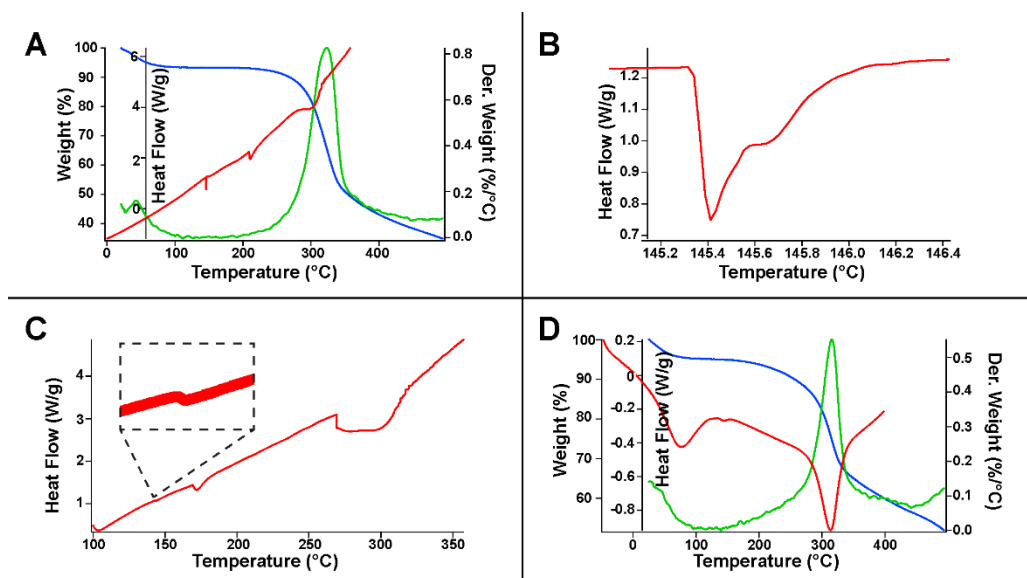


Figure 6 Thermal analyses of historical and modern silk samples. A) DSC, TGA, and DTG (differential thermogravimetry) curves of Mod2 (Red line: DSC; Green line: DTG; Blue line: TGA); B) Detail of the first DSC event on Mod 2; C) DSC curve of Hist1; D) DSC, TGA, and DTG curves of Hist3 (Red line: DSC; Green line: DTG; Blue line: TGA).

Mod1-2 showed similar thermal behavior, with three main and two minor events in the DSC curve (see Fig. 6. A). Hist1 and Hist3 showed different curves, with a decreased number of thermal events (see Fig. 6. C, D). The TGA curves of all samples showed a minor event below 100 °C, and one main event after 300 °C, which can be assigned to, respectively, the loss of water and the degradation of the polymer backbone, in agreement with the literature [39,40].

In the DSC curves of all samples, the endothermic peak related to the loss of water [39,40] has low intensity and is barely observable between 50 and 100 °C (the peak is clearly observed when higher quantities of the samples are analyzed). In the curves of the modern commercial silk samples, a sharp peak is observed above 140 °C (Mod1: 148.5 °C; Mod2: 145.4 °C) followed by a broad shoulder (see Fig. 6B). We hypothesized that this peak is due to a transition of crystalline domains unfolding into semi-crystalline structures. The second main

DSC event is a broad endothermic and (Mod1: 248.7; Mod2: 211.3 °C), assigned to the glass transition of amorphous domains, according to the literature [40,41]. Two minor thermal events are observed between 150 and 240 °C, probably related to minor structural changes due to residual sericin left after the degumming process, as reported by Mazzi et al., Liang et al. and Dinh [39,40,42]. Yazakawa et al. reported an exothermic peak around 220 °C for B. mori silk films, attributed to β -sheet crystallization [43], which is not observed in the case of degummed fibers. The last event (Mod1: 273.8e312.8 °C; Mod2: 303.9-315.5 °C) is associated with a significant weight loss (46-48%), which is ascribable to the thermal decomposition of the protein [17] as observed with DTG.

The historical samples exhibited different behavior. Hist1 showed a barely observable event around 143.8 °C, followed by an event at 175.5 °C, and a degradation peak from 290 °C to 313.9 °C (see Fig. 6C). The lower intensity of the peak around 140 °C (as compared to Mod1-2) suggests a decrease of crystalline domains and an increase of random/amorphous structures, consistently with the FTIR deconvolution results. The onset temperature of the protein degradation peak (290 °C) is lower than that of Mod2 (ca. 304 °C), which is consistent with the increase of amorphous regions over crystalline domains owing to natural aging. As reported in the literature, the temperature value of the degradation peak is dependent on crystallinity and molecular orientation: amorphous silk decomposes at lower temperatures, while well oriented and crystallized silk fibroin (such as fresh fibers) decomposes at higher temperatures [44].

Hist3 showed a first main event at 73.6 °C, a minor event at 144.2 °C, and a degradation peak with an onset temperature of 262.5 °C; however, the peak

extends up to 380.0 °C, with a sharper profile than Hist1 (see Fig. 6D). Li et al. showed that decomposition temperatures closer to those of fresh silk result from the copresence of high crystallinity and low degree of orientation [17]. Therefore, the results suggest that in the case of Hist3, the crystalline domains are composed of smaller units not linked to each other (as opposed to Mod1-2). The presence of small and scarcely linked microcrystallites would also explain the low intensity of the peak at 144.2 °C.

Some considerations can also be made regarding the weight loss observable in the TGA curves of all samples below 100 °C, ascribed to the release of adsorbed water. In crystalline silk, the OH groups of the proteins are largely involved in intramolecular bonds that hold together the folded structures. Therefore, less hydroxyls are available to interact with free water, i.e. in a more crystalline system less water will be bound [43]. Indeed, Wojcieszak et al. had previously reported that the amount of water seems to be lower in ordered regions, as indicated by the analysis of the Raman spectra of silk fibers in the 3100-3700 cm^{-1} region [45]. The values of weight loss below 100 °C (Mod1: 6.3%; Mod2: 6.0%; Hist3: 4.9%) confirm the significant presence of crystalline domains in Hist3.

Overall, the combined FTIR and thermal analyses indicate that the degradation of Hist1 and Hist3 might have followed different paths: for Hist1, the process seemed to involve the partial transformation of crystalline domains into amorphous regions; for Hist3, on the other hand, degradation involved the amorphous regions, leaving small and poorly interconnected crystalline domains. Several authors reported that the degradation molecular mechanism of silk fibroin involves changes of the amorphous regions in the first stages,

followed by alteration of crystalline or organized domains. According to Li et al., at the initial stage of degradation the amorphous regions are mainly affected, leaving crystalline regions intact; thus, the loss of disorder makes crystallinity increase. As degradation progresses, it affects both amorphous and crystalline regions, leading to loss of alignment of β -sheets, and decreased crystallinity. At the latest stage of degradation, short range order is also lost, accompanied by scission of the polypeptide chain, with dramatic decrease of crystallinity [17]. Previously, Garside et al. had analyzed pristine and historical silk samples, founding that during natural aging the amorphous regions break down and the crystallites progressively lose alignment with the fiber axis, but stay intact until the ultimate stage of degradation [16]. Vilaplana et al. and Hirabayashi et al. showed that hydrolysis, UV and UV-Vis radiation promote chain scission of amorphous regions, followed by rearrangement of crystalline structures, and finally scission in the crystalline domains [12,15]. Therefore, it seems reasonable to hypothesize that, in our case, the historical samples exhibit differential progress of the aforementioned degradation path, i.e. Hist 1 seems to be farther through the degradation process (which affected also crystalline regions), as opposed to Hist 3 (which shows mainly degradation of amorphous regions, leaving small crystallites).

Moreover, the photo-aged Mod2 sample shows secondary structures with features similar to those of Hist1-3 (see Supplementary information). Namely, after accelerated aging, oxidation bands increased, reaching values close to those of Hist2 sample. Elsewhere, the oxidation of amorphous phases following photoaging has been reported [12]. A rearrangement of the b-turns was also observed: b-turns at 1671 cm^{-1} markedly increased up to values closer to those of Hist1-3, while those at 1663 cm^{-1} decreased down to values similar

to Hist3. Noticeably, aging also produced a drastic decrease of β -sheet intermolecular bands (1616, 1622 cm^{-1}), accompanied by a marked increase of the β -sheet intramolecular band at 1628 cm^{-1} , features in common with the Hist1-3 samples. Finally, random coils/extended chains (1638-1646 cm^{-1}) decreased, while both random coils (1647-1655 cm^{-1}) and α -helices increased. Overall, we concluded that photo-aging produced the oxidation of amorphous phases, the formation of smaller and less interconnected crystallites (β -sheets), and the partial transformation of crystalline domains into less-ordered structures (α -helices, random coils). This suggests that UV-Vis photo-aging has contributed to the degradation of the historical silk samples, as expected by the fact that these have been kept over the last 200 years in a museum environment, where they were subjected to illumination during temporary or permanent exhibitions in mild environmental conditions (T, RH). The differences observed in the secondary structures of the samples indicate that, besides light aging, different factors (hydrolysis, temperature fluctuations) may have partially contributed to produce unique degradation histories [17].

A further test was considered, where the extraction of silk samples was carried out in ethanol. It is well known that ethanol interacts with hydroxyl groups of proteins, replacing water molecules and denaturing the protein structure [45,46]. It is expected that the process result in the extraction of amorphous chains (if present), leaving the protein sample with higher proportion of crystalline domains. Thermal analysis (DSC, TGA), FE-SEM and FTIR were then used to characterize both the extracted phases and the remaining fibers. The data were used to deduct information on the structure of the fibers before the treatment, supporting the previous analyses.

After extraction with ethanol, the fibers of Mod2 appear as made of filaments ca. 5 mm thick (see Fig. 7. A), while the extracted material is composed of micron-sized aggregates without any apparent structure (See Fig. 7. B). The treated Mod2 fibers exhibit a different thermal behavior than the pristine sample (see Fig. 8): in the TGA curve, a decrease of 1.7% in the water release indicates a higher content of crystalline domains; in the DSC curve, it is possible to observe a slight decrease in the temperature of the first event (change of crystalline domains into amorphous), and a more evident temperature decrease ($\Delta T = 6.5\text{ }^{\circ}\text{C}$) and flattening of the second peak (ascribed to the glass transition of amorphous domains) (see Table 1). Moreover, the minor thermal events between 150 and 240 $^{\circ}\text{C}$ were no longer observable. Overall, the thermal behavior suggests that, after extraction, the number of amorphous domains is reduced. Because the latter are able to relax thermal stress, their absence also results in a reduction of the thermal energy required to degrade the crystallites.

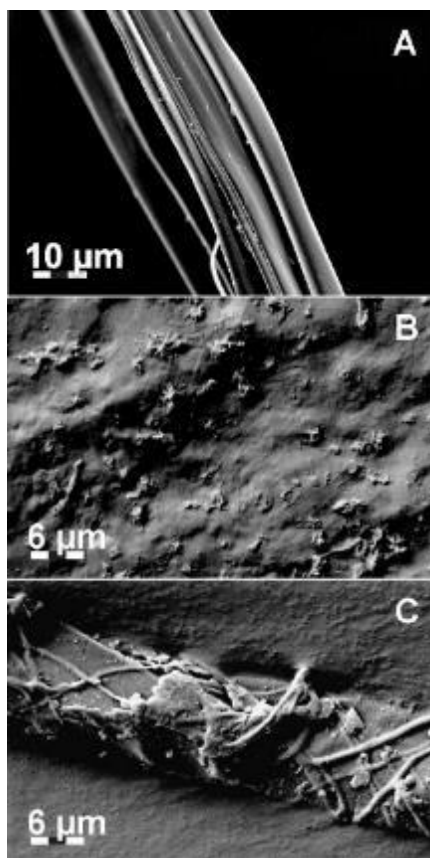


Figure 7 Field emission scanning electron microscopy images of: A) Fiber of Mod2 after extraction in EtOH; B) Material extracted from Mod2; C) Fiber of Hist2 after extraction in EtOH.

The fibers of Hist2 appear, after treatment with ethanol, as shrunk (with more evident “vein-like” features) and heterogeneously covered with microfibrils (less than 1 mm thick) (See Fig. 7. C). This can be explained considering that the treatment probably led to the extraction of amorphous phases (and of non-covalently linked domains), leaving fibrillar structures mainly composed of crystallites. The reduced amount of historical sample available did not allow further destructive analyses, and more information was gained through non-invasive FTIR mapping.

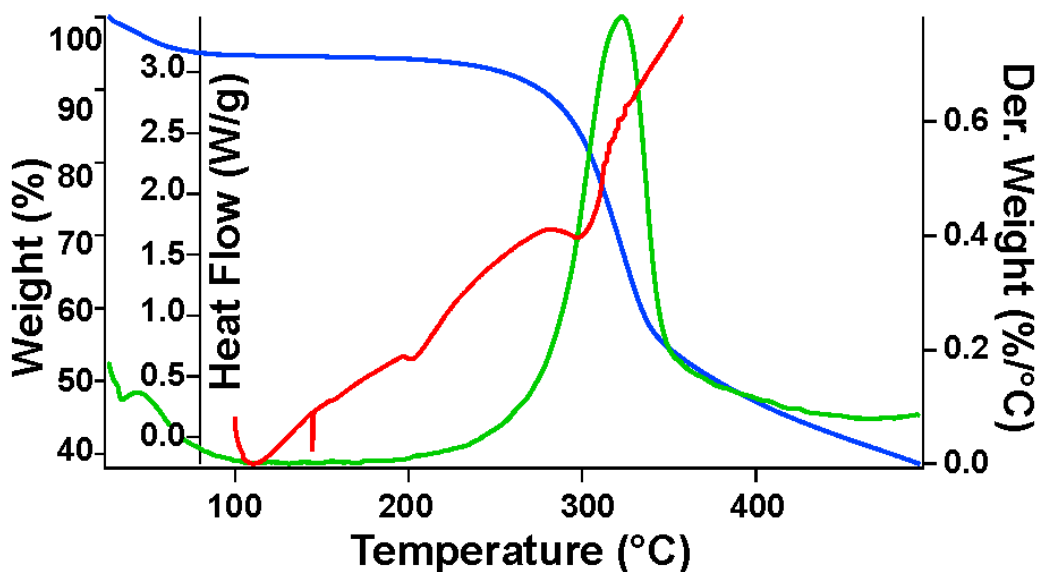


Figure 8 DSC, TGA, and DTG (differential thermogravimetry) curves of Mod2 after extraction in EtOH; (Red line: DSC; Green line: DTG; Blue line: TGA).

The intensity maps of the whole Amide A band ($3440\text{--}3160\text{ cm}^{-1}$) after immersion in ethanol showed differences as compared to the untreated samples. For Mod2, red areas are less continuous after the treatment, and appear as discrete regions of ca. 5-20 mm along the fiber axis (see Fig. 9). For Hist2, there is an increase of low-intensity areas (green regions). Accordingly, the deconvolution of spectra from high-intensity pixels showed in both cases differences from the untreated samples. Mod2 sample exhibited an increase of extended chains, aggregate b-strand/intermolecular β -sheets, α -helices and b-turns around 1671 cm^{-1} , as well as a decrease of b-turns (around 1686 and 1663 cm^{-1}), inter and intramolecular β -sheets, and side chains (See Fig. 9). The extracted material over the aluminum vessel presented a “silk-like” spectrum with an Amide I band centered around 1650 cm^{-1} , indicating an amorphous phase. Therefore, the ethanol treatment affected the secondary structure of Mod2, where intramolecular β -sheets are lost, increasing the amount of random coil/extended chains, and stabilizing helical structures. The combined

thermal and FTIR analysis of Mod2 after ethanol treatment corroborates the hypothesis that the fiber is originally composed of microfibrils well organized in covalently bound structures (as reported in the literature), surrounded by a non-covalent bonded matrix, possibly P25 and other minor proteins.

The Hist2 sample after extraction with ethanol shows a decrease in intramolecular β -sheets, α -helices, random coils, random coils/extended chains, and β -turns structures around 1663 cm^{-1} (See Fig. 9). An increase of intermolecular β -sheets and oxidation bands was found as well. Therefore, the removal of the amorphous/noncovalently linked phases by ethanol revealed the presence of domains in the fibers, mainly composed of small clusters of β -sheets. Elsewhere, Hu et al. showed that similar changes in the secondary structure were obtained by exposure to methanol [19].

Overall, the combined FTIR and thermal analyses supported the hypothesis that the natural aging of the Hist2 sample led to a combined amorphous-crystalline degradation, where crystalline domains were partially transformed in amorphous regions, which in turn underwent oxidation and depolymerization. Based on the degradation mechanisms reported in the literature and discussed in the previous paragraphs, it seems that Hist2 shows an advanced stage of degradation, where crystalline domains have started to transform after initial chain scission of amorphous regions.

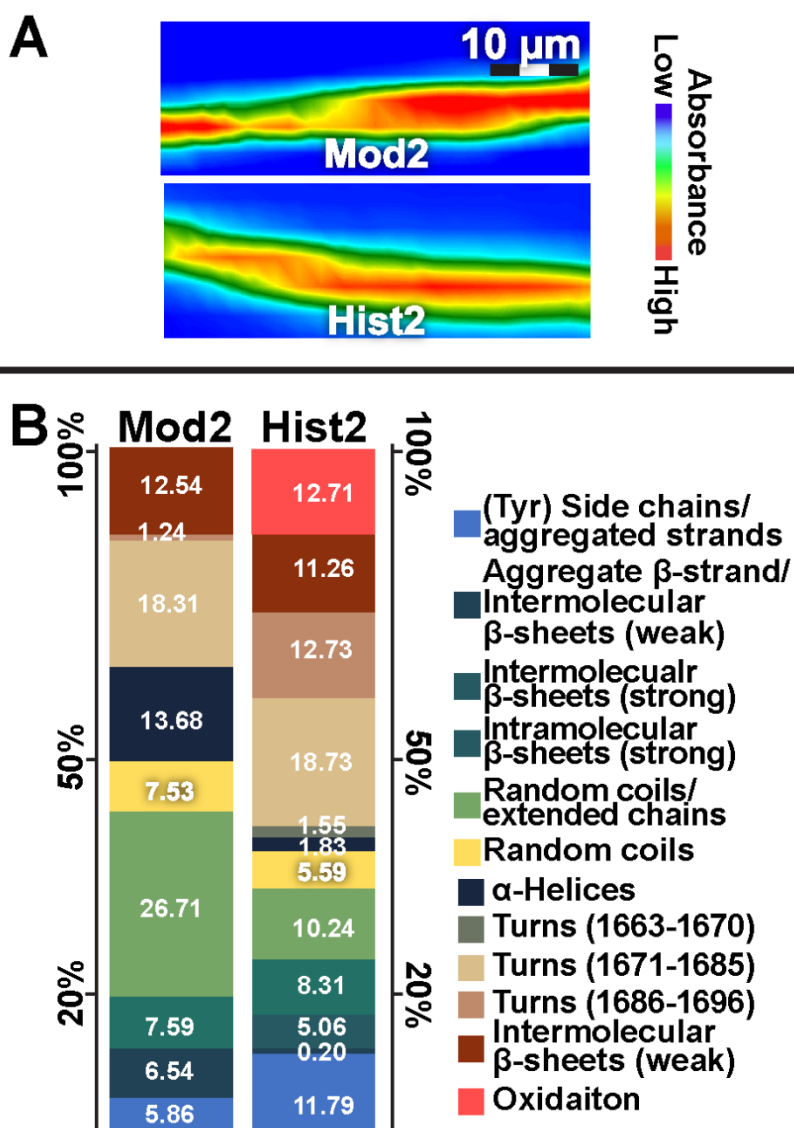


Figure 9 A) FTIR 2D Imaging-Chemical maps of the Amide A band intensity (in the 3440- 3160 cm^{-1} range) for Mod2 and Hist2 samples after extraction in ethanol; B) results of the deconvolution and fitting of the Amide I band, for Mod2 and Hist2 samples after extraction in ethanol. For each sample, the distribution is averaged on five pixels from the Amide A FTIR 2D Imaging-Chemical mapping.

9.4. Conclusions

An inclusive set of analytical techniques was used to characterize modern commercial and historical silk samples. The FTIR 2D Imaging-Chemical mapping of the fibers provided information on the secondary structure of the proteins, highlighting differences in the samples conservation status. Mod2 represents a pristine sample, where crystalline domains (composed by intra- and intermolecular β -sheets, and α -helices) are well interconnected by amorphous regions. Mod1, despite being a modern sample, shows smaller crystalline domains that are less interconnected, which was ascribed to alteration caused by possible manufacturing processes (e.g. bleaching). Each historical sample showed a unique distribution of protein secondary structures. Hist 1 showed a prevalence of amorphous domains over crystalline structures; Hist2 exhibited oxidized groups, and a loss of intermolecular aggregate β -strand/ β -sheets structures and b-turns (similarly to Mod1). Hist3 showed a prevalence of crystalline domains over amorphous structures, where the crystalline domains were probably composed of small aggregates of β -sheets, rather than extended sheet structures. These results were supported both by thermal analysis, and by the investigation of the fibers after extraction in ethanol.

Based on the investigation of the secondary structures of the historical samples, it was possible to hypothesize the different degradation paths followed by each sample through natural aging. For Hist1, degradation is likely to have produced the partial transformation of crystalline domains into amorphous regions. For Hist2 a combined amorphous-crystalline degradation could have been reached, where crystalline domains transformed into

amorphous regions, which in turn oxidized and depolymerized. Finally, the amorphous regions in Hist3 fibers underwent chain scission, to leave small and poorly interconnected crystalline domains. It seems thus that the historical samples show differential degradation, i.e. Hist 1 and 2 seem to be farther through the degradation process (which affected also crystalline regions), while Hist 3 shows mainly degradation of amorphous regions, leaving small crystallites.

Finally, FTIR analysis showed that photo-aged Mod2 fibers exhibit secondary structures similar to those of Hist1-3, confirming that photo-aging must have played a significant role in the degradation of the historical samples. Overall, FTIR 2D Imaging-Chemical mapping emerged as a promising technique to achieve the non-invasive characterization of silk microsamples, opening new perspectives in the diagnostics of both historical artifacts and manufactured fibers. The obtained results can also be beneficial as a preliminary step to formulate adequate materials for the re-introduction of silk components that were lost to degradation.

References

- [1] N. Luxford, in: P.A. Annis (Ed.), *Understanding and Improving the Durability of Textiles*, Woodhead Publishing Limited, Cambridge, 2012, pp. 205e232.
- [2] F. Vollrath, D. Porter, C. Dicko, In the structure of silk, in: S. Eichhorn, J.W.S. Hearle, M. Jaffe, T. Kikutani (Eds.), *Handbook of Textile Fibre Structure*, vol. 2, Woodhead Publishing, 2009, pp. 146e198.
- [3] X. Liu, K. Zhang, In silk fiber - molecular formation mechanism, structureproperty relationship and advanced applications, in: C. Lesieur (Ed.), *Oligomerization of Chemical and Biological Compounds*, Intech, 2014, <https://doi.org/10.5772/57611>.
- [4] S.K. Vyas, S.R. Shukla, Comparative study of degumming of silk varieties by different techniques, *J. Text. Inst.* 107 (2016) 191e199.
- [5] K.M. Babu, in: *Silk. Processing, Properties and Applications*, Woodhead Publishing, 2013.
- [6] S. Inoue, K. Tanaka, F. Arisaka, S. Kimura, K. Ohtomo, S. Mizuno, Silk fibroin of *Bombyx mori* is secreted, assembling a high molecular mass elementary unit consisting of H-chain, L-chain, and P25, with a 6:6:1 molar ratio, *J. Biol. Chem.* 275 (2000) 40517e40528.
- [7] R. Fedic, M. Zurovec, F. Sehnal, The silk of Lepidoptera, *J. Insect Biotechnol. Sericol.* 71 (2002) 1e15.
- [8] F. Cilurzo, et al., An investigation into silk fibroin conformation in composite materials intended for drug delivery, *Int. J. Pharm.* 414 (2011) 218e224.
- [9] J. Zhong, X. Liu, D. Wei, J. Yan, P. Wang, Effect of incubation temperature on the self-assembly of regenerated silk fibroin: a study using AFM, *Int. J. Biol. Macromol.* 76 (2015) 195e202.
- [10] J. Zhong, M. Ma, W. Li, J. Zhou, Z. Yan, D. He, Self-assembly of regenerated silk fibroin from random coil nanostructures to antiparallel β -sheet nanostructures, *Biopolymers* 101 (2014) 1181e1192.
- [11] M.A. Koperska, D. Pawcenis, J. Bagniuk, M.M. Zaitz, M. Missori, T. Lojewski, J. Lojewska, Degradation markers of fibroin in silk through infrared spectroscopy, *Polym. Degrad. Stabil.* 105 (2014) 185e196.
- [12] F. Vilaplana, J. Nilsson, D.V.P. Sommer, S. Karlsson, Analytical markers for silk degradation: comparing historic silk and silk artificially aged in different environments, *Anal. Bioanal. Chem.* 407 (2014) 1433e1449.
- [13] D. Aytemiz, T. Asakura, in: T. Asakura, T. Miller (Eds.), *Biotechnology of Silk*, Springer, Netherlands, 2014, pp. 69e85.
- [14] D. Gong, H. Yang, The discovery of free radicals in ancient silk textiles, *Polym. Degrad. Stabil.* 98 (2013) 1780e1783.
- [15] K. Hirabayashi, Y. Yanagi, S. Kawakami, K. Okuyama, W. Hu, Degradation of silk fibroin, *J. Sericultural Sci. Jpn.* 56 (1987) 18e22.
- [16] P. Garside, P. Wyeth, Crystallinity and degradation of silk: correlations between analytical signatures and physical condition on ageing, *Appl. Phys. A* 89 (2007) 871e876.
- [17] M.Y. Li, Y. Zhao, T. Tong, X.H. Hou, B.S. Fang, S.Q. Wu, X.Y. Shen, H. Tong, Study of the degradation mechanism of Chinese historic silk (*Bombyx mori*) for the purpose of conservation, *Polym. Degrad. Stabil.* 98 (2013) 727e735.
- [18] A. Cincinelli, C. Scopetani, D. Chelazzi, E. Lombardini, T. Martellini, A. Katsoyiannis, M.C. Fossi, S. Corsolini, Microplastic in the surface waters of the Ross Sea (Antarctica): occurrence, distribution and characterization by FTIR, *Chemosphere* 175 (2017) 391e400.
- [19] X. Hu, D. Kaplan, P. Cebe, Determining β -sheet crystallinity in fibrous proteins by thermal analysis and infrared spectroscopy, *Macromolecules* 39 (2006) 6161e6170.
- [20] J. Kong, S. Yu, Fourier transform infrared spectroscopic analysis of protein secondary structures, *Acta Biochim. Biophys. Sin.* 39 (2007) 549e559.
- [21] I. Degano, E. Ribechini, F. Modugno, M.P. Colombini, Analytical methods for the characterization of organic dyes in artworks and in historical textiles, *Appl. Spectrosc. Rev.* 44 (2009) 363e410.
- [22] M. Goodway, Fiber identification in practice, *J. Am. Inst. Conserv.* 26 (1987) 27e44.
- [23] J. Robertson, C. Roux, in: J.A. Siegel, P.J. Saukko (Eds.), *Fiber: Protocols for Examination in Encyclopedia of Forensic Sciences*, Academic Press, 2013, pp. 124e128.

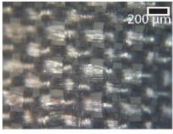
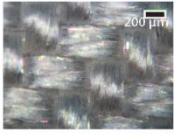
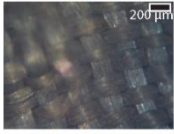
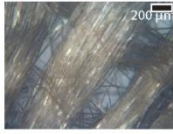






PART III. MOLECULAR STUDY OF SILK

- [24] R.H. Walters, O.A. Hougen, I. Silk Degumming, Degradation of silk sericin by alkalis, *Textil. Res. J.* 5 (1934) 92e104.
- [25] S. Ling, Z. Qi, D.P. Knight, Z. Shao, X. Chen, Synchrotron FTIR microspectroscopy of single natural silk fibers, *Biomacromolecules* 12 (2011) 3344e3349.
- [26] M. Boulet-Audet, F. Vollrath, C. Holland, Identification and classification of silks using infrared spectroscopy, *J. Exp. Biol.* 218 (2015) 3138e3149.
- [27] B. Aksakal, Temperature effect on the recovery process in stretched *Bombyx mori* silk fibers, *Spectrochim. Acta Mol. Biomol. Spectrosc.* 152 (2016) 629e636.
- [28] X. Zhang, P. Wyeth, Using FTIR spectroscopy to detect sericin on historic silk, *Sci. China Chem.* 53 (2010) 626e631.
- [29] A. Barth, Infrared spectroscopy of proteins, *Biochim. Biophys. Acta BBA Bioenerg.* 1767 (2007) 1073e1101.
- [30] J. Perez-Rigueiro, M. Elices, J. Llorca, C. Viney, Effect of degumming on the tensile properties of silkworm (*Bombyx mori*) silk fiber, *J. Appl. Polym. Sci.* 84 (2015) 1431e1437.
- [31] Y. Shen, M.A. Johnson, D.C. Martin, Microstructural characterization of *Bombyx mori* silk fibers, *Macromolecules* 31 (1998) 8857e8864.
- [32] S.W. Watt, I.J. McEwen, C. Viney, Stability of molecular order in silkworm silk, *Macromolecules* 32 (1999) 8671e8673.
- [33] Y. Kawahara, Influence of steam treatment on crystalline regions of silks: text, *Res. J.* 68 (1998) 385.
- [34] F. Lucas, J.T.B. Shaw, S.G. Smith, Amino acid analysis with fluorodinitrobenzene, *Anal. Biochem.* 6 (1963) 335e351.
- [35] H. Ito, et al., Structure and chemical composition of silk proteins in relation to silkworm diet, *Textil. Res. J.* 65 (1995) 755e759.
- [36] M. Wojcieszak, et al., Origin of the variability of the mechanical properties of silk fibers: 4. Order/crystallinity along silkworm and spider fibers, *J. Raman Spectrosc.* 45 (2014) 895e902.
- [37] P. Colomban, H.M. Dinh, A. Bunsell, B. Mauchamp, Origin of the variability of the mechanical properties of silk fibres: 1 - the relationship between disorder, hydration and stress/strain behaviour, *J. Raman Spectrosc.* 43 (2012) 425e432.
- [38] A. Percot, et al., Water dependent structural changes of silk from *Bombyx mori* gland to fibre as evidenced by Raman and IR spectroscopies, *Vib. Spectrosc.* 73 (2014) 79e89.
- [39] S. Mazzi, E. Zulker, J. Buchicchio, B. Anderson, X. Hu, Comparative thermal analysis of Eri, Mori, Muga, and Tussar silk cocoons and fibroin fibers, *J. Therm. Anal. Calorim.* 116 (2014) 1337e1343.
- [40] H.M. Dinh, Raman/ir Study of the Variability of Proteic Fibres: Relationship between Local Structure, Treatments and (Nano)mechanical Properties of Silk Fibres and Films, *Universite Pierre et Marie Curie, 2010 (UPMC Paris 6)*.
- [41] M. Tsukada, G. Freddi, M. Nagura, H. Ishikawa, N. Kasai, Structural changes of silk fibers induced by heat treatment, *J. Appl. Polym. Sci.* 46 (1992) 1945e1953.
- [42] L.J. Zhu, J.M. Yao, K. Hirabayashi, Relationship between the adhesive property of sericin protein and cocoon reelability, *J. Sericultural Sci. Jpn.* 67 (1998) 129e133.
- [43] K. Yazawa, K. Ishida, H. Masunaga, T. Hikima, K. Numata, Influence of water content on the b-sheet formation, thermal stability, water removal, and mechanical properties of silk materials, *Biomacromolecules* 17 (2016) 1057e1066.
- [44] M. Tsukada, M. Obo, H. Kato, G. Freddi, F. Zanetti, Structure and dyeability of *Bombyx mori* silk fibers with different filament sizes, *J. Appl. Polym. Sci.* 60 (1996) 1619e1627.
- [45] D. Mohanta, S. Santra, G.N. Reddy, S. Giri, M. Jana, Residue specific interaction of an unfolded protein with solvents in mixed water/ethanol solutions: a combined molecular dynamics and ONIOM study, *J. Phys. Chem.* 121 (2017) 6172e6186.
- [46] D. Soto, S. Escobar, F. Guzman, C. Cardenas, C. Bernal, M. Mesa, Structure reactivity relationships on the study of b-galactosidase folding/unfolding due to interactions with immobilization additives: triton X-100 and ethanol, *Int. J. Biol. Macromol.* 96 (2017) 87e92.

Supplementary Information

Chapter 9

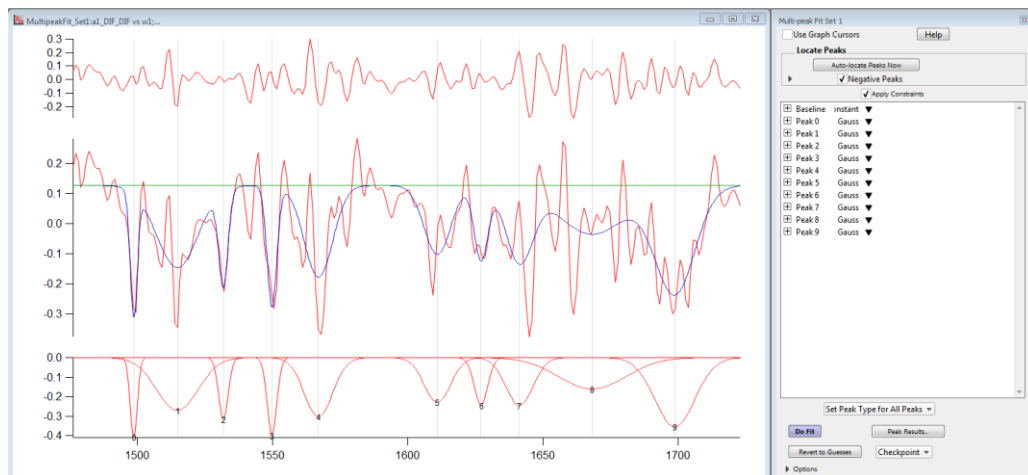
PART III. MOLECULAR STUDY OF SILK

Mod1	Mod2	Hist1	Hist2	Hist3
				
		 105 cm x 34 cm ca. 1538	 150 cm x 150 cm ca. 1815	 168 cm x 162,5 cm ca. 1808
ca. 2000	ca. 2015			

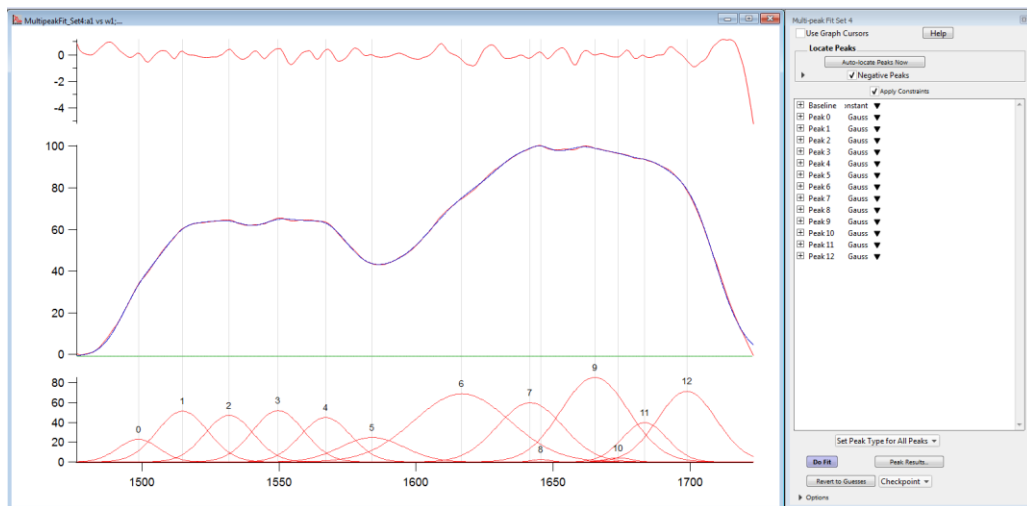
Supplementary Image 1. Photography and detail of the historical Flags and modern commercial textiles

Example of deconvolution process carried on the Amide I and II region of the spectra took in one red pixel of Mod2

1. Second derivate possible bands



2. Deconvolution/Fitting process result over Amide I and II with help of the second derivate bands



Supplementary Table 1. List of bands fund after the deconvolution of the Amide I and II

Type	Location	Amplitude	Amp δ	Area	Area δ	FWHM	FWHM δ
Gauss	1498.7	22.8074	0	426.991	0	17.58	0
Gauss	1514.8	51.2291	0.4520	1191.28	10.95	21.84	0.169
Gauss	1531.8	47.0277	0.5376	1045.47	15.05	20.88	0.298
Gauss	1549.7	51.8377	0.7580	1214.42	20.27	22.00	0.311
Gauss	1567	44.8097	1.730	1018.8	40.47	21.35	0.334
Gauss	1584	24.6602	1.934	718.49	100.15	27.37	1.802
Gauss	1616.7	68.7337	0.793	3013.41	136.03	41.18	1.494
Gauss	1641.6	59.7765	2.372	1788.23	79.19	28.10	0.350
Gauss	1645.4	2.50559	0.6180	20.9487	9.16	7.85	2.010
Gauss	1665.1	85.3378	0.7092	2643.45	42.97	29.10	0.434
Gauss	1673.7	4.20861	0.5864	49.1526	9.73	10.97	1.456
Gauss	1683.4	39.6723	1.0916	807.532	20.78	19.12	0.351
Gauss	1698.8	71.3388	0.4920	1912.74	11.64	25.18	0.147

PART III. MOLECULAR STUDY OF SILK

Supplementary Table 2. Assignment of the percentage of structures on the respective bands found after the deconvolution process of the amide I. Amide I area normalized to 100%

Protein structure assigned	Location cm ⁻¹	Area	%
(Tyr) side chains/aggregated strands	-	0.0	0.0
Aggregate beta-strand/Intermolecular β -sheets (weak)	1616.7	3013.41	29.43
β -sheets (strong) ^a	-	0.0	0.0
β -sheets (strong) ^b	-	0.0	0.0
random coils/extended chains	1641.6	1788.23	17.47
random coils/extended chains	1645.5	20.95	0.20
random coils	-	0.0	0.0
α -helices	-	0.0	0.0
turns (1663-1670)	1665.2	2643.45	25.83
turns (1671-1685)	1673.8	49.15	0.48
turns (1671-1685)	1683.4	807.53	7.89
turns (1671-1685)	-	0.0	0.0
Intermolecular β -sheets (weak)	1698.8	1912.74	18.69
Total Amide I Area		10235.46	100

Supplementary Table 3. Average of five results after the deconvolution process of the Amide I

Secondary protein structure of Mod2	Red Pixel					Percentage%	
	1	2	3	4	5	Average	St. Dev
(Tyr) side chains/aggregated strands	0.0	8.5	5.6	24.0	6.6	9.0	8.0
Aggregate β -strand/ β -sheets (weak) ^a	29.4	0.0	0.0	0.0	0.0	5.9	11.8
β -sheets (strong) ^a	0.0	0.0	31.2	0.0	24.9	11.2	13.9
β -sheets (strong) ^b	0.0	0.0	0.0	11.1	0.0	2.2	4.4
random coils/extended chains	17.7	61.0	0.0	14.5	0.0	18.7	22.4
random coils	0.0	0.0	0.0	10.2	28.4	7.7	11.1
α -helices	0.0	0.0	41.2	0.0	0.0	8.2	16.5
turns (1663-1670)	25.8	0.0	0.0	9.9	13.4	9.8	9.6
turns (1671-1685)	0.5	17.8	9.3	13.5	19.0	12.0	6.7
turns (1686-1696)	7.9	8.3	0.0	14.3	0.0	6.1	5.5
β -sheets (weak) ^a	18.7	4.3	12.6	2.4	7.6	9.1	5.9
Oxidation	0.0	0.0	0.0	0.0	0.0	0.0	0.0

a: Intermolecular; b: Intramolecular

Chapter 10.

Understanding the structural degradation of Mesoamerican historical silk: A Focal Plane Array (FPA) FTIR and multivariate analysis

Abstract

Silk artifacts constitute an invaluable heritage, and to preserve such patrimony it is necessary to correlate the degradation of silk fibroin with the presence of dyes, pollutants, manufacturing techniques, etc. Fourier Transform Infrared Spectroscopy with a Focal plane array detector (FPA FTIR) provides structural information at the micron scale. We characterized the distribution of secondary structures in silk fibers for a large set of South American historical textiles, coupling FTIR with multivariate statistical analysis to correlate the protein structure with the age of the samples and the presence of dyes. We found that the pressure applied during attenuated total reflectance (ATR) measurements might induce structural changes in the fibers, producing similar spectra for pristine and aged samples. Reflectance spectra were thus used for the rigorous characterization of secondary structures. Some correlation was highlighted between the age of the samples (spanning over five centuries) and specific changes in their secondary structure. A correlation was found between

Chapter 10. Understanding the structural degradation of Mesoamerican historical silk: A Focal Plane Array (FPA) FTIR and multivariate analysis

the color of the samples and structural alterations, in agreement with the chemical nature of the dyes. Overall, we demonstrated the efficacy of reflectance FPA μ -FTIR, combined with multivariate analysis, for the rigorous and non-invasive description of protein secondary structures on large sets of samples.

THIS CHAPTER HAS BEEN PUBLISHED ON: “Scientific Reports” [Diego Badillo-Sanchez, David Chelazzi, Rodorico Giorgi, Alessandra Cincinelli, Piero Baglioni, Understanding the structural degradation of South American historical silk: A Focal Plane Array (FPA) FTIR and multivariate Analysis, Scientific Reports (2019) 9:17239]

10.1. Introduction

The term “silk” is generally used to indicate the product of the transformation of domesticated *Bombyx mori* cocoon’s spun fiber after the degumming process (i.e. a chemical treatment that removes the coating of sericin protein from the fiber [1]). Silk is mainly composed of Heavy-Fibroin, Light-Fibroin, and P25 (a chaperonin-like protein), in a 6:6:1 ratio [2], distributed as amorphous and crystalline domains along the fiber axis [3,4]. Both the composition and structure of silk are responsible for its unique physical and mechanical properties, which justify its extended use in ancient fabrics and, more recently, in new bio-materials [5–10]. Historical silk artifacts constitute an invaluable heritage, usually present in museums and collections as clothes, tapestries, flags/banners and decorative objects. However, silk artifacts are often affected by degradation, mainly depending on environmental factors (relative humidity, light, temperature), and the presence of acids, oxidizing compounds, and biopollutants.

To preserve this cultural and historical patrimony, in-depth research into silk degradation mechanisms is a necessary step, prior to the design of cleaning and consolidation materials. The literature reports on numerous methodologies to investigate the structure and dynamic behavior of silk [11–17]. In particular, research aims to correlate the degradation of fibroin with the presence of dyes, fibers’ manufacturing techniques, pollutants, etc. [18–21]. Both Fourier Transform Infrared Spectroscopy (FTIR) and Raman have been extensively used to analyze proteins, thanks to the possibility of correlating spectral features with structural information [22–24]. The use of FTIR microscopy (μ -FTIR) in reflectance mode is advantageous as it allows the analysis of non-transparent

textile fibers in a non-invasive way. Since the amount of light reflected by some samples may be rather low, the reflectance spectra obtained with standard mercury cadmium telluride (MCT) detectors typically show low signal-to-noise (S/N) ratios [25,26]. Higher quality spectra are therefore usually obtained by attenuated total reflectance measurements (ATR-FTIR), which guarantee a higher S/N. In fact, many authors have elected ATR as the standard technique for investigating textiles, including silk. For instance, this method has highlighted remarkable changes in the secondary structure of fibroin films induced by solvents or thermal treatment [27]; Belton et al. have shown the utility of ATR spectra fitting (without the use of peak deconvolution) to elucidate the conformational make up of silk protein in self-regenerated silk films [28]; however, in the case of naturally or artificially aged silk textiles, ATR analysis showed less evident changes in the secondary structure of aged fibroin compared to pristine silk. Vilaplana et al. reported that aged samples showed only a small increase in oxidation bands ($1775\text{-}1700\text{ cm}^{-1}$), while no changes were observed in the Amide I region ($1700\text{-}1600\text{ cm}^{-1}$) [29]. Smith et al. demonstrated the efficacy of ATR for identifying silk in historical textiles from characteristic absorptions, however the ATR spectra of the aged silk samples showed no significant differences from those of reference pristine silk [30]. In addition, Koperska et al. used variations in the intensity ratio of Amide I, II and III bands in historical silk ATR spectra, as estimators of crystallinity, oxidation, and depolymerization; while some relevant differences in the estimators were highlighted, the spectra of the aged and unaged samples showed similar profiles in the Amide I-II region ($1700\text{-}1450\text{ cm}^{-1}$) [31]. Garside et al. provided further insight by developing the use of polarized (Pol-) FTIR-ATR and near infrared (NIR) spectroscopy, and correlated the breaking strength of historical fibers with an

orientated crystallinity parameter derived from the Pol-ATR spectra (i.e. comparing the ratio of β -sheet/ α -helix absorption intensities for fibers aligned perpendicular and parallel to the incident electric vector) [32]. Nevertheless, no reproducible crystallinity index could be obtained through the more rigorous spectral deconvolution (peak fitting) [32].

In this study, both reflectance and ATR measurements were carried out on pristine and historical silk fibers, comparing the results obtained through the systematic spectral deconvolution of the Amide I band. Measurements were performed using a Focal Plane Array (FPA) detector, consisting of a grid of light-sensitive elements, which guarantees the possibility of simultaneously acquiring a large number of spectra on areas ranging from thousands of μm^2 to tens of mm^2 , with high lateral resolution (e.g. 1.1-5.5 μm). Unless FPA detectors are used, such resolution is typically accessible only with synchrotron light [33]. FPA μ -FTIR 2D Imaging is an advantageous and feasible approach when investigating samples that have a heterogeneous structure and composition down to the micron-scale. Recently, we demonstrated the efficacy of this technique for studying the distribution of secondary structures in silk fibers [34]. In particular, we showed that three samples with different age and color (e.g. fibers of flag banners from the 16th and 19th century) had reached different stages of a degradation process affecting the amorphous and crystalline domains of the fibroin. However, no pattern was observed linking the age (or color) of the samples with the progress of the degradation process.

To fill this gap, in this work we have investigated the correlation of the protein structure of a large set of historical silk samples with their age, and with the presence of dyes. To this purpose, FPA μ -FTIR was carried out on samples of historical flags and banners of different origins, obtained from the textile

collection of the National Museum of Colombia, where the objects were kept in the last 200 years under identical conditions (in terms of light, relative humidity, temperature, etc.), without undergoing any restoration intervention. First of all, the difference between the information obtained through ATR and reflectance measurements was critically evaluated. Then, the analysis of the complete sample set was carried out in reflectance mode, followed by the spectral deconvolution of the Amide I band for each sample, in order to clarify the secondary structure of the fibroin on the micron-scale. Finally, principal components analysis (PCA) was performed to correlate the different structures with the age and color of the samples.

10.2. Methods

10.2.1. Silk samples

A textile of modern industrial production (used as a representative pristine silk standard) and 61 historical silk samples were analyzed (See Supplementary Information, SI Table 1-3). The modern sample (hereinafter “Mod”) was a beige silk with a density of 2.57 g/cm³ obtained from a local market in Florence. The 61 historical samples (named “HS 1-61”) came from the textile collection of the National Museum of Colombia. The age of these historical samples range from ca. 100 to 500 years. Most samples are dyed blue, yellow or red; six samples exhibited different colors (orange, green, purple and black). None of the textiles has been restored or treated during storage and exhibition in the collections.

10.2.2. Treatment of modern silk

In order to produce, through accelerated aging, observable changes in the secondary structure of fibroin induced by acid hydrolysis and photo-oxidation, the modern silk samples were treated as follows: 1 cm² of Mod textile was immersed in 2 mL of a solution at pH 4 (Buffer Solution, pH 4, Potassium hydrogen phthalate-based, J.T. Baker Analyzed[®] Reagent, Mallinckrodt Baker, Inc., Phillipsburg, USA), and kept in darkness at room temperature for 24 hours. Then, the sample was rinsed using water purified by a Millipore system (resistivity >18 MΩ cm), and dried at room temperature. This sample was labeled as “Mod1”. To investigate the effects of UV-Vis light, a Mod sample of 1 cm² was placed in a UV-Vis chamber for 30 days, following a procedure reported elsewhere [34]. These illumination conditions are meant to accelerate the natural aging that would be experienced by objects on display in museums, where illuminations of 50-100 lux are typically used. The photo-aged sample was labeled as “Mod2”.

10.2.3. Fourier Transform Infrared (FTIR) 2D Imaging-Chemical mapping

Individual fibers (length 5 mm) were manually separated from the original textile samples and analyzed (without any pre-treatment) with a Cary 670 FTIR spectrophotometer coupled to a Cary 620 FTIR microscope (Agilent Technologies). Measurements were carried out in ATR and reflectance mode (over a gold-plated reflective surface); background spectra were collected either in air (ATR) or directly on the gold-plated surface (reflectance). The FTIR settings were as follows: 512 scans for each acquisition, spectral resolution of 2 cm⁻¹, open windows, and spectral range of 3900-900 cm⁻¹. ATR data were collected

using a Ge crystal, while for reflectance measurements a 15x Cassegrain objective was used. For both ATR and reflectance measurements, a Focal Plane Array (FPA) detector was used: for ATR measurements, a 64 x 64 pixels grid (each pixel providing an independent spectrum related to an area of $1.1 \mu\text{m}^2$); for reflectance measurements, a 128 x 128 pixels grid (each pixel related to an area of $5.5 \mu\text{m} \times 5.5 \mu\text{m}^2$). Each analysis produced a “tile” of $70 \times 70 \mu\text{m}^2$ (ATR), or $700 \times 700 \mu\text{m}^2$ (reflectance). In the FTIR 2D maps, the chromatic scale shows the bands’ intensity, following the order red > yellow > green > blue.

10.2.3.1. Analysis of the secondary protein structures

An IR map was collected (in ATR or reflectance mode) on a chosen spot for each silk fiber. Then, from each map, five spectra with high Amide A absorbance, and fifteen spectra of the air in contact with the Ge crystal (ATR), or of the golden platelet (reflectance), were selected. The spectra of air (or of the Au surface) were averaged to obtain a single spectrum, which was used as a reference to subtract environmental water absorptions from the fiber spectra. Then, each of the five fiber spectra underwent the following process: 1) Manual spectral subtraction of the reference air (or Au) spectrum; the subtraction factor was adjusted manually until no absorption at 1654 cm^{-1} (OH bending, H_2O) was observable in the fiber spectra; 2) Smoothing with an SG quad-cubic function of 13-15 points, taking care not to alter any diagnostic feature of the spectra; 3) Spectrum truncation down to the $1720\text{-}1480 \text{ cm}^{-1}$ range (Amide I–II region); 4) Baseline correction using a linear function connecting the two extremes of the truncated spectra; 5) Each spectrum was normalized to the maximum absorbance value of the Amide I band. Operations 1-5 were carried out using the Agilent Resolution Pro software (Agilent technologies). Each resultant

spectrum was deconvoluted and fitted using the multipeak fitting package of the Igor Pro software, version 7 (WaveMetrics, Inc). First, the second derivative of the convoluted spectra was used to locate the position of bands. Then, the spectra were deconvoluted using Gaussian curves and a constant baseline (constrained at zero absorbance), in two steps: 1) The position and width of the bands were hold; the height of all bands constrained to a maximum of 80 and a minimum of 0; the fitting was then iterated until no changes were reported between two successive iterations; 2) The width was let change in the 0-20 limit, and the height was let change with a minimum limit of 0; the fitting was iterated until no changes were reported between two successive iterations. The resultant deconvoluted bands composing Amide I were assigned to the different secondary structures of the protein as follows [35,36]: (Tyr) side chains/aggregated strands, 1605-1615 cm^{-1} ; aggregate β -strand/intermolecular β -sheets (weak), 1616-1621 cm^{-1} ; intermolecular β -sheets (strong), 1622-1627 cm^{-1} ; intramolecular β -sheets (strong), 1628-1637 cm^{-1} ; random coils/extended chains, 1638-1646 cm^{-1} ; random coils, 1647-1655 cm^{-1} ; α -helices, 1656-1662 cm^{-1} ; β -turns, 1663-1670, 1671-1685, and 1686-1696 cm^{-1} ; intermolecular β -sheets (weak), 1697-1703 cm^{-1} oxidation bands, 1703-1720 cm^{-1} .

10.2.4. Statistical data analysis

The secondary structures of the different silk samples, as obtained by the FTIR deconvolution/fitting process, were subjected to multivariate statistical analysis through Principal Component Analysis (PCA), using the Simca software Vs 16.0.1 (Sartorius stedim data analytics AB, Germany). PCA fundamentals on data treatment can be found elsewhere^{37–42}. Data acquired on historical and aged samples were centered on the values obtained for pristine silk (“Mod” sample).

10.2.5. Fiber Optics Reflectance Spectroscopy (FORS)

FORS analysis was performed to identify dyes on the silk fibers, using a portable optical fiber spectrophotometer Prime™ X (B&W Tec Inc., Newark, DE, USA) with a back-thinned CCD array detector (1024 pixel), connected to a Deuterium/Tungsten light source and a bifurcated fiber reflectance probe that combines optical fibers (7 fibers, $\varnothing = 200 \mu\text{m}$ each). Spectra were collected for each sample in the 200-900 nm interval, avoiding areas affected by noticeable defects; a 99 % Teflon diffuse reflectance metrological standard from BW Tech (Newark, DE, USA) was employed for calibration. Each spectrum was collected averaging 50 cycles of 50 ms each to enhance S/N; both incident and acquisition angles are perpendicular to the surface. A dedicated software (BWSpec 3.27 by B&W Tec Inc.) was used for spectra acquisition and colorimetric data collection. Spectra collected were compared with those reported in the literature for the identification of dyes [43–47].

10.3. Results and Discussion

Figure 1 shows the ATR-FTIR spectra of pristine commercial silk (“Mod”), and of a set of 18 historical silk samples, in the 1720-1480 cm^{-1} range. This interval was highlighted, as it is used in the deconvolution/fitting process to evaluate the distribution of the protein’s secondary structure. All the spectra exhibit the typical absorptions of *Bombyx mori* silk (as reported in the literature [29,48]) across the full Mid IR range explored by the FPA detector (3900-900 cm^{-1} , see SI Figure 2 and 4). Each spectrum in Figure 1 refers to a single pixel (1.1 x 1.1 μm^2) from the 2D Imaging map of the corresponding sample. The spectra were normalized to the maximum absorbance of Amide I, and a linear baseline was applied between 1720 and 1480 cm^{-1} , prior to the deconvolution step. The

normalization also facilitates the qualitative comparison of the spectral profiles. Almost all spectra exhibit Amide I and II absorptions that resemble those of non-aged *Bombyx mori* silk ("Mod") [29]. In particular, the Amide I band is centered at 1625 cm^{-1} , with only weak band components observable in some cases, between 1640 and 1690 cm^{-1} . The main exceptions are samples HS50 and HS49, respectively a blue (168 years) and a yellow (143 years) textiles, which exhibit a broader band with a shoulder at 1647 cm^{-1} .

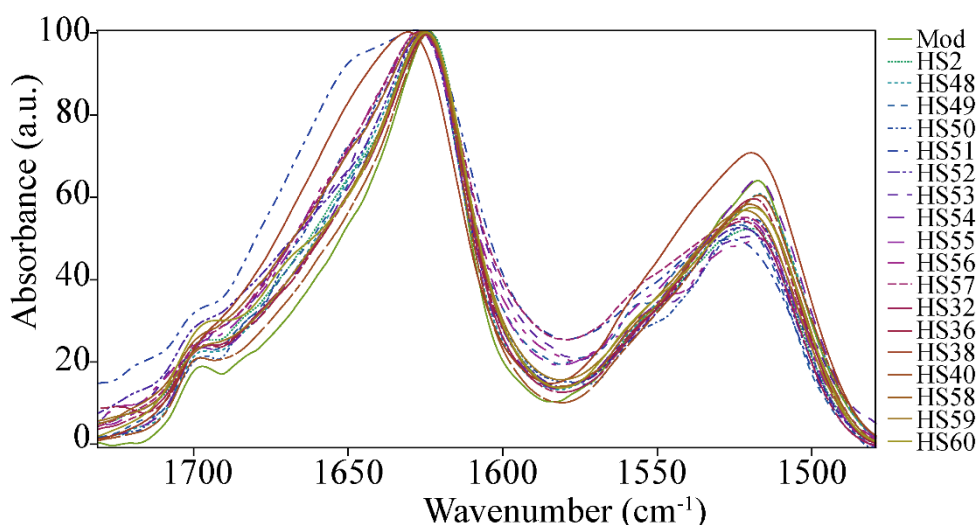


Figure 1 FPA ATR μ -FTIR spectra of pristine commercial silk ("Mod"), and of a subset of 18 historical silk samples, showing the Amide I and II region (1720 - 1480 cm^{-1}). Each spectrum refers to a single pixel ($1.1 \times 1.1\ \mu\text{m}^2$) from the 2D Imaging map of the corresponding sample (representative ATR maps of pristine and historical samples are shown in Figure S12 and S14).

To get further insight, five spectra for each sample (related to five different pixels in each sample's 2D Imaging map) were deconvoluted, and the average resulting structures are shown in Figure 2. As a general trend, the proportion between β -sheets and random coils is close to 54:40, which is in agreement with the description (obtained via X-Ray Diffraction, XRD) of fibroin crystallites uniformly embedded in an amorphous matrix, commonly reported in the literature for standard *Bombyx mori* silk [27,29,36,49]. However, when the detailed composition of the secondary structure of the different samples is

critically analyzed, a striking feature emerges, i.e. the absence of several characteristic types of structures that are normally expected (with different proportions) both in pristine and historical samples. In particular, intramolecular β -sheet (strong) ($1637\text{-}1628\text{ cm}^{-1}$), aggregate β -strand/intermolecular β -sheet (weak) ($1621\text{-}1616\text{ cm}^{-1}$), and random coils/extended chains ($1646\text{-}1638\text{ cm}^{-1}$) are completely missing in all samples. This is in strong disagreement with what we had previously observed in reflectance mode for the Mod sample and three historical samples (see also SI, Figure 1, 3, and 5, and SI Table 4), where these structures were found to be present [34]. While it might be possible that in some (but reasonably not all) historical samples these crystalline structures disappear (as a result of late degradation stages [49]), such structures should be present at least for the pristine *Bombyx mori* silk [27]. Similar considerations apply to α -helices ($1662\text{-}1656\text{ cm}^{-1}$) and two types of β -turns ($1670\text{-}1663$, and $1696\text{-}1686\text{ cm}^{-1}$), which are absent in the ATR spectra of the majority of the samples (including pristine silk). Moreover, other types of structures in the ATR spectra are either significantly overexpressed (intermolecular β -sheet (strong) at $1627\text{-}1622\text{ cm}^{-1}$, random coils at $1655\text{-}1647\text{ cm}^{-1}$, and side chains/aggregated strands at $1615\text{-}1605\text{ cm}^{-1}$) or under-expressed (intermolecular β -sheet (weak) at $1703\text{-}1697\text{ cm}^{-1}$) as opposed to reflectance measurements [34]. The proportion of β -turns ($1685\text{-}1671\text{ cm}^{-1}$) and oxidation bands ($1720\text{-}1703\text{ cm}^{-1}$) are instead consistent with reflectance data. Overall, the deconvolution of ATR-FTIR spectra would suggest that almost all the considered historical samples have secondary structures similar to that of modern pristine silk, which is in contrast with the macroscopic evidence that all historical samples in the set (61 specimens) exhibit significantly poorer mechanical properties than the Mod sample. In fact,

it is well known that mechanical properties depend on the arrangement of secondary structures in silk fibers [50,51].

Similarly, aging the Mod textile did not produce any significant change in the ATR spectra of the samples (see SI, Figure 6 and 7), which again show profiles that match that of pristine silk, regardless of the aging protocol (i.e. using acid pH or UV-Vis photo-aging).

We hypothesized that the pressure applied during the ATR measurements might produce structural changes that favor the formation of some motifs over others, resulting in similar profiles for both pristine and naturally (or artificially) aged samples. In fact, in order to obtain adequate band intensities, an intimate contact is required between the Ge crystal and the textile samples during the ATR experiments, and the inevitable pressure on the fibers might induce microstructural modifications [52]. This is reasonable considering that silk fibroin is a polymorphic material whose structure and structural dynamics are sensitive to experimental conditions such as pH, temperature, and pressure [35,53]. He et al. recently investigated the effects of low pressure on secondary structure transitions in wet films of regenerated silk fibroin [54]; these authors found that the application of low pressure in ATR experiments favors the formation of β -sheets, as seen by increasingly stronger absorptions in the ATR spectra around 1618 cm^{-1} , analogously to what we observed here on silk fibers. Elsewhere, the conversion of silk III structure (threefold extended helix) to silk II (a β -sheet structure) due to surface pressure on a Langmuir trough has also been reported [55].

In conclusion, while ATR is typically considered as a standard tool for inquiring changes in commercial and historical textiles [29,36,56–58], our

results clearly show that, although in some cases partial changes in the spectra profile are observable, this technique is unsuitable when a rigorous characterization of the silk secondary structure is needed, probably owing to the effects of the pressure applied during the measurement. Therefore, detailed information on the structural changes of the naturally and artificially aged silk samples was obtained through reflectance μ -FTIR measurements.

The distribution of the secondary structures for the full set of samples (Mod, Mod1-2, HS1-47), obtained by reflectance μ -FTIR, is shown in Figure 3 (see also SI Table 5). A more heterogeneous distribution of structures is observed (as opposed to the ATR measurements), which was reasonably expected for samples with various origins, age, content (e.g. dyes), and that were likely exposed to different manufacturing processes. Artificial aging of pristine silk at pH 4 (Mod1) produced a strong decrease of aggregate β -strand/intermolecular β -sheets (weak), intermolecular β -sheets (strong and weak), random coils/extended chains, and random coils; an increase in (Tyr) side chains/aggregate, intramolecular β -sheets (strong), β -turns ($1685\text{-}1671\text{ cm}^{-1}$), and oxidation bands was also observed. This is consistent with the hydrolysis of amorphous phases, and the consequent formation of smaller, more isolated crystalline domains [36,59]. UV-Vis aging (Mod2) produced a decrease of aggregate β -strand/intermolecular β -sheets (weak), intermolecular β -sheets (strong and weak), random coils/extended chains, and β -turns ($1670\text{-}1663\text{ cm}^{-1}$), and an increase of (Tyr) side chains/aggregate, intramolecular β -sheets (strong), β -turns ($1685\text{-}1671\text{ cm}^{-1}$), random coils, α -helices, and oxidation bands; this result is consistent with the oxidation of side chains and amorphous domains following irradiation, as reported in the literature [49,59,60].

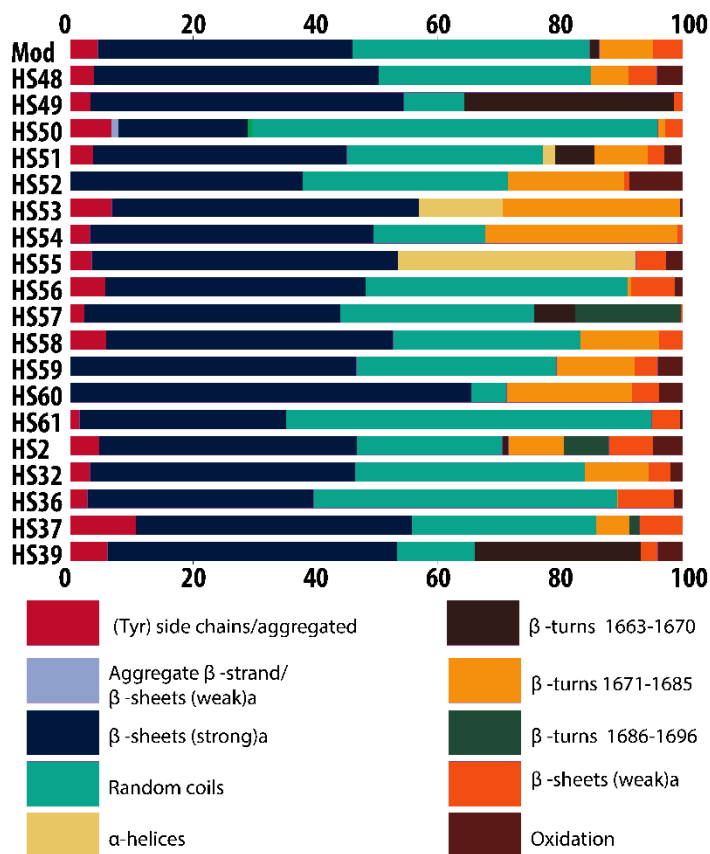


Figure 2. Assigned secondary structures (%) of silk protein, obtained from the deconvolution of the Amide I and II region ($1720\text{--}1480\text{ cm}^{-1}$) of the FPA ATR μ -FTIR spectra of commercial (Mod) and historical silk (subset of 18 samples).

In order to inquire the presence of possible correlations among the secondary structures of the samples, we analyzed the experimental data through a PCA model, an approach that has been extensively used to classify calculated structures in proteins [61], identify spectroscopic markers [29,48,62], and determine protein dynamics [63]. The model uses as variables the percentage amount of the structures obtained by the deconvolution/fitting of the μ -FTIR reflectance spectra (all the 12 different secondary structures), plus the samples age, for 50 silk samples (Mod, Mod1-2, HS1-47). The observations were centered around the values of pristine silk (Mod) so as to highlight differences in the historical samples with respect to non-aged silk. The PCA

Chapter 10. Understanding the structural degradation of Mesoamerican historical silk: A Focal Plane Array (FPA) FTIR and multivariate analysis

model yields a cumulative R² of 0.78 (R₁= 0.67; R₂= 0.11) and a Q₂ of 0.40 (Q₁= 0.43; Q₂= 0.40) for the first two principal components. These results were deemed as acceptable, considering the high variability in the secondary structure exhibited by historical samples with different provenance, aging, and storing conditions prior to their inclusion in a monitored collection.

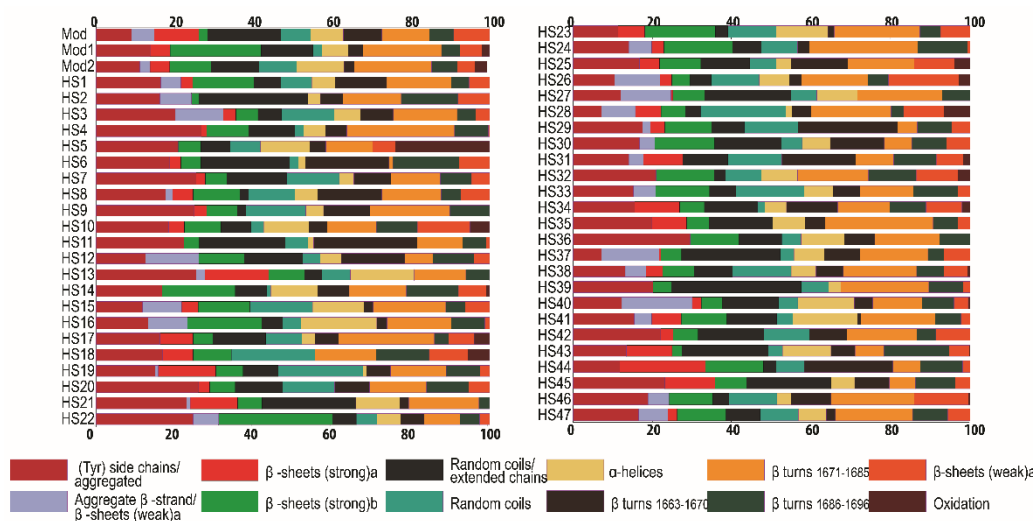


Figure 3 Assigned secondary structures (%) of silk protein, obtained from the deconvolution of the Amide I and II region (1720-1480 cm^{-1}) of reflectance FPA μ -FTIR spectra of commercial (Mod, Mod1-2) and historical silk samples (full set, HS1-47).

The loading plot (see Figure 4) of the first two principal components (PC1,2), shows that PC1 mainly accounts for the variance of crystalline structures, while variance of amorphous structures is predominant in PC2. Positive contributions to PC1 mainly come from (Tyr) side chains/aggregated strands, intramolecular β -sheets (strong), and β -turns (1671-1685 cm^{-1}), along with the age of the samples; oxidation bands provide a smaller contribution. Aggregate β -strand/intermolecular β -sheets (weak), inter-molecular β -sheets (strong), random coils/extended chains, and to a lesser extent α -helices, provide negative contributions. For the considered set of historical silk samples, age can be thus correlated with the degradation of amorphous regions, which produces

smaller and more isolated crystal-line domains. These findings are in good agreement with the literature, where the degradation of fibroin is reported by some authors to start at the amorphous domains, progressively affecting crystalline regions and leading to loss of alignment of β -sheets, until short range order is lost at the latest stage, accompanied by chain scission and strong decrease of crystallinity [29,36,49,59]. However, it is also evident from the model that age cannot be univocally considered as the sole parameter to evaluate changes in the secondary structure. This observation is supported by archeological findings showing that older silk artifacts do not necessarily exhibit worse conservation status than more recent objects [32,45,58,64–68]. Other factors are thus expected to play significant roles in determining changes of the silk protein.

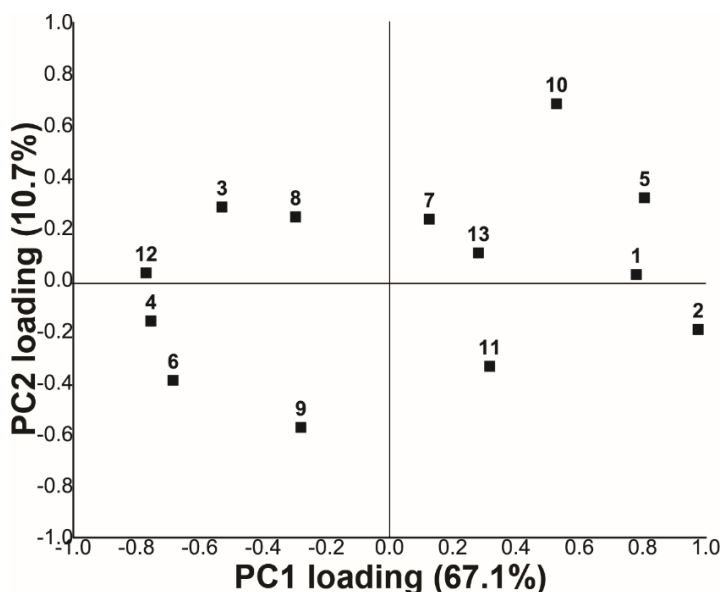


Figure 4. Loading plot (first two principal components, PC1,2) of the PCA model applied to the secondary structures and age of a set of 50 silk samples (Mod, Mod1-2 and HS1-47). The variables are numbered in the plot as follows: age (1), (Tyr) Side chains/aggregated β -strands (2), aggregate β -strand/ β -sheets (weak) (3), intermolecular β -sheets (strong) (4), intramolecular β -sheets (strong) (5), random coils/extended chains (6), random coils (7), α -helices (8), β -turns (1663-1670 cm^{-1}) (9), β -turns (1671-1685 cm^{-1}) (10), β -turns (1686-1696 cm^{-1}) (11), intermolecular β -sheets (weak) (12), oxidation (13).

The score plot obtained from PC1 and PC2 shows a distribution of the samples, with pristine silk (Mod) at the origin of axes, and historical (HS1-47) and artificially aged (Mod1-2) samples shifted to positive values of PC1 (x axis) and positive or negative values of PC2 (y axis). When only the position of the samples in the plot is considered (see SI, Figure 8), no major groups can be distinguished among the silk samples. However, when each sample is associated to its color (Figure 5), some groups and trends are clearly high-lighted. Namely, red samples tend to be located at farther distances from Mod, with large positive values of PC1, i.e. their secondary structure is the most dissimilar from pristine fibers, with the highest increase of intramolecular β -sheets (strong) and (Tyr) side chains/aggregated strands, and some increase of oxidation bands. Blue and yellow samples are in general grouped closer to Mod, roughly halfway along the PC1 axis, but blue samples tend to have negative values of PC2 (increase of random coils/extended chains), while yellow samples have mostly positive PC2 values (increase of α -helices, random coils, and oxidation bands). The yellow samples show also a tighter grouping around Mod1-2. It must be noticed that samples within the same color group have different ages.

The identification of dyes in the historical samples, using FORS (see SI, Table 6 and Figures 9-12), allowed further explanation of the observed trends.

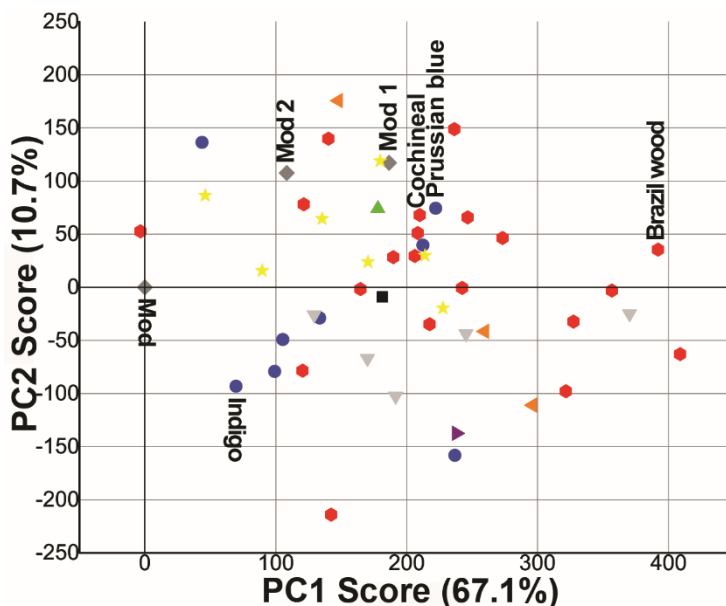


Figure 5. Score plot for PC1 and PC2 of the PCA applied to the different secondary structures and the age for a set of 50 silk samples (Mod, Mod1-2 and HS1-47). In the plot, each silk sample is associated with its color, or marked as gray if non-dyed. Names of the main dyes are specified for each portion of the plot.

The red dyes were found to be cochineal, brazilwood, and madder (see SI, Figure 9). These dyes contain polycyclic aromatic groups, including anthraquinone structures, which are able to form complexes with proteins and metal ions used in the dyeing treatment (e.g. Al ions [69]). Such complexes include extended conjugated structures able to promote the photo-oxidation and weakening of silk proteins; in fact, anthraquinone derivatives are known to be protein photocleavers [70]. Moreover, anthraquinoid dyes are in some cases applied at acidic pH values, in order to achieve the desired hue and stability [69]. These features are consistent with the fact that the red dyed historical fibers have secondary structures characterized by smaller and less inter-connected crystalline domains, decreased amorphous content, and more oxidized groups than pristine silk. For some of the red samples (e.g. Brazil wood, see Figure 5) this trend is more pronounced, while others (e.g. Cochineal) are relatively less degraded and closer in structure to Mod1-2.

Blue dyes were identified as Prussian Blue and Indigo (see SI, Figure 10). Overall, the blue samples exhibit secondary structures that resemble those of pristine silk more than red samples, even though some (including one Prussian Blue) are also close to Mod1-2. In general, blue samples exhibit some increase of (Tyr)side-chains/aggregated strands, random coil/extended chains and β -turns (1696-1686 cm^{-1}). This indicates that slight degradation of the crystalline domains has occurred, leading to an increase of amorphous structures, and to the exposure, rather than scission, of side chains. Macroscopically, the blue dyed fibers show better mechanical behavior than red and yellow samples. In fact, Indigo does not form complexes with the silk protein groups, as opposed to anthraquinoids; instead, the dye-protein interaction is based on ionic and secondary bonds (hydrogen bonds, polar forces and Van der Waals interactions) [71]. The absence of extended conjugated structures is thus expected to limit the photo-oxidation (and consequent degradation) of the indigo dyed fibers.

Most of the yellow dyed samples are grouped around Mod1 and Mod2. Overall, these fibers show secondary structures with decreased intermolecular β -sheets, and increased oxidation groups and random coils, which is consistent with exposure to acidity and photo-oxidative aging [29]. Even though it was not possible to unequivocally identify the yellow dyes by FORS, their spectra resemble those of some natural dyes commonly and historically used, such as hydroxy and methoxy derivatives of flavones and isoflavones, dihydropyrans, anthocyananidins and carotenoids (see SI, Figure 11). These dyes are typically linked to the fibers by the addition of a mordant, in most cases a metal salt whose cation bridges to the fibers through complexation [72]. Even in this case, strong absorption of Vis (blue) and UV light by the complexes can result in oxidation of the fibers. Black silk samples have also some proximity with Mod 1-

2, suggesting that degradation might have occurred also through thermal transformation of oxidized products over prolonged exposition to light and thermal oscillations.

Samples with secondary colors (green, orange, purple) exhibit secondary structures with features ascribable to the presence of the different dyes mixed in their manufacture. Green samples (combination of blue and yellow dyes) show features and degradation patterns similar to those of yellow samples; orange samples (combination of red and yellow dyes) and purple samples (combination of red and blue dyes) followed degradation paths similar to those of red and blue samples, respectively.

10.4. Conclusions

A large set of historical and pristine silk samples was analyzed through FPA μ -FTIR, comparing the information obtained from ATR and reflectance measurements. Even though the ATR spectra of the historical samples exhibit partial differences from pristine silk, the rigorous deconvolution of the Amide I absorptions showed the absence of characteristic types of structures that are expected both in pristine and historical silk. In contrast, the structures obtained from the deconvolution of reflectance spectra showed a heterogeneous distribution of structures, consistent with the typical degradation paths that silk textiles undergo during natural aging. We concluded that the pressure applied during ATR measurements might be enough to induce structural changes in the silk fibers, favoring the formation of some structural motifs (e.g. intermolecular β -sheet strong) over others, producing similar spectral profiles for pristine and aged samples.

The structures obtained by reflectance measurements for the full set of samples were then used as variables for the PCA multivariate analysis aimed to investigate the correlation of age with the degradation of silk textiles. Our results show that there is only a slight correlation between the historical samples' age (spanning over five centuries) and changes in their secondary structure with respect to pristine commercial silk; this suggests that aging time cannot be univocally considered as the main parameter in silk degradation. On the other hand, a correlation was found between the color of the samples and alterations of structures. In particular, silk samples containing red (anthraquinoids) and yellow (flavonoids) dyes exhibited secondary structures similar to those of acid- or photo-aged silk; this is consistent with the formation

of complexes between the dyes, metal cations (mordants) and the proteins, producing large conjugated structures that favor the photo-oxidative degradation of the fibers. Silk containing blue (indigo) dyes show less significant structural alterations, which was explained considering that indigo binds to proteins mostly through ionic and secondary interactions, without the formation of complexes with extended conjugation.

Overall, we demonstrated the efficacy of FPA μ -FTIR in reflectance mode, combined with multivariate analysis, for the rigorous and non-invasive description of the protein secondary structure of large sets of samples. The developed approach constitutes a feasible analytical protocol for the investigation of structural changes in polymeric materials, with potential applications in several fields, including cultural heritage preservation (diagnostics), forensics, material science, industrial quality control, and pharmaceuticals.

References

- [1] Vyas, S. K. & Shukla, S. R. Comparative study of degumming of silk varieties by different techniques. *The Journal of The Textile Institute* 107, 191–199 (2016).
- [2] Inoue, S. et al. Silk Fibroin of *Bombyx mori* Is Secreted, Assembling a High Molecular Mass Elementary Unit Consisting of H-chain, L-chain, and P25, with a 6:6:1 Molar Ratio. *J. Biol. Chem.* 275, 40517–40528 (2000).
- [3] Wojcieszak, M. et al. Origin of the variability of the mechanical properties of silk fibers: 4. Order/crystallinity along silkworm and spider fibers. *Journal of Raman Spectroscopy* 45, 895–902 (2014).
- [4] Vollrath, F., Porter, D. & Dicko, C. 5 - The structure of silk. in *Handbook of Textile Fibre Structure* 2, 146–198 (Woodhead Publishing, 2009).
- [5] Kaplan, D., Adams, W. W., Farmer, B. & Viney (Eds.), and C. *Silk Polymers. Materials Science and Biotechnology.* (American Chemical Society, 1994).
- [6] Weber, R. S., Craig (auth.), C. L., Asakura, T. & Miller (eds.), T. *Biotechnology of Silk.* (Springer Netherlands, 2014).
- [7] Hu, X. et al. Stability of Silk and Collagen Protein Materials in Space. *Scientific Reports* 3, 3428 (2013).
- [8] Jiang, P. et al. Spider silk gut: Development and characterization of a novel strong spider silk fiber. *Scientific Reports* 4, 7326 (2014).
- [9] Rockwood, D. N. et al. Materials Fabrication from *Bombyx mori* Silk Fibroin. *Nat Protoc* 6, (2011).
- [10] Min, K., Kim, S. & Kim, S. Silk protein nanofibers for highly efficient, eco-friendly, optically translucent, and multifunctional air filters. *Sci Rep* 8, (2018).
- [11] Darshan, G. H., Kong, D., Gautrot, J. & Vootla, S. Physico-chemical characterization of *Antheraea mylitta* silk mats for wound healing applications. *Scientific Reports* 7, 10344 (2017).
- [12] Yarger, J. L., Cherry, B. R. & van der Vaart, A. Uncovering the structure–function relationship in spider silk. *Nature Reviews Materials* 3, 18008 (2018).
- [13] Pérez-Rigueiro, J. et al. Emergence of supercontraction in regenerated silkworm (*Bombyx mori*) silk fibers. *Scientific Reports* 9, 2398 (2019).
- [14] Qin, N. et al. Nanoscale probing of electron-regulated structural transitions in silk proteins by near-field IR imaging and nano-spectroscopy. *Nature Communications* 7, 13079 (2016).
- [15] Vollrath, F., Hawkins, N., Porter, D., Holland, C. & Boulet-Audet, M. Differential Scanning Fluorimetry provides high throughput data on silk protein transitions. *Scientific Reports* 4, 5625 (2014).
- [16] Koski, K. J., Akhenblit, P., McKiernan, K. & Yarger, J. L. Non-invasive determination of the complete elastic moduli of spider silks. *Nature Materials* 12, 262–267 (2013).
- [17] Lepore, E., Isaia, M., Mammola, S. & Pugno, N. The effect of ageing on the mechanical properties of the silk of the bridge spider *Larinioides cornutus* (Clerck, 1757). *Scientific Reports* 6, 24699 (2016).
- [18] Aguayo, T., Carolina Araya, M., Mónica Icaza, T. & Campos-Vallette, M. A vibrational approach for the study of historical weighted and dyed silks. *Journal of Molecular Structure* 1075, 471–478 (2014).
- [19] Das, D., Datta, D. B. & Bhattacharya, P. Simultaneous Dyeing and Finishing of Silk Fabric With Natural Color and Itaconic Acid. *Clothing and Textiles Research Journal* 32, 93–106 (2014).
- [20] Degano, I., Biesaga, M., Colombini, M. P. & Trojanowicz, M. Historical and archaeological textiles: An insight on degradation products of wool and silk yarns. *Journal of Chromatography A* 1218, 5837–5847 (2011).
- [21] Egerton, G. S. Some Aspects of the Photochemical Degradation of Nylon, Silk, and Viscose Rayon. *Textile Research Journal* 18, 659–669 (1948).
- [22] Barth, A. Infrared spectroscopy of proteins. *Biochimica et Biophysica Acta (BBA) - Bioenergetics* 1767, 1073–1101 (2007).
- [23] Arrondo, J. L. R., Muga, A., Castresana, J. & Goñi, F. M. Quantitative studies of the structure of proteins in solution by fourier-transform infrared spectroscopy. *Progress in Biophysics and Molecular Biology* 59, 23–56 (1993).

- [24] Percot, A. et al. Water dependent structural changes of silk from *Bombyx mori* gland to fibre as evidenced by Raman and IR spectroscopies. *Vibrational Spectroscopy* 73, 79–89 (2014).
- [25] Chalmers, J. M., Overall, N. J. & Ellison, S. Specular reflectance: A convenient tool for polymer characterization by FTIR-microscopy? *Micron* 27, 315–328 (1996).
- [26] Fringeli, U. P. ATR and Reflectance IR Spectroscopy, Applications. in *Encyclopedia of Spectroscopy and Spectrometry (Third Edition)* (eds. Lindon, J. C., Tranter, G. E. & Koppenaal, D. W.) 115–129 (Academic Press, 2017). doi:10.1016/B978-0-12-803224-4.00104-7
- [27] Hu, X., Kaplan, D. & Cebe, P. Determining Beta-Sheet Crystallinity in Fibrous Proteins by Thermal Analysis and Infrared Spectroscopy. *Macromolecules* 39, 6161–6170 (2006).
- [28] Belton, D. J., Plowright, R., Kaplan, D. L. & Perry, C. C. A robust spectroscopic method for the determination of protein conformational composition – Application to the annealing of silk. *Acta Biomaterialia* 73, 355–364 (2018).
- [29] Vilaplana, F., Nilsson, J., Sommer, D. V. P. & Karlsson, S. Analytical markers for silk degradation: comparing historic silk and silk artificially aged in different environments. *Anal Bioanal Chem* 407, 1433–1449 (2014).
- [30] Smith, M. J., Thompson, K. & Hermens, E. Breaking down banners: analytical approaches to determining the materials of painted banners. *Heritage Science* 4, 23 (2016).
- [31] Koperska, M. A. et al. Degradation markers of fibroin in silk through infrared spectroscopy. *Polymer Degradation and Stability* 105, 185–196 (2014).
- [32] Garside, P., Lahlil, S. & Wyeth, P. Characterization of historic silk by polarized attenuated total reflectance Fourier transform infrared spectroscopy for informed conservation. *Appl Spectrosc* 59, 1242–1247 (2005).
- [33] Ryu, M. et al. Orientational Mapping Augmented Sub-Wavelength Hyper-Spectral Imaging of Silk. *Scientific Reports* 7, 7419 (2017).
- [34] Badillo-Sanchez, D., Chelazzi, D., Giorgi, R., Cincinelli, A. & Baglioni, P. Characterization of the secondary structure of degummed *Bombyx mori* silk in modern and historical samples. *Polymer Degradation and Stability* 157, 53–62 (2018).
- [35] Kong, J. & Yu, S. Fourier Transform Infrared Spectroscopic Analysis of Protein Secondary Structures. *Acta Biochimica et Biophysica Sinica* 39, 549–559 (2007).
- [36] Garside, P. & Wyeth, P. Crystallinity and degradation of silk: correlations between analytical signatures and physical condition on ageing. *Appl. Phys. A* 89, 871–876 (2007).
- [37] Martens, H. & Næs, T. Multivariate calibration. I. Concepts and distinctions. *TrAC Trends in Analytical Chemistry* 3, 204–210 (1984).
- [38] Næs, T. & Martens, H. Multivariate calibration. II. Chemometric methods. *TrAC Trends in Analytical Chemistry* 3, 266–271 (1984).
- [39] Slutsky, B. *Handbook of Chemometrics and Qualimetrics: Part A* By D. L. Massart, B. G. M. Vandeginste, L. M. C. Buydens, S. De Jong, P. J. Lewi, and J. Smeyers-Verbeke. *Data Handling in Science and Technology Volume 20A*. Elsevier: Amsterdam. 1997. xvii + 867 pp. ISBN 0-444-89724-0. \$293.25. *J. Chem. Inf. Comput. Sci.* 38, 1254–1254 (1998).
- [40] Ratola, N., Amigo, J. M. & Alves, A. Comprehensive assessment of pine needles as bioindicators of PAHs using multivariate analysis. The importance of temporal trends. *Chemosphere* 81, 1517–1525 (2010).
- [41] Lee, L. C., Liong, C.-Y. & Jemain, A. A. A contemporary review on Data Preprocessing (DP) practice strategy in ATR-FTIR spectrum. *Chemometrics and Intelligent Laboratory Systems* 163, 64–75 (2017).
- [42] Bereton, R. G. *Pattern Recognition*. in *Applied Chemometrics for Scientists* 145–191 (John Wiley & Sons, Ltd, 2007). doi:10.1002/9780470057780.ch5
- [43] Maynez-Rojas, M. A., Casanova-González, E. & Ruvalcaba-Sil, J. L. Identification of natural red and purple dyes on textiles by Fiber-optics Reflectance Spectroscopy. *Spectrochimica Acta Part A: Molecular and Biomolecular Spectroscopy* 178, 239–250 (2017).
- [44] Angelini, L. G. et al. Characterization of Traditional Dyes of the Mediterranean Area by Non-Invasive Uv-Vis-Nir Reflectance Spectroscopy. *Studies in Conservation* 55, 184–189 (2010).

Chapter 10. Understanding the structural degradation of Mesoamerican historical silk: A Focal Plane Array (FPA) FTIR and multivariate analysis

- [45] Gulmini, M. et al. Identification of dyestuffs in historical textiles: Strong and weak points of a non-invasive approach. *Dyes and Pigments* 98, 136–145 (2013).
- [46] Acquaviva, S., D’Anna, E., De Giorgi, M. L., Della Patria, A. & Baraldi, P. Physical and chemical investigations on natural dyes. *Appl. Phys. A* 100, 823–828 (2010).
- [47] Leona, M. & Winter, J. Fiber Optics Reflectance Spectroscopy: A Unique Tool for the Investigation of Japanese Paintings. *Studies in Conservation* 46, 153–162 (2001).
- [48] Peets, P., Leito, I., Pelt, J. & Vahur, S. Identification and classification of textile fibres using ATR-FT-IR spectroscopy with chemometric methods. *Spectrochimica Acta Part A: Molecular and Biomolecular Spectroscopy* 173, 175–181 (2017).
- [49] Li, M.-Y. et al. Study of the degradation mechanism of Chinese historic silk (*Bombyx mori*) for the purpose of conservation. *Polymer Degradation and Stability* 98, 727–735 (2013).
- [50] Colomban, P., Dinh, H. M., Bunsell, A. & Mauchamp, B. Origin of the variability of the mechanical properties of silk fibres: 1 - The relationship between disorder, hydration and stress/strain behaviour. *Journal of Raman Spectroscopy* 43, 425–432 (2012).
- [51] Jauzein, V. & Colomban, P. 6 - Types, structure and mechanical properties of silk. in *Handbook of Tensile Properties of Textile and Technical Fibres* (ed. Bunsell, A. R.) 144–178 (Woodhead Publishing, 2009).
- [52] Van Nimmen, E. et al. FT-IR spectroscopy of spider and silkworm silks: Part I. Different sampling techniques. *Vibrational Spectroscopy* 46, 63–68 (2008).
- [53] Wilson, D., Valluzzi, R. & Kaplan, D. Conformational Transitions in Model Silk Peptides. *Biophysical Journal* 78, 2690–2701 (2000).
- [54] He, Z., Liu, Z., Zhou, X. & Huang, H. Low pressure-induced secondary structure transitions of regenerated silk fibroin in its wet film studied by time-resolved infrared spectroscopy. *Proteins* 86, 621–628 (2018).
- [55] Valluzzi, R., Gido, S. P., Zhang, W., Muller, W. S. & Kaplan, D. L. Trigonal Crystal Structure of *Bombyx mori* Silk Incorporating a Threefold Helical Chain Conformation Found at the Air–Water Interface. *Macromolecules* 29, 8606–8614 (1996).
- [56] Huang, D. et al. A new consolidation system for aged silk fabrics: Effect of reactive epoxide-ethylene glycol diglycidyl ether. *Reactive and Functional Polymers* 73, 168–174 (2013).
- [57] Liu, J. et al. Identification of ancient textiles from Yingpan, Xinjiang, by multiple analytical techniques. *Journal of Archaeological Science* 38, 1763–1770 (2011).
- [58] Nilsson, J., Vilaplana, F., Karlsson, S., Bjurman, J. & Iversen, T. The Validation of Artificial Ageing Methods for Silk Textiles Using Markers for Chemical and Physical Properties of Seventeenth-Century Silk. *Studies in Conservation* 55, 55–65 (2010).
- [59] Hirabayashi, K., Yanagi, Y., Kawakami, S., Okuyama, K. & Hu, W. Degradation of silk fibroin. *The Journal of Sericultural Science of Japan* 56, 18–22 (1987).
- [60] Lu, Q. et al. Degradation Mechanism and Control of Silk Fibroin. *Biomacromolecules* 12, 1080–1086 (2011).
- [61] Howe, P. W. A. Principal components analysis of protein structure ensembles calculated using NMR data. *J Biomol NMR* 20, 61–70 (2001).
- [62] Yu, X. et al. Surface enhanced Raman spectroscopy distinguishes amyloid B-protein isoforms and conformational states. *Protein Science* 27, 1427–1438 (2018).
- [63] David, C. C. & Jacobs, D. J. Principal component analysis: a method for determining the essential dynamics of proteins. *Methods Mol. Biol.* 1084, 193–226 (2014).
- [64] Liu, M. et al. Identification of Ancient Silk Using an Enzyme-linked Immunosorbent Assay and Immuno-fluorescence Microscopy. *Analytical Sciences* 31, 1317–1323 (2015).
- [65] Zhang, X. & Wyeth, P. Using FTIR spectroscopy to detect sericin on historic silk. *Sci. China Chem.* 53, 626–631 (2010).
- [66] Barrigón, M. Textiles and Farewells: Revisiting the Grave Goods of King Alfonso VIII of Castile and Queen Eleanor Plantagenet. *Textile History* 46, 235–257 (2015).
- [67] Karl, B. Silk and Propaganda — Two Ottoman Silk Flags and the Relief of Vienna, 1683. *Textile History* 45, 192–215 (2014).

PART III. MOLECULAR STUDY OF SILK

- [68] Levey, S. M. Illustrations of the History of Knitting Selected from the Collection of the Victoria and Albert Museum. *Textile History* 1, 183–205 (1969).
- [69] Bechtold, T. Natural Colorants – Quinoid, Naphthoquinoid and Anthraquinoid Dyes. in *Handbook of Natural Colorants* (eds. Bechtold, T. & Mussak, R.) 151–182 (John Wiley & Sons, Ltd, 2009).
- [70] Suzuki, A., Hasegawa, M., Ishii, M., Matsumura, S. & Toshima, K. Anthraquinone derivatives as a new family of protein photocleavers. *Bioorganic & Medicinal Chemistry Letters* 15, 4624–4627 (2005).
- [71] Steingruber, E. Indigo and Indigo Colorants. in *Ullmann's Encyclopedia of Industrial Chemistry* (Wiley-VCH Verlag GmbH & Co. KGaA, 2000).
- [72] Rosenberg, E. Characterisation of historical organic dyestuffs by liquid chromatography–mass spectrometry. *Anal Bioanal Chem* 391, 33–57 (2008).

Supplementary Information

Chapter 10

PART III. MOLECULAR STUDY OF SILK

SI Table 1. List of Flags (belonging to the National Museum of Colombia), from which silk samples were collected and analyzed in this study

Museum ID flag reference	Name	Possible provenance	Date (year)	Dimensions (cm)
97	Coat of arms of the royal audience of Santa Fe	Spain	Ca. 1550	164 x 133 x 5
99	Flag with the coat of arms of Castilla y León	Spain	Ca. 1700	159 x 155
100	Flag of the infantry regiment of "los Cazadores de Extremadura, second battalion"	Spain	Ca. 1815	158 x 150
101	Flag of the Spanish regiment "of Burgos"	Spain	Ca. 1815	145 x 143
103	Flag of a Spanish battalion of infantry	Spain	Ca. 1813	150 x 140
104	Flag of the Numancia battalion	Spain	Ca. 1813	148 x 145
105	Gran Colombia's flag from the Hussars' battalion	Colombia	Ca. 1824	73 x 78
106	Gran Colombia's flag from the Hussars del centro' battalion	Colombia	Ca. 1824	79 x 88
107	Gran Colombia's flag from the Milicias Regladas de Cartagena' battalion	Colombia	Ca. 1823	168 x 162,5
108	Flag of the first military auxiliary battalion of the province of Bogota	Colombia	Ca. 1824	153 x 153
109	Flag with the coat of arms of King Carlos IV of Spain	Spain	Ca. 1790	104,5 x 160
110	Gran Colombia's flag of the Ligeros No1' battalion	Spain	Ca. 1824	160,7 x 153
111	Gran Colombia's flag of the National Artillery Brigade, of Cundinamarca	Colombia	Ca. 1824	143 x 195
113	Flag from one of the Colombian civil wars	Colombia	Ca. 1850	147,8 x 166
114	"Estados Unidos de Colombia's Flag", dedicated to the Cauca's liberators	Colombia	Ca. 1861	255 x 155
115	Banner taken at the Panama Chagres capitulation	Spain	Ca. 1815	98 x 124
116	Flag with the coat of arms of Castilla y León from the "Escuadrón de Vaqueanos del Batallón General"	Spain	Ca. 1700	74 x 106
117	Banner with the Spanish coat of arms	Spain	Ca. 1808	168 x 162,5
118	Banner with the Castilla y León coat of arms	Spain	Ca. 1808	134 x 111

Supplementary Information Chapter 10

120	Venezuelan flag taken at the Garrapecera battle	Venezuela	1901	144 x 185
122	Gran Colombia's flag from the Simón Bolívar No. 17 battalion	Colombia	1824	178,5 x 253
124	Arequipa's coat of arms	Peru	Ca. 1875	107 x 80
126	Colombian Sovereignty flag which sailed over the amazon river after the Salomón Lozano frontiers treaty	Colombia	1929	65 x 95,5
129	Colombian flag gifted to the Gr. Manuel Briceño	Colombia	1885	247 x 233,5
1948	Estados unidos de Colombia's coat of arms	Venezuela	s. XIX	173 x 183
3044	Colombian flag that owns to José Hilario López	Colombia	Ca. 1849	280 x 195
3245	Banner that owns to Gr. Pedro Alcántara Herrán	Colombia	s. XIX	49 x 54,3
3305	Estados Unidos de Colombia's coat of arms from the Chía No. 27 army battalion	Spain	Ca. 1538	105 x 34
3615	Battalion Rifles No. 14 of the republic of Colombia coat of arms	Colombia	Ca. 1899	81,2 x 64,8
6079	Colombian flag that owns to the Gr. Solón Wilches	Colombia	Ca. 1880	42 x 23
7354	Battalion Santos N° 4 flag won in the Palonegro battle for the Gr. Josué Calasanz Guevara	Colombia	1900	173 x 183

PART III. MOLECULAR STUDY OF SILK

SI Table 2. List of silk samples used for the ATR μ -FTIR analysis

Sample	Date	Museum ID flag
Mod	2015	--
HS2	1901	120
HS48	1880	6079
HS49	1875	124
HS50	1850	113
HS51	1901	1948
HS52	1860	3245
HS53	1824	108
HS54	1824	106
HS55	1823	107
HS56	1815	115
HS57	1813	103
HS32	1813	104
HS36	1808	118
HS38	1790	109
HS40	1700	116
HS58	1700	99
HS59	1700	99
HS60	1550	97
HS61	1538	3305

SI Table 3. List of silk samples used for the reflectance μ -FTIR analysis. MNC: Fiber not colored, originally located inside a metal thread in the artifact; NC: Not colored; --: Not measured

Sample	Date	Museum ID flag	Color	Age
Mod	2015	MOD	NC	3
Mod1	2018	Mod pH 4	NC	1
Mod2	2018	Mod UV	NC	1
HS1	1929	126	Red	89
HS2	1901	120	Red	117
HS3	1901	1948	Red	117
HS4	1900	7354	Yellow	118
HS5	1900	7354	Red	118
HS6	1899	3615	Red	119
HS7	1885	129	Yellow	133
HS8	1885	129	Orange	133
HS9	1880	6079	Red	138
HS10	1875	124	Black	143

Supplementary Information Chapter 10

HS11	1875	124	Purple	143
HS12	1861	114	Blue	157
HS13	1861	114	Red	157
HS14	1849	3044	Blue	169
HS15	1849	3044	Red	169
HS16	1840	3245	Yellow	178
HS17	1824	111	Green	194
HS18	1824	111	Red	194
HS19	1824	110	Red	194
HS20	1824	122	Red	194
HS21	1824	105	Orange	194
HS22	1824	106	MNC	194
HS23	1823	107	Orange	195
HS24	1823	107	Red	195
HS25	1815	100	Yellow	203
HS26	1815	100	Yellow	203
HS27	1815	101	Blue	203
HS28	1815	101	Red	203
HS29	1815	100	MNC	203
HS30	1815	101	MNC	203
HS31	1813	103	Blue	205
HS32	1813	104	Red	205
HS33	1808	118	Blue	210
HS34	1808	117	Red	210
HS35	1808	117	Red	210
HS36	1808	118	Red	210
HS37	1790	109	Yellow	228
HS38	1790	109	Red	228
HS39	1700	116	Yellow	318
HS40	1700	116	Red	318
HS41	1700	99	MNC	318
HS42	1700	116	MNC	318
HS43	1550	97	Blue	468
HS44	1550	97	MNC	468
HS45	1538	3305	Blue	480
HS46	1538	3305	Blue	480
HS47	1538	3305	Red	480

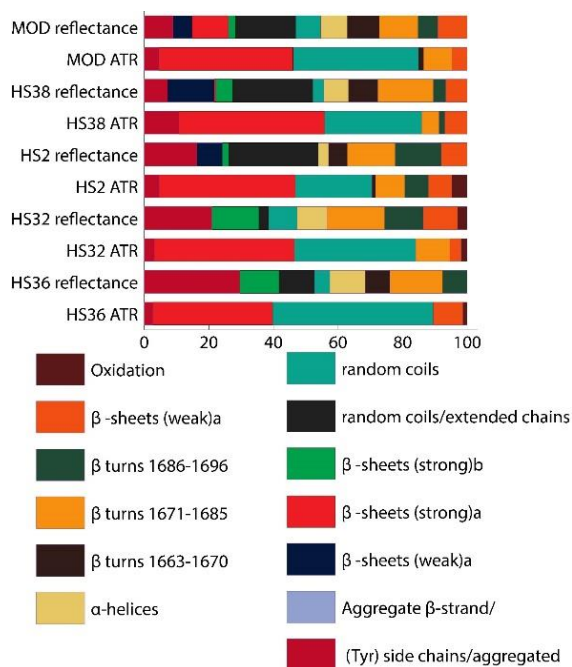
PART III. MOLECULAR STUDY OF SILK

SI Table 4. Assigned secondary structures (%) of silk protein obtained from the deconvolution of the Amide I and II region (1720-1480 cm⁻¹) of the FPA ATR and reflectance μ -FTIR spectra of commercial ("Mod") and historical silk ("HS2,32,36,38").

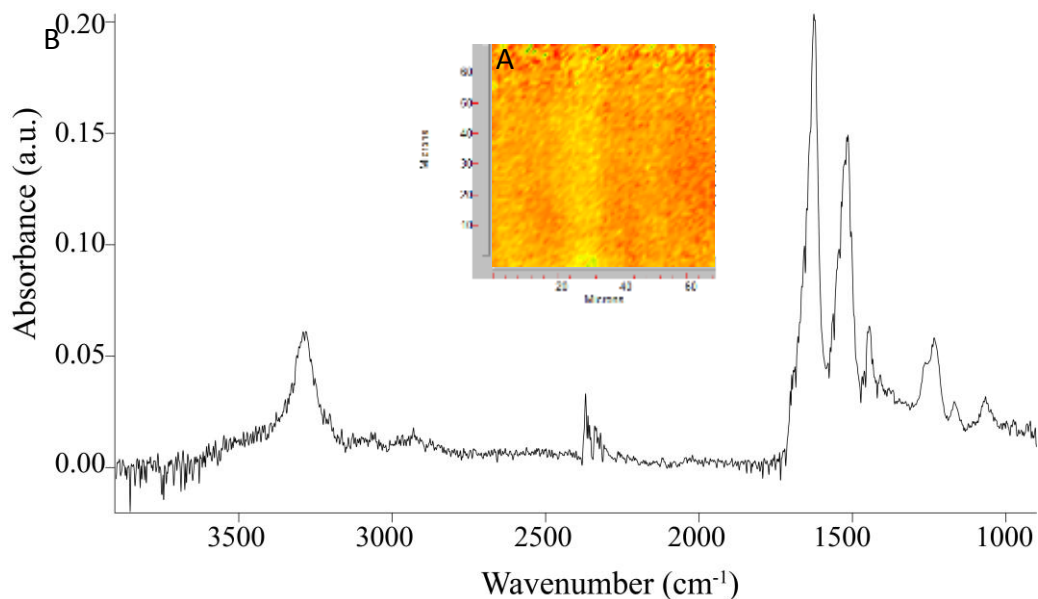
Protein secondary structure	MOD reflect.	MOD ATR	HS38 reflect.	HS38 ATR	HS2 reflect.	HS2 ATR	HS32 reflect.	HS32 ATR	HS36 reflect.	HS36 ATR
(Tyr) side chains/aggregated	8.95	4.51	7.26	10.66	16.30	4.67	20.93	3.18	29.61	2.77
Aggregate β -strand/ β -sheets (weak)a	5.89	0.00	14.43	0.00	7.88	0.00	0.00	0.00	0.00	0.00
β -sheets (strong)a	11.21	41.59	0.48	45.17	0.00	42.15	0.00	43.35	0.00	36.97
β -sheets (strong)b	2.22	0.00	5.15	0.00	1.97	0.00	14.60	0.00	12.17	0.00
Random coils/extended chains	18.65	0.00	24.92	0.00	27.75	0.00	2.96	0.00	10.86	0.00
Random coils	7.72	38.78	3.42	30.10	0.00	23.70	8.85	37.50	4.87	49.69
α -helices	8.24	0.00	7.58	0.00	3.14	0.00	9.22	0.00	10.91	0.00
β turns 1663-1670	9.84	1.57	9.09	0.00	5.81	1.07	0.00	0.00	7.68	0.00
β turns 1671-1685	12.04	8.74	17.16	5.40	14.78	9.04	17.86	10.51	16.27	0.10
β turns 1686-1696	6.10	0.00	3.82	1.70	14.32	7.36	12.02	0.00	7.63	0.00
β -sheets (weak)a	9.13	4.81	6.67	6.98	8.05	7.20	10.60	3.56	0.00	9.11
Oxidation	0.00	0.00	0.00	0.00	0.00	4.81	2.96	1.91	0.00	1.37

For β -sheets: "a": intermolecular; "b": intramolecular.

Supplementary Information Chapter 10

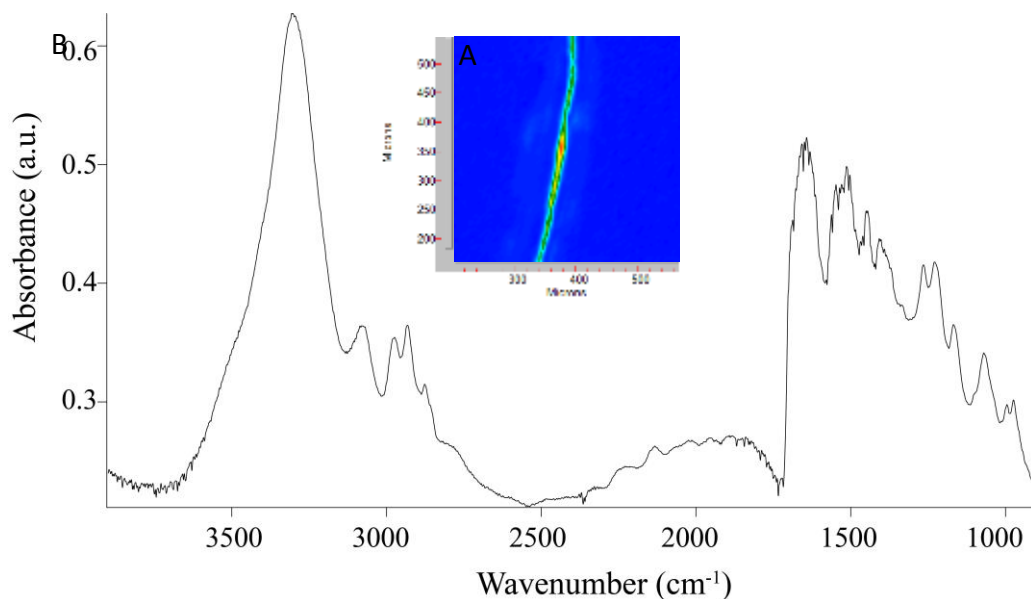


SI Figure 1. Bar plot of the assigned secondary structures (%) of silk protein (also shown in SI Table 4), obtained from the deconvolution of the Amide I and II region (1720-1480 cm^{-1}) of the FPA ATR and reflectance μ -FTIR spectra of commercial ("Mod") and historical silk ("HS2,32,36,38").

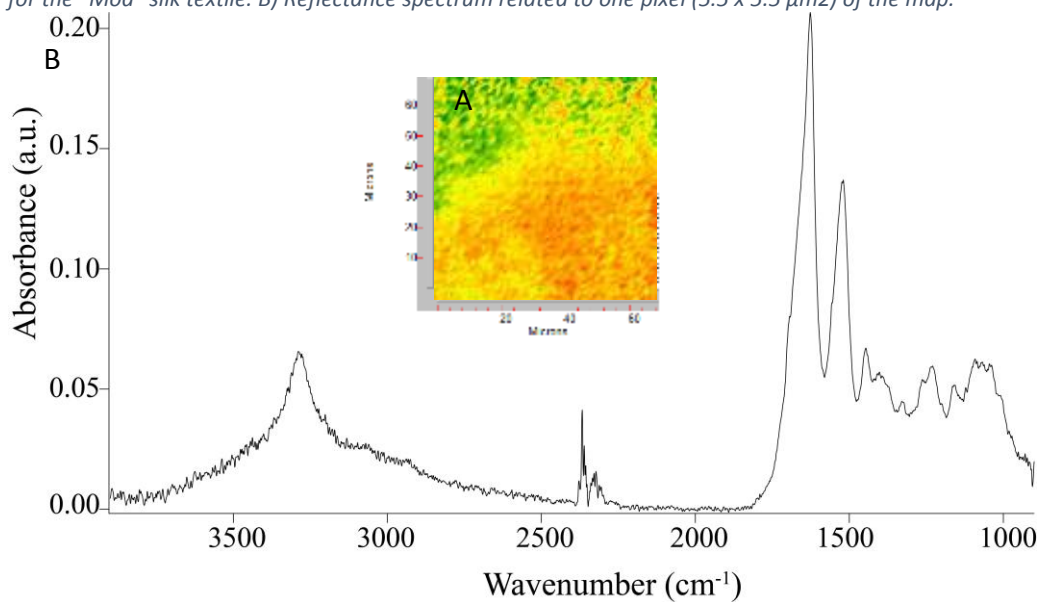


SI Figure 2. A) ATR 2D FPA map of the intensity of the Amide A band (in the 3440-3160 cm^{-1} range) for the "Mod" silk textile. B) ATR spectrum related to one pixel (1.1 x 1.1 μm^2) of the map.

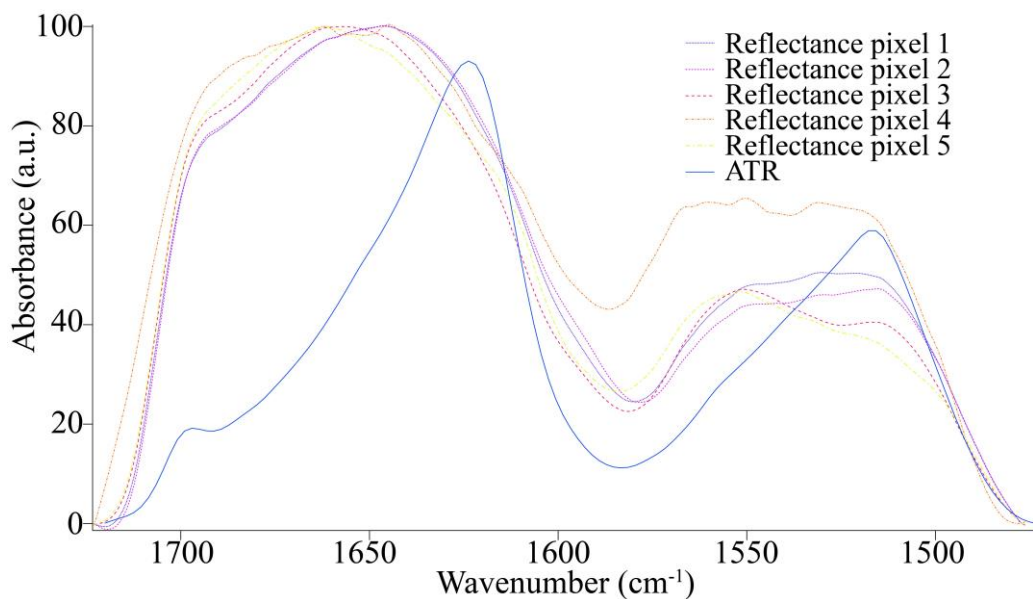
PART III. MOLECULAR STUDY OF SILK



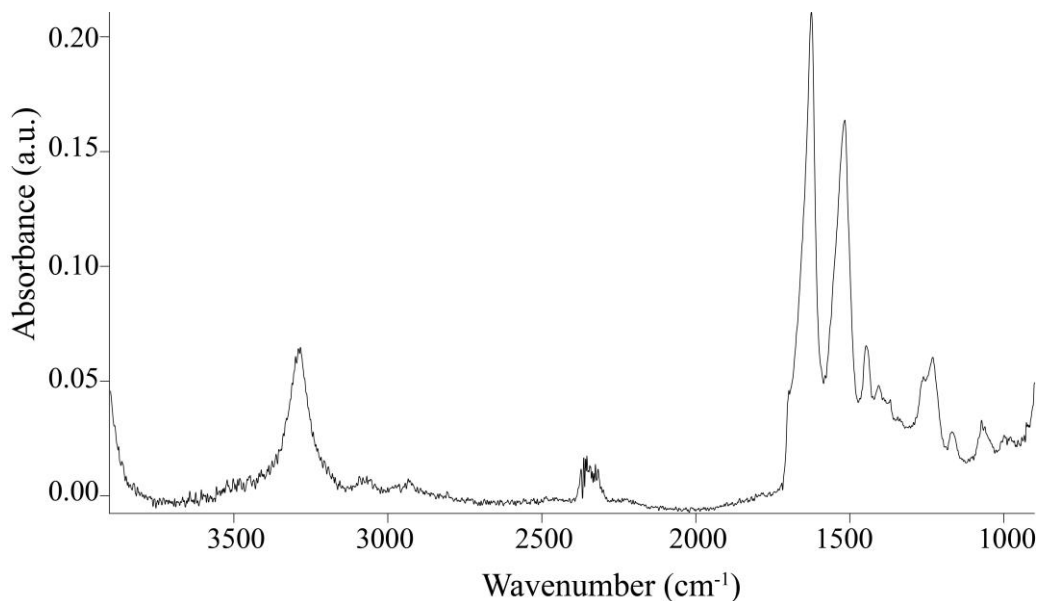
SI Figure 3. A) Reflectance 2D FPA map of the intensity of the Amide A band (in the 3440-3160 cm⁻¹ range) for the "Mod" silk textile. B) Reflectance spectrum related to one pixel (5.5 x 5.5 μm²) of the map.



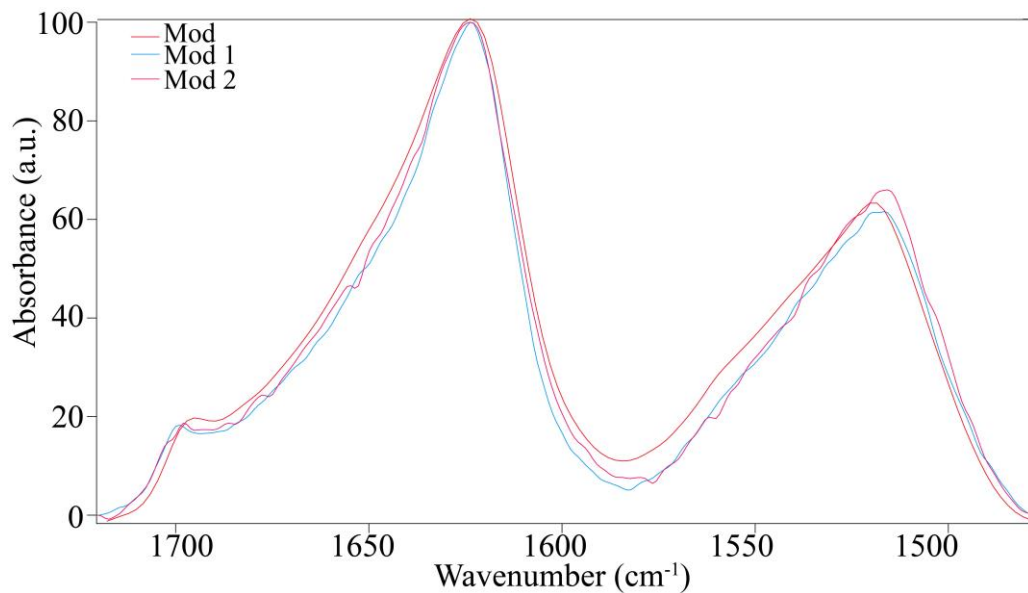
SI Figure 4. A) ATR 2D FPA map of the intensity of the Amide A band (in the 3440-3160 cm⁻¹ range) for the "HS2" silk textile. B) ATR spectrum related to one pixel (1.1 x 1.1 μm²) of the map



SI Figure 5. Comparison of an ATR spectrum (related to one pixel from the 2D FTIR map shown in Figure SI2B) and five reflectance spectra (related to five different pixels from the 2D FTIR map shown in Figure SI3B) of the “Mod” sample in the Amide I and II region (1750-1450 cm^{-1})



SI Figure 6. ATR Spectra (3900-900 cm^{-1}) of the “Mod2” sample.



SI Figure 7. Comparison of ATR spectra of the "Mod", "Mod1" and "Mod2" samples, in the Amide I and II region (1750-1450 cm⁻¹).

Supplementary Information Chapter 10

SI Table 5. Assigned secondary structures (%) of silk protein obtained from the deconvolution of the Amide I and II region (1720-1480 cm⁻¹) of the FPA reflectance μ -FTIR spectra of commercial (“Mod”, “Mod1-2”) and historical silk (“HS1-47”). (For β -sheets: “a”: intermolecular; “b”: intramolecular.)

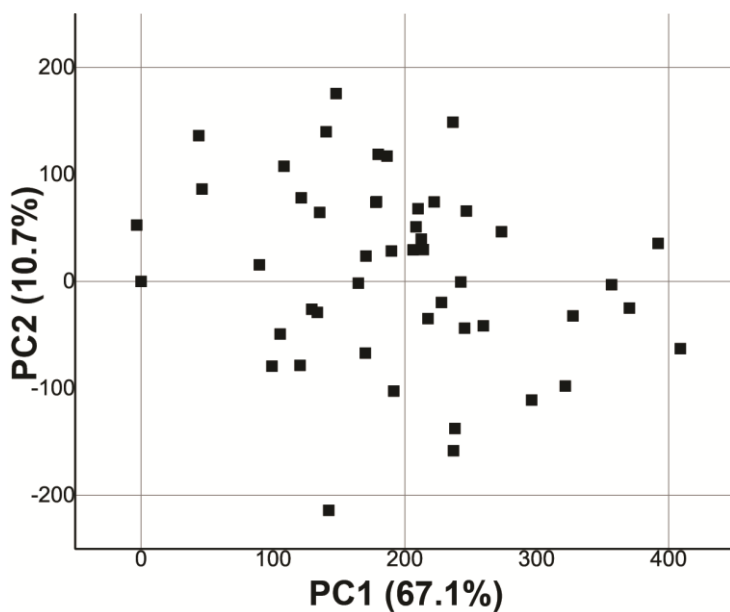
Sample	(Tyr) side chains/ aggregated	Aggregate β -strand/ β -sheets (weak)a	β -sheets (strong)a	β -sheets (strong)b	Random coils/ extended chains	Random coils	α -helices	β -Turns 1663-1670	β -Turns 1671-1685	β -Turns 1686-1696	β -sheets (weak)a	Oxidation
Mod	8.95	5.89	11.21	2.22	18.65	7.72	8.24	9.84	12.04	6.10	9.13	0.00
Mod1	13.73	0.00	5.18	23.11	13.07	2.37	6.70	3.67	19.95	4.70	5.62	1.89
Mod2	11.06	2.64	4.99	10.53	12.26	9.51	12.04	2.62	19.65	6.54	4.43	3.17
HS1	16.45	5.10	3.02	15.49	6.82	7.98	5.87	13.17	16.42	4.46	5.22	0.00
HS2	16.30	7.88	0.00	1.97	27.75	0.00	3.14	5.81	14.78	14.32	8.05	0.00
HS3	20.19	12.08	3.29	5.62	5.95	13.50	6.53	8.41	16.24	4.63	3.57	0.00
HS4	26.73	0.00	1.40	10.53	11.83	2.35	5.52	5.41	27.37	8.68	0.20	0.00
HS5	20.90	0.00	0.00	5.77	7.42	7.77	12.51	4.11	11.85	0.00	5.78	23.90
HS6	18.79	0.00	2.77	5.08	22.60	2.19	1.82	21.23	1.02	16.77	7.73	0.00
HS7	25.45	0.00	2.37	5.37	15.24	13.40	3.72	9.43	12.58	7.95	4.50	0.00
HS8	17.70	1.74	5.20	11.96	2.07	11.82	5.79	16.39	15.10	4.85	7.38	0.00
HS9	24.91	0.00	3.22	7.73	2.22	15.26	4.44	11.92	20.23	10.07	0.00	0.00
HS10	18.51	0.00	3.88	9.35	7.62	3.26	11.55	4.61	12.45	10.49	13.28	5.00
HS11	22.23	0.00	0.00	4.00	21.87	5.85	1.38	26.30	11.57	5.95	0.84	0.00
HS12	12.53	13.55	0.00	11.58	14.88	4.46	5.35	16.16	7.11	10.43	3.95	0.00
HS13	25.43	2.22	16.27	9.00	4.54	7.20	16.22	0.00	13.17	5.94	0.00	0.00
HS14	16.81	0.00	0.00	18.62	7.98	0.93	11.98	8.01	14.49	13.30	7.02	0.86
HS15	11.80	9.96	4.23	13.05	0.15	15.88	12.99	2.43	18.43	4.90	6.18	0.00

PART III. MOLECULAR STUDY OF SILK

HS16	13.20	10.03	0.00	18.93	5.23	4.77	19.17	2.68	16.39	8.46	1.16	0.00
HS17	16.25	0.00	8.41	5.12	13.28	9.28	3.17	6.12	24.38	3.53	6.61	3.84
HS18	22.96	0.94	12.11	6.26	23.73	0.00	11.28	2.15	17.93	2.64	0.00	0.00
HS19	16.89	0.00	7.75	9.75	0.00	21.29	0.00	0.00	15.50	13.52	9.77	5.53
HS20	15.05	0.82	14.64	6.86	8.87	21.65	0.86	6.15	14.20	8.58	2.31	0.00
HS21	25.98	0.00	2.93	6.49	12.08	13.17	0.00	8.85	14.47	10.73	5.30	0.00
HS22	24.62	6.51	0.00	28.99	6.01	5.29	6.01	5.97	9.03	5.14	2.42	0.00
HS23	11.48	0.00	6.60	17.87	3.06	12.29	13.01	1.54	21.59	5.19	7.39	0.00
HS24	14.15	5.69	3.04	17.39	7.10	9.12	0.00	3.19	27.25	12.49	0.57	0.00
HS25	12.09	12.57	0.52	8.08	21.79	6.33	10.28	0.00	21.44	6.91	0.00	0.00
HS26	7.36	8.43	6.46	6.10	3.74	21.58	1.44	4.89	20.10	3.22	10.19	6.48
HS27	16.83	0.00	5.01	10.36	12.28	6.69	3.76	14.39	16.75	0.00	10.00	3.91
HS28	10.50	11.41	2.99	4.69	5.20	12.17	7.60	3.08	16.71	5.28	17.66	2.72
HS29	17.69	1.88	3.64	11.78	8.16	13.58	0.00	25.08	4.95	8.68	4.56	0.00
HS30	16.85	3.75	0.00	15.10	16.78	5.27	7.02	13.60	7.08	8.74	5.81	0.00
HS31	14.14	3.64	9.94	0.00	11.26	13.65	0.00	18.66	9.54	10.77	6.76	1.64
HS32	20.93	0.00	0.00	14.60	2.96	8.85	9.22	0.00	17.86	12.02	10.60	2.96
HS33	15.19	5.71	0.00	13.55	6.62	17.17	7.25	6.78	13.49	11.26	2.98	0.00
HS34	15.67	0.00	11.23	6.19	13.36	2.01	5.24	12.97	13.19	9.15	8.99	2.00
HS35	19.94	0.00	8.65	5.54	16.26	0.00	8.05	5.07	27.22	6.28	2.98	0.00
HS36	29.61	0.00	0.00	12.17	10.86	4.87	10.91	7.68	16.27	7.63	0.00	0.00
HS37	7.26	14.43	0.48	5.15	24.92	3.42	7.58	9.09	17.16	3.82	6.67	0.00
HS38	13.22	5.30	4.14	7.85	9.69	14.88	6.10	6.92	18.46	7.00	5.91	0.53
HS39	20.15	0.00	0.00	4.63	32.74	7.03	2.89	0.00	22.22	8.67	1.66	0.00

Supplementary Information Chapter 10

HS40	12.24	17.77	2.40	5.32	14.07	4.89	14.17	4.66	12.56	7.88	3.65	0.40
HS41	15.49	4.32	7.42	11.48	12.64	4.13	16.16	0.94	18.66	6.65	2.11	0.00
HS42	22.11	0.00	3.18	6.29	16.53	11.57	0.00	9.36	17.60	4.72	8.64	0.00
HS43	13.53	0.00	11.49	2.51	21.63	3.65	12.19	6.14	7.17	16.42	5.14	0.13
HS44	11.85	0.00	21.56	14.61	3.19	7.07	0.00	22.34	6.92	10.66	1.79	0.00
HS45	23.08	0.00	12.78	7.81	21.39	0.00	5.98	8.70	6.57	10.08	3.61	0.00
HS46	19.00	5.29	0.00	11.02	4.09	11.99	3.64	10.05	20.81	0.00	13.78	0.33
HS47	16.62	7.34	2.29	12.36	8.51	9.70	7.07	2.18	19.56	8.93	5.45	0.00



SI 8. Score plot obtained from PCA considering as variables the relative amounts (%) of different secondary structures (from FTIR measurements and deconvolution fitting process) for a set of 50 silk samples (Mod, Mod1-2 and HS1-47), and the age of the samples.

PART IV.
SILK CONSOLIDATION

Chapter 11.

Self-regenerated silk fibroin with controlled crystallinity for the reinforcement of silk

Abstract

Silk artifacts constitute a fundamental cultural and historical heritage, yet they are affected by degradation that alters the secondary structure of fibroin and weaken the mechanical properties of textiles, hindering their preservation. Feasible and compatible consolidants for silk are still largely needed. Here, we propose a robust and reliable method to restore the mechanical properties of fragile, aged silk fibers, based on the application of self-regenerated silk fibroin (SRSF) with controlled crystallinity, prepared from waste silk. By varying the concentration of fibroin dispersions, the content of crystalline and amorphous domains in SRSF films can be tuned, as demonstrated by 2D micro-Fourier transform infrared spectroscopy Imaging and thermal analysis. Namely, the application of amorphous films (random coils/extended chains > 60%) completely recovered the mechanical properties of aged silk fibers, without inducing unwanted alterations. The possibility to feasibly confer desired mechanical properties to degraded silk fibers open new perspectives in textile conservation, biomaterials and materials engineering, and in the preparation of composites with enhanced properties.

11.1. Introduction

Silk has been employed by mankind since ancient times to produce different types of artifacts, tapestries, and garments [1,2]. The most frequently used raw material is the domesticated *Bombyx mori* cocoon's spun fiber, which undergoes a degumming process to remove the coating of sericin protein [3]. The resulting silk fibers have a hierarchical structure, with filaments that are typically 7-12 μm wide, composed of fibrillar elements (ca. 1 μm wide), in turn made up of 10 nm wide microfibrils [4]. Degummed silk is mainly composed of Heavy-Fibroin, Light-Fibroin, and P25 (a chaperonin-like protein), in a 6:6:1 ratio [5], present as amorphous and crystalline domains oriented along the fiber axis [2,6]. The composition and structure of this proteinaceous material account for its valuable physical and mechanical properties, i.e. strength, lightness, smoothness and luster, which explain its use in ancient and modern fabrics, as well as in recently developed bio-materials [7–10].

Historical silk objects are an invaluable cultural and artistic patrimony, mainly comprising clothes, tapestries, flags, banners and decorative objects. However, silk is affected by several degradation pathways, e.g. oxidation, hydrolysis, chain scission and chain rearrangements, mainly induced by environmental factors (relative humidity, light, temperature), and by the presence of acids, oxidizing compounds, metal components, and biopollutants [1,8,11]. The resulting changes in the secondary structures of silk fibers cause the alteration of their mechanical properties [12,13], and as a result historical samples can be fragile and exhibit scarce flexibility [14–16]. To avoid the loss of this heritage, there is the strong need to find feasible and reliable methodologies for the consolidation of weakened silk artifacts.

The traditional textile conservation practice includes repairs and lining, and the use of synthetic polymers (adhesives, glues, etc.). Repairs, such as the introduction of new silk or paper elements, are used to provide mechanical support to weakened silk objects [17–19]. However, these methods introduce non-original components in the artifacts, and do not provide the *in situ* reinforcement (at the micro scale) needed by the original fibers, which are still exposed to degradation processes. Synthetic polymers (e.g. acrylates, vinyl acetates, epoxy resins) are widely used as consolidants owing to their good adhesion and mechanical properties [20], however these materials present several drawbacks. Natural aging can cause the yellowing of the polymers, producing aesthetical alteration of the textiles. Vinyl polymers undergo deacetylation and loss of organic acids [21] that are detrimental to silk. Besides, aging produces changes in the molecular weight of the synthetic polymers due to cross-linking or chain scission reactions, affecting the polymers solubility in their original solvents, and hindering their safe removal from the artifacts [22–25]. Huang et al. used epoxide-ethylene glycol diglycidyl ether (EGDE) to crosslink with tyrosine and lysine in amorphous domains of silk fibroin, producing mechanical strengthening [26], and previously Cai et al. had modified silk fibers with a silicone-containing epoxide, producing significant changes of physical and chemical properties [27].

Alternatively, biopolymers represent an attractive and sustainable source of potential consolidants for silk. Cellulose has been widely employed to formulate composites with silk fibroin [28–32], mainly to produce films, membranes, foams, and gels of biomaterials for *in vivo* use. For instance, cellulose nanofibrils (CNFs) are promising candidates owing to their strength and biocompatibility [28,33], and cellulose is able to give strong hydrogen

bonding, electrostatic interactions and covalent bonds to fibroin, inducing structural changes (e.g. increase of β -sheets and decrease of random coils) in blended cellulose-fibroin films [34,35]. Bacterial cellulose films have been recently adopted by Wu et al. to reinforce ancient silk fabrics, with promising results [25], however the process involves some time-consuming steps (bacteria culturing, extraction) and the need to efficiently remove the bacteria to avoid potential damage to the silk fibers.

In principle, fibroin is the ideal consolidant for silk as it exhibits physico-chemical compatibility, and its application does not involve the introduction of foreign components into the silk objects. Self-regenerated silk fibroin (SRSF) can be obtained and processed through a variety of methods [36–39]. Composites of fibroin (from silkworm cocoons) and silk have been widely explored in the framework of biomaterials and materials engineering, and are typically meant to be significantly stronger than pristine natural silk [40–44]. For instance, Yuan et al. embedded silk fibers into SRSF matrices (0.2 mm thick), and observed that by increasing the amount (wt%) of fibers it is possible to obtain a significant enhancement of the films' mechanical properties [40,44]. Wojcieszak et al. investigated the behavior of pristine fibers either mono-reinforced with small amounts of films, or embedded in thicker film matrices (up to ca. half centimeter). The film processing method (filtration, evaporation temperature) was shown to affect the order of the resultant matrix, as qualitatively observed through Raman spectroscopy by measuring the full width at half maximum (FWHM) of amide I and amide III bands, and the presence or disappearance of bands in the 1100-800 cm^{-1} region (associated with β -sheets and CH_3 deformations). Composites with thicker and disordered matrices showed the highest enhancement of mechanical behavior as compared to natural silk [43].

In the present contribution, we propose a new sustainable method to restore the mechanical properties of fragile (aged and degraded) silk fibers, meant for the treatment of historical objects. Specifically, we wanted the following features: 1) avoid to embed the fibers in thick coatings, so as to preserve the aesthetics of the treated artifacts; 2) restore the mechanical properties of aged/historical silk back to those of pristine natural silk, rather than obtaining 'super strong' fibers with highly enhanced mechanical behavior; 3) achieve the controlled tuning of the secondary structure of the SRSF, in particular of the relative amount of crystalline structures, playing on the fibroin concentration of the SRSF precursor solutions. This point is based on the following rationale: crystalline SRSF films (e.g. combined amount of β -sheets and β -turns > 60%) are expected to improve the fibers' tensile strength, while highly amorphous films (e.g. β -sheets + β -turns < 30%), where the fibroin chains have higher mobility, might increase the elongation of the aged/degraded fibers. Recovering the ductility of the fibers is particularly desirable for brittle historical textiles where the original amorphous component was lost to degradation [14,45]. On such samples, improved elongation is needed to allow handling during exhibition and restoration of the artifacts, as well as to increase the lifespan of the objects.

Waste silk textiles, rather than silkworm cocoons, were used to obtain SRSF films, a choice recommended in the past [46] so as to propose a sustainable and inexpensive approach that can be easily upscaled, based on the responsible use of bioresources. The SRSF films, cast from dispersions, were studied with Fourier Transform Infrared (FTIR) 2D Imaging, to characterize the secondary structure of the films, and with scanning electron microscopy (SEM); then, SRSF dispersions were applied onto artificially aged silk fibers, and the same

analytical set was used to investigate the distribution of the coatings on the fibers. Finally, the mechanical behavior of the treated fibers was studied through tensile strength tests, and compared to that of pristine silk.

11.2. Materials and methods

11.2.1. Chemicals used

Nitric acid (HNO₃, 90% ACS, Sigma Aldrich), ethanol (EtOH, anhydrous, analytical grade, Carlo Erba), and calcium chloride (anhydrous CaCl₂, ≥ 99.9%, Sigma Aldrich) were used. MilliQ water (resistivity 18.2 MΩ cm) was used.

11.2.2. Pristine and aged silk samples

A commercial non-dyed modern silk textile (Georgette Silk) with a density of 51 mg/cm³ was used as reference pristine silk (labeled “PS”). In order to alter, through accelerated aging, the secondary structure of fibroin and the mechanical properties of the silk fibers, three types of treatment were carried out on pristine silk. To induce changes by temperature, PS strips (10 x 15 cm²) were heated in a convection oven at 130 °C for 4 hours (samples labeled as “AS1”). To induce changes by acid hydrolysis, small PS strips (4 x 0.5 cm²) were treated by dripping 10 μL of nitric acid (diluted to 1.8% v/v) over each PS sample, and then the samples were heated in a microwave oven at 570W for 20 seconds (samples labeled as “AS2”). The microwave oven heating was meant to accelerate the reaction between nitric acid and fibroin (acid hydrolysis, oxidation, xanthoproteic reaction [47], without using prolonged exposure to temperature and concentrated acid, which could lead to the complete destruction of the fibers. After the treatment, the samples were rinsed with MilliQ water and let dry at room temperature before analysis. To induce photo-

oxidative degradation, PS strips (10 x 15 cm²) were irradiated with UV-Vis light (samples labeled as “AS3”), as follows [45]: a Neon Light Color 765 Basic daylight Beghelli Lamp was used (160 mW/lm, 380e700 nm), placing the silk samples in a closed chamber for 30 days at room conditions (36 °C, RH 40%), where the samples’ surface was exposed to ca. 11000 Lux of homogeneous illumination. These conditions are meant to accelerate the natural aging that would be experienced by objects on display in museums, where illuminations of 50-100 lux are typically used.

11.2.3. Self-regenerated silk fibroin (SRSF) solutions

The SRSF solutions were obtained starting from waste scraps of Taffeta silk (density: 2.57 g/cm³). SRSF solutions were prepared following procedures reported in the literature [39,48]: the silk textiles were washed with ethanol four times to remove impurities and industrial additives, and let dry at room temperature; then, 0.5 g of textile was immersed in a 5 mL solution of CaCl₂:H₂O:EtOH (molar ratio of 1:8:2), heated at 60 °C and agitated until complete dissolution of the silk. The solution was then dialyzed with a membrane cell MC18 14 Kpa (Sigma Aldrich), against 1 L water (MiliQ) for two days, replacing the water at 1 h, 4 h, 10 h, 20 h, 32 h and 40 h, since the dialysis started. The dialyzed solution (12 mL, labeled “SRSF-A”) was centrifuged twice at 9000 rpm, and the supernatant separated. The final concentration of SRSF-A is 5.34% (w/v). Two diluted solutions (“SRSF-B”, 1.18% w/v; “SRSF- C”, 0.15% w/v) were prepared from the SRSF-A solution. All the solutions were stored at 4°C for 1 day before use.

11.2.4. SRSF coatings

A set of coated silk samples was prepared for each type of aged silk (AS1-3). Each set of 4 comprised small silk strips (4 x 0.5 cm²) treated with, respectively: SRSF-A; SRSF-B; SRSF-C, followed by drying and immersion in SRSF-B. The treatment consisted in dripping 15 µL of SRSF solution over the silk strip, taking care of wetting the fibers homogeneously so as to obtain a uniform coating. The coated samples (12) were kept in a container at 22 °C and a relative humidity (RH) of 43% for one week before analyses. The samples were labeled according to the aging and coating treatment, e.g.: AS1-A, AS1-B, AS1-C, AS2-A, etc.

11.2.5. Fourier Transform Infrared (FTIR) 2D Imaging-Chemical mapping

The SRSF films and the silk fibers (pristine, aged, and coated) were analyzed (without any pre-treatment) with a Cary 670 FTIR spectrophotometer coupled to a Cary 620 FTIR microscope (Agilent Technologies), using a 15x Cassegrain objective. Measurements were carried out in reflectance mode over a gold plated reflective surface; background spectra were collected directly on the gold-plated surface. Acquiring the spectra in reflectance mode was preferred to performing Attenuated Total Reflectance (ATR) on the films, as we previously showed that the pressure applied during ATR measurements might induce structural changes in the silk fibers, hindering the rigorous characterization of the films secondary structure via spectral deconvolution (peak fitting). The FTIR settings were as follows: 512 scans for each acquisition, spectral resolution of 2 cm⁻¹, open windows, and spectral range of 3900-900 cm⁻¹. A 128 x 128 pixels Focal Plane Array (FPA) detector was used (each pixel

related to an area of $5.5 \mu\text{m} \times 5.5 \mu\text{m}^2$). Each analysis produced a “tile” of $700 \times 700 \mu\text{m}^2$. In the FTIR 2D maps, the chromatic scale shows the bands’ intensity following the order red > yellow > green > blue.

11.2.5.1. Analysis of the secondary protein structures

An IR map was collected on a chosen spot of the SRSF films or silk fibers. Then, from each map, five spectra with high amide A absorbance, and fifteen spectra of the golden platelet were selected. The spectra of the Au surface were averaged to obtain a single spectrum, which was used as a reference to subtract environmental water absorptions from the spectra of the film/fiber. Then, each of the five film/fiber spectra underwent the following process: 1) Manual spectral subtraction of the reference Au spectrum; the subtraction factor was adjusted manually until no absorption at 1654 cm^{-1} (OH bending, H₂O) was observable in the spectra over the protein amide I band; 2) Smoothing with an SG quad-cubic function of 13-15 points, taking care not to alter any diagnostic feature of the spectra; 3) Spectrum truncation down to the $1720\text{--}1480 \text{ cm}^{-1}$ range (amide I–II region); 4) Baseline correction using a linear function connecting the two extremes of the truncated spectra; 5) Each spectrum was normalized to the maximum absorbance value of the amide I band. Operations 1-5 were carried out using the Agilent Resolution Pro software (Agilent technologies). Each resultant spectrum was deconvoluted and fitted using the multiplex fitting package of the Igor Pro software, version 7 (WaveMetrics, Inc). First, the second derivative of the convoluted spectra was used to locate the position of bands. Then, the spectra were deconvoluted using Gaussian curves and a constant baseline (constrained at zero absorbance), in two steps: 1) The position and width of the bands were hold; the height of all bands constrained to a maximum of 80 and a minimum of 0; the fitting was then iterated until no

changes were reported between two successive iterations; 2) The width was let change in the 0-20 limit, and the height was let change with a minimum limit of 0; the fitting was iterated until no changes were reported between two successive iterations. The resultant deconvoluted bands composing amide I were assigned to the different secondary structures of the protein as follows [49,50]: (Tyr) side chains/aggregated strands, 1605-1615 cm^{-1} ; aggregate β -strand/intermolecular β -sheets (weak), 1616-1621 cm^{-1} ; intermolecular β -sheets (strong), 1622-1627 cm^{-1} ; intramolecular β -sheets (strong), 1628-1637 cm^{-1} ; random coils/extended chains, 1638-1646 cm^{-1} ; random coils, 1647-1655 cm^{-1} ; α -helices, 1656-1662 cm^{-1} ; β -turns, 1663-1670, 1671-1685, and 1686-1696 cm^{-1} ; intermolecular β -sheets (weak), 1697-1703 cm^{-1} ; oxidation bands, 1703-1720 cm^{-1} .

11.2.6. Field Emission Scanning Electron Microscopy (FE-SEM)

FE-SEM investigation of the SRSF films and silk samples was carried out using a SIGMA instrument (Carl Zeiss Microscopy GmbH, Germany). Samples were gold coated, and images acquired using the secondary electron detector as well in-lens secondary electron detector in an acceleration potential of 5 kV. For FE-SEM analyses, SRSF films were cast on glass slides by dripping 100 μL of SRSF solution and letting dry in a desiccator at room temperature.

11.2.7. Differential Scanning Calorimetry (DSC)

A Q2000 DSC (TA Instruments, New Castle, DE, USA) instrument was used. Aluminum hermetic pans (TZero Aluminum Hermetic, TA Instruments) were used as sample holders and as a reference. The DSC measurements on the SRSF films were done with the following temperature program: initial

isothermal for 2 min at 0°C, heat ramp of 10 °C/min from 0°C to 400°C; nitrogen atmosphere (flow rate 50 mL/min). Reproducible results could be obtained using ca. 1 mg of silk sample for each measurement. The obtained data were elaborated with the Q Series software, version 5.4.0. Two measurements were carried out for each sample.

11.2.8. Tensile tests

Tensile measurements were performed at room conditions (T= 23°C, RH= 43%) using a Discovery HR-3 rheometer from TA Instruments, equipped with an extension accessory, recording the elongation and tensile force. The samples consisted of 16 types of silk textile (PS, AS1-3 and their corresponding coated samples A-D); for each type, ten samples were tested, averaging the obtained values. Each sample contained 18 vertical threads of 100 µm diameter and 4 cm length. The gap length was set as 1 cm and the elongation speed set at 94 µm/s. Recorded data was transformed in strain strength values for analysis and discussion.

11.3. Results and discussion

Uniform films of SRSF were obtained starting from waste silk scraps, after the dissolution, dialysis and centrifugation steps. No coagulates or inhomogeneities were evident under visual inspection. The SRSF-A film is translucent and opaque, while SRSF-B and SRSF-C are transparent. Both SRSF-A and SRSF-B are rigid films, while SRSF-C is flexible. Figure 1 shows the FTIR 2D maps and SEM images of the films cast on glass slides. In all cases the films look smooth and homogeneous down to micron scale, without holes or cracks; a thicker rim was observed at the border of the SRSF-C, formed upon drying. The FTIR spectra collected on the films exhibit the characteristic bands of *Bombyx*

mori silk fibroin, at 3300 (amide A), 3077 (amide B), 2981, 2935, 2879 (CH stretching), 1729-1594 (amide I), 1594-1479 (amide II), 1452 (vibration modes of residues), 1384 (CH₂ bending), 1260 (amide III, β -sheet), 1240 (amide III, random coil and helical conformation), 1172 (N-CH stretching), and 1058 cm⁻¹ (skeletal stretching) [11,51,52]. No bands ascribable to other types of synthetic or natural compounds (e.g. additives and impurities that in principle could be present in the waste silk scraps), were observed. In general, the intensity of the fibroin bands follows the order SRSF-A > SRSF-B > SRSF-C, as expected considering that the films were cast from solutions at decreasing concentration (SRSF-A, 5.34% w/v; SRSF-B, 1.18% w/v; SRSF-C, 0.15% w/v). Besides, significant differences in the shape of the amide I and II bands of the films were observed. The SRSF-A film exhibit peaks centered at 1656 and 1537 cm⁻¹, and different components of the amide absorptions, related to different secondary structures, are observable. Conversely, SRSF-B and SRSF-C show asymmetrical amide peaks, where the contribution of some structures is evidently dominant with respect to the others. Namely, the spectra of SRSF-B show maxima at 1675 (amide I) and 1552 cm⁻¹ (amide II), while those of SRSF-C exhibit enhanced absorptions at 1644 and 1523 cm⁻¹. The inset in Figure 1 (panel 3) shows the 1729-1594 cm⁻¹ region (amide I), where the intensity of the band component centered at 1644 cm⁻¹ (random coils/extended chains [49]) was mapped. It is evident from the maps (Figure 1, panels 1A-1C) that the content of amorphous structures follows a reverse trend with concentration, i.e. SRSF-A < SRSF-B < SRSF-C. This feature is observed homogeneously all across the films' surface down to the micron scale.

The deconvolution of the amide I region of the SRSF films allowed to detail differences in the secondary structure of the fibroin obtained after casting

from solutions at different concentrations. The waste silk used to produce the SRSF films was considered as a reference to understand structural rearrangements due to the solubilization and film formation processes. Results are shown in Figure 2. Intermolecular β -sheets (weak) decrease passing from waste silk to SRSF-A and SRSF-B, and completely disappear in SRSF-C, where intermolecular β -sheets (strong) and intramolecular β -sheets are also absent. α -helices are more present in SRSF-A than in the original waste fabric, but disappear in SRSF-C. The total content of β -turn structures is similar for waste silk and SRSF-A, but SRSF-A exhibits an increase of turns at 1686-1696 cm^{-1} and a decrease of turns at 1671-1685 cm^{-1} . The latter are significantly enhanced and the main structure in SRSF-B, where almost no turns at 1663-1670 cm^{-1} are observed. SRSF-C shows β -turn contents similar to waste silk, but a dramatically higher content of random coils/extended chains, which are the main type of secondary arrangement in this film. Overall, we concluded that increasing the concentration of fibroin in the solutions leads to progressive ordering of the protein structure in the SRSF films, i.e. from random coils/extended chains to β -turns, α -helices, and eventually ordered β -sheets. β -turns seem to represent an intermediate step in the transition from highly amorphous to more crystalline films. Models of transition from β -turns in un-spun silk I ('disordered') to β -sheets in spun silk II ('crystallized') have been proposed on the basis of NMR, X-ray diffraction, IR, circular dichroism, and Raman scattering [13]. Previously, Magoshi et al. [53] suggested that conformational change between random coils (or α -helices) and β -sheets can occur by concentration variations in fibroin solutions (less than 3 wt%), even though no details of the effect of concentration on the conformation were given. Xie and Liang [54] carried out differential scanning calorimetry (DSC) and Raman spectroscopy on concentrated (15-37

wt%) regenerated silk fibroin aqueous solutions, and speculated that concentration increase resulted in close arrangement of the fibroin molecules and transition from random coil and α -helices to β -sheets.

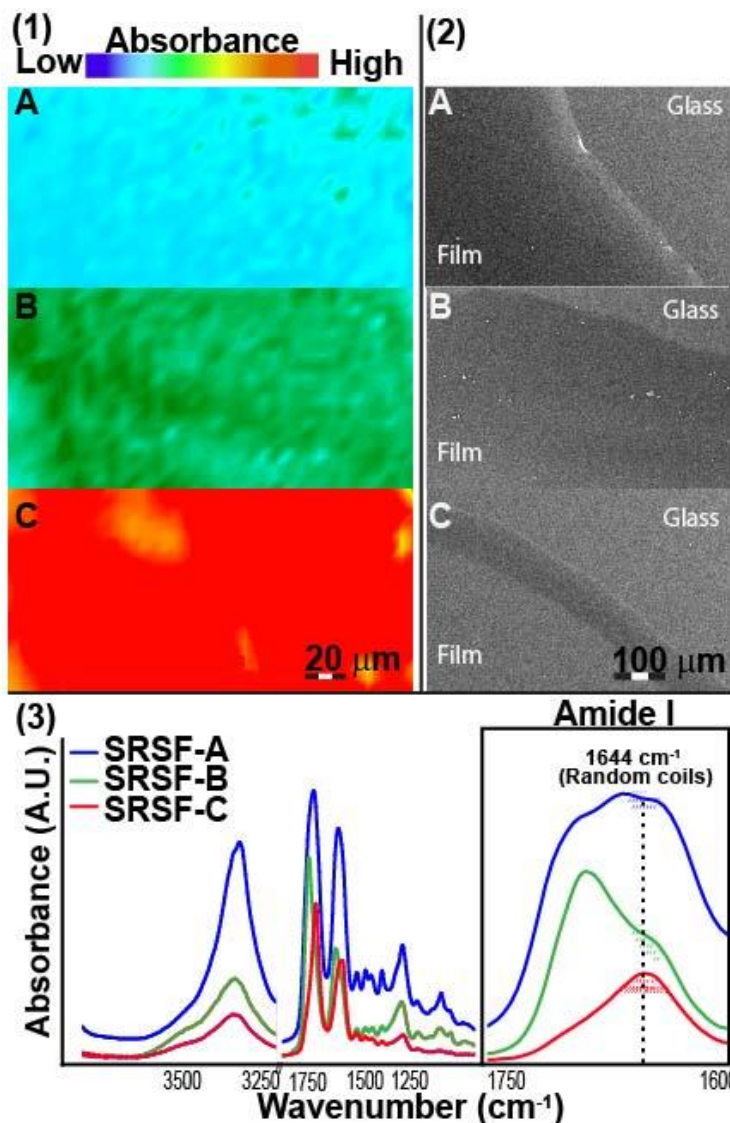


Figure 1 FTIR 2D Imaging-Chemical mapping and SEM images of SRSF films cast from dispersions of waste silk. (1) FTIR 2D maps of the intensity of the 1652-1634 cm^{-1} region (amide I band, random coils/extended chains) for the SRSF-A (A), SRSF-B (B), and SRSF-C (C) films. (2) SEM images of the SRSF-A (A), SRSF-B (B), and SRSF-C (C) films cast on glass slides. (3) Representative examples of FTIR spectra, each corresponding to one pixel ($5.5 \times 5.5 \mu\text{m}^2$) in the Imaging maps. The inset shows the 1750-1600 cm^{-1} region of the spectra (amide I), and the mapped portions of the peaks' areas (shaded areas, 1652-1634 cm^{-1}).

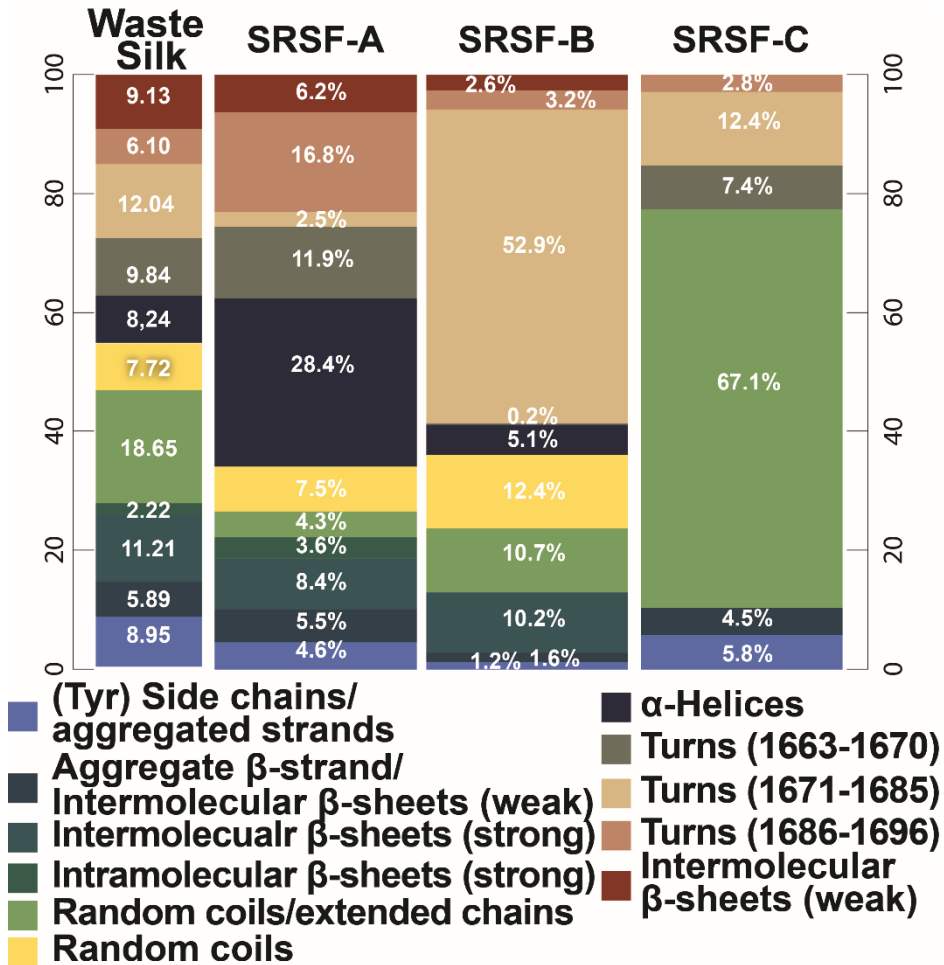


Figure 2 Assigned secondary structures (%) of silk protein, obtained from the deconvolution of the amide I and II region ($1720-1480\text{ cm}^{-1}$) of reflectance FPA μ -FTIR spectra of waste silk and SRSF-A-C films.

In order to support the results obtained with FPA FTIR 2D Imaging, we carried out thermal analysis on the prepared SRSF films. Figure 3 shows the DSC curves of the SRSF A-C films. SRSF-C exhibits a broad endothermic event between 30 and 160°C , which Motta et al. ascribed to the evaporation of water from amorphous fibroin, after the material crossed the glass transition it has at that level of water content [55]. The same authors suggested that this thermal event is also probably associated with some conformational changes that take place in the water moistened fibroin after it reaches the glass transition

temperature (T_g) [55], and Xie et al. argued that a temperature-induced transition from random coils (or α -helices) to β -sheets occurs in the 30-160°C range [54]. A weak but clear glass transition of amorphous fibroin is also observable for SRSF-C at 175°C, in agreement with the literature [55]. Then, SRSF-C shows an exothermic peak around 220°C, which has been previously assigned to a random coil to β -sheet conformational transition [55–57]. The wide endothermic peak centered at 288°C is due to the thermal degradation of the fibroin chains [58].

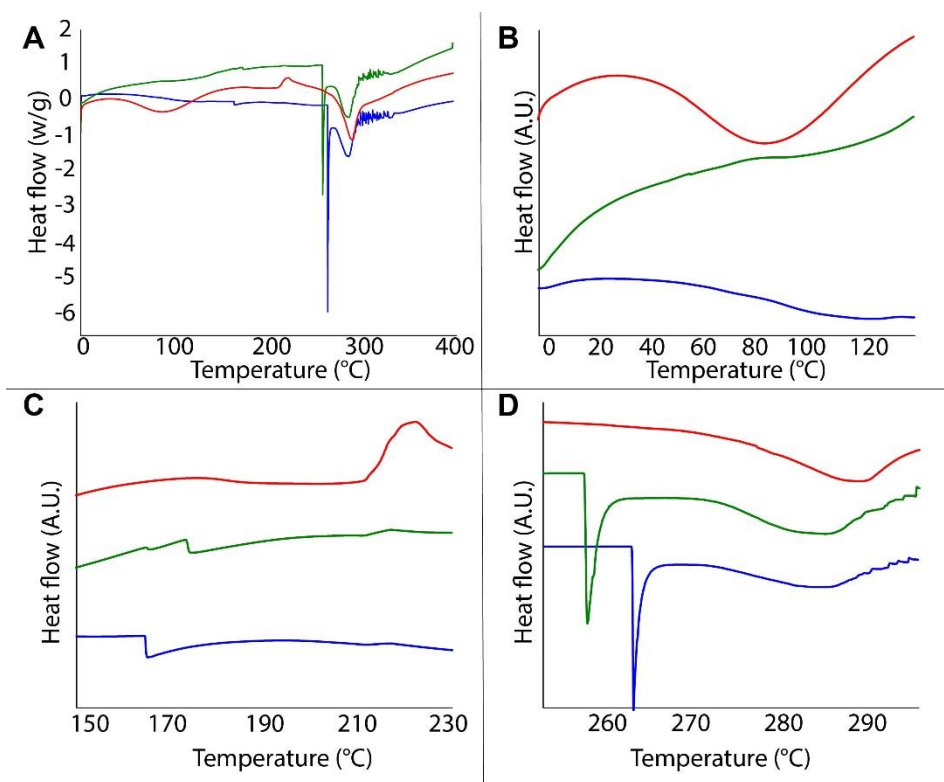


Figure 3 (A) DSC curves of the SRSF films (SRF-A: blue curve; SRF-B: green curve; SRF-C: red curve). (B-D) Insets highlighting the three main thermal events observed for the SRSF films, in the 0-120°C (loss of water), 150-230°C (glass transition), and 250-300°C (melting and protein decomposition).

SRSF-A and -B show similar DSC curves, characterized by different thermal events than SRSF-C. A weak and broad endothermic event is observed

between 60 and 150°C, possibly due to the loss of water [59]. The reduced intensity of this event in SRSF-A and -B indicates the presence of crystalline domains, where the OH groups of the proteins are largely involved in intramolecular bonds, and less hydroxyls are thus available to interact with free water [60,61]. The second event is a glass transition, respectively at 163°C (SRSF-A) and 168°C (SRSF-B), followed by weak exothermic events at 215°C. The latter are significantly less intense than the correspondent peak in the SRSF-C curve. The most notable feature is the presence of sharp endothermic peaks at 263 (SRSF-A) and 258°C (SRSF-B), which can be associated with the melting transition of the proteins. No such transition is observed in the SRSF-C curve. According to the literature, this transition can be obscured by the thermal decomposition of fibroin at slow heating rates [62]; however, in the case of SRSF-A and -B intense peaks were observed, well separated from the decomposition event (observed after 280°C), and the melting peak of SRSF-A is sharper and more intense than that of SRSF-B. Opening the pans after the DSC measurements revealed the presence of flattened, molten and charred residues in the case of SRSF-A and -B, while a more powdery, voluminous and granular charred residue, with no evident sign of melting, was observed for SRSF-C. Overall, the results obtained through DSC support FTIR data, indicating that the increase in fibroin concentration from SRSF-C to -B, and -A results in a rearrangement of the fibroin chains from amorphous (random coils, extended chains) into ordered structures (α -helices, β -sheets). Importantly, the film preparation can be feasibly tuned playing on the concentration of fibroin in the starting solutions, so as to obtain either highly amorphous (random coils/extended chains > 60%) or crystalline films (α -helices + β -sheets > 50%, without counting the β -turns).

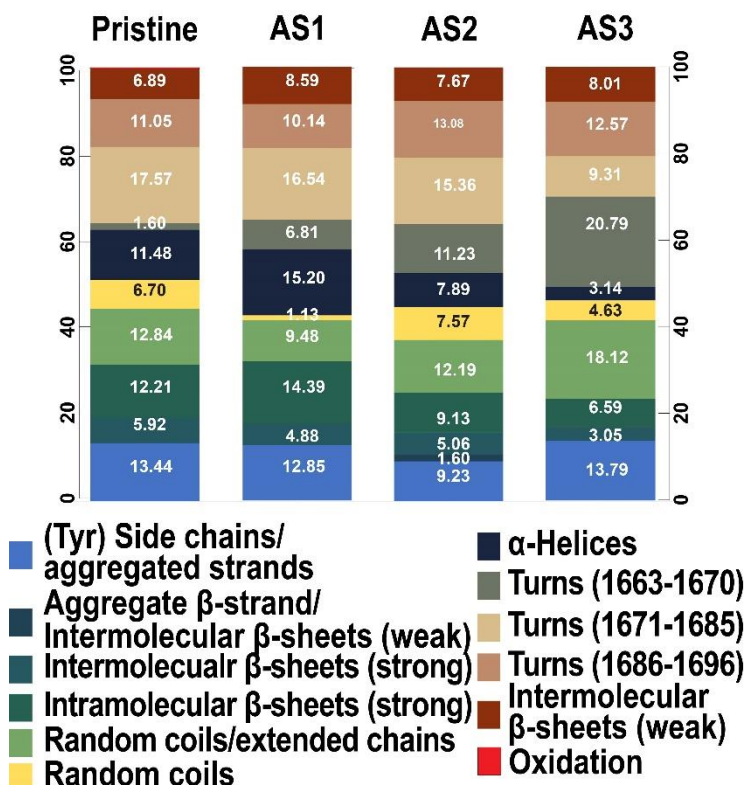


Figure 4 Assigned secondary structures (%) of silk protein, obtained from the deconvolution of the amide I and II region ($1720\text{-}1480\text{ cm}^{-1}$) of reflectance FPA μ -FTIR spectra of commercial silk either pristine, or artificially aged using temperature (AS1), nitric acid (AS2), or UV-Vis light (AS3).

As mentioned in the introduction, the possibility of tuning the secondary structure of the SRSF films is attractive for the conservation of aged and degraded silk fibers, because crystalline or amorphous coatings are expected to produce different effects on the mechanical behavior of the treated fibers. Namely, coatings rich in crystalline domain should increase the stiffness of the fibers, while amorphous coatings (with more mobile fibroin chains) are expected to increase the ductility of the fibers. The concept of applying coatings with tunable composition to degraded textiles was also recently proposed for the conservation of canvases by Kolman et al., who combined polyelectrolyte-

treated silica (SNP) to cellulose nanofibrils (CNF), varying the SNP/CNF ratio to balance the stiffness and ductility increase of the canvas fibers [63].

The degraded silk fibers considered in the present contribution were obtained starting from pristine commercial silk that was artificially aged using temperature, nitric acid, or UV-Vis light. These treatments were aimed to alter the secondary structure of the silk fibers and induce different changes in their mechanical behavior, prior to the application of the SRSF coatings. Figure 4 shows the secondary structure of the commercial silk before and after the aging treatments. The pristine commercial fibers (Georgette silk) has similar structural motifs to the waste silk used to prepare the SRSF films; the only differences regard the lack of aggregate β -strand/intermolecular β -sheets (weak), and a decrease of β -turns at $1670\text{-}1663\text{ cm}^{-1}$ with respect to the other β -turns bands. The UV-Vis aging produced a significant decrease of intramolecular β -sheets and α -helices, and an increase of random coils/extended chains and β -turns at $1670\text{-}1663\text{ cm}^{-1}$; this indicates the formation of smaller crystallites (β -sheets), and the partial transformation of crystalline domains into less-ordered structures (random coils), as previously observed for photo-aged silk [45]. However, differently from previous studies, no significant increase in oxidation bands occurred. Treatment with nitric acid (sample AS2) resulted in the appearance of aggregate β -strand/intermolecular β -sheets (weak), the increase of β -turns at $1670\text{-}1663\text{ cm}^{-1}$, and the decrease of α -helices. The treatment also produced a significant yellowing of the sample. Thermally treated commercial silk (sample AS3) exhibited an increase of α -helices and a decrease of random coil structures.

We thus investigated the tensile behavior of the treated silk fibers, to correlate it with the structural and molecular changes observed via FTIR

imaging. In fact, both the tensile strength and the elongation length of silk fibers are intimately related to their secondary structure [42,64–66]. Table 1 shows the tensile strength, elongation length and Young's modulus of commercial fibers either pristine, aged, or coated (after aging) with the SRSF dispersions.

Thermal aging caused some decrease in the elongation length, and an increase in tensile strength. This is consistent with what observed with FTIR, i.e. the decrease in amorphous structures (random coil, extended chains) that provide mobility and ductility to the fibers. According to Tsukada et al., thermal treatment of *B. mori* silk fibers produces an increase in the number and size of crystalline regions, due to close packing of laterally ordered regions adjacent to the crystalline domains. The same authors reported a decrease in ductility of the thermally treated fibers, which exhibit a slight contraction from room temperature to 120°C, attributed to the evaporation of humidity followed by a rearrangement of the structure [67]. The samples aged with nitric acid exhibit a high dispersion in the values of tensile strength, which are in average closer to those of pristine fibers than thermally and photo-aged samples. However, treatment with nitric acid produced the highest elongation length, consistently with the reduction of ordered structures (α -helices) observed with FTIR. Photo-aging did not affect significantly tensile strength, which remained similar to that of pristine sample, but decreased the fibers' elongation length, similarly to thermal aging. In fact, it has been reported that photo-aging of silk results in increased brittleness of the fibers [68,69]. This is in agreement with the presence of smaller crystalline domains observed with FTIR.

PART IV. SILK CONSOLIDATION

Table 1 Elongation (%), tensile strength (MPa) and Young's modulus (MPa/mm) of commercial silk textiles, either pristine, artificially aged, and coated after aging. AS1: silk thermally aged; AS2: silk aged with nitric acid; AS3: silk aged with UV-Vis light. A-C refers to the type of SRSF applied onto the textiles. Standard deviations (σ) are reported along with the values.

Sample	Elongation		Tensile strength		Young's modulus	
	%	σ	MPa	σ	MPa/mm	σ
Pristine	50	4	158	13	422	41
AS1	41	5	189	16	630	30
AS1-A	42	3	107	8	309	33
AS1-B	51	5	122	15	282	31
AS1-C	66	8	148	31	351	81
AS2	63	4	161	15	444	94
AS2-A	47	10	101	22	287	34
AS2-B	54	7	121	19	344	37
AS2-C	64	10	141	29	351	49
AS3	40	3	149	11	431	20
AS3-A	29	3	94	8	365	53
AS3-B	35	3	102	12	367	36
AS3-C	50	3	134	10	374	56

When the aged samples are coated with the SRSF dispersions, some general trends are observable in their mechanical behavior: coating with SRSF-A tends to reduce the elongation length of the fibers, as expected from the application of a highly ordered material with reduced amorphous content. Besides, a drastic decrease in the tensile strength is observed. The application of SRSF-B results in a better mechanical behavior, where the elongation of the aged fibers is reverted to values closer to those of the pristine fibers, while the tensile strength is higher than that obtained after applying coating A, but still lower than the pristine silk. The application of SRSF-C produced the best results in terms of recovering the fibers' original mechanical behavior: the treated fibers show higher elongation than pristine and aged samples, and tensile strength comparable with that of pristine silk. Macroscopically, the treated

fibers exhibited an improved resistance to physical handling. Figure 5 shows the FTIR 2D Imaging-chemical mapping and the SEM images of pristine commercial textile after photo-aging and the application of the SRSF-C dispersion. Mapping of the fibroin band at 1230 cm^{-1} (amide III in random coil conformation [50,70]) shows that, following the application, the thread of fibers uniformly exhibits an increased amorphous content, without the presence of aggregates on the fibers, or amorphous fibroin films in the gaps between weft and warp. This indicates that the SRSF dispersion penetrates the textile and produces a homogeneous coating of the fibers, rather than simply creating a superficial film.

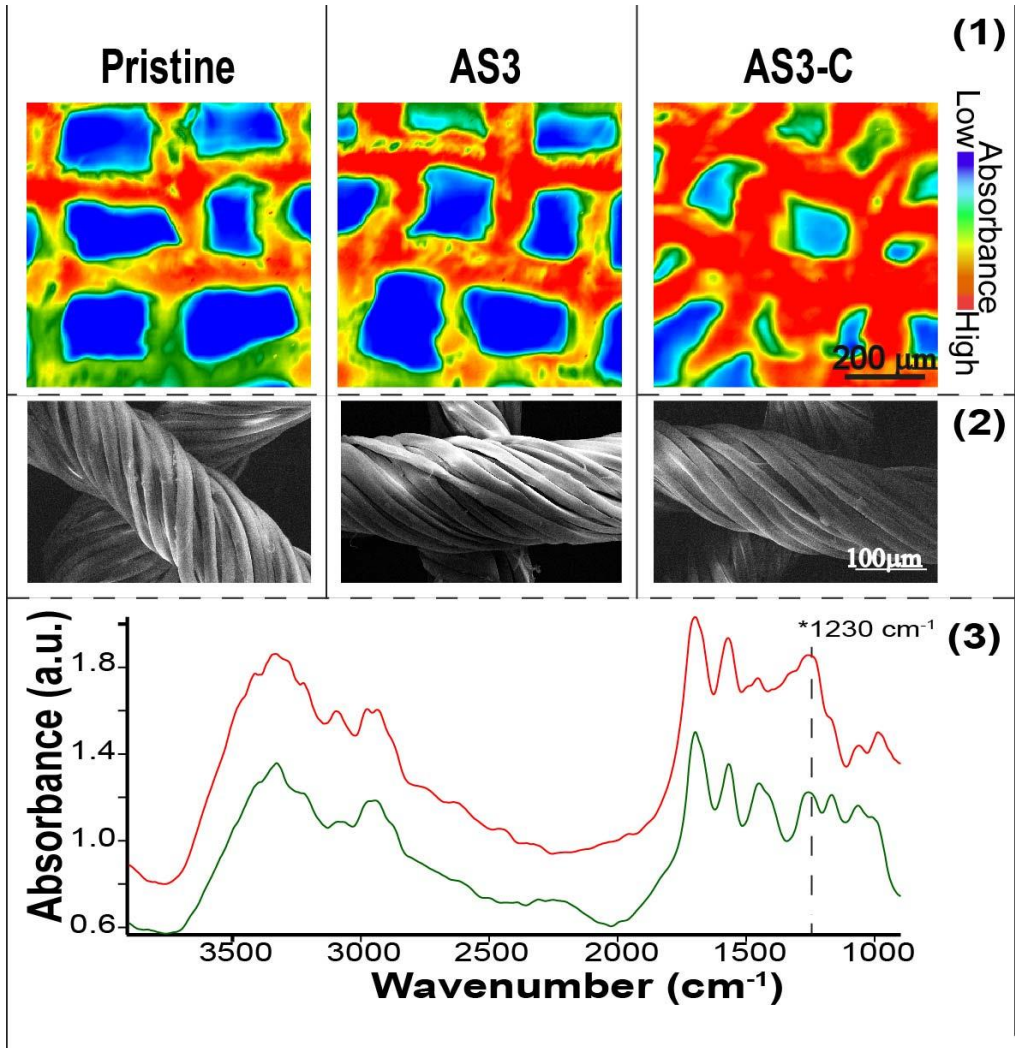


Figure 5(1) FTIR 2D Imaging-Chemical mapping of silk textiles: (left) pristine textile; (center) textile artificially aged with UV-Vis light; (right) the artificially aged textile after treatment with SRSF-C. The intensity of the 1230 cm⁻¹ peak is shown (amide III in random coil conformation). (2) SEM images of the same textiles as in (1). Both FTIR 2D Imaging and SEM confirmed that SRSF-C distributes homogeneously within the fibers, without forming a superficial coating. (3) Representative examples of FTIR spectra, each corresponding to one pixel (5.5 × 5.5 μm²) in the Imaging maps. Red and green spectra relate to pixels of the same color in the maps. The intensity of the 1230 cm⁻¹ peak is highlighted.

11.4. Conclusions

The composition of SRSF dispersions was tuned, varying the concentration of fibroin, so as to obtain films with different content of crystalline and amorphous domains. When the dispersions are applied to artificially aged and degraded silk textiles, they penetrate through the textile matrix, homogeneously coating the fibroin fibers rather than forming a superficial layer. This produces different changes in the mechanical behavior of the fibers, consistently with the amorphous content of the SRSF films. Namely, films with high content of ordered structures (α -helices + β -sheets > 50%) produce a decrease of tensile strength and elongation length, as expected from the application of a brittle material with scarce ductility. Instead, the application of highly amorphous films (random coils/extended chains > 60%) recovered the tensile strength and the elongation length of the aged silk fibers, up to values similar or higher than those of pristine silk.

Overall, we demonstrated that SRSF films can be obtained from renewable silk waste, easily tuning their secondary structure to confer desired mechanical properties to degraded silk fibers. These results open new perspectives in the conservation of textiles, where feasible consolidation materials are still needed. Besides, the use of SRSF films with tunable secondary structure is potentially useful in other fields such as biomaterials and materials engineering, and the preparation of composites with enhanced properties.

References

- [1] N. Luxford, Silk durability and degradation, in: P.A. Annis (Ed.), *Understanding and Improving the Durability of Textiles*, Woodhead Publishing Limited, Cambridge, 2012: pp. 205–232. <http://discovery.ucl.ac.uk/1366005/> (accessed December 1, 2016).
- [2] F. Vollrath, D. Porter, C. Dicko, 5 - The structure of silk, in: *Handbook of Textile Fibre Structure*, Woodhead Publishing, 2009: pp. 146–198. [//www.sciencedirect.com/science/article/pii/B9781845697303500056](http://www.sciencedirect.com/science/article/pii/B9781845697303500056) (accessed January 26, 2017).
- [3] S.K. Vyas, S.R. Shukla, Comparative study of degumming of silk varieties by different techniques, *The Journal of The Textile Institute*. 107 (2016) 191–199. doi:10.1080/00405000.2015.1020670.
- [4] Á. Tímár-Balázs, D. Eastop, *Chemical principles of textile conservation*, Oxford : Butterworth-Heinemann, 2004. <https://trove.nla.gov.au/version/8460266> (accessed March 4, 2019).
- [5] S. Inoue, K. Tanaka, F. Arisaka, S. Kimura, K. Ohtomo, S. Mizuno, Silk Fibroin of Bombyx mori Is Secreted, Assembling a High Molecular Mass Elementary Unit Consisting of H-chain, L-chain, and P25, with a 6:6:1 Molar Ratio, *J. Biol. Chem.* 275 (2000) 40517–40528. doi:10.1074/jbc.M006897200.
- [6] M. Wojcieszak, A. Percot, S. Noinville, G. Gouadec, B. Mauchamp, P. Colomban, Origin of the variability of the mechanical properties of silk fibers: 4. Order/crystallinity along silkworm and spider fibers, *Journal of Raman Spectroscopy*. 45 (2014) 895–902. doi:10.1002/jrs.4579.
- [7] D. Kaplan, W.W. Adams, B. Farmer, and C. Viney (Eds.), *Silk Polymers*. Materials Science and Biotechnology, American Chemical Society, 1994. <http://gen.lib.rus.ec/book/index.php?md5=46294b434882f15d3cec192f62b11d22>.
- [8] R.S. Weber, C.L. Craig (auth.), T. Asakura, T. Miller (eds.), *Biotechnology of Silk*, 1st ed., Springer Netherlands, 2014. <http://gen.lib.rus.ec/book/index.php?md5=f44d613bf7bb1ca80774ed6fca3a90f>.
- [9] D. Yang, H. Kim, J. Lee, H. Jeon, W. Ryu, Direct modulus measurement of single composite nanofibers of silk fibroin/hydroxyapatite nanoparticles, *Composites Science and Technology*. 122 (2016) 113–121. doi:10.1016/j.compscitech.2015.11.019.
- [10] A. Gao, Q. Yang, L. Xue, Poly (l-Lactic acid)/silk fibroin composite membranes with improved crystallinity and thermal stability from non-solvent induced phase separation processes involving hexafluoroisopropanol, *Composites Science and Technology*. 132 (2016) 38–46. doi:10.1016/j.compscitech.2016.06.011.
- [11] F. Vilaplana, J. Nilsson, D.V.P. Sommer, S. Karlsson, Analytical markers for silk degradation: comparing historic silk and silk artificially aged in different environments, *Anal Bioanal Chem.* 407 (2014) 1433–1449. doi:10.1007/s00216-014-8361-z.
- [12] P. Colomban, H.M. Dinh, A. Bunsell, B. Mauchamp, Origin of the variability of the mechanical properties of silk fibres: 1 - The relationship between disorder, hydration and stress/strain behaviour, *Journal of Raman Spectroscopy*. 43 (2012) 425–432. doi:10.1002/jrs.3044.
- [13] V. Jauzein, P. Colomban, 6 - Types, structure and mechanical properties of silk, in: A.R. Bunsell (Ed.), *Handbook of Tensile Properties of Textile and Technical Fibres*, Woodhead Publishing, 2009: pp. 144–178. [//www.sciencedirect.com/science/article/pii/B9781845693879500060](http://www.sciencedirect.com/science/article/pii/B9781845693879500060) (accessed January 26, 2017).
- [14] P. Garside, P. Wyeth, Crystallinity and degradation of silk: correlations between analytical signatures and physical condition on ageing, *Appl. Phys. A*. 89 (2007) 871–876. doi:10.1007/s00339-007-4218-z.
- [15] P. Garside, S. Lahlil, P. Wyeth, Characterization of historic silk by polarized attenuated total reflectance Fourier transform infrared spectroscopy for informed conservation, *Appl Spectrosc.* 59 (2005) 1242–1247. doi:10.1366/000370205774430855.
- [16] Y. Gong, L. Li, D. Gong, H. Yin, J. Zhang, Biomolecular Evidence of Silk from 8,500 Years Ago, *PLOS ONE*. 11 (2016) e0168042. doi:10.1371/journal.pone.0168042.
- [17] H.E. Ahmed, Y.E. Ziddan, A new approach for conservation treatment of a silk textile in Islamic Art Museum, Cairo, *Journal of Cultural Heritage*. 12 (2011) 412–419. doi:10.1016/j.culher.2011.02.004.

Chapter 11. Self-regenerated silk fibroin with controlled crystallinity for the reinforcement of silk

- [18] Y. Nishio, Maintenance of Asian paintings II: minor treatment of scroll paintings, *The Book and Paper Group Annual*, Volume 20. (2002) 15–26, ill.
- [19] J.B. Perjés, K.E. Nagy, M. Tóth, *Conserving Textiles Studies in honour of Ágnes Timár-Balázs*, ICCROM Conservation Studies 7, ICCROM, Italy, 2009.
- [20] O.M.A. Abdel-Kareem, The long-term effect of selected conservation materials used in the treatment of museum artefacts on some properties of textiles, *Polymer Degradation and Stability*. 87 (2005) 121–130. doi:10.1016/j.polymdegradstab.2004.07.014.
- [21] D. Chelazzi, A. Chevalier, G. Pizzorusso, R. Giorgi, M. Menu, P. Baglioni, Characterization and degradation of poly(vinyl acetate)-based adhesives for canvas paintings, *Polymer Degradation and Stability*. 107 (2014) 314–320. doi:10.1016/j.polymdegradstab.2013.12.028.
- [22] O. Chiantore, M. Lazzari, Photo-oxidative stability of paraloid acrylic protective polymers, *Polymer*. 42 (2001) 17–27. doi:10.1016/S0032-3861(00)00327-X.
- [23] M. Favaro, R. Mendichi, F. Ossola, S. Simon, P. Tomasin, P.A. Vigato, Evaluation of polymers for conservation treatments of outdoor exposed stone monuments. Part II: Photo-oxidative and salt-induced weathering of acrylic–silicone mixtures, *Polymer Degradation and Stability*. 92 (2007) 335–351. doi:10.1016/j.polymdegradstab.2006.12.008.
- [24] M. Lazzari, O. Chiantore, Thermal-ageing of paraloid acrylic protective polymers, *Polymer*. 41 (2000) 6447–6455. doi:10.1016/S0032-3861(99)00877-0.
- [25] S.-Q. Wu, M.-Y. Li, B.-S. Fang, H. Tong, Reinforcement of vulnerable historic silk fabrics with bacterial cellulose film and its light aging behavior, *Carbohydrate Polymers*. 88 (2012) 496–501. doi:10.1016/j.carbpol.2011.12.033.
- [26] D. Huang, Z. Peng, Z. Hu, S. Zhang, J. He, L. Cao, Y. Zhou, F. Zhao, A new consolidation system for aged silk fabrics: Effect of reactive epoxide-ethylene glycol diglycidyl ether, *Reactive and Functional Polymers*. 73 (2013) 168–174. doi:10.1016/j.reactfunctpolym.2012.08.019.
- [27] Z. Cai, G. Jiang, Y. Qiu, Chemical modification of Bombyx mori silk with epoxide EPSIB, *Journal of Applied Polymer Science*. 91 (2004) 3579–3586. doi:10.1002/app.13590.
- [28] Y. Feng, X. Li, M. Li, D. Ye, Q. Zhang, R. You, W. Xu, Facile Preparation of Biocompatible Silk Fibroin/Cellulose Nanocomposite Films with High Mechanical Performance, *ACS Sustainable Chem. Eng.* 5 (2017) 6227–6236. doi:10.1021/acssuschemeng.7b01161.
- [29] H.J. Kim, Y.J. Yang, H.J. Oh, S. Kimura, M. Wada, U.-J. Kim, Cellulose–silk fibroin hydrogels prepared in a lithium bromide aqueous solution, *Cellulose*. 24 (2017) 5079–5088. doi:10.1007/s10570-017-1491-7.
- [30] E. Marsano, P. Corsini, M. Canetti, G. Freddi, Regenerated cellulose–silk fibroin blends fibers, *International Journal of Biological Macromolecules*. 43 (2008) 106–114. doi:10.1016/j.ijbiomac.2008.03.009.
- [31] G. Yang, L. Zhang, Y. Liu, Structure and microporous formation of cellulose/silk fibroin blend membranes: I. Effect of coagulants, *Journal of Membrane Science*. 177 (2000) 153–161. doi:10.1016/S0376-7388(00)00467-1.
- [32] L. Zhou, Q. Wang, J. Wen, X. Chen, Z. Shao, Preparation and characterization of transparent silk fibroin/cellulose blend films, *Polymer*. 54 (2013) 5035–5042. doi:10.1016/j.polymer.2013.07.002.
- [33] P. Ang-atikarnkul, A. Watthanaphanit, R. Rujiravanit, Fabrication of cellulose nanofiber/chitin whisker/silk sericin bionanocomposite sponges and characterizations of their physical and biological properties, *Composites Science and Technology*. 96 (2014) 88–96. doi:10.1016/j.compscitech.2014.03.006.
- [34] S. Shang, L. Zhu, J. Fan, Intermolecular interactions between natural polysaccharides and silk fibroin protein, *Carbohydrate Polymers*. 93 (2013) 561–573. doi:10.1016/j.carbpol.2012.12.038.
- [35] D. Tian, T. Li, R. Zhang, Q. Wu, T. Chen, P. Sun, A. Ramamoorthy, Conformations and Intermolecular Interactions in Cellulose/Silk Fibroin Blend Films: A Solid-State NMR Perspective, *J. Phys. Chem. B*. 121 (2017) 6108–6116. doi:10.1021/acs.jpcc.7b02838.
- [36] J.G. Hardy, L.M. Römer, T.R. Scheibel, Polymeric materials based on silk proteins, *Polymer*. 49 (2008) 4309–4327. doi:10.1016/j.polymer.2008.08.006.

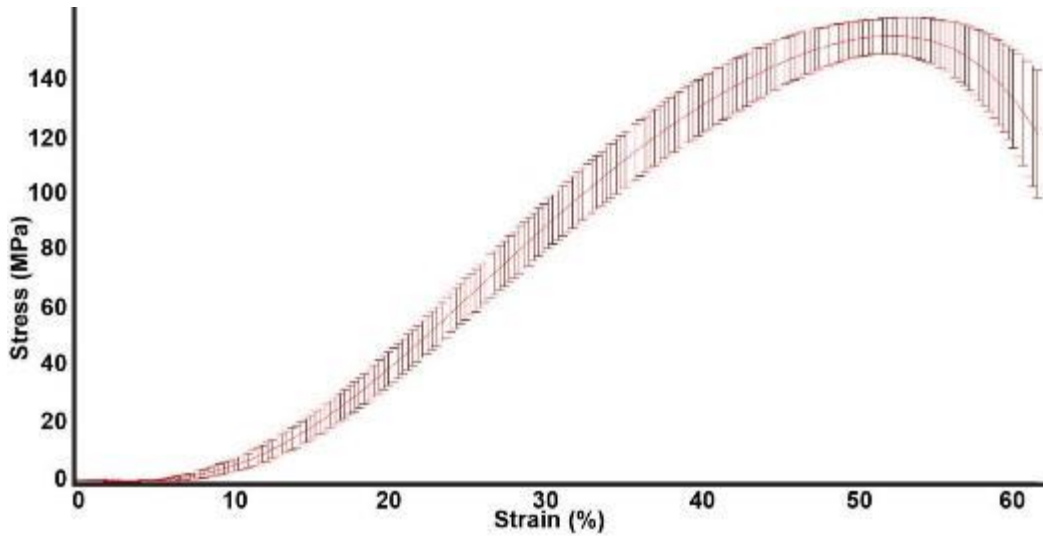
- [37] S. Kapoor, S.C. Kundu, Silk protein-based hydrogels: Promising advanced materials for biomedical applications, *Acta Biomaterialia*. 31 (2016) 17–32. doi:10.1016/j.actbio.2015.11.034.
- [38] Y. Qi, H. Wang, K. Wei, Y. Yang, R.-Y. Zheng, I.S. Kim, K.-Q. Zhang, A Review of Structure Construction of Silk Fibroin Biomaterials from Single Structures to Multi-Level Structures, *Int J Mol Sci*. 18 (2017). doi:10.3390/ijms18030237.
- [39] D.N. Rockwood, R.C. Preda, T. Yücel, X. Wang, M.L. Lovett, D.L. Kaplan, Materials Fabrication from *Bombyx mori* Silk Fibroin, *Nat Protoc*. 6 (2011). doi:10.1038/nprot.2011.379.
- [40] Y. Duan, X. Chen, Z.-Z. Shao, The Silk Textile Embedded in Silk Fibroin Composite: Preparation and Properties, *Chin J Polym Sci*. 36 (2018) 1043–1046. doi:10.1007/s10118-018-2117-8.
- [41] R.F.P. Pereira, M.M. Silva, V. de Zea Bermudez, *Bombyx mori* Silk Fibers: An Outstanding Family of Materials, *Macromol. Mater. Eng*. 300 (2015) 1171–1198. doi:10.1002/mame.201400276.
- [42] D.U. Shah, D. Porter, F. Vollrath, Can silk become an effective reinforcing fibre? A property comparison with flax and glass reinforced composites, *Composites Science and Technology*. 101 (2014) 173–183. doi:10.1016/j.compscitech.2014.07.015.
- [43] M. Wojcieszak, A. Percot, P. Colomban, Regenerated silk matrix composite materials reinforced by silk fibres: Relationship between processing and mechanical properties, *Journal of Composite Materials*. 52 (2018) 2301–2311. doi:10.1177/0021998317743563.
- [44] Q. Yuan, J. Yao, X. Chen, L. Huang, Z. Shao, The preparation of high performance silk fiber/fibroin composite, *Polymer. The International Journal for the Science and Technology of Polymers and Biopolymers*. 51 (2010) 4843–4849. doi:10.1016/j.polymer.2010.08.042.
- [45] D. Badillo-Sanchez, D. Chelazzi, R. Giorgi, A. Cincinelli, P. Baglioni, Characterization of the secondary structure of degummed *Bombyx mori* silk in modern and historical samples, *Polymer Degradation and Stability*. 157 (2018) 53–62. doi:10.1016/j.polymdegradstab.2018.09.022.
- [46] G.M. Nogueira, A.C.D. Rodas, C.A.P. Leite, C. Giles, O.Z. Higa, B. Polakiewicz, M.M. Beppu, Preparation and characterization of ethanol-treated silk fibroin dense membranes for biomaterials application using waste silk fibers as raw material, *Bioresource Technology*. 101 (2010) 8446–8451. doi:10.1016/j.biortech.2010.06.064.
- [47] G. Migliavacca, F. Ferrero, C. Tonin, Xanthoproteic reaction for the evaluation of wool antifelting treatments, *Coloration Technology*. 130 (2014) 319–326. doi:10.1111/cote.12108.
- [48] G. Cheng, X. Wang, S. Tao, J. Xia, S. Xu, Differences in regenerated silk fibroin prepared with different solvent systems: From structures to conformational changes, *J. Appl. Polym. Sci*. 132 (2015) n/a-n/a. doi:10.1002/app.41959.
- [49] X. Hu, D. Kaplan, P. Cebe, Determining Beta-Sheet Crystallinity in Fibrous Proteins by Thermal Analysis and Infrared Spectroscopy, *Macromolecules*. 39 (2006) 6161–6170. doi:10.1021/ma0610109.
- [50] J. Kong, S. Yu, Fourier Transform Infrared Spectroscopic Analysis of Protein Secondary Structures, *Acta Biochimica et Biophysica Sinica*. 39 (2007) 549–559. doi:10.1111/j.1745-7270.2007.00320.x.
- [51] M. Boulet-Audet, F. Vollrath, C. Holland, Identification and classification of silks using infrared spectroscopy, *Journal of Experimental Biology*. 218 (2015) 3138–3149. doi:10.1242/jeb.128306.
- [52] S. Ling, Z. Qi, D.P. Knight, Z. Shao, X. Chen, Synchrotron FTIR Microspectroscopy of Single Natural Silk Fibers, *Biomacromolecules*. 12 (2011) 3344–3349. doi:10.1021/bm2006032.
- [53] J. Magoshi, S. Nakamura, Physical properties and structure of silk. VIII. Effect of casting temperature on conformation of wild silk fibroin films, *Journal of Polymer Science: Polymer Physics Edition*. 23 (1985) 227–229. doi:10.1002/pol.1985.180230120.
- [54] F. Xie, H. Liang, Effect of Concentration on Structure and Properties of Concentrated Regenerated Silk Fibroin Solution, in: *Advanced Materials and Processes: ADME 2011*, Trans Tech Publications, 2011: pp. 1653–1656. doi:10.4028/www.scientific.net/AMR.311-313.1653.
- [55] A. Motta, L. Fambri, C. Migliaresi, Regenerated silk fibroin films: Thermal and dynamic mechanical analysis, *Macromolecular Chemistry and Physics*. 203 (2002) 1658–1665. doi:10.1002/1521-3935(200207)203:10/11<1658::AID-MACP1658>3.0.CO;2-3.

Chapter 11. Self-regenerated silk fibroin with controlled crystallinity for the reinforcement of silk

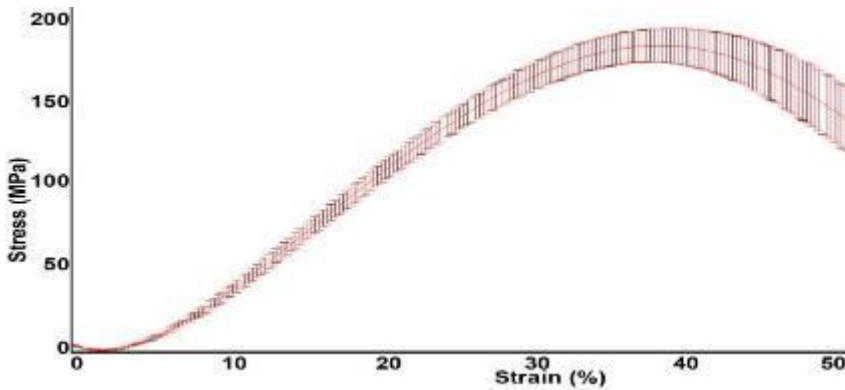
- [56] J. Magoshi, M. Mizuide, Y. Magoshi, K. Takahashi, M. Kubo, S. Nakamura, Physical properties and structure of silk. VI. Conformational changes in silk fibroin induced by immersion in water at 2 to 130°C, *Journal of Polymer Science: Polymer Physics Edition*. 17 (1979) 515–520. doi:10.1002/pol.1979.180170315.
- [57] J. Magoshi, S. Nakamura, Studies on physical properties and structure of silk. Glass transition and crystallization of silk fibroin, *Journal of Applied Polymer Science*. 19 (1975) 1013–1015. doi:10.1002/app.1975.070190410.
- [58] Y. Gotoh, M. Tsukada, T. Baba, N. Minoura, Physical properties and structure of poly(ethylene glycol)-silk fibroin conjugate films, *Polymer*. 38 (1997) 487–490. doi:10.1016/S0032-3861(96)00665-9.
- [59] X. Hu, D. Kaplan, P. Cebe, Dynamic Protein–Water Relationships during β -Sheet Formation, *Macromolecules*. 41 (2008) 3939–3948. doi:10.1021/ma071551d.
- [60] D. Mohanta, S. Santra, G.N. Reddy, S. Giri, M. Jana, Residue Specific Interaction of an Unfolded Protein with Solvents in Mixed Water–Ethanol Solutions: A Combined Molecular Dynamics and ONIOM Study, *J. Phys. Chem. A*. 121 (2017) 6172–6186. doi:10.1021/acs.jpca.7b05955.
- [61] K. Yazawa, K. Ishida, H. Masunaga, T. Hikima, K. Numata, Influence of Water Content on the β -Sheet Formation, Thermal Stability, Water Removal, and Mechanical Properties of Silk Materials, *Biomacromolecules*. 17 (2016) 1057–1066. doi:10.1021/acs.biomac.5b01685.
- [62] P. Cebe, X. Hu, D.L. Kaplan, E. Zhuravlev, A. Wurm, D. Arbeiter, C. Schick, Beating the Heat - Fast Scanning Melts Silk Beta Sheet Crystals, *Scientific Reports*. 3 (2013) 1130. doi:10.1038/srep01130.
- [63] K. Kolman, O. Nechyporchuk, M. Persson, K. Holmberg, R. Bordes, Combined Nanocellulose/Nanosilica Approach for Multiscale Consolidation of Painting Canvases, *ACS Appl. Nano Mater.* 1 (2018) 2036–2040. doi:10.1021/acsanm.8b00262.
- [64] J. Pérez-Rigueiro, M. Elices, J. Llorca, C. Viney, Effect of degumming on the tensile properties of silkworm (*Bombyx mori*) silk fiber, *Journal of Applied Polymer Science*. 84 (n.d.) 1431–1437. doi:10.1002/app.10366.
- [65] J. Pérez-Rigueiro, C. Viney, J. Llorca, M. Elices, Silkworm silk as an engineering material, *J. Appl. Polym. Sci.* 70 (1998) 2439–2447. doi:10.1002/(SICI)1097-4628(19981219)70:12<2439::AID-APP16>3.0.CO;2-J.
- [66] Ph. Colomban, G. Gouadec, Raman and IR micro-analysis of high performance polymer fibres tested in traction and compression, *Composites Science and Technology*. 69 (2009) 10–16. doi:10.1016/j.compscitech.2007.10.034.
- [67] M. Tsukada, G. Freddi, M. Nagura, H. Ishikawa, N. Kasai, Structural changes of silk fibers induced by heat treatment, *Journal of Applied Polymer Science*. 46 (1992) 1945–1953. doi:10.1002/app.1992.070461107.
- [68] G.S. Egerton, The Mechanism of the Photochemical Degradation of Textile Material, *Journal of the Society of Dyers and Colourists*. 65 (1949) 764–780. doi:10.1111/j.1478-4408.1949.tb02558.x.
- [69] R.L. Feller, Accelerated aging: photochemical and thermal aspects, Getty Conservation Institute, 1994.
- [70] M.A. Koperska, D. Pawcenis, J. Bagniuik, M.M. Zaitz, M. Missori, T. Łojewski, J. Łojewska, Degradation markers of fibroin in silk through infrared spectroscopy, *Polymer Degradation and Stability*. 105 (2014) 185–196. doi:10.1016/j.polymdegradstab.2014.04.008.

Supplementary Information

Chapter 11

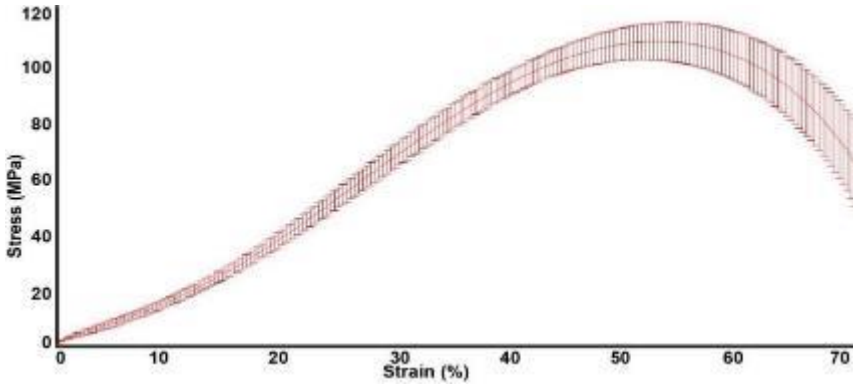


Supplementary Figure 1. Strain-stress plot (average of 10 curves) of pristine commercial silk (Georgette). Each sample is composed of 18 threads, each of 4 cm length, with a gap length set as 1 cm and an elongation speed set at 94 $\mu\text{m/s}$

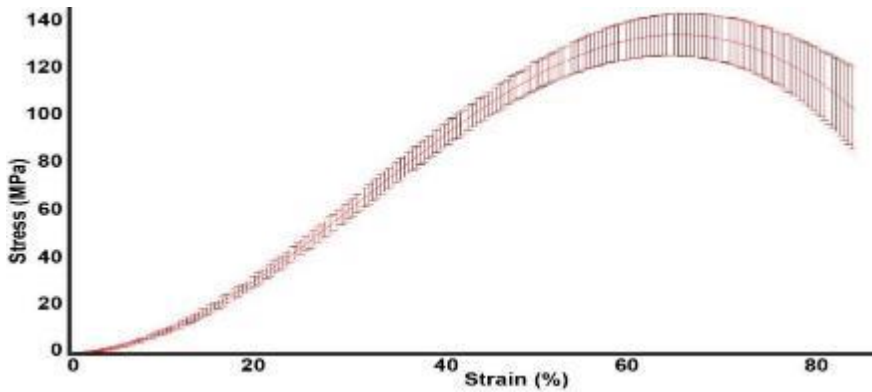


Supplementary Figure 2. Strain-stress plot (average of 10 curves) of commercial silk (Georgette), aged for 4 hours at 130°C (AS1). Each sample is composed of 18 threads each of 4 cm length, with a gap length set as 1 cm and an elongation speed set at 94 $\mu\text{m/s}$.

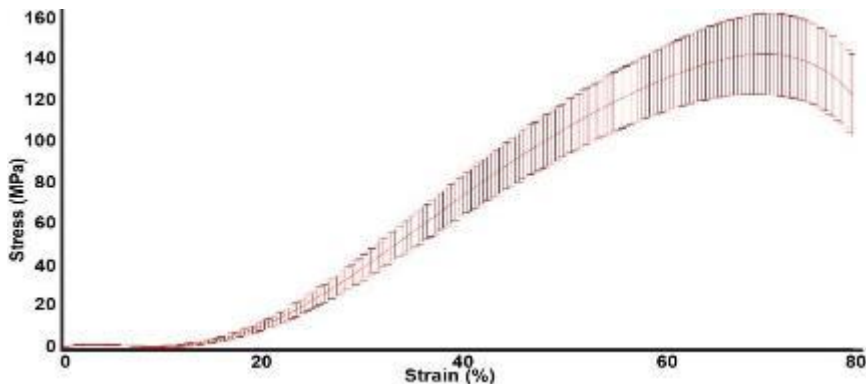
PART IV. SILK CONSOLIDATION



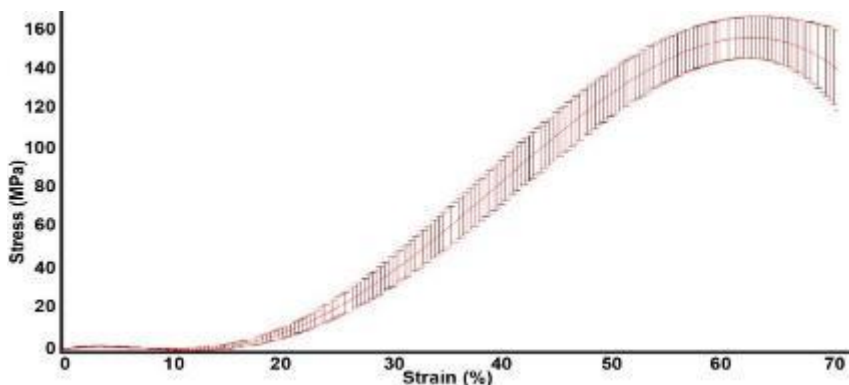
Supplementary Figure 3. Strain-stress plot (average of 10 curves) of commercial silk (Georgette), aged for 4 hours at 130°C and then treated with SRSF-A (AS1-A). Each sample is composed of 18 threads each of 4 cm length, with a gap length set as 1 cm and an elongation speed set at 94 $\mu\text{m/s}$.



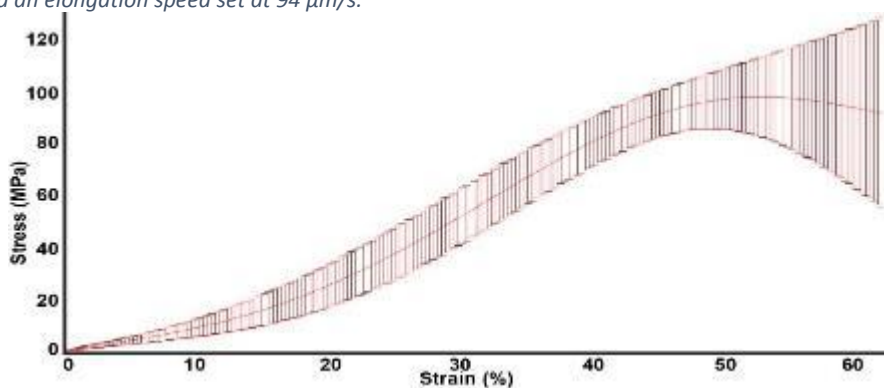
Supplementary Figure 4. Strain-stress plot (average of 10 curves) of commercial silk (Georgette), aged for 4 hours at 130°C and then treated with SRSF-B (AS1-B). Each sample is composed of 18 threads each of 4 cm length, with a gap length set as 1 cm and an elongation speed set at 94 $\mu\text{m/s}$.



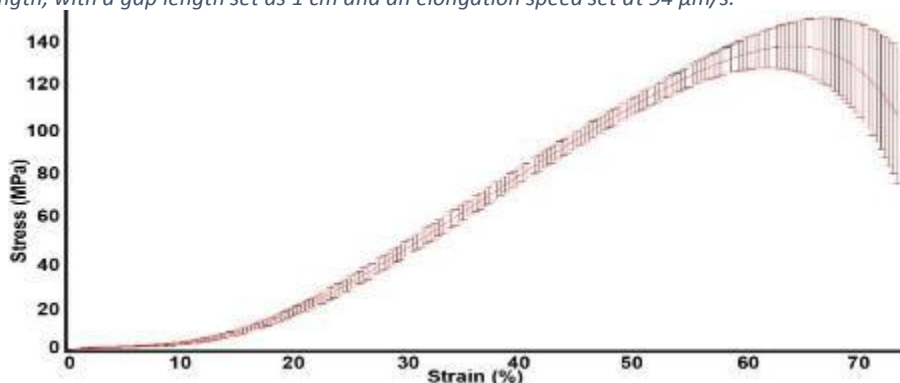
Supplementary Figure 5. Strain-stress plot (average of 10 curves) of commercial silk (Georgette), aged for 4 hours at 130°C and then treated with SRSF-C (AS1-C). Each sample is composed of 18 threads each of 4 cm length, with a gap length set as 1 cm and an elongation speed set at 94 $\mu\text{m/s}$.



Supplementary Figure 6. Strain-stress plot (average of 10 curves) of commercial silk (Georgette), aged with HNO₃ 1.8% (AS2). Each sample is composed of 18 threads each of 4 cm length, with a gap length set as 1 cm and an elongation speed set at 94 μm/s.

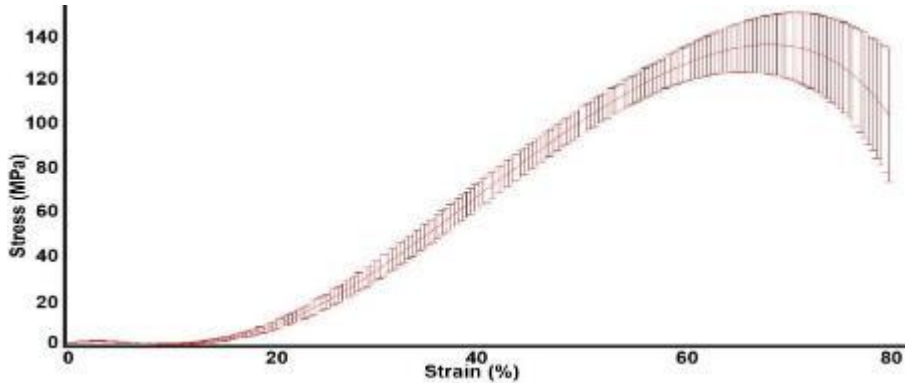


Supplementary Figure 7. Strain-stress plot (average of 10 curves) of commercial silk (Georgette), aged with HNO₃ 1.8% (AS2) and then treated with SRSF-A (AS2-A). Each sample is composed of 18 threads each of 4 cm length, with a gap length set as 1 cm and an elongation speed set at 94 μm/s.

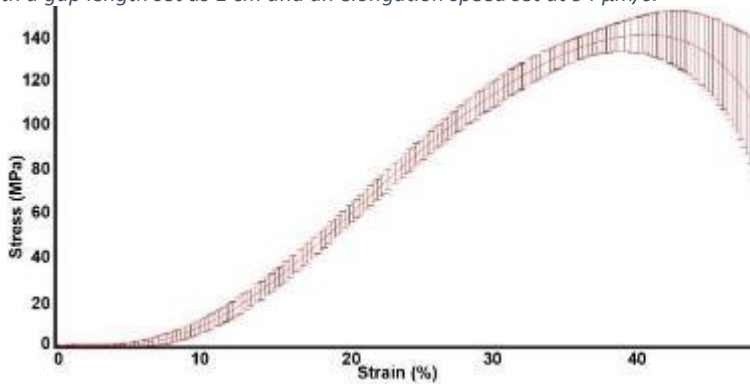


Supplementary Figure 8. Strain-stress plot (average of 10 curves) of commercial silk (Georgette), aged with HNO₃ 1.8% (AS2) and then treated with SRSF-B (AS2-B). Each sample is composed of 18 threads each of 4 cm length, with a gap length set as 1 cm and an elongation speed set at 94 μm/s.

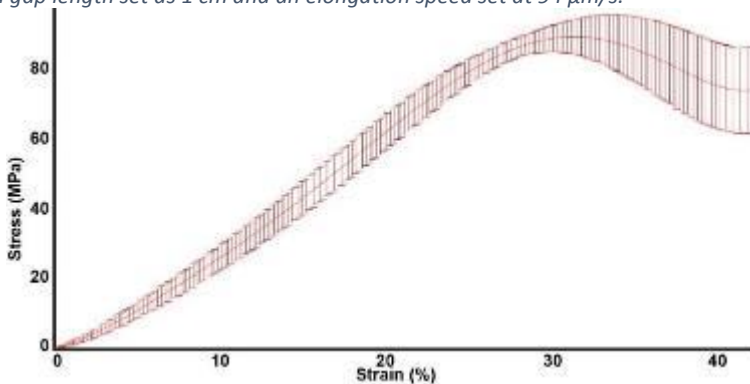
PART IV. SILK CONSOLIDATION



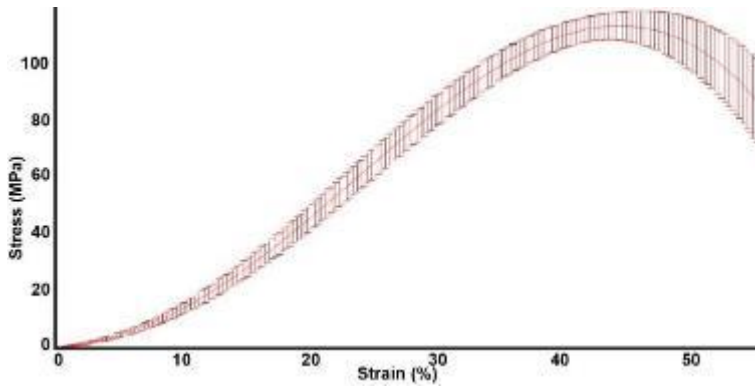
Supplementary Figure 9. Strain-stress plot (average of 10 curves) of commercial silk (Georgette), aged with HNO₃ 1.8% (AS2) and then treated with SRSF-C (AS2-C). Each sample is composed of 18 threads each of 4 cm length, with a gap length set as 1 cm and an elongation speed set at 94 μm/s.



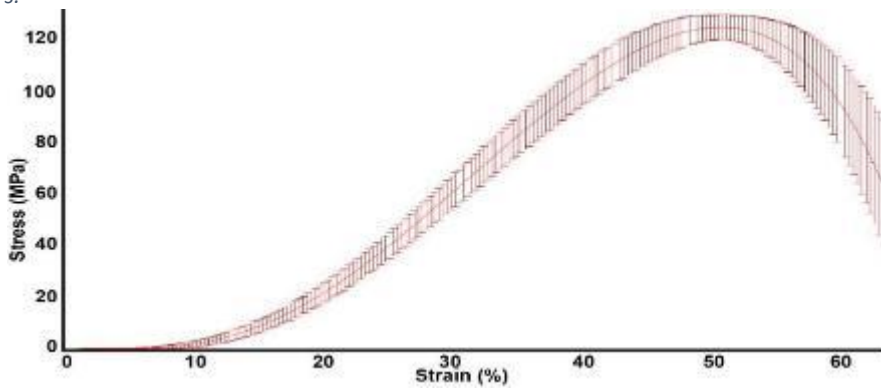
Supplementary Figure 10. Strain-stress plot (average of 10 curves) of commercial silk (Georgette), aged UV-Vis for 30 days at room temperature and RH (AS3). Each sample is composed of 18 threads each of 4 cm length, with a gap length set as 1 cm and an elongation speed set at 94 μm/s.



Supplementary Figure 11. Strain-stress plot (average of 10 curves) of commercial silk (Georgette), aged UV-Vis for 30 days at room temperature and RH (AS3) and then treated with SRSF-A (AS3-A). Each sample is composed of 18 threads each of 4 cm length, with a gap length set as 1 cm and an elongation speed set at 94 μm/s.



Supplementary Figure 12. Strain-stress plot (average of 10 curves) of commercial silk (Georgette), aged UV-Vis for 30 days at room temperature and RH (AS3) and then treated with SRSF-B (AS3-B). Each sample is composed of 18 threads each of 4 cm length, with a gap length set as 1 cm and an elongation speed set at 94 $\mu\text{m/s}$.






Supplementary Figure 13. Strain-stress plot (average of 10 curves) of commercial silk (Georgette), aged UV-Vis for 30 days at room temperature and RH (AS3) and then treated with SRSF-C (AS3-C). Each sample is composed of 18 threads each of 4 cm length, with a gap length set as 1 cm and an elongation speed set at 94 $\mu\text{m/s}$.

APPENDIX




Appendix 1.

List of flags and samples




Appendix 1. List of Flags and Samples

Historical textile object (Images © National Museum of Colombia)	National Museum Register Number	Name - Date - Dimensions (cm)	List of samples
	97	Royal Audience of Santa Fe' Coat of arms Ca. 1550 164 x 133	1-22
	99	Flag with the Castilla and Leon's coat of arms Ca. 1700 159 x 155	23-39
	100	Spanish flag of the Infantry regiment of the Extremadura hunters, second battalion Ca. 1815 158 x 150	91-110




APPENDIX

	<p>101</p>	<p>Spanish Colonel Flag of the Burgos regiment Ca. 1815 145 x 143</p>	<p>111-130</p>
	<p>102</p>	<p>Spanish flag of the Infantry battalion of the line of Huamanga Ca. 1824 146 x 143</p>	<p>131-141</p>
	<p>103</p>	<p>Spanish flag of the infantry battalion Of Ayohuma Ca. 1813 150 x 140</p>	<p>142-158</p>


Appendix 1. List of Flags and Samples

	104	Spanish flag of the battalion Bandera Numancia Ca. 1813 148 x 145	159-170
	105	Gran Colombia flag, for 1 st squadron of the hussar battalion Ca. 1824 73 x 78	260-265
	106	Gran Colombia flag for the hussar battalion of the center Ca. 1824 79 x 88	266-276




APPENDIX

	<p>107</p>	<p>Gran Colombia flag for the 1st battalion of the ruled militias of Cartagena Ca. 1823 168 x 162.5</p>	<p>40-48</p>
	<p>108</p>	<p>Flag for the 1st battalion of the auxiliary militia of the province of Bogotá Ca. 1824 153 x 153</p>	<p>171-178</p>
	<p>109</p>	<p>Flag with the King of Spain Carlos IV's coat of arms Ca. 1790 104.5 x 160</p>	<p>49-51</p>




Appendix 1. List of Flags and Samples

	<p style="text-align: center;">110</p>	<p style="text-align: center;">Gran Colombia flag for the fast battalion N° 1 Ca. 1824 160.7 x 153</p>	<p style="text-align: center;">179-186</p>
	<p style="text-align: center;">111</p>	<p style="text-align: center;">Gran Colombia flag for the national brigade of artillery Ca. 1824 143 x 195</p>	<p style="text-align: center;">59-69</p>
	<p style="text-align: center;">112</p>	<p style="text-align: center;">Flag of one of the Colombian civil wars Ca. 1850 143 x 195</p>	<p style="text-align: center;">187-190</p>
	<p style="text-align: center;">113</p>	<p style="text-align: center;">Flag of one of the Colombian civil wars Ca. 1850 147,8 x 166</p>	<p style="text-align: center;">70-74</p>





APPENDIX

	<p>114</p>	<p>Republic of the New Grenade flag Ca. 1861 255 x 155</p>	<p>225-239</p>
	<p>115</p>	<p>Spanish flag taken on the Chagres capitulation Ca. 1815 98 x 124</p>	<p>201-207</p>
	<p>116</p>	<p>Flag with the Castilla and León coat of arms from the Vaqueanos squadron of the general battalion Ca. 1700 74 x 106</p>	<p>277-287</p>




Appendix 1. List of Flags and Samples

	<p style="text-align: center;">117</p>	<p>Flag with the Spanish coat of arms Ca. 1808 168 x 162,5</p>	<p style="text-align: center;">52-57</p>
	<p style="text-align: center;">118</p>	<p>Flag with the Castilla and León coat of arms Ca. 1808 134 x 111</p>	<p style="text-align: center;">191-200</p>
	<p style="text-align: center;">120</p>	<p>Venezuelan flag taken by the conservator government in the Garrapecera war 22.8.1901 144 x 185</p>	<p style="text-align: center;">75-80</p>





APPENDIX

	<p>122</p>	<p>Great Colombia flag for the battalion Simón Bolívar N° 17 1824 178,5 x 253</p>	<p>240-249</p>
	<p>124</p>	<p>Arequipa's coat of arms Ca. 1875 107 x 80</p>	<p>288-300</p>
	<p>125</p>	<p>Republic of Colombia coat of arms for the Cauca's hunter regiment, 1st battalion Ca. 1932 43,5 x 37</p>	<p>301-309</p>
	<p>126</p>	<p>Colombian flag used as act of sovereignty in the Amazon river after the Salomón Lozano treaty</p>	<p>334-339</p>



Appendix 1. List of Flags and Samples

		1929 65 x 95,5	
	129	Colombian flag offered to Manuel Briceño in the 1885 campaign 247 x 233,5	81-90
	131	United states of Colombia's coat of arms for the Chia battalion N° 27 of the reserve army Ca. 1861 59,5 x 53	323-333
	1948	United states of Colombia's coat of arms Ca. 1861 59,5 x 53	353-367

APPENDIX

	<p>3044</p>	<p>Republic of the New Grenade flag that belonged to José Hilario López Ca. 1849 280 x 195</p>	<p>208-220</p>
	<p>3245</p>	<p>Flag that belonged to General Pedro Alcántara Herrán s. XIX 49 x 54,3</p>	<p>372-378</p>
	<p>3305</p>	<p>Fragment of almaizal Ca. 1538 105 x 34</p>	<p>310-322</p>
	<p>3615</p>	<p>Republic of Colombia's coat of arms for the rifle battalion N° 14 Ca. 1899 81,2 x 64,8</p>	<p>340-352</p>

Appendix 1. List of Flags and Samples

		6079	Colombian flag with coat of arms that belonged to General Solón Wilches Ca. 1880 42 x 23	368-371
		7354	Battalion Santos N° 4 flag, won on the Palonegro battle 1900 173 x 183	250-259

Appendix 2. Sampling protocol

2.1. Proposal for sampling protocol in art objects and/or cultural heritage goods for scientific research

The art objects and/or cultural heritage goods, by their value (not in economic terms) must to be subject to different studies to extract its information. The results coming from those researches on the objects has as consequence the building up of identity and culture among the societies who own them, at the same time gives an increase of scientific information of the objects. To arrive to those results, it must first to follow a process in which the possible research conclusions will be directly affected: the sampling process.

The sampling process from art objects and/or cultural heritage goods, it is a complex process which vary between each object, nevertheless, it is possible to do some general recommendations in aims to guide both, as to the personal whom will take the sampling, as to the analyst whom carry next the respective studies, trying in this way to obtain objective samples which allows to obtain correct answers without false-negative or false-positive conclusions.

The study of art objects and/or cultural heritage goods, it is based on the analysis of the object completely and/or in portions of it, to obtain the respective results from the object itself or to make some comparisons with another objects by context, composition or age. By this reason, it is necessary take in account the sampling strategy to do on the object, avoiding statistical

problems, keeping in mind that the precision of the result could vary according to the number of samples taken.

2.1.1. Sampling process responsible

The representativity of each taken sample from the art object and/or cultural heritage good cannot be subject to interpretations, subjective ideas, believes based on speculation, on the contrary, it must to be a methodic process, judicious and objective, giving as result accurate samples for the following analysis to be done on the object, by this reason, the sampling process cannot be an independent process of only one person.

To obtain a correct sampling from an art object and/or cultural heritage good, it is necessary a team to study the object, it must to be composed by at least: One conservator/restorer specialized on the material to study, a scientific specialized on archaeometry or cultural heritage studies, a curator and an administrative person at charge of the documentation of the process (detailed writing of the process and video or photography register). With this is pretended that the decision making on the sampling process will not slanted to one particular vision, will be protected the object, will be clarified why its relevant the sampling process, how will be done the sampling process and the possible consequences of the intervention to the object, guaranty on this way an optimal selection of samples which will be representative of the art object and/or cultural heritage good, giving the chance to different academic communities of different backgrounds to participate on the process to obtain the correct questions which could be answered with the analysis of the object.

2.1.2. Preliminary studies before the sampling process

Each art object and/or cultural heritage good is a unique object itself (even if exist similar reproductions) from which it is possible to extract information not only of its physical-chemical composition, of its conservational condition, of its degradation processes, of who being exhibit and/or store, but also information related with its elaboration process/technique, the artist or handcraft, about the cultural context and historic moment in which was manufactured, about the raw materials employed on it and more.

With the above, it is evident that any kind of analysis on which is necessary a sampling process of an art object and/or cultural heritage good, must to follow a scientific process in its acquisition to allow to obtain the biggest number of results which might give answer to the different scientific/historical questions that exist on the object or which might appear on the future. To obtain this, the team of experts must to execute a documented inspection to the object previous to the intervention, guaranty to obtain a deep knowledge on the analytical process on the object and on the process, which will be hold next.

On this stage, must be foreseen the “How” and with which elements will hold the sampling process, as well as to define the possible risks which could be subject the object on the intervention, being mandatory to clearly define all and every one of the required instruments to do the sampling process, guarantying the safety of the intervened object. Do not improvise at risk of loss and/or contaminate the sample, neither over-expose the art object and/or cultural heritage good.

It is important to underline that art objects and/or cultural heritage goods, for being objects handled by physical-chemical transformation on its manufacture, has by itself a natural tendency to change across the time, which must to be keep in mind on the sampling process, due to the original status/composition could vary with the time, being necessary a discussion by the expert team about it before to the sampling process.

2.1.3. Sampling process methods

The sampling process which is a process to obtain accurate samples to be given to an expert or a specialized team to develop its research, being this samples previously agreed and accepted by the personal at charge of the custody and protection of the art object and/or cultural heritage good. The sampling process could be executed by two procedures: *in situ* or by direct material extraction from the object.

It is relevant to underline that always that will be possible the *in-situ* procedure must to be chosen before than any other kind of sampling procedure.

2.1.3.1. *In situ* sampling

The samples obtained by the in-situ sampling procedure are those which do not depend neither require an extraction of a portion of the object for its next analysis either on the same location or in a distant laboratory. This kind of sampling it is based on the inspection of the object on stablished areas by analytic and statistical parameters. This procedure is given by the availability of personal and portable/mobile analytical techniques which allow to make measurements with high reproducibility, high sensibility, and high accuracy, either on the location where rest the object or by the possibility to move the object by its dimensions to the laboratory where will be subject to analysis by

the specialist without the requirement to subtract any kind of material from the object studied.

The *in-situ* procedure, not by the direct absence of material subtraction from the object, could be interpreted as an indication of a direct risk absence for the object. This process as any other kind of procedure on the object implies damage risk and/or deterioration, nevertheless, thanks to the modern techniques and the ability of the specialist at charge, the bigger risk falls on the handling expertise of the art object and/or cultural heritage good by means of the analyst team and of course the conservational status of the object.

2.1.3.2. Direct extraction sampling

The different samples that are obtained by direct material extraction from the art object and/or cultural heritage good, are those which imply a direct contact with the object, whereas, as is named, a portion of the object is subtracted from its original location and it is carried over to the following external location to be analyzed. This procedure is done due to the next reasons: first, by the specific necessity to obtain results to questions about the object that would be impossible to answer in another way and second, due to the impossibility to execute an *in-situ* analysis on the object.

The direct extraction sampling procedure on the art objects and/or cultural heritage goods, it is a regular practice on the cultural heritage research field, having nowadays the advantage that, with the development of new technologies and its miniaturization, the sample dimension requirements could arrive to be of relative insignificant sizes respect to the full body size of the object even of a microscopic scale.

This process it is based on the extraction of a portion of the object due to be considered intrusive and destructive must to have in mind the following considerations:

- The samples to be taken cannot be extracted without an initial clear question and a precise analytic procedure to be executed on the samples.
- The resulting samples from each object must to be taken by specialist with the knowledge on this kind of procedure, avoiding in this way bigger damages or collateral effects on the object. The specialist must to register and keep record of its actions through a report with the name and position of the person(s) at charge, the date, the light and environmental conditions, as well as to indicate any possible risk condition that will be found on the room, support of the object and/or any location where is the object which would be a possible risk on a future for the art object and/or cultural heritage good.
- It must to keep a record with great accuracy of the exact location where will be taken the extracted sample, as well a description of its composition, dimensions and weight.
- The sample to be extracted as far as possible, must to be from an area where is already a deterioration, nevertheless, it cannot have a composition different from the original object.
- The sampling process cannot increase the deterioration on the object, neither bring out new deterioration phenomena on the object.
- The resultant sample must to be representative of the different elements which is composed the object, containing the bigger number of elements by area as far as possible.
- The size of the resultant sample to be taken must to be of the minimal dimensions possible from which will be possible to execute its analyze, each analytical technique has its own requirements, by this reason, if will be execute different analyzes on the object it must to keep in mind the requirements of each specialty on the stage of the preliminary study before to the sampling process.
- The sample dimension of the resultant sample cannot crate perceptible gaps on the object from the perspective of a naked eye of the spectator.

Appendix 2. Sampling protocol

- The total number of samples to be taken from a same object will depend as much of the availability of each object that will be found after its inspection after the preliminary study (being guided by the homogeneity composition of the object), as by the different questions done on the object for its study.
- The resultant sample must to be previously established if it will be analyzed by a stratigraphic cross section, guaranty in this way that in its extractions the sample keep the different layers/strata present on the object as well as the respective indication of its orientation.
- The resulting samples obtained by scraping, it must to be executed with the bigger accuracy possible, with trained staff and in minimal quantities, guaranty in this way to obtain a sample only from the wanted material and exclusively from the location desired established on the preliminary study done to the object.
- Each resultant sample must to be kept on individual containers, clearly labeled with its ID, date and responsible.
- The resultant samples, even in its most minimal dimension, kept its value as art object and/or cultural heritage good and therefore must to be kept on custody as it is protecting its chain of custody.
- Each resultant sample must to give the possibility to be studied with scientific rigor, otherwise, it must not be collected.
- Each resultant sample must to be kept on custody to be shared as far as possible with another researcher to allow its study to corroborate results or to obtain new ones.
- The availability of samples previously taken must to be keep on mind for all the studies to be executed on the object.
- The resultant sample cannot contain foreign materials apart of its original composition, but if it is contained, it must to be known and registered the possible processes which could transform the respective sampling area, knowing in this way the possible materials which could have an influence on the respective conclusions on the results of the analysis of those samples.
- If the resultant sample extracted corresponds from an area with a previous cleaning process, it must to be clearly registered this process, avoiding in this way any kind of interference on the conclusions obtained from the results of the analyses of those samples.

- The extracted sample must to be of optimal quality for the respective analytical process on which will be analyzed.
- The resulting samples extracted for radiocarbon dating analyzes must to be specially identified and stored in special containers which avoid its contamination with organic material which could affect its respective dating.
- The representativity of the resultant extracted sample it must to attempt that the results of its analyses give conclusions with high reproducibility in the face of another samples with similar characteristics of the object.
- The direct extraction sampling procedure must to attempt to minimize the future extraction of new samples of the object, decreasing the number of interventions which could increase the object deterioration.
- The resultant samples as far as possible to be able to relate them in time, context and/or composition with objects of similar characteristics.
- If it should exist doubts on the results to be obtained after the respective analysis to be executed on the sample, said samples must to be split on the moment of the extraction sampling process and send to peer laboratories for its analyses.
- On the collection of each sample it must to be avoided the introduction of foreign material (contaminants) to the object.
- Each resultant sample must to be kept on optimal conditions of relative humidity, temperature and light exposure according to the composition of each sample, avoiding in this way transformations or changes on the sample which could carry out wrong or incongruous results.

It is important to underline that even if the samples are extracted by a direct subtraction of material from the object, it does not imply that said samples will be destroyed partially or completely on all the study cases, on the contrary, several analytic studies done to the cultural heritage objects nowadays are executed with a nondestructive character, whereby, at the end of the research on the samples, even, those can be relocated on its original location.

2.1.4. Final consideration

It is important to have present that the research processes on which are involved the art objects and/or cultural heritage goods, give as result that no in all the cases it is possible to achieve the expected conclusions, which means, that exist the possibility that after a rigorous process, will be obtained as result that there is not an answer, either due to the analytic method it was inadequate (sensitivity, detection limits, etc.) or due to the own conditions of the material does not allow to obtain results, being own conditions of the experimentation, which only after of the execution of the test can be known. Consequently, the sampling process must to be followed in aims to diminish this possibility, attempting to omit the human error.

References

1. Artioli, G. *Scientific Methods and Cultural Heritage: An introduction to the application of materials science to archaeometry and conservation science*. (Oxford University Press, USA, 2010).
2. Derrick, M., Stulik, D. & Landry, J. M. *Infrared Spectroscopy in Conservation Science*. (Getty Conservation Institute, 2000).
3. Doménech-Carbó, D. A., Doménech-Carbó, P. D. M. T. & Costa, P. D. V. in *Electrochemical Methods in Archaeometry, Conservation and Restoration* (eds. Doménech-Carbó, D. A., Doménech-Carbó, P. D. M. T. & Costa, P. D. V.) 1–32 (Springer Berlin Heidelberg, 2009).
4. Terry J. Reedy, C. L. R. in *Statistical Analysis in Art Conservation Research*: Available at: <http://www.getty.edu/publications/virtuallibrary/0892360976.html>. (Accessed: 12th December 2016)

2.2. Sampling protocol agreed with the national museum of Colombia

1. OBJETIVO

El presente texto genera los lineamientos o directrices básicas, para la toma de muestras en los Bienes de Interés Cultural (BIC), con el fin de ser una herramienta para la investigación científica de este tipo de objetos.

2. ALCANCE

Aplica a las actividades ejecutadas por los conservadores e investigadores de museos del Ministerio de Cultura para la toma de muestras de un BIC con el fin de obtener información científica del mismo.

3. INTRODUCCIÓN

Como parte del Sistema Integrado de Conservación (SIC), se encuentra el Programa de Investigación, el cual no debe ser excluido de las actividades que desarrolla el Área de Conservación de la entidad y se le debe dar el peso y ayuda que éste necesita.

Éste programa contempla dos componentes: Investigaciones solicitadas por la curaduría e investigaciones solicitadas por alguna entidad académica.

Appendix 2. Sampling protocol

Tabla 1 Tipos de fuentes de estudios a realizar en Bienes de Interés Cultural

Programa	Componentes
Investigación	Curatorial
	Académica

Por lo general el Área de Conservación del Museo, puede resolver preguntas o interrogantes de las piezas de la colección respecto a la técnica o materialidad que tiene un objeto, en especial si éste hace parte de los guiones curatoriales, o si se requiere para sustentar intervenciones de restauración por medio de los estudios preliminares de las piezas.

Entonces, el Área de Conservación es la encargada de generar los análisis físicos – químicos a las obras que lo requieran, con el fin de que esta información, verifique o evalúe la posibilidad de inclusión de las piezas en los guiones curatoriales y/o las posibilidades de intervención, pues “todos los proyectos de conservación deben iniciarse mediante una investigación científica sólida y rigurosa”¹. El objeto de tales investigaciones es encontrar la máxima información posible, tanto de carácter histórico como estético y técnico, sobre el soporte material del bien y por ello requiere una aproximación interdisciplinaria.

Lo anterior, abre cabida a las investigaciones académicas, que son todas aquellas que se generan a partir de un proyecto de investigación asociada a un programa académico, que por lo general tiene vinculación con el Ministerio de Cultura.

¹ PRINCIPIOS PARA LA PRESERVACIÓN, CONSERVACIÓN Y RESTAURACIÓN DE PINTURAS MURALES (2003) Ratificados por la 14ª Asamblea General del ICOMOS, en Victoria Falls, Zimbabue, octubre de 2003, pág. 2

Es de aclarar, que estos proyectos académicos deberán ser aprobados por el museo y por lo tanto el museo deberá tener conocimiento de los mismos. Así mismo, el tema del proyecto académico deberá estar relacionado con el Sistema Integrado de Conservación (SIC), de lo contrario no podrá ser atendido por el Área de Conservación del Museo.

En ese orden de ideas, el presente documento es una base para investigaciones de carácter científico que requieran el análisis de los componentes, materialidad o técnica de los BIC, ya sea para investigaciones que requiere el personal del Museo o para las investigaciones académicas con fines eminentemente científicos.

Cabe mencionar que la “seguridad de una intervención de conservación y restauración en cualquier tipo de Bien Cultural sólo puede garantizarse si previamente se ha realizado un análisis riguroso, serio y específico que pueda ofrecer una información veraz y actualizada de su composición, estructura y estado de conservación”², y esto solo se logra a través de análisis científicos efectuados a las colecciones, sin embargo, en el medio de la Conservación – Restauración, existe una amplia polémica respecto al uso de análisis destructivos para obtener información de las colecciones, prefiriendo el uso de análisis no destructivos para ello, aunque muchos de ellos no generan la información suficiente para responder las problemáticas planteadas en la investigación.

² ESTUDIOS SOBRE EL ARTE ACTUAL, NO. 1. Del microanálisis al macro análisis en el bien cultural: una aproximación a las nuevas tecnologías. Ainhoa Rodríguez López y Fernando Bazeta Gobantes, Julio 2013. Pág. 1

De acuerdo con el libro *Ciencia y Arte IV*, en el artículo de *Consideraciones en torno a los estudios científicos aplicados a la conservación del Patrimonio cultural*, “existe un evidente rechazo a la aplicación de técnicas tradicionales clasificadas como destructivas”, pues en la actualidad las técnicas que ayudan “en la caracterización de materiales de los BIC pueden ser destructivas o mínimamente invasivas y no destructivas (TND, técnicas no destructivas)”³.

No obstante, el uso de una u otra técnica de muestreo para someter el BIC a un análisis científico, dependerá de la posibilidad de respuesta por la técnica empleada, donde en ocasiones será de obligatoriedad el uso de protocolos invasivos. Por consiguiente, se presenta la necesidad de tener un protocolo establecido para proteger el BIC y garantizar la obtención de resultados precisos y certeros en el proceso investigativo.

4. NECESIDAD DE INVESTIGACIÓN CIENTÍFICA

El acercamiento más tradicional que se realiza a los bienes patrimoniales “es desde las humanidades, y lo estudios científicos, en algunas ocasiones, son motivo de desconfianza y controversia, a pesar que, en las últimas décadas, es cada vez más común la introducción de estudios científicos y técnicos previos a la intervención”⁴.

Esta situación obliga a ser especialmente cuidadoso en la toma de muestras, los usos de las técnicas, en los métodos para reducir los riesgos, la comunicación e interpretación de los resultados, de tal forma,

³ Ibid, pág. 2

⁴ CONSIDERACIONES EN TORNO A LOS ESTUDIOS CIENTÍFICOS APLICADOS A LA CONSERVACIÓN DEL PATRIMONIO CULTURAL. Del Egidio Marian, Juanes David y Bueso Miriam, Pág. 8

que ésta sea clara, útil y transparente. “Esta generación de confianza, es necesaria para trabajar con profesionales relacionados con la gestión, tutela, conservación y preservación; así como la investigación del patrimonio, es un aspecto muy presente entre los científicos. Si no se cuida adecuadamente, puede impedir la existencia de una participación o cooperación adecuada y necesaria, para la conservación de los bienes culturales.”⁵

Entonces, por lo general los objetos BIC, deben ser siempre sometidos a diversos estudios para extraer información, los resultados de las diferentes investigaciones en las piezas tienen el fin de la construcción de identidad y cultura, así como el incremento de información con carácter científico de los mismos.

Para llegar a dichos resultados científicos se debe evaluar las razones por las cuales se desea analizar y cuál es el objetivo de las investigaciones, siendo así necesario realizar primero un proceso de relación entre el muestreo o proceso de toma de muestras y las preguntas científicas a ser resueltas en la investigación, para obtener resultados satisfactorios y congruentes a las necesidades que se están buscando.

La toma de muestras, es un proceso complejo que varía de objeto a objeto, sin embargo, se pueden hacer algunas consideraciones generales que darán lineamientos básicos tanto al personal que realizara la toma de la muestra, como a los científicos quienes realizan su posterior

⁵ Ibidem.

análisis, con el fin de obtener muestras de estudio objetivas que no conlleven a “falsos negativos o falsos positivos⁶”.

Es importante tener en cuenta que el estudio de los BIC se basa en el análisis del objeto en su totalidad y/o porciones del mismo, para obtener resultados del objeto o para generar comparaciones con otros objetos, ya sea por contexto, composición o edad.

Por este motivo, se debe tener en cuenta la estrategia de muestreo a realizar en el objeto, para evitar problemas estadísticos, teniendo presente que dependiendo del número de muestras tomadas puede variar la precisión del resultado.

5. RESPONSABLES DEL PROCESO DE TOMA DE MUESTRAS

La representatividad de la muestra tomada del objeto no puede ser sometido a subjetividades, creencias o ideas basadas en especulaciones, al contrario, debe ser un proceso metódico, juicioso y objetivo, dando como resultado muestras certeras para los análisis, por lo cual la toma de muestras no puede ser un proceso independiente de una única persona.

Para la correcta toma de muestras de un BIC, se debe contar con un equipo de análisis del objeto, el cual debe estar compuesto al menos por:

⁶ Entiéndase como “falsos negativos o falsos positivos” a resultados erróneos que no cumplen las expectativas de la investigación y que hacen creer que la información es verídica, cuando realmente no lo es.

- Un conservador – restaurador de bienes muebles con conocimiento en el material a estudiar.
- Un científico especialista en estudios del patrimonio o arqueometría,
- Un curador, quien determina la importancia, significación y necesidad del análisis,
- Un auxiliar o persona a cargo de la toma documental del proceso (escritura en detalle del proceso y toma documental por video o fotografía).

Con esto se busca que la toma de decisiones en el proceso de muestreo no sea sesgada por una única visión, se proteja el objeto, se comprenda el para qué, el cómo y las consecuencias del procedimiento, garantizando de este modo una selección de muestras que serán representativas del BIC brindándole así la oportunidad a una comunidad con diferentes conocimientos a entablar preguntas que pueden derivarse del objeto.

Es importante tener en cuenta que las personas que están en contacto directo con las piezas y/o muestras, ya sea los científicos y los conservadores – restauradores, deben contar con los elementos de protección (EPP)⁷ necesarios para garantizar el bienestar tanto de los operarios como la calidad de muestras a tomar y analizar.

⁷ Para mayor información ver, Protocolo para el uso y manejo de elementos de protección personal (EPP) para la manipulación de obras, Área de Conservación – Museo Nacional de Colombia. 2016.

6. ESTUDIO PRELIMINAR A LA TOMA DE MUESTRAS

Cada objeto se debe considerar como único (así existan similares reproducciones), de las muestras estudiadas del BIC se puede extraer información no solo de su composición físico-química, de su estado de conservación, de sus procesos de degradación, de cómo exhibirse, cómo almacenarse, sino también información relacionada con su proceso de elaboración, del artista y/o fabricante, del contexto cultural en el cual fue creado, del momento histórico en el que se elaboró, de los insumos disponibles en su tiempo, entre otros.

Con lo anterior, se puede ver que cualquier tipo de análisis en el cual sea necesario la toma de una muestra de un objeto, debe tener un principio científico en su proceso de adquisición para que de esta se pueda extraer el mayor número de resultados que den respuesta a las diversas preguntas científicas, históricas y estéticas que existan en el momento del objeto, o que puedan existir en un futuro.

Con este fin, el Área de Conservación con ayuda del equipo de estudio seleccionado de la entidad deberá realizar una inspección previa del BIC, garantizando poseer el conocimiento concreto del proceso analítico al cual va a ser sometido el objeto en estudio durante toda su investigación.

En esta etapa, que comienza con una inspección a profundidad del objeto para conocer su estado material, se debe prever el cómo y con qué instrumentación se procederá a hacer el muestreo, así como definir los posibles riesgos que pueden presentarse en el procedimiento, siendo obligatorio definir con claridad todos y cada uno de los elementos

requeridos para hacer un “procedimiento de toma de muestra” efectivo, pues es indispensable evitar la improvisación, dado que se pone en riesgo tanto el BIC, como la toma de la muestra, ya sea perdiéndola o contaminándola.

Es importante resaltar, que los objetos, por ser parte las colecciones de los museos, han sido manipulados, ya sea para procesos de exhibición y almacenamiento o en su propia fabricación, lo cual genera una transformación físico-química de sus elementos, pues tienen la tendencia natural al cambio a través de su tiempo de vida y uso, lo cual debe ser tenido en cuenta en el proceso de muestreo, dado que pueden versen alterados, el estado y/o composición original al pasar el tiempo.

En ese orden de ideas, es indispensable que el equipo de trabajo evalúe el estado de conservación del objeto y la integridad del mismo, con el fin de tomar muestras que sean efectivas y certeras para la investigación, establezcan el número de muestras a tomar, las técnicas de análisis a ser empleadas, las preguntas a responder y los posibles efectos y/o impactos del estudio a realizar.

7. PROCEDIMIENTO CIENTÍFICO EN LA OBTENCIÓN DE MUESTRAS DE BIC

Los estudios científicos a los cuales son sometidos los BIC, hacen necesario como primera medida que sean sujetos a un proceso de muestreo para obtener los puntos de análisis de donde se copilará o extraerá la información correspondiente del objeto con el fin de llegar a las conclusiones necesarias para responder las preguntas entabladas en

la investigación. Dichos estudios, se basan en una “serie de tecnologías científicas para obtener resultados fiables”⁸ de los cuales pueden ser técnicas de análisis destructivos o no destructivos, sin embargo, es importante resaltar, que los procedimientos de análisis solo se pueden ejecutar como un proceso posterior al muestreo, siendo cierto que el muestreo también puede ser destructivo o no destructivo.

Por lo anterior, la toma de muestras se hace previo acuerdo y aceptación, tanto por los científicos que la analizan, como por los conservadores que las toman. El muestreo se puede desarrollar por dos procedimientos: *in situ* o por extracción directa de material del objeto

Es importante resaltar qué, siempre que sea posible se debe ejecutar el procedimiento *in situ* antes de cualquier otro proceso de muestreo.

a. Muestreo *in situ*

Las muestras en el análisis *in situ* son aquellas que no dependen, ni necesitan de una extracción directa del material para ser posteriormente analizada, ya sea en el mismo recinto o en un laboratorio, por lo tanto, se puede establecer que el muestreo *in situ* se realiza al tiempo con el proceso de análisis del objeto. Entonces, las técnicas *in situ* son “aquellas en que la muestra analizada queda inalterada al finalizar el proceso de análisis. Estas técnicas se basan en la aplicación de fenómenos físicos tales como ondas electromagnéticas, acústicas, elásticas, emisión de partículas subatómicas, y cualquier tipo de prueba que no implique una

⁸ Del Egido. Op Cit, pág. 3

alteración de la muestra examinada... por lo tanto, dichas técnicas no generan modificaciones en las propiedades físicas o químicas del objeto.”⁹

Este tipo de muestreo se basa en la inspección del objeto en sectores establecidos por parámetros analíticos y estadísticos. Este procedimiento se da por disponibilidad de personal y técnicas analíticas portátiles/móviles que permitan hacer mediciones con alta reproducibilidad, sensibilidad y precisión en el lugar donde reposa el objeto o por la posibilidad de trasladar el objeto (por sus dimensiones) al laboratorio donde será sometido a análisis por los científicos.

Es importante considerar que, al realizar el procedimiento *in situ*, aunque no se extraiga material del objeto, también pueden generar alteraciones en el objeto que modifican radicalmente el estado de conservación del objeto, no obstante, gracias a las técnicas modernas y la capacitación de los especialistas a cargo, el mayor riesgo recae en la manipulación del objeto por parte del equipo de científicos.

Lo anterior, debe ser tenido en cuenta por el grupo de profesionales en el estudio preliminar al muestreo, a la hora de realizar estudios científicos, pues el hecho de que una técnica de análisis no requiera muestras, no implica necesariamente que la técnica sea inocua para el objeto.

⁹ Del Egido. Op Cit, Pág. 10

b. Muestreo por extracción directa

Las muestras que se obtienen por extracción directa de material del objeto, son aquellas que implican un contacto directo con la pieza, donde, como su nombre lo indica, una porción de la obra es extraída de su posición inicial y es llevada para su posterior análisis en una locación externa o laboratorio.

Este procedimiento se lleva a cabo debido a dos motivaciones: primero por la necesidad específica de obtener resultados a preguntas sobre el objeto que de otro modo sería imposible responder y segundo debido a la imposibilidad de realizar análisis de tipo *in situ* sobre el objeto.

De acuerdo con el artículo “*Consideraciones en torno a los estudios científicos aplicados a la conservación del patrimonio cultural*”, uno de los más grandes problemas que presentan la toma de las muestras para análisis destructivos, es falta de concientización o necesidad de efectuar el análisis, por parte de quienes custodian las obras, “pues en muchas ocasiones, se llega a extremos en los que está mal visto, o directamente se niega el permiso para la toma de muestras de una fachada de un monumento porque es una técnica destructiva, sin tener en cuenta que por ejemplo, la erosión debida al viento, la lluvia y contaminación genera una pérdida de material mucho mayor en un año, que la pérdida que sufre el monumento por tomar esa micro muestra... así mismo, tampoco se tiene en cuenta que la información que puede aportar esa pequeña cantidad puede permitir un diseño del proceso de intervención más

adecuado y evitar intervenciones desastrosas que generen graves daños por falta de información.”¹⁰

“Los estudios con micro muestras son esenciales para responder aquellas cuestiones que derivan de los estudios sin toma de muestra proporcionando una inestimable ayuda en los procesos de intervención, aconsejando el empleo de un determinado producto de restauración, la eliminación de alguna sustancia o elemento de deterioro o desaconsejando un método nocivo o proponer nuevos materiales anteriormente contrastados. Estos datos son indispensables para determinar si el protocolo de actuación está acorde a las necesidades o requiere de una nueva revisión,”¹¹ así mismo, las técnicas de análisis con toma de micro muestras, también aportan una gran cantidad de información desde el punto de vista histórico y artístico.

El procedimiento de extracción de muestras es una práctica común, teniendo que en la actualidad se cuenta con nuevas tecnologías y la miniaturización de los análisis, por lo tanto, el requerimiento de las dimensiones de las muestras puede llegar a ser de tamaños absolutamente minúsculos respecto al volumen del objeto e incluso microscópicos.

Cuando se decide proceder a la toma de muestras es indispensable, no solo contar las herramientas necesarias para su extracción, sino también con una ficha modelo, la cual debe tener los siguientes ítems: 1.

¹⁰ Del Egado. Op Cit, Pág. 14

¹¹ Ibidem.

identificación de la obra, con sus dimensiones y número de registro, etc., y 2 un gráfico en el que se señale la ubicación de cada una de las muestras extraídas.

El proceso de muestreo que inicia con el estudio preliminar del objeto donde por un estudio organoléptico de la superficie del objeto se determinan aquellas zonas susceptibles a la extracción de muestras por su interés estilístico, técnico y material. Concluye con la acción de la extracción del material, donde a cada muestra extraída se le asigna un código para su identificación.

Para la extracción del material, el proceso se basa en la toma de una porción del material del objeto, teniendo en cuenta las siguientes consideraciones:

- Las muestras a ser extraídas no pueden ser obtenidas sin una clara pregunta inicial y un definido procedimiento analítico a ejecutarse en ellas.
- Las muestras obtenidas de cada objeto deben ser tomadas por los conservadores del museo o por especialistas con conocimiento en dicho procedimiento, evitando de este modo surjan daños mayores o colaterales en el objeto.

En las medidas de las posibilidades se recomienda registrar la toma de muestras con el nombre y cargo de la(s) persona(s), la fecha, las condiciones medioambientales y de luz del día de la toma, así como indicar la ubicación o mueble de almacenamiento

donde se encuentre el objeto que pueda llegar a generar un efecto negativo a futuro en el objeto.

- Se debe documentar con precisión la ubicación del punto de toma de cada muestra, así como en las medidas de la posibilidad la descripción de su composición, dimensiones y peso.
- Procurar realizar la extracción en aquellas zonas que presentan craquelados y lagunas o que manifiesten deterioro, para respetar tanto las partes intactas sin lagunas, como las zonas muy afectadas y con escasos fragmentos. Sin embargo, la muestra resultante no debe tener composición diferente a la buscada en el objeto original.
- La toma de la muestra no debe aumentar el deterioro, ni producir nuevas alteraciones en el objeto.
- La muestra debe ser representativa de los diferentes elementos que componen el objeto, conteniendo el mayor número de elementos que sea posible.
- El tamaño de la muestra a tomar debe ser de la menor dimensión posible de la cual se pueda hacer su estudio, pues cada técnica analítica requiere una dimensión diferente, por lo cual, si se van a realizar varios estudios sobre la muestra, se debe tener en cuenta los requerimientos de cada especialidad en el estudio preliminar de muestreo.
- El tamaño de la muestra no puede generar vacíos perceptibles en el objeto muestreado.
- El número de muestras a tomar de un mismo objeto, dependerá tanto de la disponibilidad que cada pieza arroja luego de su inspección preliminar (guiándose en la homogeneidad del objeto),

como de las diferentes preguntas realizadas sobre éste para ser estudiadas.

- Antes de la toma de cada muestra debe tener previamente establecido si la muestra será sometida a análisis estratigráfico, garantizando así que, en el procedimiento de toma se conserve los diferentes estratos presentes en el objeto, así como la indicación de las capas, con la orientación del corte estratigráfico según las capas de la pieza.
- Las tomas realizadas por raspado, se deben llevar a cabo con la mayor precisión posible y en cantidades mínimas, garantizando así la colección de material única y exclusivamente del sitio y composición de interés.
- Cada muestra obtenida se debe embalar en contenedores individuales con clara especificación de su identificación, fecha de muestreo y responsable.
- En la medida de las posibilidades las muestras obtenidas, en su más mínima dimensión, siguen siendo parte de los BIC y por ende deben ser custodiadas como tal, salvaguardando su cadena de custodia.
- Cada muestra obtenida debe brindar la posibilidad de ser estudiada con rigurosidad científica, de lo contrario no debe ser extraída.
- Cada muestra en lo posible debe ser custodiada para ser estudiada y ser compartida con otros investigadores para corroborar los resultados, con el fin de poder obtener nuevos hallazgos.

- La disponibilidad de muestras de un objeto previamente adquiridas, deben ser tenidas en consideración para los estudios a realizar en el objeto.
- La muestra obtenida no debe contener material ajeno a su elaboración original y de contenerlo se debe conocer y documentar a que proceso de tratamiento fue sometido el objeto en dicha área, conociendo así de antemano posibles materiales que puedan influir en las conclusiones obtenidas de los resultados en el análisis.
- Si la pieza fue sometida anteriormente a procesos de limpieza química o tratamientos de restauración, debe ser aclarado con exactitud, con el fin de evitar errores en el análisis de los resultados obtenidos en las muestras.
- La muestra extraída debe ser de óptimas cualidades para el proceso analítico al cual será sometida.
- Las muestras a ser sometidas a análisis de datación por radiocarbono deben ser especialmente identificadas y almacenadas en contenedores que eviten su contaminación con material orgánico que pueda afectar su respectiva datación.
- La representatividad de la muestra debe procurar buscar que los resultados de su análisis arrojen conclusiones de alta reproducibilidad ante el estudio de otra muestra con similares características del objeto.
- La extracción de muestras debe procurar minimizar la futura extracción de muestras del objeto en el futuro, disminuyendo el número de intervenciones que pueden aumentar el deterioro del objeto.

- Las muestras obtenidas deben en lo posible poder relacionarse en tiempo, contexto y/o composición con objetos de similares características.
- Si llegasen a existir dudas en los resultados a ser obtenidos luego de los estudios a ejecutarse en las muestras, dichas muestras deben ser divididas en el momento de su toma y deben ser enviadas a laboratorios pares para su análisis.
- En el proceso de toma de muestras se debe eliminar la introducción de material extraño (contaminación) al objeto.
- Cada muestra debe ser almacenada en condiciones de temperatura, humedad relativa y exposición a la luz acordes a la composición de la misma, evitando así transformaciones o cambios en la muestra que puedan llevar a resultados erróneos o incongruentes.
- Es importante resaltar que, aún si las muestras obtenidas por extracción directa implican la remoción de parte del objeto, no implica que estas muestras sean destruidas parcial o completamente en todos los estudios que se realicen en estos, al contrario, varios de los estudios analíticos que se realizan en el patrimonio cultural actualmente son de carácter no destructivo, con lo que, al finalizar su estudio, la muestra puede llegar a ser reposicionada en su ubicación original.

En conclusión, la toma de las muestras ha de ser minuciosa, dado que siempre se ha de tener presente el provocar el menor daño o deterioro posible a la obra y ha de estar muy bien documentada para ayudar en el proceso de interpretación de los resultados obtenidos con las nuevas

tecnologías de análisis que tras el muestreo se emplean sobre las muestras tomadas.

Finalmente, es importante señalar que la toma de micro muestras posibilita la existencia de que esta información sea cargada a Colecciones Colombianas, la cual puede consultarse o revisarse durante generaciones sin necesidad de recurrir nuevamente al objeto analizado. Lo anterior debe tenerse muy presente, pues con el uso de las nuevas tecnologías, se permitirá en el futuro tener resultados cada vez más exactos.

c. Resultados esperados

El análisis de los materiales permite obtener una visión general y completa de las piezas tanto a nivel técnico y material, por lo tanto, la recopilación y clasificación de los resultados deberá facilitar su lectura y comprensión, en especial, para aquellas áreas no directamente relacionadas con las ciencias como los conservadores – restauradores y curadores, quienes ansiosamente desean conocer las respuestas a los interrogantes establecidos sobre los objetos de estudio.

En los casos donde se estudie un mismo tipo de soporte¹², lo más apropiado será generar una tabla por cada componente del soporte o por cada estrato presente en los objetos estudiados. Por ejemplo, si se está

¹² Entiéndase como soporte, el material principal o clasificación de material primario que compone un objeto, es decir, pintura de caballete, maderas, metales, textiles, papel, etc.

estudiando pintura de caballete, la tabla deberá tener los materiales de base de preparación, imprimaturas, capa pictórica y capa de protección.

En caso de estar estudiando objetos que no tienen estratigrafía se recomienda colocar en la primera columna de la tabla el código del objeto, para de este modo relacionar la información obtenida.

Las tablas generadas deberán tener las siguientes divisiones en las columnas indicando: Materiales inorgánico y orgánicos, espesor (indicado en μm), código de obra y el código de la muestra de la cual la información se ha extraído.

La exposición de los resultados analíticos en tablas, deberá estar complementado con su descripción en forma narrativa acompañada con las técnicas de laboratorio empleadas para cada caso.

Por último, es importante que en los estudios se realicen comparaciones de diferencias y similitudes con el fin de comprender o justificar las técnicas y/o materiales identificados.

8. CONSIDERACIONES FINALES

Es importante tener presente que los procesos de estudio a los que son sometidos los objetos dan como resultado que no en todas las ocasiones se puedan obtener las conclusiones esperadas, lo cual significa, que existe la posibilidad que luego de un riguroso estudio, se obtenga como resultado que no se obtuvo una respuesta, ya sea porque el método no es adecuado (sensibilidad, límites de detección, etc.), o porque las

condiciones de la pieza no permitieron obtener resultados, siendo condiciones propias de la experimentación, que solo luego de la ejecución de las pruebas se puede conocer. Por consiguiente, el procedimiento de toma de muestras debe hacerse en miras de disminuir dicha posibilidad, buscando omitir errores humanos.

Por otra parte, si se quiere mantener la terminología sobre destructividad o no, es necesario evaluar la no destructividad, destructividad o micro destructividad de la técnica utilizada para cada caso y tomar decisiones individualizadas.

Es importante comprender que lo que se busca desde el punto de vista de la conservación sería una técnica perfecta, que difiera mucho de la técnica ideal en el procesos de diagnóstico, es decir, una técnica que permitiera análisis globales y puntuales de daños estructurales, que su vez proporcionaran información sobre los materiales o elementos químicos y las estratigrafías con los espesores de las capas, sin la necesidad de la extracción de muestras y que éstas técnicas fueran inocuas, portátiles, pudieran realizarse *in situ* y on-line, que fueran muy económicas y que estuvieran en un sistema asistido de análisis que facilitara la interpretación de los datos. Sin embargo, a la fecha, esta idealización del procedimiento de estudio de los BIC no se encuentra, siendo inevitable que para obtener resultados similares esa necesario acudir a varias metodologías que permitan obtener la información requerida, sin llegar a alterar los valores históricos y estéticos del objeto.

Los análisis que se realizan, deben seguir una secuencia científicamente establecida, en la que los resultados de una técnica puedan llegar a servir

de base para un subsecuente estudio, teniendo presente que las técnicas de análisis que se empleen en las muestras obtenidas de los objetos, deben ser las apropiadas con el tipo de objeto a estudiar y al objetivo que se quiere conseguir con los análisis.

En conclusión, la puesta en práctica en varias de las entidades culturales, demuestran que los estudios analíticos, con extracción directa de muestra o no, proporcionan algún tipo de resultado, sin embargo, la combinación entre las técnicas destructivas y las *in situ* potencializan los hallazgos en las investigaciones científicas que puede enriquecer enormemente los resultados para responder las problemáticas del estudio del objeto y puede ser de gran relevancia para la preservación del patrimonio cultural colombiano.

Finalmente, es necesario reconocer que el uso de los análisis científicos es una excelente herramienta de documentación, no solo para la investigación, sino también para la conservación de las colecciones de los museos, pues los encargados de las Áreas de Conservación deberán ser los responsables de dicha gestión y pueden utilizar esta información como instrumento de planificación para establecer prioridades de intervención y salvaguarda del patrimonio.

REFERENCIAS

- Artioli, G. *Scientific Methods and Cultural Heritage: An introduction to the application of materials science to archaeometry and conservation science*. (Oxford University Press, USA, 2010).
- Del Egido Marian, Juanes David y Bueso Miriam. *La Ciencia y el arte IV. Consideraciones en torno a los estudios científicos aplicados a la conservación del patrimonio cultural*. (Ministerio de educación, cultura y deporte de España, 2013)
- Derrick, M., Stulik, D. & Landry, J. M. *Infrared Spectroscopy in Conservation Science*. (Getty Conservation Institute, 2000).

APPENDIX

Doménech-Carbó, D. A., Doménech-Carbó, P. D. M. T. & Costa, P. D. V. in *Electrochemical Methods in Archaeometry, Conservation and Restoration* (eds. Doménech-Carbó, D. A., Doménech-Carbó, P. D. M. T. & Costa, P. D. V.) 1–32 (Springer Berlin Heidelberg, 2009).

Rodríguez López Ainhoa y Bazeta Gobantes Fernando. *Estudios sobre el arte actual. Del micro análisis en el bien cultural: una aproximación a las nuevas tecnologías*. Número 1, (España, julio 2013).

Terry J. Reedy, C. L. R. in *Statistical Analysis in Art Conservation Research*: Available at: <http://www.getty.edu/publications/virtuallibrary/0892360976.html>. (Accessed: 12th December 2016)

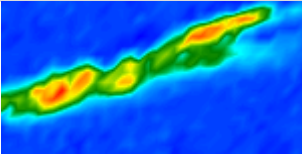
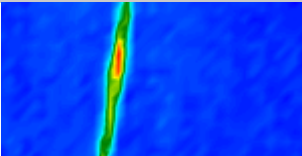
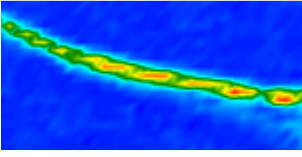
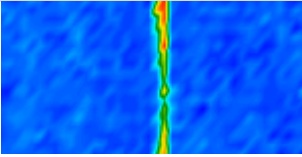
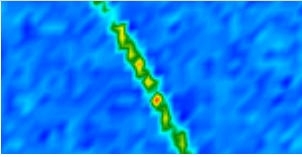
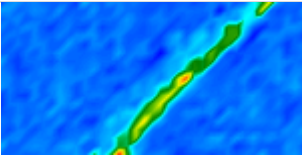
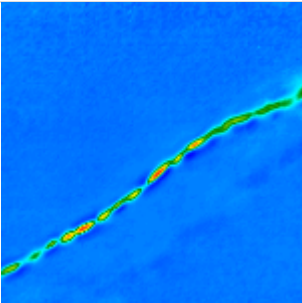
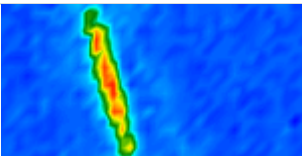
El presente documento fue elaborado en conjunto por Diego Armando Badillo Sánchez como parte de su proyecto de Doctorado en Ciencias Química – Ciencias de Conservación del Patrimonio Cultural Universidad de Florencia (Italia) y María Catalina Plazas Garcia, coordinadora del Área de Conservación del Museo Nacional de Colombia.

Visto Bueno y aprobación de Fernando López (Jefe de Gestión de Colecciones) y María Paola Rodríguez (Curadora de historia).

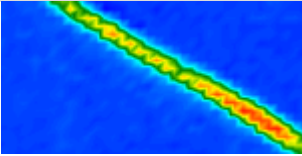
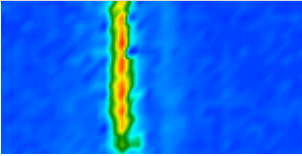
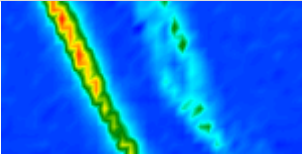
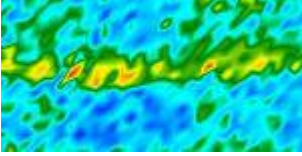
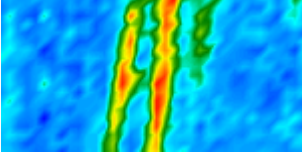
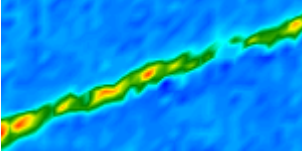
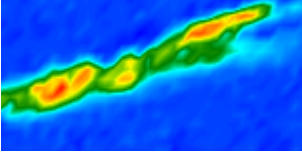
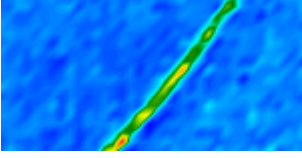
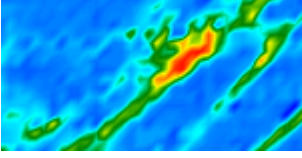
Museo Nacional de Colombia.
Diciembre 2016

Appendix 3.
FPA μ -FTIR 2D chemical mapping
on historical samples

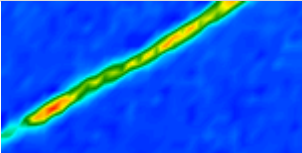
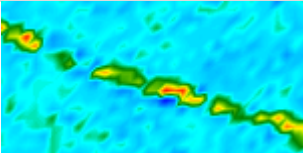
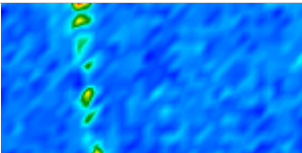
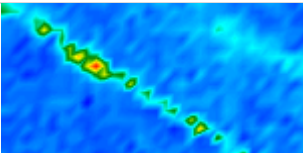
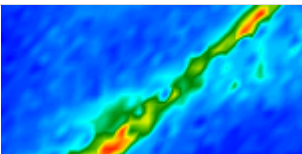
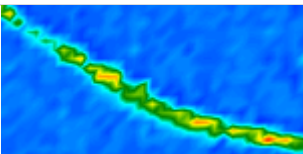
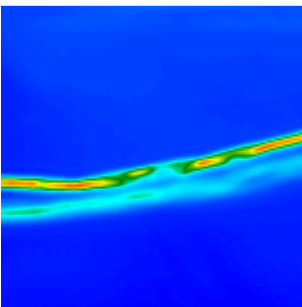
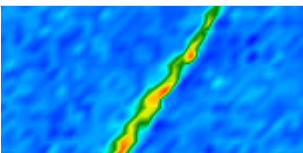
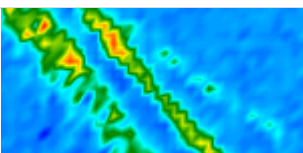
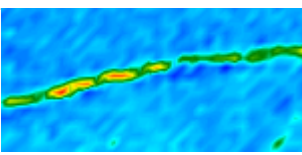
APPENDIX

Sample	Color	Date	Amide A Map (3300±30 cm ⁻¹) 100x200 μm ² Intensity: auto scale	S6	Blue	1550	
Pristine Silk	No colored	2015		S19	No colored – metal thread core		
S311	Blue	1538		S32	Yellow – metal thread core	1700	
S312	Blue			S34	White (Cotton)		
S317	Red						S278

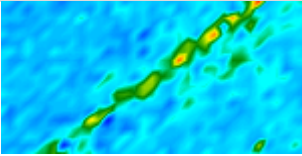
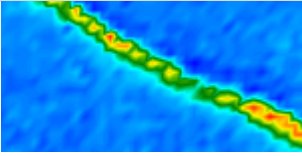
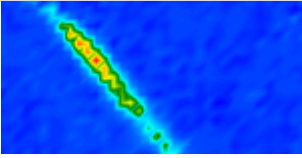
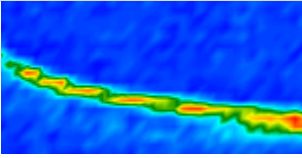
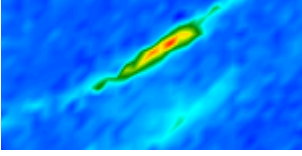
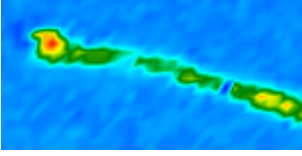
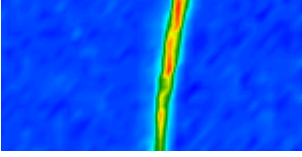
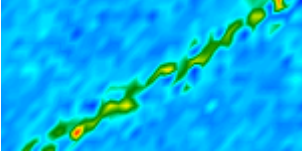
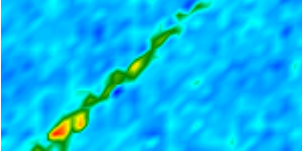
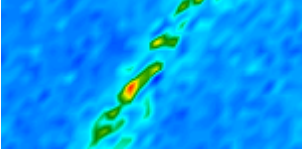
Appendix 3. FPA μ -FTIR 2D Chemical Mapping on Historical Samples

S49	Red	1790		S197	Blue		
S51	Yellow			S168	Red		1813
S52	Red	1808		S148	Blue	1813	
S53	Red			S91	Yellow	1815	
S192	Red	1808		S102	Brown		

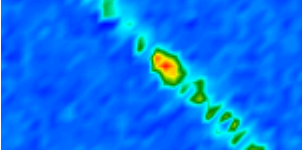
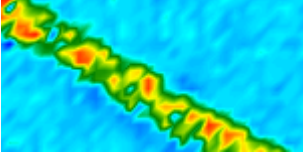
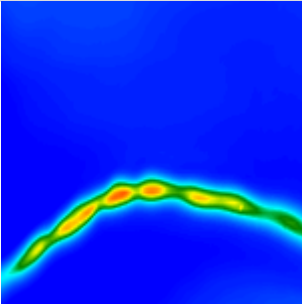
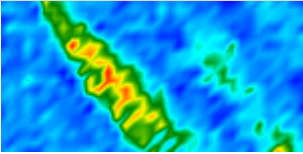
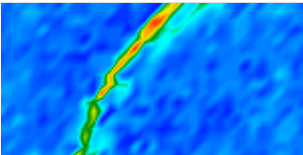
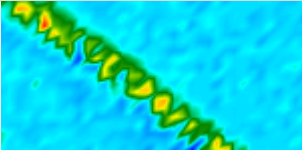
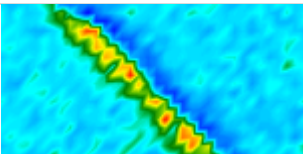
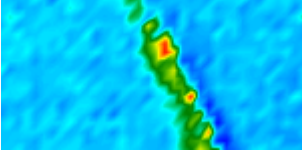
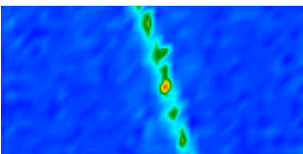
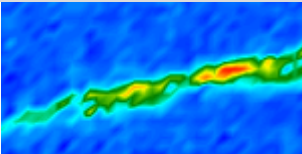
APPENDIX

S105	No colored – metal thread core			S44	Red		
S118	Red	1815		S265	Red	1824	
S205	Yellow	1815		S268	No colored – metal thread core	1824	
S207	Cotton			S59	Red	1824	
				S63	Green		
S43	Yellow	1823					

Appendix 3. FPA μ -FTIR 2D Chemical Mapping on Historical Samples



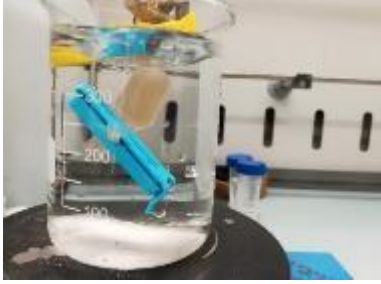
S240	Red	1824		S229	Blue	1861	
S186	Red	1824		S236	Red		
S375	Yellow	1845		S365	Red	1863	
S219	Red	1849		S289	Purple	1875	
S220	Blue			S291	No colored – metal thread core		

APPENDIX

S296	Black			S342	Red	1899	
S297	Brown (Cotton)			S251	Yellow	1900	
				S259	Red		
S370	Red	1880		S75	Red	1901	
S84	Green	1885		S335	Blue	1929	
S87	Red						

Appendix 4.
Annexed information for
different processes on the thesis
research

4.1. Description of the preparation of solutions for silk reconsolidation

Image	Description process
	Waste Silk used as raw material for the preparation of the self-regenerated silk fibroin coatings
	Waste Silk dispersed in $\text{CaCl}_2:\text{H}_2\text{O}:\text{EtOH}$ (1:12:8)
	Dispersed silk solution at the beginning of the dialysis

Appendix 4. Detailed Information for Different Processes on the Thesis
Research





	<p>Dispersed silk solution after 3 days of dialysis</p>
	<p>Final dispersed silk fibroin solution after centrifugation</p>
	<p>SRSF drop film of the final concentrated dispersed fibroin solution for concentration control</p>
	<p>Initial drop of SRSF solution over silk textile</p>

APPENDIX




SRSF solution spread over the silk textile after 5-7 minutes.

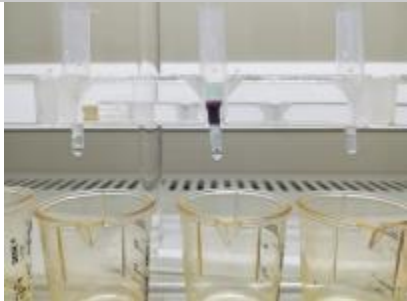


4.2. Tensile tests

Image	Description
	Pristine Silk samples before tensile test
	Rheometer used for the tensile test of the different textile sample
	Detail of silk sample on the clamp of the instrument
	Pristine Silk samples after tensile test

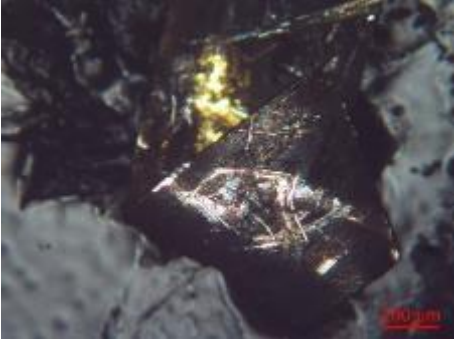
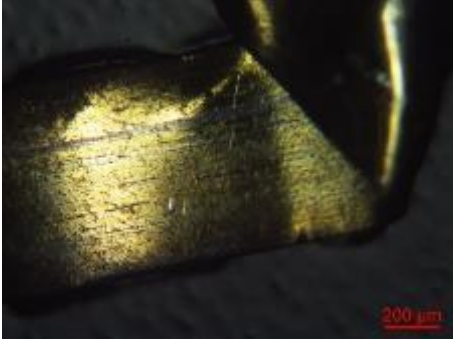

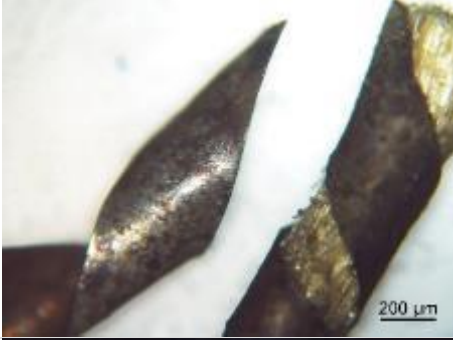
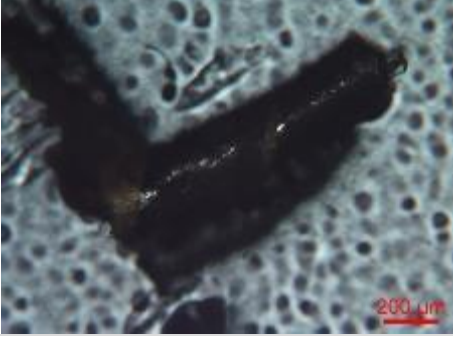

APPENDIX

			<p>Detail of the change of color of the pristine silk after the treatment with the nitric acid solution in the micro Owen</p>
--	---	--	---



4.3. Lead purification columns for lead isotope analysis on MC-ICP-MS

Image	Description
	Change of color of the resin in the process of purification/separation of the lead in micro samples of metal decorations for lead isotope analysis
	Cleaning step before to collect the lead from the micro samples of metal decorations for isotope analysis
	Final lead collected after the purification process for the isotope analysis

4.4. Example of some metal decorations chemically cleaned before SEM-EDS analysis

Sample	Before	After cleaning with HNO ₃ 1%
S26		
S17		
S135		

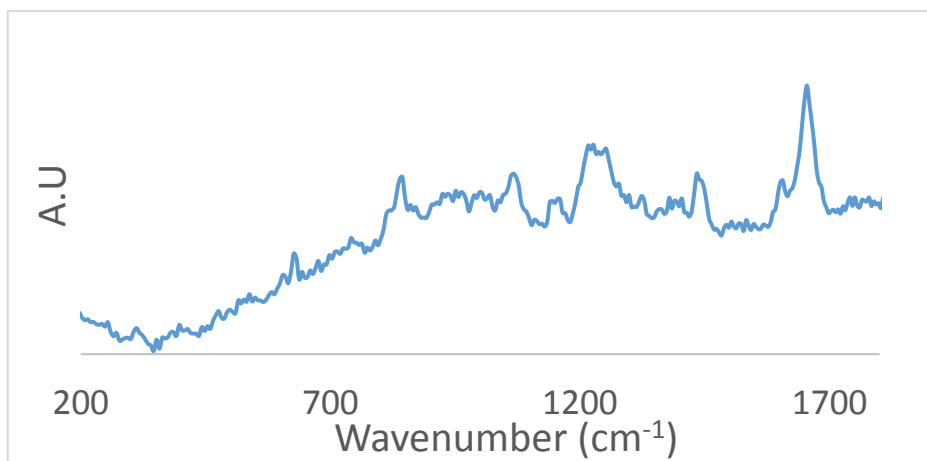
4.5. Example of the thermal decomposition of silk textile sample on a TGA chamber

Description	Image
<p>Top empty reference pan, bottom red sample before being thermally treated</p>	
<p>Top empty reference pan, bottom red sample after being thermally treated</p>	
<p>Microphotograph detail of charred silk textile after decomposition at 400°C</p>	
	

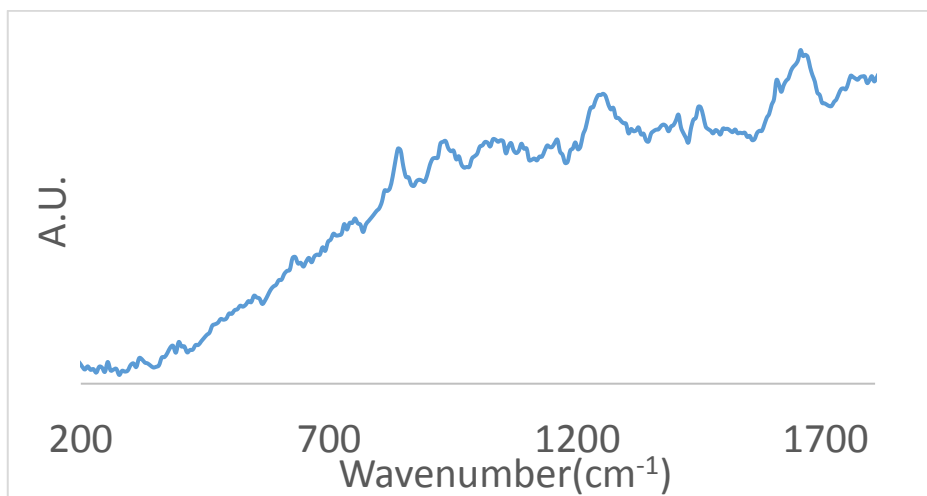
Appendix 5.
Raman spectra on the region
200-1800 cm^{-1} of the SRSF films
prepared from waste silk

Appendix 5. Raman Spectra on the Region 200-1800 cm^{-1} of the SRSF Films Prepared from Waste Silk

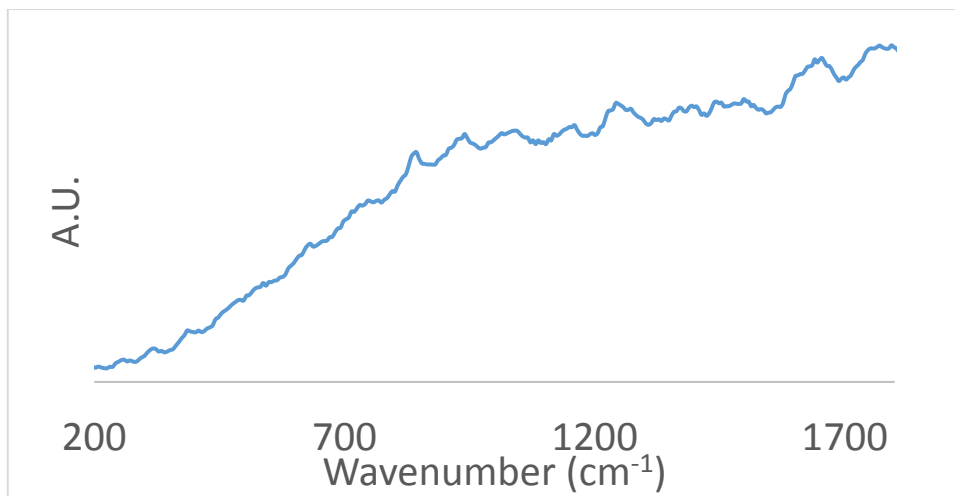
SRSF-A



SRSF-B



SRSF-C



ACKNOWLEDGEMENTS

When everything goes to the end, it is the time when you look behind and try to remember in which circumstances and who help you to finish and accomplish your goals, this operation which could seem like a cold and forced obligation instead of a true feeling of gratitude, could be addressed to acknowledge only some people as in a list, as if just they were the unique important person who did magnificent labor on you, but you know that is not true. When you look behind, you feel that sensation that embraces your soul and makes you put into consideration the great impact of each one of the participants that crossed your path, intentional and unintentionally, those with who you expend the most of your time, but as well those with who you just saw once at a coffee break or at lunchtime, or even those with who you never talk, being all of them equally important to be recognized, because each one of them have put a grain of help in what you have done, on how you have arrived, and in what you have transformed.

After three years, with incredible demands, dreams, and works of a great project that just seems like an illusion when you compare with what you could be done in the past, and what you have achieved now, it is time to acknowledge to every person who walked with you during this time, and at the same time to those who will take the time to read, discuss, continue or critique this work.

For that reason, from the keys on my desk, Thanks!